MOLECULAR MODELLING OF POLYMERIC GLASSES

by

DOROS NICOLAS THEODOROU

Diploma Chem. Eng., National Technical University
of Athens (1981)

M.S. Chem. Eng., Massachusetts Institute of Technology
(1983)

SUBMITTED TO THE DEPARTMENT OF
CHEMICAL ENGINEERING
IN PARTIAL FULFILLMENT OF THE
REQUIREMENTS FOR THE DEGREE OF

DOCTOR OF PHILOSOPHY

at the

MASSACHUSETTS INSTITUTE OF TECHNOLOGY
(September 1985)

Signature of Author _____
Department of Chemical Engineering
June 10, 1985

Certified by _____
Professor Ulrich W. Suter
Thesis Supervisor

Accepted by _____
Professor William M. Deen, Chairman
Departmental Committee on Graduate Students

MOLECULAR MODELLING OF POLYMERIC GLASSES

by

DOROS NICOLAS THEODOROU

Submitted to the Department of Chemical Engineering
on June 10, 1985 in partial fulfillment of the
requirements for the Degree of Doctor of Philosophy in
Chemical Engineering

ABSTRACT

A method is developed for the detailed atomistic modelling of well-relaxed amorphous glassy polymers. Atactic polypropylene at -40°C is used as an example. The model system is a cube with periodic boundaries, filled with segments from a single "parent chain." An initial guess structure is generated using a modified Markov process, based on Rotational Isomeric State theory, and incorporating long-range interactions. This initial guess is then "relaxed" by potential energy minimization, to reach a static model structure that satisfies the conditions of detailed mechanical equilibrium.

Theoretical estimates of the cohesive energy and the Hildebrand solubility parameter, obtained from an ensemble of 15 such model structures, agree very well with experiment. The conformation of single chains in the relaxed model system closely resembles that of unperturbed chains. Pair distribution functions and bond direction correlation functions show that the predominant structural features are intramolecular, and that long-range orientational order is completely absent.

Well-characterized samples of atactic polypropylene are prepared by catalytic epimerization of the isotactic form of the polymer to stereochemical equilibrium. The structure of these samples is studied by X-ray and neutron diffraction. Theoretical diffraction patterns, predicted directly from the pair distribution functions of the model, are consistent with the experimental scattering results.

The model is used to predict the elastic constants of an amorphous glassy polymer. A thermodynamic analysis of deformation shows that entropic contributions to the elastic response can be neglected in polymeric glasses. A statistical mechanical analysis further indicates that vibrational contributions associated with bond length and bond angle variation are not significant, so that estimates of the elastic constants can be obtained from changes in the total potential energy of static model structures subjected to simple deformations. Methods are developed for the atomistic simulation of deformation, and

applied to glassy atactic polypropylene. Predicted elastic constants are always within 15% of the experimental values, without the use of adjustable parameters. An estimate of the thermal expansion coefficient is also obtained.

The ensemble of undeformed and deformed microscopic states is used to probe local structure in the glass, and to explore the mechanism of small-strain elastic deformation. The concept of atomic level stresses is extended to bonded systems and applied to the polymer model. Chain topology influences the atomic level stresses strongly. The structural changes brought about by shear and tension deformations are examined. Atomic displacements are found to deviate markedly from local affine behavior. Considerable directional correlation of atomic motion is observed both intra- and intermolecularly. Deformation in the glassy bulk is accompanied by concerted displacement of chain segments approximately 10 bonds long.

Thesis Supervisor : Professor Ulrich W. Suter

Title : Texaco-Mangelsdorf Associate Professor of Chemical Engineering

ACKNOWLEDGEMENTS

I wish to express my gratitude to my supervisor, Professor Ulrich W. Suter, for the guidance and support he offered during the course of this work. Not only did he provide invaluable scientific input, but he also created a warm, collaborative atmosphere, in which doing research has been a real pleasure.

I would also like to thank the members of my Thesis Committee, Professors Robert E. Cohen, Robert C. Reid, James Wei and Ioannis V. Yannas, for vigorous and helpful discussions that broadened my point if view and further stimulated my interest in this work.

Thanks are due to Dr. Herbert A. Mook of the Solid State Division, Oak Ridge National Laboratory, for offering us beam time at the High Flux Isotope Reactor and for making his expertise on neutron scattering available to us; also to Professor T. Egami of the Department of Materials Science and Engineering, University of Pennsylvania, for the X - ray diffraction measurements performed on our samples.

I appreciated the help of undergraduate students Vykki Rodak, Donna Bennett and Bob Huang with the experiments.

The financial support provided for this project by the National Science Foundation, through grant No DMR-8312694 (Polymers Program) is gratefully acknowledged.

TABLE OF CONTENTS

LIST OF TABLES

LIST OF FIGURES

1. INTRODUCTION

1.1. MOTIVATION

The macroscopic properties of polymers are determined to a large extent by the molecular structure of constituent chains. It is very important to understand and to be able to reliably predict these properties from the knowledge of the chain structure. Up to now, however, the exploration of structure - property relations in polymers has been primarily heuristic, descriptive rather than predictive. At present new polymeric materials are usually obtained by trial synthesis and a'posteriori searching for possible applications. We need to develop new, reliable methods for the quantitative prediction of polymer properties, that will enable us to explore new structures and to rationally design new materials. If such sound methods of property prediction become available, one may some day be able to invert the prediction process and effectively construct polymers with specific applications in mind.

The statistical mechanical theory of single polymer chains in dilute solution has received considerable attention. On the contrary, theories of the amorphous bulk, which is much more relevant for engineering applications, have traditionally been much cruder. The reason for this is the inherent complexity of dense multichain systems. With the advent of modern computers, however, it is possible, and it is becoming increasingly so, to apply the principles of statistical mechanics to real life systems. Computer simulation has provided much needed insight on the properties of dense fluids, and is promising as a means of expanding our knowledge of bulk polymers.

This work attempts the step from chemical structure to the mechanical properties of an amorphous polymeric glass. It involves the development of a methodology for deducing technologically important macroscopic properties from "first principles." Some simplifying assumptions have to be introduced, as in any modelling effort of this complexity. This, however, can be done in a well controlled and justifiable way, so as to retain a satisfactory level of molecular detail and at the same time enhance the predictive power of the model.

The practical necessity for replacing empiricism by a rigorous "molecular engineering" approach, involving "computer aided design" of materials, was one of the main factors that triggered the author's intense interest in this work. The basic scientific need to improve our fundamental understanding of polymers and to resolve some fascinating questions pertaining to the structure and macroscopic behavior of glasses also provided strong motivation. It is hoped that the results of the research presented in this writing will be of some use in both respects.

1.2. OBJECTIVES

Briefly stated, the objectives of this thesis have been:

(a) to develop a quantitative computer model of molecular structure in an amorphous polymer (atactic polypropylene) below its glass formation temperature. The model is more realistic than any existing models and involves no adjustable parameters. It provides detailed information on

on the conformation and relative arrangement of chains in the bulk, as well as estimates of thermodynamic quantities such as the cohesive energy and Hildebrand's solubility parameter.

(b) to arrive, by simulating small-strain mechanical deformation of this model system, at theoretical estimates of the elastic constants (isothermal compressibility κ_T, Young's modulus of elasticity E, shear modulus G, Poisson ratio ν.)

(c) to test model predictions against experiment. Predictions of macroscopic properties were compared with measurements available in the literature. For testing the structural predictions of the model, however, an experimental program was undertaken for producing well characterized samples of the modelled polymer and for studying their molecular structure by X-ray and neutron scattering.

The theoretical foundations of the molecular model are laid in chapters 1 and 2 of this writing. An exposition of the model itself and of the structural and thermodynamic information obtained from it is given in chapters 3 and 4. The method developed for the simulation of deformation and the prediction of mechanical properties are described in chapter 5. Chapter 6 deals with detailed atomistic information, provided by the model, on the local topology of the glassy polymeric bulk and on the mechanism of its elastic deformation. Finally, an account of the experimental part of this work is given in chapter 7.

1.3. PREVIOUS WORK

An accurate description of glassy polymers in detailed molecular terms is not available to date, and as a result there is no theoretical treatment of deformation and relaxation phenomena in polymeric glasses based on "first principles." As a consequence, phenomenological concepts which defy precise definition, such as "free volume" [12], must be invoked. Chain packing in the amorphous bulk has been studied extensively, and newer experimental data, especially from neutron scattering, strongly suggest ([41],[14],[5],[27]) that the chain macromolecules assume essentially unperturbed random coil conformations, in the "equilibrium" melt and even in well-relaxed glasses. Flory [25] has suggested this decades ago, but the complete absence of long-range orientational correlation, implied by the random coil model, is nevertheless not universally accepted [48]. We will not discuss the extensive experimental work done in the past to elucidate the physical structure of amorphous polymers [3]. We will also not dwell on the numerous publications presenting experimental data on the mechanical behavior of amorphous polymers above and below their glass formation temperature.

Previous theoretical work of some relevance to our objectives roughly falls into two categories:

(a) Computer simulations of the structure of amorphous polymers.

(b) Theoretical predictions of mechanical properties.

(a) Theoretical investigations of structure in the amorphous polymeric bulk have typically involved Monte Carlo simulations of the topology of multichain systems. Polymer molecules are frequently modelled as self-avoiding random walks on a discrete lattice of sites with cyclic boundary conditions. Primitive cubic ([2],[18],[20],[52]) lattices, as well as more realistic "diamond" lattices ([19],[38]), or even regular two-dimensional lattices of various coordination numbers [72] have been used. Various sampling methods have been devised to limit sample attrition, which is severe at high densities. The objective is usually investigation of the effects of the volume fraction and the length of the chains on conformation-related quantities such as the mean squared end-to-end distance, $\langle r^2 \rangle$, and the mean squared radius of gyration, $\langle s^2 \rangle$. A general conclusion is that $\langle r^2 \rangle$, $\langle s^2 \rangle$, and $\partial \ln \langle r^2 \rangle / \partial \ln n$ fall as the volume fraction increases toward unity, approaching the values characteristic of an unperturbed random walk. Residual differences between some Monte Carlo simulations and Flory's "unperturbed random coil" theory are probably partly due to the simplifying assumptions and sampling techniques used.

A somewhat more sophisticated Monte-Carlo model for a "liquid" polymer has been published by Bishop et al. [6]. Chains are pictured as freely-jointed strings of beads, which interact with each other through a Lennard-Jones potential, and which are connected by bonds of finite extensibility. A reptation algorithm is used to sample configuration space.

Considerably more realistic is a computer model of the molecular arrangement in a polymer liquid, consisting of short linear polymethylene chains, advanced by Vacatello et al. [69]. The system modelled is a cubic cell with periodic

boundaries of edge length 30.4 Å and filled with 31 triacontane chains. The packing corresponds to the experimental density of the paraffinic liquid. Chains are modelled as sequences of methylene units connected by bonds of fixed length, and bond angles are given tetrahedral values. The chains are initially grown "in situ" in a lattice, starting from randomly oriented trimethylene units. The system is subsequently "equilibrated" by a Monte Carlo procedure which resembles reptation, but allows for continuous variation of bond angles. Hence, the final model is not a lattice model. The methylene-methylene nonbonded interaction potential is changed during "equilibration" to save computer time. The structure is evaluated only during the latter stages of equilibration, so that the number of microstates sampled is much smaller than in an ordinary Metropolis Monte Carlo procedure. Predicted X-ray scattering curves agree satisfactorily with experimental data, and characteristic quantities of the chains indicate an essentially unperturbed conformation.

A molecular dynamics approach to the problem of modelling the structure of amorphous polymers has been introduced by Weber and Helfand [74]. Their system is a "liquid" periodic polyethylene chain in a box of edge length 18.2 Å, containing 200 carbon centers, at 425 K. Structural and dynamic information is accumulated from a run simulating the temporal evolution of the system.

To summarize the situation: Early lattice models for the computer simulation of the amorphous bulk rest on artificial assumptions and employ time-consuming methods for sampling configuration space by chain movement; they give information on qualitative trends, but are rather inappropriate for making quantitative predictions. More refined models, which account for chain chemistry and interatomic interactions in a more realistic way, can be successful in predicting experimentally

observed aspects of bulk polymeric structure. Polyethylene seems to be the only polymer chain on which realistic modelling of the structure of the amorphous bulk has been attempted, and these attempts have been restricted to the liquid state. No computer simulation has ever been performed at densities corresponding to a glass.

(b) Theoretical work attempting to derive macroscopic mechanical properties of polymers from "first principles" is not extensive. Previous efforts pertain almost exclusively to the crystalline state,in which the existence of a well-defined periodic structure permits drastic simplification. An early statistical mechanical treatment of crystalline polymethylene by Pastine led to a P-V-T equation of state that compares favorably with experiment. More recently, Tashiro, Kobayashi and Tadokoro ([62],[63]) derived elastic constants for a variety of crystalline polymers. Their model predictions are within 35% of the experimentally observed quantities.

Mechanical properties of glassy amorphous polymers have not yet been connected to their detailed molecular structure. Existing theoretical work on the mechanical properties of polymeric glasses is largely phenomenological in character. Haward and MacCallum [32] proposed that the adiabatic compressibility of a polymeric glass is mainly determined by interchain forces. Based on a Lennard-Jones type relation between total potential energy and the cubic root of the molar volume they arrived at an expression of the form

$$\kappa_S = f(V_o / V) \qquad (1.1)$$

where κ_S is the adiabatic compressibility, V is the molar volume (cm^3/mol units) and V_o is the molar volume under conditions such that

$$\left.\frac{\partial U}{\partial V}\right|_T = 0$$

This compressibility-volume correlation compares favorably with experimental data, thus indicating that mechanical properties are predictable on the basis of conventional intermolecular force relationships.

Unlike other fields of polymer engineering, the field of estimation of mechanical properties by means of additive group contribution methods is not very developed. For amorphous polymers an estimate of the compressibility can be arrived at by use of the Schuyer correlation ([71], p.267.)

$$\frac{B}{\rho} = \frac{1}{\kappa_T \rho} = \left(\frac{\bar{u}_{Rao}}{V}\right)^6 \qquad (1.2)$$

where V is the molar volume and $\bar{u}_{Rao}$ is the Rao function or molar sound velocity, defined as

$$\bar{u}_{Rao} = V \, u_{long}^{1/3} \left[\frac{1 + \nu}{3 (1 - \nu)} \right]^{1/6} \qquad (1.3)$$

where u_{long} is the longitudinal sound velocity in the material and ν the Poisson ratio. There exist tables of group contributions for both $\bar{u}_{Rao}$ and V. The Young's modulus E and shear modulus G can only be obtained through the compressibility, using an estimate for the Poisson ratio ν. Note that, according to correlation (1.2), mechanical properties are determined solely by the the material's density and chemical structure.

Yannas ([78],[79],[80]) considers displacements, on the molecular level, brought about by mechanical deformation of glassy polymers and finds that deformation of a macromolecular segment occurs primarily by rotation around skeletal bonds,

rather than by distortion of bond angles and distances. The term "strophon" is introduced to characterize a 3-virtual-bond-long segment, which is the smallest possible part of the chain that can undergo change of its end-to-end distance upon deformation. The force required to overcome inter- and intramolecular barriers to bond rotation is estimated on the basis of a simple single-strophon model. The comparative contribution of these barriers to the small-strain modulus is used as a basis for distinguishing between two mechanisms of deformation. In vinyl polymers the inter- and intramolecular contributions are found to be equally significant.

An atomistic approach to plastic deformation in amorphous metals has been introduced by Maeda and Takeuchi [43], and by Srolovitz, Vitek and Egami [55]. The work presented in this writing, although developed completely independently, and although referring to bonded systems, small deformations and a nonzero absolute temperature, has certain aspects in common with their approach.

2. FUNDAMENTAL ANALYSIS

2.1. THERMODYNAMIC CONSIDERATIONS

In trying to develop a computer model capable of predicting the elastic constants of polymeric glasses I started from some fundamental thermodynamic considerations, which are briefly presented in the following.

In the continuum formulation of thermoelasticity ([75], Chapter 1) a body is regarded as a collection of material particles, whose positions are denoted by

$$\underset{\sim}{r}_o = (r_{o_1} , r_{o_2} , r_{o_3}) \equiv (x_o , y_o , z_o)$$

in the reference (undeformed) state, and by

$$\underset{\sim}{r} = (r_1 , r_2 , r_3) \equiv (x , y , z)$$

in the deformed state. The vector $\underset{\sim}{t}$, with components

$$t_\alpha = r_\alpha - r_{o_\alpha}$$

we will call the displacement vector.
The material strain tensor, $\underline{\underline{\varepsilon}}$, is defined by:

$$\varepsilon_{LM} = \frac{1}{2} \left(\sum_{\alpha=1}^{3} \frac{\partial r_\alpha}{\partial r_{o_L}} \frac{\partial r_\alpha}{\partial r_{o_M}} - \delta_{LM} \right) =$$

$$= \frac{1}{2} \left(\frac{\partial t_L}{\partial r_{o_M}} + \frac{\partial t_M}{\partial r_{o_L}} \right) + \frac{1}{2} \sum_{\alpha=1}^{3} \frac{\partial t_\alpha}{\partial r_{o_M}} \frac{\partial t_\alpha}{\partial r_{o_L}} \qquad (2.1)$$

Since this work is concerned entirely with small deformations, terms second order in the derivatives of displacement with respect to position will be neglected in defining $\underline{\underline{\varepsilon}}$,

and no distinction will be drawn between material and spatial strain (compare formulation in [11], chapter 13.)

The material stress tensor is denoted by $\underline{\underline{\tau}}$. Again, no distinction is made between material and spatial stress. The element τ_{LM} is taken equal to the force per unit area acting an element of surface perpendicular to axis L, and along the direction M. Thus, if $d\underline{F}$ is the surface traction on an element of surface dS, where the unit normal vector directed toward the exterior of the surface is $\underline{n}$,

$$d\underline{F} = \underline{\underline{\tau}}^T \cdot \underline{n} \; dS \tag{2.2}$$

By virtue of their symmetry, the tensors $\underline{\underline{\varepsilon}}$ and $\underline{\underline{\tau}}$ will also be represented, in Voigt notation, as vectors of six components ([75], p.14). The two notations will be used interchangeably; the particular notation employed will be evident from the number of subscripts.

$$\varepsilon_1 = \varepsilon_{11} \; , \; \varepsilon_2 = \varepsilon_{22} \; , \; \varepsilon_3 = \varepsilon_{33} \; , \; \varepsilon_4 = 2\varepsilon_{23} \; , \; \varepsilon_5 = 2\varepsilon_{31} \; , \; \varepsilon_6 = 2\varepsilon_{12} \tag{2.3}$$

$$\tau_1 = \tau_{11} \; , \; \tau_2 = \tau_{22} \; , \; \tau_3 = \tau_{33} \; , \; \tau_4 = \tau_{23} \; , \; \tau_5 = \tau_{31} \; , \; \tau_6 = \tau_{12}$$

The thermodynamics of elastic solids is formulated in terms of the tensors $\underline{\underline{\varepsilon}}$ and $\underline{\underline{\tau}}$. The fundamental equation for an elastic system at constant chemical composition assumes the form

$$dU = T\,dS + V_o \sum_{LM} \tau_{LM} d\varepsilon_{LM} = T\,dS + V_o \sum_{I} \tau_I \, d\varepsilon_I \tag{2.4}$$

(The subscript o denotes the undeformed state.)

For the Helmholtz energy $A = U - T\,S$ we obtain, in differential form

$$dA = -S\,dT + V_o \sum_{LM} \tau_{LM} d\varepsilon_{LM} = -S\,dT + V_o \sum_{I} \tau_I\, d\varepsilon_I \qquad (2.5)$$

The fourth-order tensor of isothermal elastic coefficients, C_{LMNK}, is defined by:

$$C_{LMNK} = \left.\frac{\partial \tau_{LM}}{\partial \varepsilon_{NK}}\right|_{T,\varepsilon_{[NK]}} = \frac{1}{V_o} \left.\frac{\partial^2 A}{\partial \varepsilon_{LM} \partial \varepsilon_{NK}}\right|_{T,\varepsilon_{[LM,NK]}} \qquad (2.6)$$

As a result of the Voigt symmetry relations ([75], p.32) it can be condensed into a symmetric 6x6 matrix C_{IJ}, by replacing index pairs by single indices, as was done in eqns (2.3).

For an isotropic material, such as an amorphous glassy polymer, the $\underline{\underline{C}}$ matrix assumes the form:

$$\underline{\underline{C}} = \begin{bmatrix} 2\mu+\lambda & \lambda & \lambda & 0 & 0 & 0 \\ \lambda & 2\mu+\lambda & \lambda & 0 & 0 & 0 \\ \lambda & \lambda & 2\mu+\lambda & 0 & 0 & 0 \\ 0 & 0 & 0 & \mu & 0 & 0 \\ 0 & 0 & 0 & 0 & \mu & 0 \\ 0 & 0 & 0 & 0 & 0 & \mu \end{bmatrix} \qquad (2.7)$$

where λ, μ are the Lame' constants.

The Young's modulus E, shear modulus G, bulk modulus B and Poisson ratio ν are related to λ and μ by:

$$E = \mu \frac{3\lambda+2\mu}{\lambda+\mu} \qquad G = \mu$$

$$B \equiv \frac{1}{\kappa_T} = \lambda + \frac{2}{3}\mu \qquad \nu = \frac{\lambda}{2(\lambda+\mu)} \tag{2.8}$$

The strain dependence of entropy under constant temperature is expressed by the Grüneisen tensor ([75], p.34) $\underline{\underline{\gamma}}$:

$$\gamma = \frac{1}{\rho_o c_\varepsilon V_o} \left. \frac{\partial S}{\partial \varepsilon_{LM}} \right|_{T,\, \varepsilon_{[LM]}} =$$

$$= - \frac{1}{\rho_o c_\varepsilon} \left. \frac{\partial \tau_{LM}}{\partial T} \right|_{\underline{\underline{\varepsilon}}} \tag{2.9}$$

where c_ε is a specific heat per unit mass of material at constant strain. The tensor $\underline{\underline{\gamma}}$ can again be represented in condensed notation.

For an isotropic solid,

$$\gamma_{LM} = \gamma\, \delta_{LM} = \frac{1}{\rho_o c_\varepsilon} \frac{\alpha_P}{\kappa_T} \tag{2.10}$$

where α_P is the volumetric thermal expansion coefficient, and γ the Grüneisen parameter.

Consider an arbitrary elastic solid subjected to an arbitrary isothermal small-strain deformation. If we Taylor-expand the internal energy, U, around the undeformed state to second order, and use the definitions introduced above, we have:

$$U = A + TS = U_o + V_o \sum_{LM} \left[\tau_{LM} + \rho_o c_\varepsilon T\, \gamma_{LM} \right] \varepsilon_{LM} +$$

$$+ \frac{1}{2} V_o \sum_{LM} \sum_{NK} \left[C_{LMNK} - T \frac{\partial}{\partial T} C_{LMNK} \Big|_{\underline{\underline{\varepsilon}}} \right] \varepsilon_{LM}\, \varepsilon_{NK} \tag{2.11}$$

The first terms in the brackets come from the strain derivatives of the Helmholtz energy; the second terms come from the corresponding derivatives of entropy.

The quantity

$$\frac{1}{3}\,\mathrm{Tr}\left(\underline{\underline{\tau}} + \rho_o c_\varepsilon T\,\underline{\underline{\gamma}}\right) = -P + \frac{\alpha_P T}{\kappa_T} = \left.\frac{\partial U}{\partial V}\right|_T \qquad (2.12)$$

is sometimes termed "internal pressure".

The tensor

$$\underline{\underline{\sigma}} = \underline{\underline{\tau}} + \rho_o c_\varepsilon T\,\underline{\underline{\gamma}} \qquad (2.13)$$

we will call, by analogy, the "internal stress tensor." Concentrating on the second order term of (2.11), we have, more explicitly:

$$V_o C_{LMNK} = \left.\frac{\partial^2 A}{\partial \varepsilon_{LM}\,\partial \varepsilon_{NK}}\right|_{T,\ \varepsilon_{[LM,NK]}} =$$

$$= \left.\frac{\partial^2 U}{\partial \varepsilon_{LM}\,\partial \varepsilon_{NK}}\right|_{T,\ \varepsilon_{[LM,NK]}} - T \left.\frac{\partial^2 S}{\partial \varepsilon_{LM}\,\partial \varepsilon_{NK}}\right|_{T,\ \varepsilon_{[LM,NK]}} =$$

$$= \left.\frac{\partial^2 U}{\partial \varepsilon_{LM}\,\partial \varepsilon_{NK}}\right|_{T,\ \varepsilon_{[LM,NK]}} - T \left.\frac{\partial}{\partial T} C_{LMNK}\right|_{\underline{\underline{\varepsilon}}} \qquad (2.14)$$

It is interesting to explore the relative significance of internal energy and entropic contributions to the elastic coefficients, as expressed by eqn. (2.14).

Entropic effects are relatively unimportant if the dimensionless ratio

$$\left| \frac{1}{C_{LMNK}} \left(T \left. \frac{\partial C_{LMNK}}{\partial T} \right|_{\underline{\underline{\varepsilon}}} \right) \right| = \left| \left. \frac{\partial \ell n C_{LMNK}}{\partial \ell n T} \right|_{\underline{\underline{\varepsilon}}} \right| << 1 \qquad (2.15)$$

Temperature derivatives of the elastic coefficients at constant strain are not convenient to measure experimentally. For an isotropic solid, and under the condition that the reference (undeformed) state is characterized by an isotropic stress distribution, the criterion of eqn.(2.15) is transformed to (see Appendix A):

$$\left| \frac{1}{C_{LMNK}} \left(T \left. \frac{\partial C_{LMNK}}{\partial T} \right|_{P} + \frac{\alpha_P T}{\kappa_T} \left. \frac{\partial C_{LMNK}}{\partial P} \right|_{T} \right) \right| << 1 \qquad (2.16)$$

Consider the particular case of a uniform hydrostatic compression. The relevant elastic constant is

$$B = C_{11} + C_{22} + C_{33} + 2C_{23} + 2C_{31} + 2C_{12} \qquad (2.17)$$

If the individual elastic constants satisfy eqn.(2.16), then we must have

$$\left| \frac{1}{B} \left(T \left. \frac{\partial B}{\partial T} \right|_{P} + \alpha_P T \, B \left. \frac{\partial B}{\partial P} \right|_{T} \right) \right| << 1 \quad , \text{ or} \qquad (2.19)$$

$$\left| \frac{T}{\kappa_T} \left. \frac{\partial \kappa_T}{\partial T} \right|_{P} + \frac{\alpha_P T}{\kappa_T^2} \left. \frac{\partial \kappa_T}{\partial P} \right|_{T} \right| << 1$$

Consider now the case of a pure shear, e.g. perpendicular to z and in the direction x. The relevant elastic constant is

$$C_{3131} = C_{55} = \mu = G \qquad (2.20)$$

The criterion [eqn.(2.16)] takes the form

$$\left| \frac{T}{G} \left. \frac{\partial G}{\partial T} \right|_P + \frac{\alpha_P T}{\kappa_T} \frac{1}{G} \left. \frac{\partial G}{\partial P} \right|_T \right| << 1 \qquad (2.21)$$

A set of excellent experimental data, which permits direct evaluation of the left-hand side of criteria (2.19) and (2.21) for a typical polymer glass can be found in [42]. Using their measurements on glassy PMMA at T = 20°C, P = 1 atm and a frequency of 4 MHz, we obtain:

$$\alpha_P = 18.7 \cdot 10^{-5} K^{-1}, \quad \kappa_T = 1.70 \cdot 10^{-4} MPa^{-1}, \quad G = 1.88 \cdot 10^{3} \text{ MPa}$$

$$\left. \frac{\partial \kappa_T}{\partial P} \right|_T = -1.59 \cdot 10^{-7} MPa^{-2}, \quad \left. \frac{\partial \kappa_T}{\partial T} \right|_P = 2.16 \cdot 10^{-7} MPa^{-1} K^{-1}$$

$$\left. \frac{\partial G}{\partial P} \right|_T = 3.44 \quad , \quad \left. \frac{\partial G}{\partial T} \right|_P = -4.69 \text{ MPa } K^{-1}$$

whence:

$$\left| \frac{T}{\kappa_T} \left. \frac{\partial \kappa_T}{\partial T} \right|_P + \frac{\alpha_P T}{\kappa_T^2} \left. \frac{\partial \kappa_T}{\partial P} \right|_T \right| = 0.071 < 1 \qquad (2.22)$$

$$\left| \frac{T}{G} \left. \frac{\partial G}{\partial T} \right|_P + \frac{\alpha_P T}{\kappa_T} \frac{1}{G} \left. \frac{\partial G}{\partial P} \right|_T \right| = 0.14 < 1 \qquad (2.23)$$

Thus, criteria (2.19) and (2.21) are fulfilled for an amorphous polymer below its glass formation temperature, far from regions in which dynamic transitions are observed.

Our thermodynamic analysis has shown that, in a polymeric glass, the internal energy contribution to the elastic response to deformation is much more important than the entropic contribution. In the following we choose to concentrate on the internal energy contribution only.

2.2. STATISTICAL MECHANICAL CONSIDERATIONS

2.2.1. General Formulation

Consider a system of polymer chains within a cube of bulk amorphous polymer, of total volume V. For simplicity in the statistical mechanical description we impose periodic boundary conditions, forming the entire contents of the cube from a single vinyl "parent chain" of the type

$$R - CHR - (CH_2 - CHR)_{x-1} - R$$

where R is a substituent with no internal structure. (This representation is further discussed in chapter 3.)

A full microscopic description of the system in configuration space is given by specifying:

(a) The location of the chain start, $\underset{\sim}{r}_{C_o}$

(b) Three "Eulerian angles" $\underline{\psi} = (\psi_1, \psi_2, \psi_3)$, specifying the overall orientation of the "parent chain" with respect to a fixed frame of reference.

(c) All torsion angles $\underline{\phi} = (\phi_2, \phi_3, \ldots, \phi_{2x-1})$ of all skeletal bonds of the chain but the first and last.

(d) All bond lengths in the system. These are 6x-2 in number, and are collectively denoted by $\underline{\ell}$.

(e) All bond (valence) angles in the system. These are 10x-5 in number, and are collectively denoted by $\underline{\theta}$.

Variables $\underset{\sim}{r}_{Co}, \Psi$ are "external", while variables ϕ, $\underset{\sim}{\ell}$, $\underset{\sim}{\theta}$ are "internal." Variables $\underset{\sim}{r}_{C_o}$, Ψ , Φ are termed "soft," whereas variables $\underset{\sim}{\ell}$ and $\underset{\sim}{\theta}$ are termed "hard."
The total number of soft variables in the system is $N_s = 2x+4$; that of hard variables is $N_h = 16x-7$. The total number of atoms is $N = 6x-1 = 1/3(N_s+N_h)$.

To describe the system in momentum space one needs another 3N variables, so that the overall phase space of our system is (36x-6)-dimensional.

A detailed analysis of the partition function in a polymer system has been given by Gō and Scheraga [29]. According to their findings, motion associated with the soft degrees of freedom can be treated classically, whereas vibrational motion associated with the hard degrees of freedom must be treated quantum-mechanically.

Extending their single-chain analysis to the bulk polymer, we can write the most general ("exact") partition function of our system as:

$$Z = \left(\frac{1}{2 \pi \beta \hbar^2} \right)^{N_s/2} V \left(\sum_{k=1}^{N} m_k \right)^{3/2} \times$$

$$\times \int \left[\prod_{i=1}^{N_h} \left(\frac{\exp(-\beta \hbar \omega_i/2)}{1 - \exp(-\beta \hbar \omega_i)} \right) \right] \left[\frac{1}{\det(\underset{\sim}{G})} \right]^{1/2} \times \qquad (2.24)$$

$$\times \exp \left[-\beta \, U^{pot}(\Psi , \Phi) \right] \, d\Psi \, d\Phi$$

where $\beta = \frac{1}{k_B T}$

The first term in the above expression arises from the momentum integration of the soft variables, treated classically. The volume term comes from integrating out $\underset{\sim}{r}_{C_o}$,while the

term involving frequencies arises from the quantum treatment of the hard degrees of freedom. The quantity $U^{pot}(\Psi , \Phi)$ denotes the total potential energy as a function of Eulerian and torsion angles, with all hard variables kept fixed at their equilibrium positions. $\underline{\underline{G}}$ is a transformation matrix, depending on atomic masses and the system configuration. It arises during the transformation from a representation cast in terms of individual atom coordinates to a representation involving internal variables.
In our system,

$$(\underline{\underline{G}}^{-1})_{ij} = \sum_{k=1}^{N} \sum_{\alpha=1}^{3} m_k \frac{\partial r_{k,\alpha}}{\partial q_i} \frac{\partial r_{k,\alpha}}{\partial q_j} \qquad (2.25)$$

where m_k and $r_{k,\alpha}$ denote the mass and Cartesian coordinates of atom k, and $\underline{q} = [\Psi , \Phi]^T$ is the (N_s-3)-dimensional vector of Eulerian and rotation angles.

The thermodynamics of a multichain polymer system in equilibrium can be deduced, in principle, from the partition function, within the framework of the canonical ensemble. The Helmholtz energy, A, and the internal energy, U, are simply related to Z by:

$$A = - \frac{1}{\beta} \ln Z \qquad (2.26)$$

$$U = - \frac{\partial \ln Z}{\partial \beta} \qquad (2.27)$$

2.2.2 Harmonic Approximation

A polymer glass is not in thermodynamic equilibrium, so it cannot "freely" sample the entire configuration space. Chains have lost the ability to rearrange themselves within the time

scale of ordinary measurements. At temperatures $T \leq T_g - 20^{\circ}C$, which are of interest in this work, polymeric glasses are solids for all practical purposes. Characteristic times for volume relaxation are of the order of years ([7], p.387). Thermal motion consists predominantly of solid-like vibrations of atoms about their average equilibrium positions ([82], p.14), and mechanical response to small deformations is adequately described by linear elasticity ([77], p.108).

For the purpose of modelling this "solidlike," elastic response of a glass to deformation, we consider it as being "locked" in the vicinity of a local minimum of the total potential energy in configuration space. We symbolize that minimum as $U^{pot}_{min} = U^{pot}(\Psi_{min} , \Phi_{min})$. We assume that the glass "has no way of knowing" what happens outside the neighborhood of the minimum, and formulate a "quasi-thermodynamics" around this minimum, as we would do for a crystalline solid. Expanding the function $U^{pot}(\Psi , \Phi)$ around $(\Psi_{min} , \Phi_{min})$ to second order, we get:

$$U^{pot}(\Psi , \Phi) = U^{pot}_{min} + \underline{g}^{T}_{min} \begin{bmatrix} \Delta\Psi \\ \Delta\Phi \end{bmatrix} + \frac{1}{2} [\Delta\Psi^{T} \; \Delta\Phi^{T}] \; \underline{\underline{H}}_{min} \begin{bmatrix} \Delta\Psi \\ \Delta\Phi \end{bmatrix} \tag{2.28}$$

where $\Delta\Psi = \Psi - \Psi_{min}$, $\Delta\Phi = \Phi - \Phi_{min}$,

$\underline{g}_{min} = \underline{g} (\Psi_{min} , \Phi_{min})$ (gradient),

$\underline{\underline{H}}_{min} = \underline{\underline{H}} (\Psi_{min} , \Phi_{min})$ (Hessian).

By definition, $\underline{g}_{min} = \underline{0}$ and $\underline{\underline{H}}_{min}$ positive definite. From eqn. (2.28):

$$U^{pot}(\Psi, \Phi) = U^{pot}_{min} + \frac{1}{2} [\Delta\Psi^T \Delta\Phi^T] \underline{\underline{H}}_{min} \begin{bmatrix} \Delta\Psi \\ \Delta\Phi \end{bmatrix} \tag{2.29}$$

To formulate a local thermodynamics for the glass we assume that the entire contribution to the integral in (2.24) comes from the vicinity of (Ψ_{min} , Φ_{min}). Furthermore, we assume that $\underline{\underline{G}}$ and the frequencies ω_i do not vary very much with Ψ and Φ near this minimum, so that they can be taken out of the integration. Then, using eqn.(2.29), the integral in eqn.(2.24) reduces to a (N_s-3)-dimensional Gaussian integral, which readily gives ([49], p.310):

$$Z = \left(\frac{1}{2 \pi \beta \hbar^2} \right)^{N_s/2} V \left(\sum_{k=1}^{N} m_k \right)^{3/2} \times$$

$$\times \left[\prod_{k=1}^{N_h} \left(\frac{\exp(-\beta\hbar\omega_i/2)}{1 - \exp(-\beta\hbar\omega_i)} \right) \right] \left[\frac{1}{\det(\underline{\underline{G}}_{min})} \right]^{1/2} \times$$

$$\times \left(\frac{2\pi}{\beta} \right)^{\frac{N_s-3}{2}} \left[\frac{1}{\det(\underline{\underline{H}}_{min})} \right]^{\frac{1}{2}} \exp[-\beta U^{pot}_{min}] =$$

$$= \left[\frac{\sum_{k=1}^{N} m_k}{2 \pi \beta \hbar^2} \right]^{3/2} \left[\frac{1}{\beta \hbar} \right]^{N_s-3} \left[\frac{V^2}{\det(\underline{\underline{G}}_{min} \underline{\underline{H}}_{min})} \right]^{1/2} \times$$

$$\times \left[\prod_{k=1}^{N_h} \left(\frac{\exp(-\beta\hbar\omega_i/2)}{1 - \exp(-\beta\hbar\omega_i)} \right) \right] \exp[-\beta U^{pot}_{min}] \tag{2.30}$$

The last three factors of eqn.(2.30) incorporate all the spatial dependence of the partition function.

By eqns (2.26) and (2.27):

$$A = U^{pot}_{min} + \frac{1}{2\beta} \ln \left[\frac{\det(\underline{\underline{G}}_{min} \underline{\underline{H}}_{min})}{V^2} \right] - \tag{2.31}$$

$$- \frac{1}{\beta} \ln \left[\left(\frac{\sum_{k=1}^{N} m_k}{2 \pi \beta \hbar^2} \right)^{3/2} \left(\frac{1}{\beta \hbar} \right)^{N_s - 3} \right] + A_{vib}$$

$$U = U^{pot}_{min} + \left(N_s - \frac{3}{2} \right) \frac{1}{\beta} + U_{vib} \tag{2.32}$$

where

$$A_{vib} = - \frac{1}{\beta} \ln Z_{vib} \quad , \quad U_{vib} = - \frac{\partial \ln Z_{vib}}{\partial \beta} \tag{2.33}$$

$$Z_{vib} = \prod_{k=1}^{N_h} \left[\frac{\exp(-\beta \hbar \omega_i / 2)}{1 - \exp(-\beta \hbar \omega_i)} \right]$$

Let ξ be any space related quantity, such as volume, or a strain component. We concentrate on the derivatives

$\left. \frac{\partial U}{\partial \xi} \right|_T$ (internal pressure and internal stress tensor; compare eqn. (2.11)), and

$\left. \frac{\partial^2 A}{\partial \xi^2} \right|_T$ (bulk modulus of elasticity and isothermal compressibility; compare eqn. (2.14)).

From eqns (2.32) and (2.33) we have:

$$\left. \frac{\partial U}{\partial \xi} \right|_T = \left. \frac{\partial U^{pot}_{min}}{\partial \xi} \right|_T + \left. \frac{\partial U_{vib}}{\partial \xi} \right|_T \tag{2.34}$$

$$\left.\frac{\partial^2 A}{\partial \xi^2}\right|_T = \left.\frac{\partial^2 U^{pot}_{min}}{\partial \xi^2}\right|_T +$$

$$+ \frac{1}{2\beta}\frac{\partial}{\partial \xi}\left[\ln\left[\frac{\det(\underline{\underline{G}}_{min}\,\underline{\underline{H}}_{min})}{V^2}\right]\right]_T$$

$$+ \left.\frac{\partial^2 A_{vib}}{\partial \xi^2}\right|_T \qquad (2.35)$$

Equation (2.35) expresses the fact that only that part of the kinetic energy which is associated with the hard mode vibrations is spatially dependent. The contribution of the soft degrees of freedom, treated classically, amounts to an equipartition term [eqn.(2.32)], which does not depend on ξ.

Equation (2.35), which is actually an instance of the "quasi-harmonic approximation" ([75], p.141) applied to glassy amorphous polymers, breaks up an elastic constant into three terms.

The first term consists of a "potential energy contribution." It expresses how the energy of the minimum, to which our system is confined in configuration space, changes with changing the spatial extent and shape of the system.

The second term incorporates a "configurational entropy" contribution. It depends on the curvature ($\underline{\underline{H}}_{min}$) of the potential energy hypersurface around the minimum. It can be used to assess the importance of entropy effects on the elastic constants. Since our thermodynamic analysis showed that these effects are not significant, this term will be neglected in the following. This constitutes a "strict

harmonic approximation" ([75], p.148) for the soft degrees of freedom.

The third term expresses the volume- and strain-dependence of vibrational frequencies associated with the hard degrees of freedom.

By neglecting the configurational entropy term in equation (2.35) we are left only with potential energy and vibrational contributions in each of the eqns (2.34) and (2.35). The significance of vibrational contributions is examined in the next subsection for $\xi = V$.

2.2.3 Vibrational Contributions

The vibrational terms in eqns (2.34) and (2.35) could, in principle, be evaluated exactly by detailed consideration of all normal modes in our system. Such an exact treatment in a disordered multichain system would not be trivial (see [61], p.179, [47] for corresponding treatments in the crystalline phase.) Here we estimate the significance of hard mode vibrational contributions based on two limiting models that are frequently used for solid polymers: the Einstein model and the Debye model.

Each of these models assumes a specific distribution for the vibrational frequencies ω_i appearing in the vibrational partition function [eqn.(2.33)], thus permitting an analytical calculation of A_{vib} and U_{vib}.

According to the Einstein model ([8]),

$$\omega_i = \omega_o \quad , \qquad \Theta_E = \frac{\hbar\,\omega_o}{k_B} \tag{2.36}$$

According to the Debye model, frequencies follow a parabolic distribution

$$f(\omega) = \frac{9\,N_h}{\omega_{max}^3} \cdot \omega^2 \quad , \qquad \Theta_D = \frac{\hbar\,\omega_{max}}{k_B} \tag{2.37}$$

$$0 < \omega < \omega_{max}$$

In the following the generic symbol Θ is used to denote Θ_E or Θ_D in the case of the Einstein and the Debye model, respectively.

By a well known rule the Grüneisen parameter [compare eqn.(2.10)]

$$\gamma = - \frac{d\ \ell n\Theta}{d\ \ell nV} \tag{2.38}$$

is independent of volume within the temperature range of interest.

Both models lead to the Mie and Grüneisen equation of state, thought to be of wider validity ([8]) than each of the distributions (2.36) or (2.37):

$$P + \left.\frac{\partial U_{min}^{pot}}{\partial V}\right|_T = \gamma\,\frac{U_{vib}}{V} \tag{2.39}$$

Direct differentiation of eqn.(2.39), taking into account equations (2.10), (2.33), (2.36) to (2.38) gives:

$$B = \frac{1}{\kappa_T} = V \left.\frac{\partial^2 A}{\partial V^2}\right|_T = V \left.\frac{\partial^2 U^{pot}_{min}}{\partial V^2}\right|_T + \left.\frac{\partial U^{pot}_{min}}{\partial V}\right|_T +$$

$$+ P - \frac{\gamma^2}{V} \left(T C_{vib} - U_{vib} \right) \qquad (2.40)$$

where $$C_{vib} = \left.\frac{\partial U_{vib}}{\partial T}\right|_V \simeq \rho_o V c_\varepsilon$$

From equations (2.34), (2.39) and (2.10) the relative error committed in estimating $\left.\frac{\partial U}{\partial V}\right|_T$ by $\left.\frac{\partial U^{pot}_{min}}{\partial V}\right|_T$ (potential energy effects only) is:

$$\frac{\left.\frac{\partial U^{pot}_{min}}{\partial V}\right|_T - \left.\frac{\partial U}{\partial V}\right|_T}{\left.\frac{\partial U}{\partial V}\right|_T} = \frac{\left(\gamma \frac{U_{vib}}{V} - P\right) - \left(- P + \frac{\alpha_P}{\kappa_T} T\right)}{\left(- P + \frac{\alpha_P}{\kappa_T} T\right)}$$

$$= \frac{\gamma \frac{U_{vib}}{V} - \gamma \frac{C_{vib} T}{V}}{- P + \gamma \frac{C_{vib} T}{V}}$$

and, for ordinary pressures,

$$\frac{\left.\frac{\partial U^{pot}_{min}}{\partial V}\right|_T - \left.\frac{\partial U}{\partial V}\right|_T}{\left.\frac{\partial U}{\partial V}\right|_T} = \frac{U_{vib}}{C_{vib} T} - 1 \qquad (2.41)$$

From eqn.(2.35) after omission of the configurational entropy term, together with eqn.(2.39) and eqn.(2.40), the relative error in estimating B by

$$V \left. \frac{\partial^2 U^{pot}_{min}}{\partial V^2} \right|_T \quad \text{is:}$$

$$\frac{V \left. \frac{\partial^2 U^{pot}_{min}}{\partial V^2} \right|_T - B}{B} = - \frac{\frac{\gamma^2}{V} (T C_{vib} - U_{vib}) - \frac{\gamma}{V} U_{vib}}{B} \tag{2.42}$$

$$= - \frac{\gamma^2 C_{vib} T}{V B} \left[\frac{1 + \gamma}{\gamma} \frac{U_{vib}}{C_{vib} T} - 1 \right]$$

Equations (2.41) and (2.42) permit direct numerical evaluation of the relative error associated with neglecting vibrational contributions. For glassy atactic polypropylene, which is the polymer we are modelling in this work, values of the thermodynamic and mechanical properties at T = 233 K are (see also Chapter 5):

$\alpha_P = 2.5 \cdot 10^{-4}\ K^{-1}$ ([40], p.244; [81]; [71], p.60)

$B = \frac{1}{\kappa_T} = 3340$ MPa ([71], p.267)

$\rho_o = 892\ kg/m^3$ ([40], p.244)

$c_\varepsilon = 1320\ J/kg\ K$ ([71], p.86-89)

whence

$$\frac{C_{vib}}{V} = 1.177 \cdot 10^6\ J/m^3 K$$

$$\gamma = 0.71$$

For both models examined the quantity $\frac{U_{vib}}{C_{vib}\,T}$

is a known function of the ratio $\tilde{T} = \frac{\Theta}{T}$

For the Einstein model,

$$\frac{U_{vib}}{C_{vib}\,T} = \frac{e^{2\tilde{T}_E} - 1}{2\tilde{T}_E\, e^{\tilde{T}_E}} \quad , \quad \tilde{T}_E = \frac{\Theta_E}{T} \tag{2.43}$$

For the Debye model,

$$\frac{U_{vib}}{C_{vib}\,T} = \frac{\frac{3\,\tilde{T}_D}{8} + D(\tilde{T}_D)}{4\,D(\tilde{T}_D) - \frac{3\,\tilde{T}_D}{e^{\tilde{T}_D} - 1}} \quad , \quad \tilde{T}_D = \frac{\Theta_D}{T} \tag{2.44}$$

Values of the Debye function

$$D(x) = \frac{3}{x^3} \int_0^x \frac{z^3}{e^z - 1}\, dz$$

are tabulated in [1], p.998.

It temains to select appropriate values for Θ_E and Θ_D. Such values are obtained experimentally from low-temperature heat capacity data. According to Bondi ([7], p.398) most molecular, and especially polymeric glasses have a Θ_D of the order 120 K. Simha et al. [51] give experimental values of Θ_D and Θ_E for a variety of glassy amorphous polymers. In all cases the Debye temperature is lower than 120 K. We thus chose, for the purpose of a conservative estimate, to describe thermal vibrations in the glassy polymer by the characteristic temperatures:

$$\Theta_D = 120\ K\ , \qquad \Theta_E = \frac{3}{4}\,\Theta_D = 90\ K$$

Then $\tilde{T}_E = 0.386$ and $\tilde{T}_D = 0.515$, and, using the property values listed above, equations (2.41) to (2.44) give:

Einstein Model

$$\frac{\left.\frac{\partial U^{pot}_{min}}{\partial V}\right|_T - \left.\frac{\partial U}{\partial V}\right|_T}{\left.\frac{\partial U}{\partial V}\right|_T} = 0.025$$

$$\frac{V\left.\frac{\partial^2 U^{pot}_{min}}{\partial V^2}\right|_T - B}{B} = -0.060$$

Debye Model

$$\frac{\left.\frac{\partial U^{pot}_{min}}{\partial V}\right|_T - \left.\frac{\partial U}{\partial V}\right|_T}{\left.\frac{\partial U}{\partial V}\right|_T} = 0.027$$

$$\frac{V\left.\frac{\partial^2 U^{pot}_{min}}{\partial V^2}\right|_T - B}{B} = -0.061$$

Thus, the vibrational contribution to (2.34) and (2.35) is at most of the order 2.5% and 6%, respectively. The temperature considered in our simulations is sufficiently higher than the Debye temperature of the polymeric glass, so that the quantum nature of thermal motion associated with the hard

degrees of freedom has no profound influence on the properties of interest. In the following we choose to neglect the vibrational contribution altogether.

Our thermodynamic analysis permitted us to neglect entropic contributions and thus estimate derivatives of the Helmholtz energy using the corresponding derivatives of internal energy. Our statistical mechanical analysis now justifies using the total potential energy of the static structure in place of the internal energy. We thus replace eqns. (2.34) and (2.35) by the following, much simpler forms, which involve potential energy effects only:

$$\left.\frac{\partial U}{\partial \xi}\right|_T = \left.\frac{\partial U^{pot}_{min}}{\partial \xi}\right|_T \qquad \begin{array}{l}\text{(estimation of internal}\\ \text{pressure and stress)}\end{array} \qquad (2.45)$$

$$\left.\frac{\partial^2 A}{\partial \xi^2}\right|_T = \left.\frac{\partial^2 U^{pot}_{min}}{\partial \xi^2}\right|_T \qquad \begin{array}{l}\text{(estimation of}\\ \text{elastic coefficients)}\end{array} \qquad (2.46)$$

The considerations presented above, and the simplifications to which they lead, have been crucial in the development of a methodology for simulating structure and for predicting mechanical properties.

3. THE MOLECULAR MODEL

3.1. STUDIED POLYMER AND MODEL ASSUMPTIONS

The polymer we chose to study in this work is atactic polypropylene at 1 atm and -40°C. Several reasons contributed to this choice. The simple alkane structure of polypropylene permits the use of simple and well-known expressions for the potential energy of interatomic interactions. The atactic form ensures complete absence of crystallinity: atactic chains cannot crystallize, due to their irregular stereostructure; thus, model microstates arrived at through energy minimization are representative of a completely amorphous polymer (see chapter 4.) In addition, samples of atactic polypropylene of well defined configurational statistics can readily be obtained experimentally [59].

Some values of physical and mechanical properties of glassy atactic polypropylene available in the literature are summarized in Table 3.1. The model temperature is ca. 20°C below the glass formation temperature, T_g , of ca. -18°C. At this temperature interval below T_g polymeric glasses are solids for all practical purposes (compare introduction to section 2.2.2. and references cited there.) The density of a well-relaxed polypropylene glass at -40°C is ca. 0.892 g/cm^3.

Our molecular model rests on the following assumptions:

A. The model does not incorporate thermal motion, i.e. it is static. Temperature enters only indirectly, through specification of the density in the undeformed state.

B. The glassy polymer is pictured in configuration space as an ensemble of mutually inaccessible states of microscopic liquid disorder. Estimates of the macroscopic properties are obtained by arithmetic averaging over the individual microstates. Each undeformed microstate, as well as all deformed states obtained from it, satisfy the requirements of detailed mechanical equilibrium.

C. Bond lengths and bond angles are kept fixed. Molecular rearrangement can occur exclusively through rotation (torsion) around skeletal bonds.

D. Backbone carbons and pendant hydrogen atoms are treated explicitly, whereas methyl groups are lumped into single "quasi-atom" entities.

E. In predicting mechanical properties entropic contributions to the elastic coefficients are neglected. Only potential energy effects are considered.

F. We concentrate on the purely elastic response to deformation. Viscoelastic phenomena associated with relaxation or flow are not considered. Thus chain slippage is avoided, i.e. each deformed microstate must be structurally similar to the deformed microstate from which it came.

Assumptions A and B find justification in the thermodynamic and statistical mechanical considerations we presented in chapter 2. According to equations (2.45) and (2.46) the relevant quantity is the total potential energy U^{pot}_{min} of a local minimum in configuration space. It is the changes in this quantity that we have to monitor as a function of deformation in order to predict the mechanical properties.

Table 3.1 : Physical Properties of Amorphous Glassy Polypropylene

	PROPERTY	VALUE or Equation	SOURCE
1.	Density, ρ (kg/m^3)	$\frac{10^3}{\rho} = 1.05062 + 0.0003036\ T$ with T in K, whence ρ (-40°C) = 892 kg/m^3	Experimental curve,[40], p. 294 (temperature range -18.8°C to -70°C)
2.	Thermal expansion coefficient, α_p (K^{-1})	α_p (-40°C) = $2.7 \cdot 10^{-4}$ K^{-1} α_p (-40°C) = $2.51 \cdot 10^{-4}$ K^{-1} $\alpha_p = 2.0 \cdot 10^{-4}$ K^{-1}	Exp.,[40], p. 244 (atactic glassy PP) Exp.,[81], 18% crystallinity, prob. isotactic Deduced from exp. value given in [71] p. 60 (glassy PP)
3.	Glass transition temperature, Tg(°C)	-10°C -8°C to -20°C -20°C -18°C	Exp., [59] (equilibrium epimerized polypropylene, extrapolated to zero cooling rate) Exp., [53] (NMR linewidth measurements for the investigation of molecular motion in atactic PP) Exp., [9], p. 8 (atactic PP) Exp.,[10], p. V-23 Exp.,[40], p. 244
4.	Bulk modulus of elasticity, $B = \frac{1}{\kappa_T}$	3500 MPa $\frac{1}{\kappa_T}$ (-40°C) = 3340 MPa	[71], p. 271. Exp. value for semicrystalline PP, expected to be a fairly good estimate for the amorphous glassy polymer Estimated by Schuyer Correlation, [71], p. 267
5.	Young's modulus of elasticity E (MPa)	E(-40°C) = 2650 MPa	[50] (Measurements on amorphous PP at audio frequencies, $\bar{M}w = 3 \cdot 10^5$, 0% crystallinity)
6.	Shear modulus G(MPa)	G(-40°C) = 970 MPa	Value calculated for consistency with above B and E values
7.	Poisson's ratio ν	0.37 0.33	Based on above reported B and E values [77], p. 111 - typical value for glasses
8.	Cohesive energy density $(\frac{E_{coh}}{V})$ J/m^3	$2.83 \cdot 10^8 - 3.54 \cdot 10^8$ J/m^3 $2.90 \cdot 10^8$ J/m^3	Exptl.,[71]; lower value more reliable Calculated by Van Krevelen group contribution method,[71], p. 137

Assumption A reflects the fact that we focus on the atomic positions of static mechanical equilibrium, as one would do in a crystal. By thus stripping the system of its thermal motion (and introducing only a "mean field" temperature,) we achieve a dramatic reduction in the degrees of freedom. Alternatively, a full simulation of the system, in both configuration and momentum space, could be attempted by molecular dynamics; with the present computational capabilities, however, dynamic simulations could only cover an exceedingly short time span, and one could not depart significantly from the vicinity of the initial guess structure.

Our molecular model follows Cohen and Turnbull's [68] concept of glasses being in a state of frozen-in liquid disorder. By "detailed mechanical equilibrium" we mean that the sum of all forces and all torques exerted on each atom or bond of our microscopic structures is zero. Assumption B, i.e., the requirement that the modelled microstates be in nechanical equilibrium (at local minima of the total potential energy) should not be interpreted as implying thermodynamic equilibrium (a minimum of the Helmholtz energy of the macroscopic system under constant temperature and volume would be required for this.) Each structure generated in our investigation is only one microstate, and the microstates do not comprise an equilibrium ensemble.

Assumption C follows directly from our analysis of the vibrational contributions associated with the hard degrees of freedom (section 2.2.3.) The content of this assumption is the essence of the "strophon" concept. From the computational standpoint this is a very useful assumption: Freezing the hard degrees of freedom reduces the number of variables needed to describe the system in configuration space by a factor of nine. Assumption D is also a computational expedient.

Assumption E is a consequence of our thermodynamic analysis of entropic contributions (section 2.1.)

Assumtion F leads us to consider only very small degrees of deformation for the prediction of the mechanical properties of interest. According to a rule of thumb [77] polymeric glasses are linearly elastic up to deformations of approximately 1%. In this work I limit myself to deformations considerably smaller than that.

In general, our assumptions have been designed so as to give a model which is realistic, and at the same time tractable with available computational resources.

3.2. MOLECULAR GEOMETRY AND POTENTIALS

In the undeformed state, the system we are considering in our simulations is a cube of glassy atactic polypropylene filled with segments of macromolecular chains at a density corresponding to the experimental density of the polymer. To eliminate problems associated with boundaries we introduce "periodic boundary conditions," a trick frequently encountered in molecular dynamics simulations. Our cube is imagined to be part of an "infinite polymeric medium." Given an atom $\underline{1}$ within the cube, all images generated from $\underline{1}$ by any combination of translations along the edge (or "continuation") vectors $\underline{a}_x$, $\underline{a}_y$, $\underline{a}_z$ belong to the infinite medium and, conversely, all atoms of the medium can be generated from atoms in the cube by such a combination of translations. Thus, our cube

plays the role of a "unit cell," by repetition of which "ad infinitum" we can fill space with polymer. This is not a bad representation for an amorphous material, provided that the dimensions of our cube are large compared to the range of interatomic interactions [66].

As a consequence of periodic boundary conditions, if a chain belonging to the cube crosses one of its faces, there will be an identical chain entering the cube through the opposite face. Thus, we can form the whole contents of the cube from a limited number of parent chains, by placing one of their ends in the cube, truncating and periodically displacing at each intersection with the boundaries, until the other end is reached. In this work we chose to use a single, finite linear parent chain to create our system. There are exactly two chain ends in the cube. The infinite polymeric medium to which the cube belongs consists entirely of displaced images of the same chain. The use of finite parent chains permits a clear-cut distinction between intermolecular and intramolecular quantities. On the other hand, mapping the entire system onto a single parent chain permits an elegant formulation of the computational problems addressed in this work. Periodic boundary conditions and the role of a parent chain are illustrated in Fig.3.1.

Our parent chains have the simple vinyl constitution

$$CH_3\text{-}CHR\text{-}(CH_2\text{-}CHR)_{x-1}\text{-}CH_3 \qquad (3.1)$$

The substituents R are methyl groups. These, together with the terminal methyls, are modelled, according to our assumptions, as single entities. A chain of degree of polymerization x has 2x skeletal bonds, 2x-1 skeletal carbons and 2 skeletal (terminal) methyls. It has (x-1) dyads [26], of which (x-3) are subject to (<u>meso</u>- or <u>racemo</u>-) diastereoisomerism, 2x-2

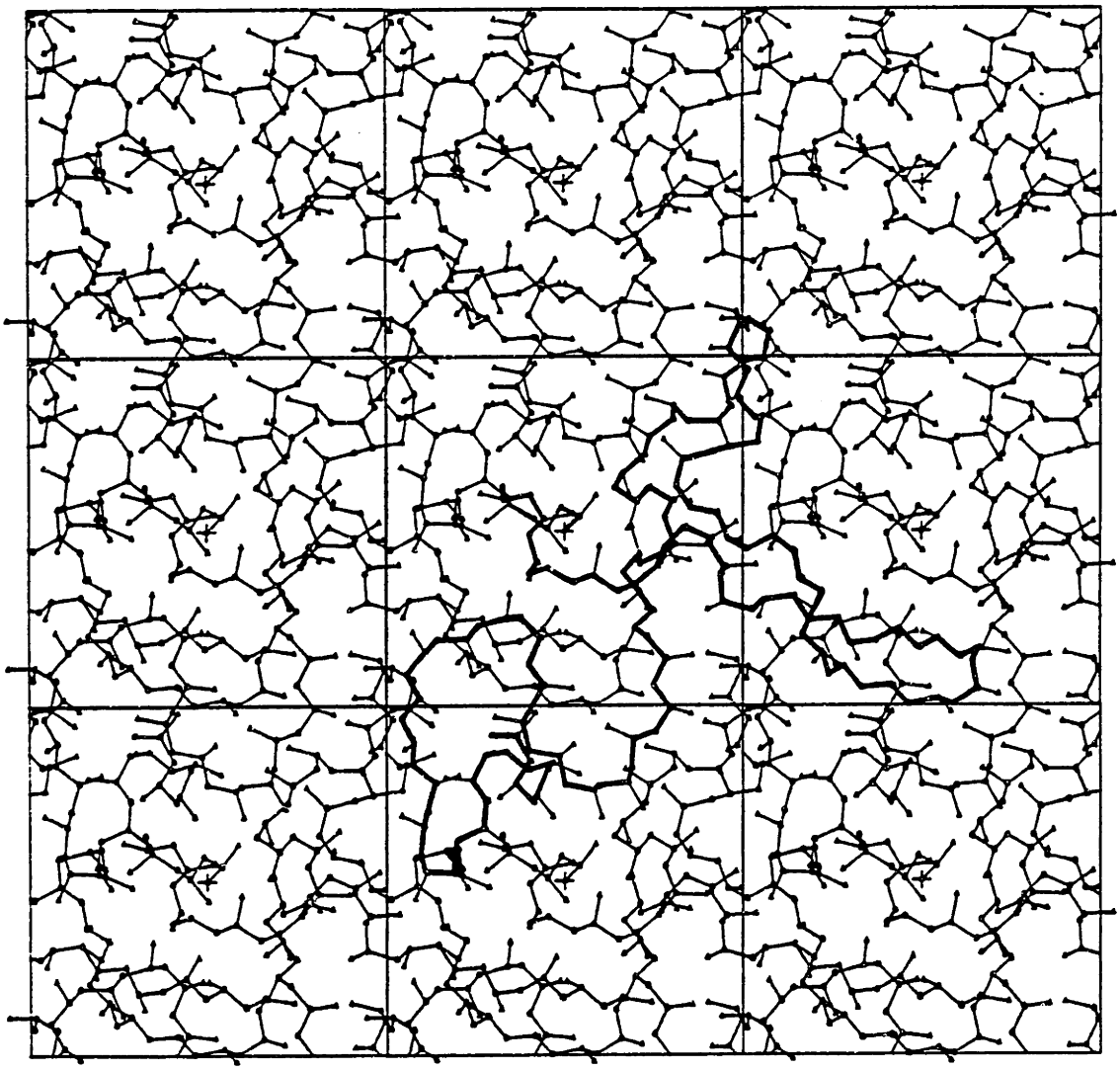

Figure 3.1

A model structure in the cube (center) and eight of its neighboring images, projected on the xy-plane. The parent chain is traced with a bold line. All carbon atoms (including methyl carbons) are indicated; hydrogen atoms are omitted for clarity

hydrogens attached to achiral skeletal carbons, x hydrogens and x methyl substituents attached to chiral skeletal carbons. The total number of interacting groups (C,H,R) is 6x-1. The size of the cube and the length of the parent chain are simply related through the polymer density as follows:

$$V = \underset{\sim}{a}_x \cdot (\underset{\sim}{a}_y \times \underset{\sim}{a}_z) = \frac{1}{\rho\, N_L} \{(M_R+3M_H+2M_C)\, x + (2M_R-2M_H-M_C)\} \quad (3.2)$$

where N_L, M_H, M_C, M_R denote the Avogadro number, the atomic weights of hydrogen and carbon, and the molecular weight of the methyl group. Computer time considerations limited the size of our parent chain to x = 76 monomeric units. The cube has then edges 18.15 Å long. This size is large enough to satisfy the "minimum image convention" ([66]). A total of 455 interacting atoms and groups are present in the cube.

With the assumptions introduced in section 3.1., the state of the system is completely defined if one specifies:

(i) the three edge vectors, $\underset{\sim}{a}_x$, $\underset{\sim}{a}_y$, $\underset{\sim}{a}_z$, of the cube

(ii) the tacticity (configuration) of the parent chain

(iii) three "Eulerian angles", ψ_1, ψ_2, and ψ_3, describing the orientation of the parent chain with respect to the frame of reference of the cube (compare section 2.2.)

(iv) the 2x-2 torsion angles ϕ_i of all skeletal bonds of the parent chain, but the first and last (conformation of the chain.)

The precise definition of the Eulerian and torsion angles in this work is explained in Appendix C, Figs C.1 and C.2.

The 2x+1 - dimensional vector

$$[\ \psi_1,\ \psi_2,\ \psi_3,\ \phi_2,\ \phi_3,\ \ldots,\ \phi_{2x-1}\ ] \equiv [\ \underline{\Psi}\ ,\ \underline{\Phi}\ ] \qquad (3.3)$$

we will call collectively the "vector of microscopic degrees of freedom" of the system.

Notice that the coordinates of the chain-start do not constitute degrees of freedom, because the system structure is invariant under translation of the cube along its edge vectors. Due to the periodicity of the infinite medium, we can choose any point within the cube as the start of the parent chain, $\underline{r}_{C_o}$, without affecting the total potential energy "enclosed" by the cube. On the contrary, Eulerian angles affect the periodic continuation and thus are degrees of freedom, contrary to what would happen in the case of an isolated single chain.

The geometrical parameters of the chain employed in this simulation have been used in earlier calculations [57]; the notation is explained in Fig.3.2 , and values are summarized in Table 3.2.

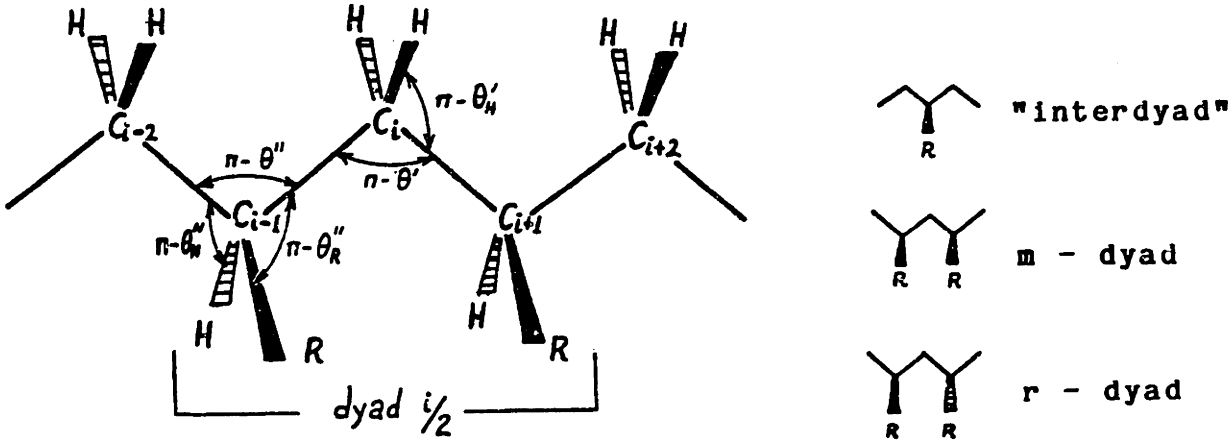

Figure 3.2 : Geometric parameters of a vinyl chain, and explanation of dyad types

Table 3.2

Molecular Geometry and Potential Parameter Values

Bond Lengths (Å)

C - C $\quad \ell = 1.53$

C - H $\quad \ell_H = 1.10$

C - R $\quad \ell_R = 1.53$

Bond Angle Supplements (degrees)

Intradyad C - C - C $\quad \theta' = 66$

Interdyad C - C - C $\quad \theta'' = 68$

Intradyad C - C - H $\quad \theta'_H = 71$

Interdyad C - C - R $\quad \theta''_R = 68$

Interdyad C - C - H $\quad \theta''_H = 73.2 = \cos^{-1}\left(\sqrt{\frac{1}{3}}\,(1-2\cos\theta'')\right)$

i	Atom or Group	Van der Waals radius (Å) r_i°	Polarizability (Å^3) α_i	Effective Number of Electrons $N_{e,i}$
1	H	1.3	0.42	0.9
2	C	1.8	0.93	5.0
3	R(methyl)	2.0	1.77	7.0

In calculating the total potential energy of nonbonded interatomic interactions, pairwise additivity is assumed. Each atom (C, H, or R) in the system acts as a site of interaction, and no distinction is made between pairs of sites belonging to the same, or to different chains. A finite range modification of the Lennard-Jones potential function is used, in which the full potential tail is substituted by a quintic spline:

$$U^{NB}(r) \begin{cases} = U^{LJ}(r) = 4\varepsilon\left\{\left(\frac{\sigma}{r}\right)^{12} - \left(\frac{\sigma}{r}\right)^{6}\right\}, & r < R_1 \\ = \varepsilon(1-\xi)^3\left\{\frac{U_1^{LJ}}{\varepsilon} + \left(3\frac{U_1^{LJ}}{\varepsilon} + \Delta\frac{U_1'^{LJ}}{\varepsilon/\sigma}\right)\xi + \right. & \\ \left. + \left(6\frac{U_1^{LJ}}{\varepsilon} + 3\Delta\frac{U_1'^{LJ}}{\varepsilon/\sigma} + \frac{\Delta^2}{2}\frac{U_1''^{LJ}}{\varepsilon/\sigma^2}\right)\xi^2\right\}, & R_1 < r < R \\ = 0, & R < r \end{cases} \quad (3.4)$$

where U_1^{LJ}, $U_1'^{LJ}$, and $U_1''^{LJ}$ stand for the value, the first and the second derivative of the Lennard-Jones function at the junction point $r = R_1$, $\Delta = (R-R_1)/\sigma$, $\xi = (r-R_1)/(R-R_1) = (r/\sigma - R_1/\sigma)/\Delta$.

Expression (3.4) is designed so that the functions

$$U^{NB}, \quad \frac{dU^{NB}}{dr}, \text{ and } \frac{d^2U^{NB}}{dr^2}$$

are continuous in the entire range of r, and assume values of zero at $r > R$.

The parameters σ_{ij} and ε_{ij} of the Lennard-Jones potential were calculated, for each of the six types of site pairs (i,j) present in our system, from literature ([7], [57]) values for atomic polarizabilities α_i, effective numbers of electrons, $N_{e,i}$, and Van der Waals radii, r_i^o, all listed in Table 3.2. The formulae used are:

$$c_{ij} = 365 \frac{\alpha_i \quad \alpha_j}{\left[\left(\frac{\alpha_i}{N_{e,i}} \right)^{1/2} + \left(\frac{\alpha_j}{N_{e,j}} \right)^{1/2} \right]} \qquad (3.5)$$

with α_i in Å^3, c_{ij} in kcal mol^{-1} Å^6 (Slater-Kirkwood formula for the description of London dispersion forces [7])

$$a_{ij} = \frac{1}{2} c_{ij} \left(r_i^o + r_j^o \right)^6 \qquad (3.6)$$

(empirical repulsion term)

$$\sigma_{ij} = \left(\frac{a_{ij}}{c_{ij}} \right)^{1/6} = \frac{1}{2^{1/6}} \left(r_i^o + r_j^o \right) \qquad (3.7)$$

$$\varepsilon_{ij} = \frac{c_{ij}^2}{4\, a_{ij}} \qquad (3.8)$$

In the calculations described in this thesis, two versions of the non-bonded potential energy function $U^{NB}(r)$ [eqn. (3.4)] are employed:

(i) the "full potential", with $R_1 = 1.45\ \sigma$ and $R = 2.30\ \sigma$, which reproduces the shape of the Lennard-Jones curve $U^{LJ}(r)$ very accurately

(ii) the "soft sphere potential", with $R_1 = 0.94\ \sigma$ and $R = 1.04\ \sigma$, which accurately reproduces the repulsive part of the Lennard-Jones, but has no attractive part.

The energy and force curves corresponding to the above two versions of $U^{NB}(r)$ are plotted in Fig. 3.3.

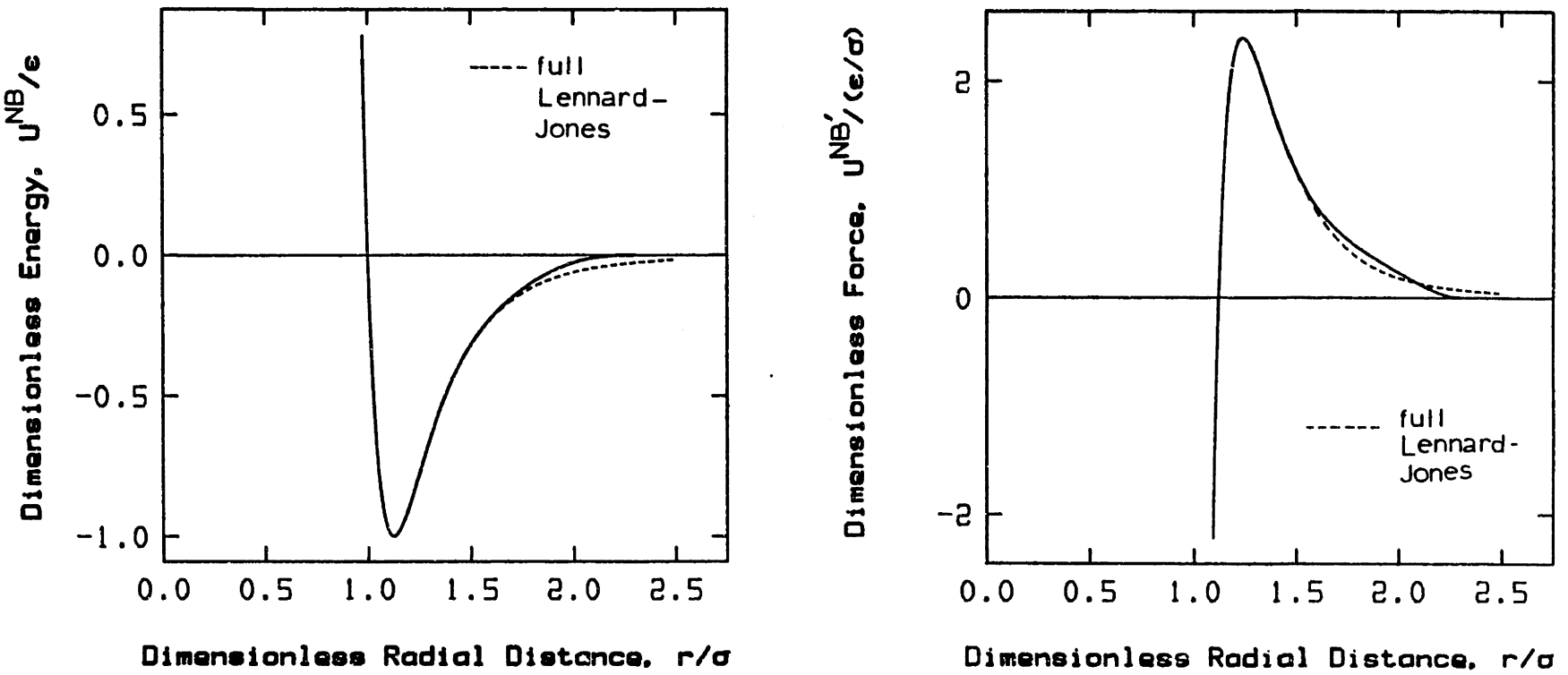

FULL POTENTIAL : $R_1/\sigma = 1.45$, $R/\sigma = 2.30$

Figure 3.3 : Dimensionless nonbonded interatomic interaction energy and force curves for the two types of potential used in this work

(a): Full Potential

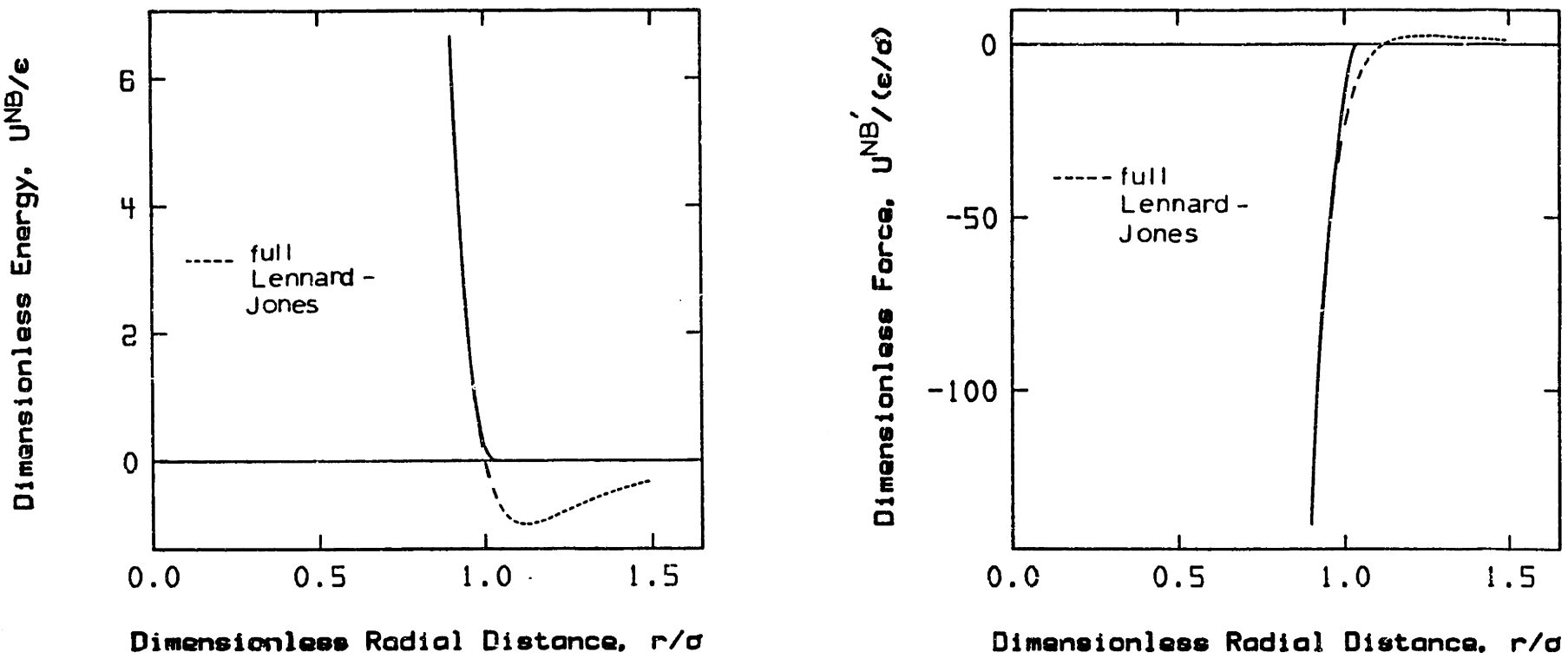

SOFT SPHERE POTENTIAL : $R_1/\sigma = 0.94$, $R/\sigma = 1.04$

Figure 3.3 : Dimensionless nonbonded interatomic interaction energy and force curves for the two types of potential used in this work

(b): Soft Sphere Potential

In addition to the nonbonded interactions, there is an intrinsic rotational potential associated with skeletal bond angle torsion. The origin of this potential is quantum mechanical ([26], p.54). It is modelled here by the standard symmetric threefold expression:

$$U_{\phi}(\phi) = \frac{k_{\phi}}{2} \quad (1 - \cos 3\phi) \qquad (3.9)$$

where ϕ is the bond torsion angle, measured from the trans - position using Flory's conventions (Fig.C.2), and the barrier height $k_{\phi} = 2.8$ kcal/mol

The three-dimensional periodicity, which characterizes our model system, gives rise to some interesting geometrical problems. Given two atoms, 1 and 2, within the primary cube, there is a total of 27 images of 2 (including the original) in the primary cube and the cubes immediately surrounding it, with which 1 may interact. If one chooses the cube size large enough [66], in comparison to the range of interatomic forces, then, for all possible locations of 1 and 2, there is at most one image of 2 with which 1 can interact (minimum image convention). In computing the energy of nonbonded interatomic interactions one needs an algorithm that can efficiently locate the minimum image. In the course of this thesis we developed and implemented new algorithms, of our own construction, to solve this and related geometrical problems. Our algorithms, unlike previous algorithms, remain valid in the case of deformed systems, where the continuation geometry is no longer cubic; i.e., they are applicable to the case of a periodic box shaped like an arbitrary parallelepiped. Details are given in [66].

3.3. GENERATION OF AN UNDEFORMED MODEL STRUCTURE

According to our assumptions, the glassy polymer will be simulated by an ensemble of static microscopic structures (states) that satisfy the conditions of detailed mechanical equilibrium. A model structure satisfying these conditions can only be obtained by an iterative process that starts with an appropriately chosen initial guess. Hence, two stages, examined separately in the following, can be identified in the generation of a realistic model structure:

(i) the creation of an initial guess structure

(ii) the "relaxation" of this structure to a state of minimal total potential energy

3.3.1. The Initial Guess

According to Flory's well-established "random coil hypothesis" ([25], p.602) chain conformation in the amorphous bulk is essentially similar to the conformation of chains in a solvent under Θ-conditions. The term "Θ-conditions" designates a state under which the tendency of a chain to expand, due to mutual interference of its segments, is compensated by a tendency to shrink due to interactions with neighboring (solvent) molecules. As a result, a Θ-chain appears "unperturbed" by long-range interactions, i.e., it behaves statistically as if it could cross itself (zero excluded volume, "phantom chain".) In a Gaussian approximation, the chain would be a self-intersecting random walk. Accepting the view that glasses are in a state of frozen-in liquid disorder also implies that the conformational statistics of the constituent chains are not too different from those of unperturbed macromolecules.

A satisfactory initial guess for our simulation could then be obtained by "random" generation of an unperturbed parent chain, and subsequent use of this chain to fill our cube to the correct density. Monte-Carlo generation of single unperturbed chains involves the generation of:

(i) a chain configuration, i.e. a dyad tacticity sequence.

(ii) a chain conformation, i.e. a sequence of rotation angles, ϕ.

In equilibrium atactic polypropylene, which we chose to model here, the configurational statistics are almost Bernoullian ([58]), with a fraction of meso-dyads equal to $w_m = 0.48$ ([58], [59]). Thus, the random generation of conformations is straightforward.

The conformational statistics of unperturbed chains are well described by the Rotational Isomeric State Theory (RIS theory, [26], [28]). This theory provides a quantitative treatment of short-range interactions. It rests on a discretization of conformation space into a finite set of rotational states. On the basis of this discretization one can compute the a' priori probabilities $p_{\xi;i}$ (bond i in state ξ), as well as the conditional probabilities $q_{\zeta\xi;i}$ (bond i in state ξ, given bond i-1 in state ζ) for all bonds in the chain. The probabilities $p_{\xi;2}$ and $q_{\zeta\xi;i}$ ($3 \leq i \leq 2x-1$) define an "equivalent Markov process", usable for the Monte-Carlo generation of correctly weighed unperturbed single chain conformations. A successful five state RIS model for polypropylene, developed by Suter and Flory [57], was used here for the generation of our parent chains. Details of the conformation generation are provided in Appendix B.

If we try to fill our cube with unperturbed chains, generated with the scheme described above, we discover that the structures obtained are characterized by excessively high energies (order of 10^{12}- 10^{15} kcal/mol) and by a very nonuniform spatial distribution of segments (see Fig. 3.4). The reason for this is that the generation procedure incorporates no information about long-range interactions, which are severe at these densities. A parent chain may be optimized with respect to short-range interactions, but when put in the cube it is not prevented from copiously intersecting itself. This does not contradict the "random coil" hypothesis; chains in the bulk are <u>on the average</u> similar to chains under Θ-conditions, but this does not mean that <u>any</u> Θ-chain can generate an appropriate space-filling model of the polymer under arbitrary periodic conditions.

Long-range interactions must be accounted for in order to obtain a realistic initial guess. To do this, we developed the following scheme:

- We choose the Eulerian angles (ψ_1, ψ_2 and ψ_3) arbitrarily and generate the chain in a bond-by-bond fashion within the cube, observing periodic boundary conditions whenever a bond-border intersection occurs.

- At each step of the conformation generation we modify the rotational isomeric state conditional probabilities $q_{\zeta\xi;i}$ using the formula:

$$q'_{\zeta\xi;i} = q_{\zeta\xi;i} \frac{\exp\left[-\frac{\Delta U^{LR}_{\xi;i}}{R\,T}\right]}{\sum_{\xi'} q_{\zeta\xi';i} \exp\left[-\frac{\Delta U^{LR}_{\xi';i}}{R\,T}\right]} \qquad (3.10)$$

where $\Delta U^{LR}_{\xi;i}$ is the increase in long-range interaction energy upon addition to the cube of the skeletal carbon i+1 and the substituents of carbon i, if bond i is assigned the rotational state ξ.

By "long range interactions" we mean nonbonded interactions between centers that are five or more bonds apart in the same chain, or belong to different chains. Flory's convention is used for the indexing of skeletal atoms (see [26], and Appendices B, C.)

The scheme proposed in eqn. (3.10) correctly blends short-range interaction energy (implicitly contained in an exponential form within the $q_{\zeta\xi;i}$ of the RIS model) with long-range interaction energy; i.e. it is a factorization of the full conformation partition function of the system into short- and long-range terms, a pair of terms assigned to each bond. Note, however, that the rotational isomeric state treatment of short-range interactions is truly bidirectional (or "equivalent" Markov, see Appendix B), while the treatment of long-range interactions is only unidirectional (or true Markov), since we cannot anticipate overlaps with segments to be generated in the future.

Using the modified conditional probabilities $q'_{\zeta\xi;i}$ we can generate initial guesses which do not depart very much from the "random coil hypothesis," have a rather uniform spatial distribution of segments, and are of relatively low energy (order of 10^6 - 10^8 kcal/mol, due almost entirely to long-range interatomic interactions.) Thus, the hybrid scheme (3.10) satisfactorily solves the problem of obtaining a good initial guess (see Fig.3.5.)

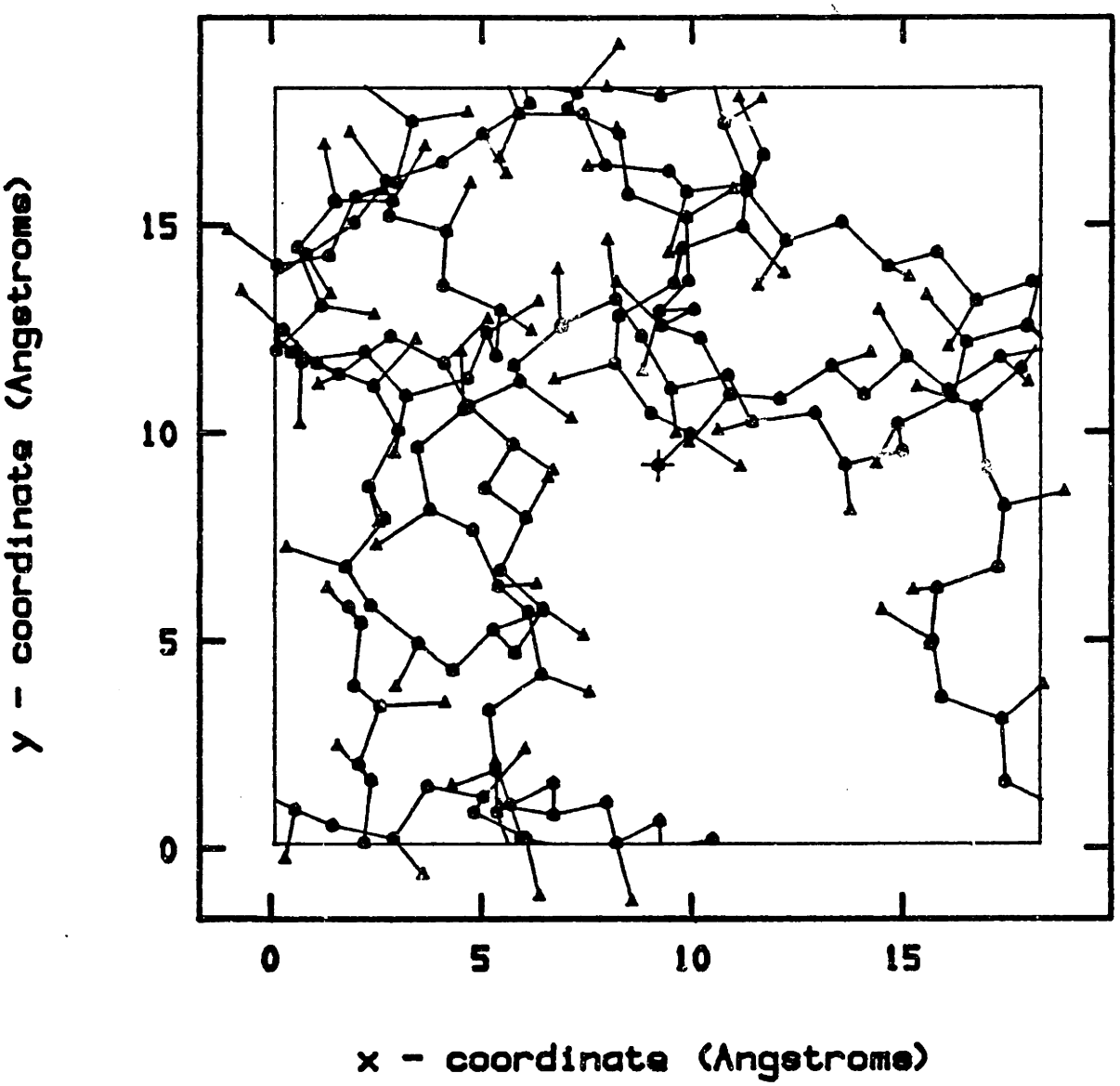

Figure 3.4

The xy-projection of an initial guess structure generated from an "unperturbed" parent chain. Skeletal carbon atoms are shown as circles, methyl carbons as triangles, and hydrogen atoms are omitted for clarity.

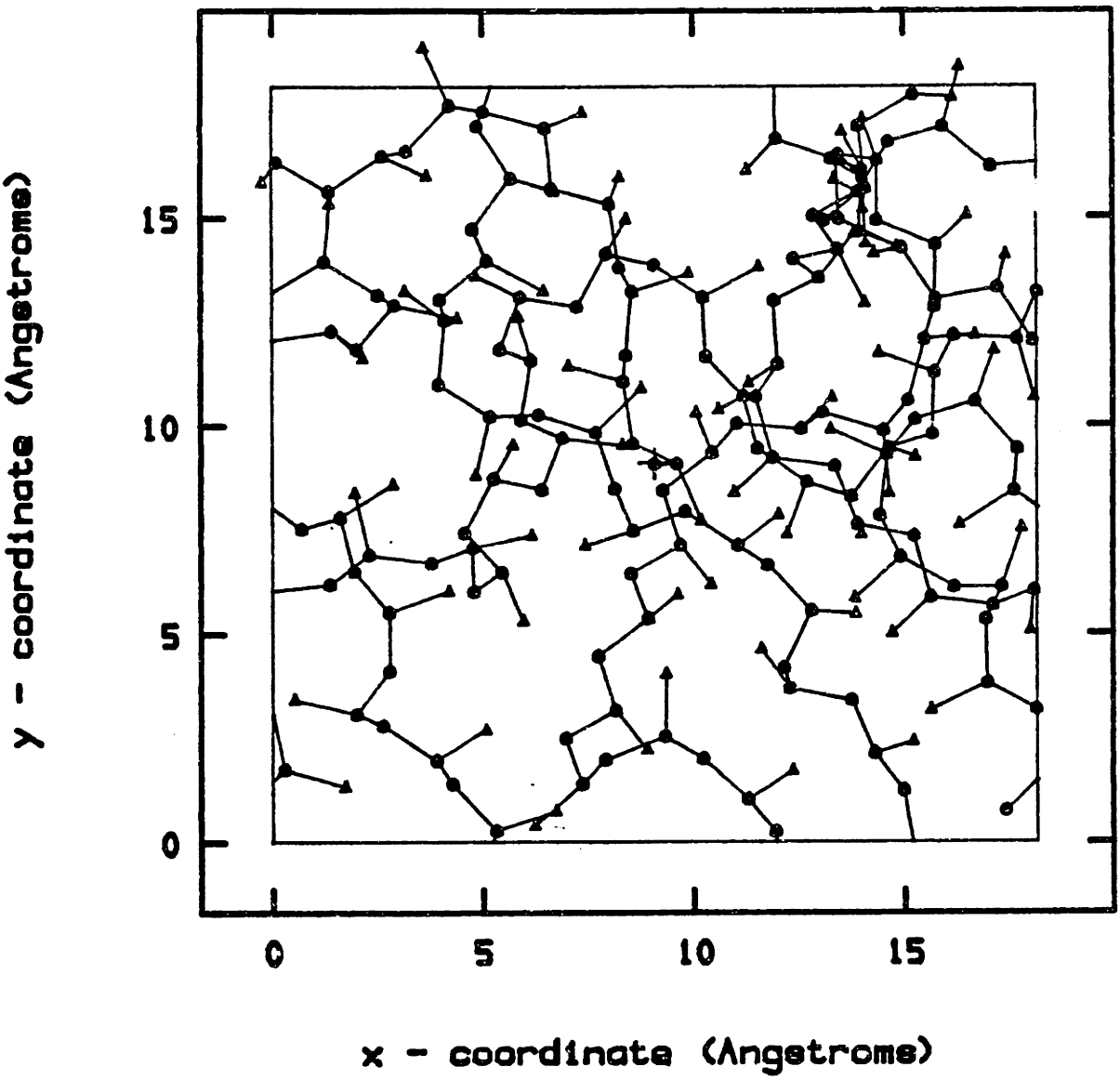

Figure 3.5

The xy-projection of an initial guess structure generated by the "hybrid scheme" of eqn. (3.10), incorporating long-range interactions. Compare with Figure 3.4.

3.3.2. The Relaxation to Mechanical Equilibrium

Each initial guess structure is subjected to a straightforward total potential energy minimization, to reach a microscopic structure that satisfies the conditions of detailed mechanical equilibrium. The total potential energy U^{pot} is the sum of all bond intrinsic rotational potentials and all nonbonded interaction potentials, computed according to the minimum image convention. The structures in mechanical equilibrium are defined by minima of the total potential energy with respect to the 2x+1 = 153 microscopic degrees of freedom ψ_1, ψ_2, ψ_3, ϕ_2, ϕ_3, ..., ϕ_{2x-1}. Because of its high dimensionality and nonlinearity the relaxation problem demands a very carefully planned method of attack.

Some key elements of the computational strategy employed are described in the following:

A. The 2x+1 Eulerian and rotation angles were directly used as variables in an unconstrained minimization problem. A formulation in terms of the individual atom coordinates would involve almost nine times as many variables, and would convert the problem to a constrained minimization, which is computationally much harder.

B. Analytical expressions were derived for the total potential energy function, its first and second derivatives with respect to the microscopic degrees of freedom, with proper consideration of the periodic boundary conditions. These derivations are presented in considerable detail in Appendix C. With our choice of potentials the objective function

$$U^{pot}(\psi, \phi) \equiv U^{pot}(\psi_1, \psi_2, \psi_3, \phi_2, \phi_3, \ldots, \phi_{2x-1}) \qquad (3.11)$$

its gradient

$$\underline{g}\ (\underline{\psi},\ \underline{\phi}) \equiv \left[\ \frac{\partial U^{pot}}{\partial \psi_1}\quad \frac{\partial U^{pot}}{\partial \psi_2}\quad \frac{\partial U^{pot}}{\partial \psi_3}\quad \frac{\partial U^{pot}}{\partial \phi_2}\ \cdots\ \frac{\partial U^{pot}}{\partial \phi_{2x-1}}\ \right]^T \tag{3.12}$$

and the Hessian matrix of second derivatives

$$\underline{\underline{H}}\ (\underline{\psi},\ \underline{\phi}) \equiv \begin{bmatrix} \dfrac{\partial^2 U^{pot}}{\partial \psi_i\ \partial \psi_k} & \dfrac{\partial^2 U^{pot}}{\partial \psi_i\ \partial \phi_k} \\ \dfrac{\partial^2 U^{pot}}{\partial \phi_i\ \partial \psi_k} & \dfrac{\partial^2 U^{pot}}{\partial \phi_i\ \partial \phi_k} \end{bmatrix} \tag{3.13}$$

are all continuous functions of the degrees of freedom. This ensures a well-behaved minimization.

C. The quasi-Newton matrix-updating algorithm of Broyden, Fletcher, Goldfarb and Shanno ([17], [35]) was implemented. The optimization routine employs our analytically calculated gradient, an aspect crucial to the success of the method. Use of a finite-difference estimation scheme for the derivatives would not only be numerically inaccurate, but also be orders of magnitude more demanding in computation time (see Appendix C.) A number of quasi-Newton and conjugate gradient optimization algorithms, as well as the direct Newton-Raphson solution of the system $\underline{g} = \underline{0}$, were extensively tested on the problem ([65]). The BFGS algorithm was found clearly superior to all methods examined.

D. The computation time for an energy and gradient evaluation increases steeply with interatomic potential range (see Table 3.3.) This led us to develop a three-stage

optimization strategy, using a different form of the total energy function at each stage:

Stage 1: Soft sphere potential (see section 3.2.); atomic radii (i.e., Lennard-Jones σ's) equal to half their actual size; no rotational barriers.

Stage 2: Soft sphere potential; radii of actual size; full rotational barriers.

Stage 3: Full potential (see section 3.2.); radii of actual size; full rotational barriers

This stagewise scheme makes the system at first "feel" and alleviate only the most severe repulsive interactions, while keeping computation time small. The second step absorbs the bulk of the optimization iterations. In the final stage the attractive part of the potential is "switched on," and the final minimum is reached.

Using the optimization procedure described above we were able to obtain minimum energy structures characterized by a Euclidean norm of the gradient vector, $|| \underline{g} ||_2$, smaller than 10^{-6} kcal/(mol degree). The exact Hessian, calculated for the final structures, is always positive definite, indicating a true minimum. A typical computer relaxation history is given in Table 3.3. The time savings effected by the stagewise scheme of "blowing up the radii" are evident. A three-dimensional view of an equilibrium structure is shown in Fig. 3.6.

Table 3.3

Typical Evolution of a Computer Relaxation

Initial guess: Generated by modified rotational isomeric state scheme $x = 76$, $w_m = 0.480$, $T = 298K$, chain start at center of cube, $\psi_1 = \psi_2 = \psi_3 = 45^\circ$, total potential energy = $0.111.10^7 \frac{kcal}{mole}$

Machine: M.I.T. HONEYWELL DPS 8/70, operating under MULTICS (approximately equivalent in computational power to a VAX 780); all calculations were made in 8-byte precision.

Potential	Starting Structure		Ending Structure		Iterations	Function Evaluations	CPU time per function evaluation (seconds)	CPU time (hours)
	Objective function (kcal/mole)	Gradient norm (kcal/mole degrees)	Objective function (kcal/mole)	Gradient norm (kcal/mole degrees)				
Soft Spheres Half Radii	$0.202.10^3$	$0.409.10^4$	$0.798.10^{-19}$	$0.123.10^{-10}$	71	179	4.0	0.20
Soft Spheres Full Radii	$0.241.10^5$	$0.284.10^5$	408.272	$0.201.10^{-5}$	1142	2297	6.8	4.34
Full Potential	112.508	10.840	108.283	$0.790.10^{-6}$	279	619	77	13.24

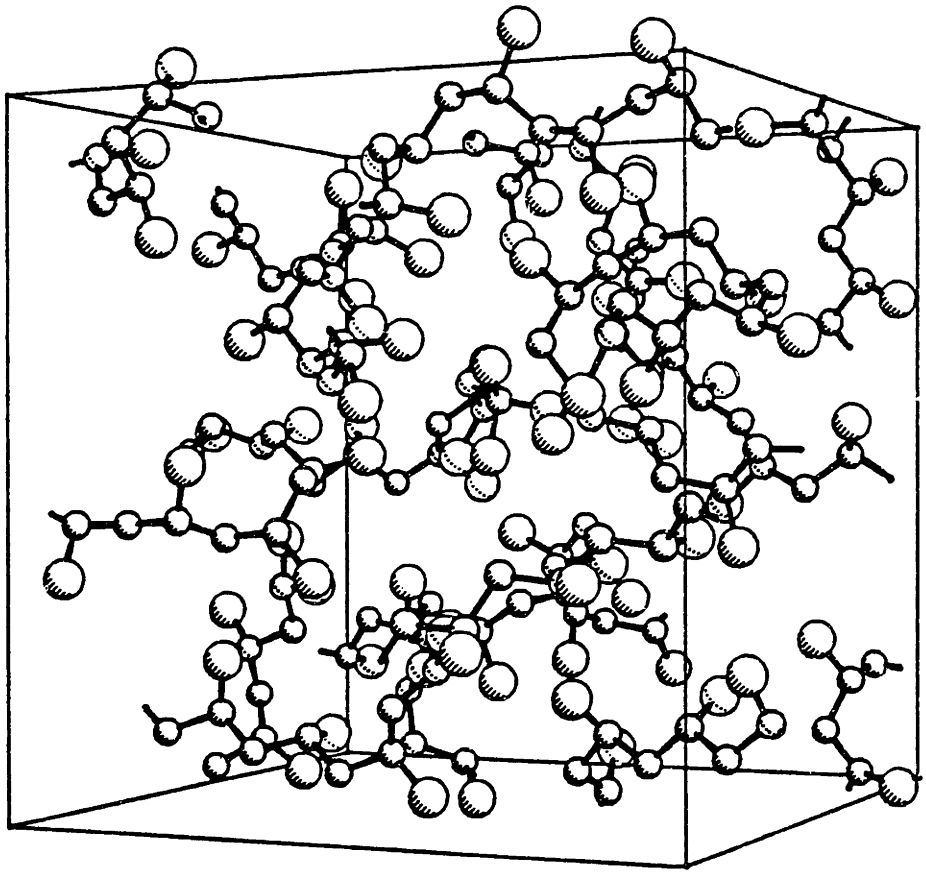

Figure 3.6

"Relaxed" model structure in detailed mechanical equilibrium. The small spheres denote skeletal carbon atoms, the large spheres methyl groups, and hydrogen atoms have been omitted for clarity.

4. THERMODYNAMIC AND STRUCTURAL PROPERTIES OF THE UNDEFORMED POLYMER

Fifteen model structures were obtained by the method described in Chapter 3. These structures comprise an ensemble, which constitutes our molecular picture of glassy atactic polypropylene in the undeformed state. This ensemble of structures provides detailed information, which is analyzed below.

4.1. COHESIVE ENERGY DENSITY AND SOLUBILITY PARAMETER

4.1.1. Theoretical Prediction

Cohesive energy, E_{coh}, is defined [71] as "the increase in internal energy per mole of substance if all molecular forces are eliminated." The square root of the cohesive energy density is the celebrated Hildebrand's solubility parameter δ.

$$\delta = \left(\frac{E_{coh}}{V} \right)^{1/2} \qquad (J/cm^3)^{1/2} \qquad (4.1)$$

E_{coh} and δ are very important thermodynamic parameters for any polymer, widely used in property correlations [71].

In our model systems each chain is surrounded by other chains, which are simply diplaced images of itself. The cohesive energy E_{coh} is the energy of interaction between these images. Each parent chain contains the same amount of matter as a model cube of the bulk polymer, and an estimate of E_{coh} can thus be obtained as the ensemble average of the difference

$$E_{coh} = U^{pot}_{tot,\ parent} - U^{pot}_{tot} \qquad (4.2)$$

where the subscript tot indicates that potential energies of interatomic interactions must be computed with the full, infinite range Lennard-Jones potential function.

The total potential energy of our 15 model structures, computed according to eqn. (C.11), falls in the range (average ± standard deviation):

$$U^{pot} = 113 \pm 20 \quad \frac{\text{kcal}}{\text{mol structures}} \qquad (4.3)$$

However, in the estimate of eqn. (4.3), we have omitted the tails of the nonbonded interaction energy functions. We therefore compute a "tail correction" to the potential energy by

$$\Delta U^{pot}_{tails} = \frac{1}{2} \sum_{\alpha=1}^{3} N_\alpha \sum_{\beta=1}^{3} \rho_\beta \left[4\pi \int_{R_{1,\alpha\beta}}^{R_{\alpha\beta}} g_{\alpha\beta}(r) \left[U^{LJ}_{\alpha\beta}(r) - U^{NB}_{\alpha\beta}(r) \right] r^2 dr + \right. \qquad (4.4)$$

$$\left. + 4\pi \int_{R_{\alpha\beta}}^{\infty} g_{\alpha\beta}(r)\ U^{LJ}_{\alpha\beta}(r)\ r^2 dr \right]$$

where N_α and ρ_α stand for the total number and number density of groups belonging to species α in the cube, summation indices 1, 2, and 3 stand for H, C, and R, respectively, $g_{\alpha\beta}$ is the pair distribution function for the species pair αβ (see below) and all other symbols have been introduced above.

We evaluated expression (4.4) using the group pair distribution functions discussed in section 4.3 for distances $r \leq 10$ Å, and assuming $g_{\alpha\beta}(r) = 1$ for $r > 10$ Å $\forall\ (\alpha,\beta)$. The result is

$$\Delta U^{pot}_{tails} = -85 \quad \frac{kcal}{mol\ structures} \tag{4.5}$$

so that

$$U^{pot}_{tot} = U^{pot} + \Delta U^{pot}_{tails} = 28\ (\pm 20) \quad \frac{kcal}{mol\ structures} \tag{4.6}$$

The contribution of the intrinsic rotational potential to U_{tot} is

$$\sum_{i=2}^{2x-1} U_{\phi}(\phi_i) = 104\ (\pm 11) \quad \frac{kcal}{mol\ structures} \tag{4.7}$$

and the rest is due to (predominantly attractive) nonbonded interatomic interactions.

The total potential energy $U^{pot}_{tot,\ parent}$ of each isolated parent chain was computed using the <u>full</u> Lennard-Jones function $U^{LJ}(r)$ [eqn. (3.4)] to describe nonbonded interatomic interactions, and including the intrinsic torsional potential; the energy U^{pot}_{tot} of the cube formed from the parent chain was subsequently subtracted from $U^{pot}_{tot,\ parent}$. The resulting difference, based on all 15 structures, is (mean ± standard deviation) :

$$E_{coh} = 174 \pm 20 \ \frac{kcal}{mol\ structures} = 227\ (\pm 26) \ \frac{kJ}{kg\ polymer} \tag{4.8}$$

whence the cohesive energy density is

$$\frac{E_{coh}}{V} = 2.0\ (\pm 0.2) \cdot 10^8 \ \frac{J}{m^3} \tag{4.9}$$

and the theoretical estimate of Hildebrand's solubility parameter is thus

$$\delta = \left(\frac{E_{coh}}{V} \right)^{1/2} = 14.2\ (\pm 0.8) \quad (J/cm^3)^{1/2} \tag{4.10}$$

4.1.2. Comparison with Experiment

Experimental values [71] for the solubility parameter (and for the cohesive energy density) are available for polypropylene of unspecified tacticity, and probably refer to the commercial isotactic form. Comparison of atactic and isotactic samples (solubility in ether; see section 7.1.2) suggests that the solubility parameter for the atactic polymer is somewhat lower than the reported one [71] of

$$\delta_{exp} = 16.8 \ (J/cm^3)^{1/2} \ , \qquad (4.11)$$

corresponding to a cohesive energy density of

$$\left(\frac{E_{coh}}{V} \right)_{exp} = 2.82 \cdot 10^8 \ J/m^3 \qquad (4.12)$$

In light of this the agreement between the theoretical prediction and experiment is excellent. This agreement indicates that the atomistic model structures are realistic, and we proceed to investigate their structural characteristics.

4.2. THE CONFORMATION OF INDIVIDUAL CHAINS IN THE BULK

4.2.1. Bond direction correlation

As a measure of orientational correlation between bonds we use the "bond direction correlation function," or "order parameter," S, defined by ([69], [74], [21])

$$S = \frac{1}{2} \left[3 \langle \cos^2 \theta \rangle - 1 \right] \qquad (4.13)$$

where θ is the angle between two skeletal bond chords of the chain (chord i is the vector connecting the midpoints of the skeletal bonds flanking carbon atom i). We denote by S_{ij} that order parameter that is obtained by taking the average in eqn. (4.13) over all chord pairs with given index difference $|i-j|$ and over all 15 structures, i.e., by averaging over the squared cosine of the angle between all chords separated by a fixed number of bonds.

Figure 4.1 shows S_{ij} as a function of $|i-j|$. The strong directional correlation between neighboring chords for very small values of $|i-j|$ vanishes rapidly with increasing distance along the chain. The absence of any long-range correlation effects indicates that the procedure used to generate the structures investigated here indeed leads to parent chains that are "random coils."

4.2.2. Distribution of Rotation Angles

To what extent, however, do these chains resemble unperturbed random coils? The distribution of rotation angles in the 15 model systems is depicted in Figure 4.2. The corresponding distribution for unperturbed chains, predicted by the RIS model [57] was obtained aa follows: We generated 100 Bernoullian configurations with x=76 and w_m = 0.48; we then computed the a' priori probabilities of each rotational isomeric state, using a generator matrix technique described in [26], and averaged them over all configurations. The a' priori probabilities thus obtained appear as "Dirac pulses" in Figure 4.2 (bold lines); this is, of course, a consequence of the discretization inherent in the RIS model. The pulse heights

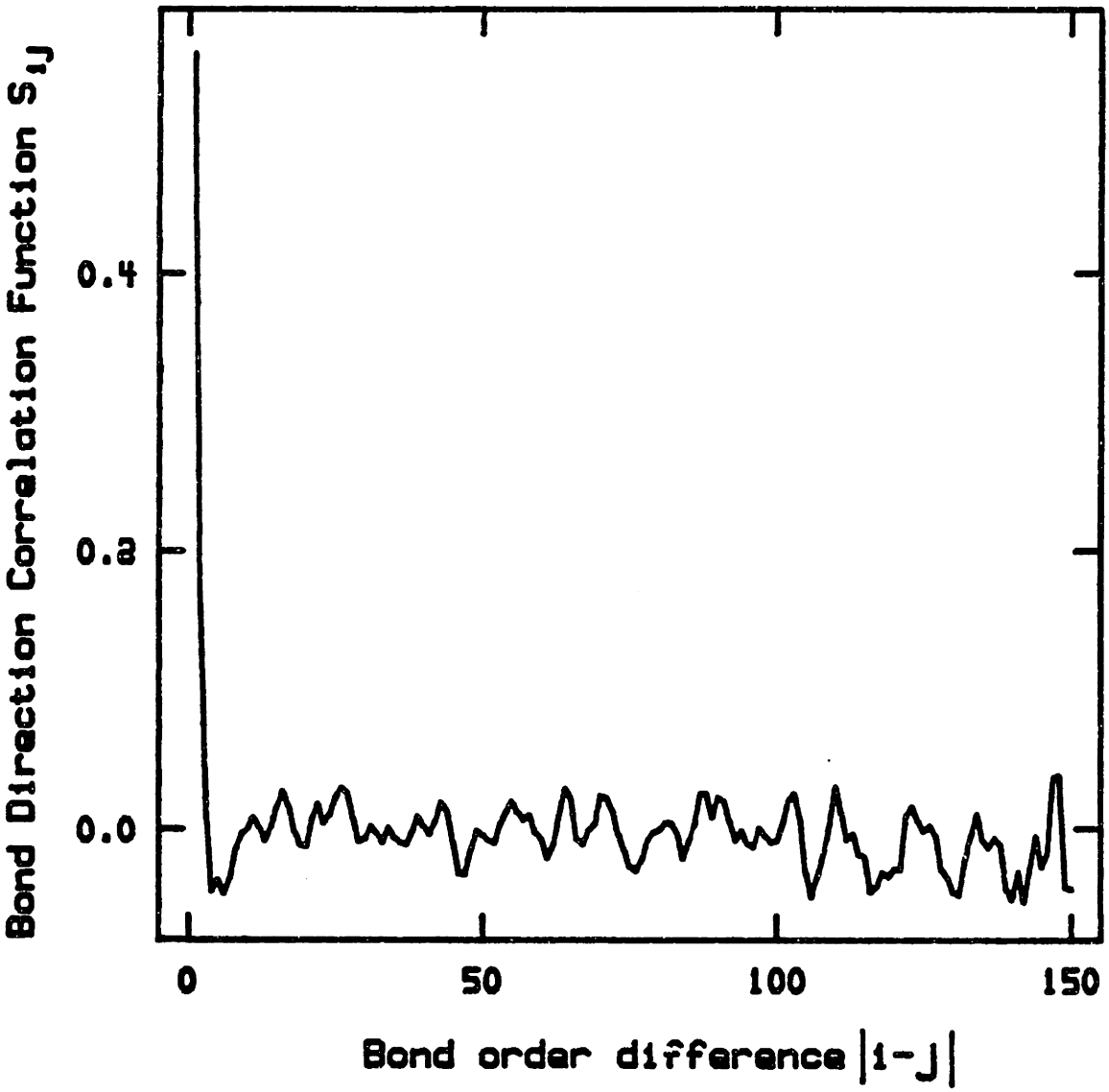

Figure 4.1

Bond direction correlation function S_{ij} between skeletal chords in the fifteen parent chains, plotted against the index difference |i-j|.

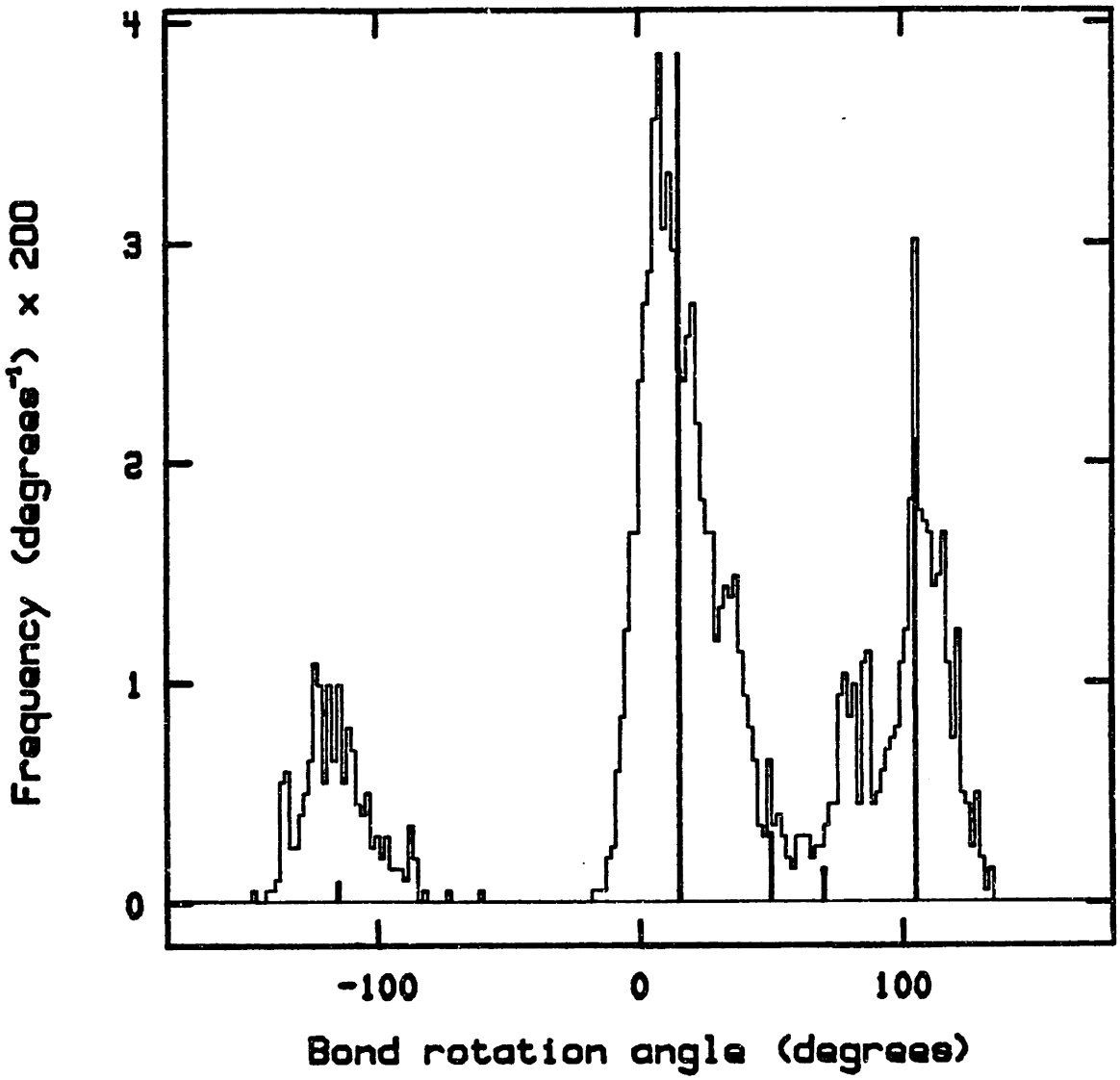

Figure 4.2

Distribution of Torsion Angles in the ensemble of fifteen undeformed model structures.
The corresponding R.I.S. values for unperturbed chains are given as relative probabilities (bold vertical lines).

are proportional to the state probabilities. We observe that rotation angles in our bulk model system concentrate in two major peaks, corresponding to the t and g rotational isomeric states. In addition, one can discern three smaller peaks near the locations of the t^*, g^*, and $\bar{g}$ states. Thus, qualitative agreement between the angle distribution in the bulk and the RIS-prediction is very good. A quantitative comparison was made by subdividing the torsion angle range into five intervals, each corresponding to a rotational state, and by integrating the rotation angle distribution to obtain the probabilities that ϕ lie in each of these intervals. These probabilities are given, together with the RIS probabilities, in Table 4.1. Although the relative population of the major states in the bulk model structures ($t/g = 1.93$) is very close to that obtained from the RIS model ($t/g = 1.84$), we observe that the states of lesser population, and in particular $\bar{g}$, are considerably more frequent in the bulk (The enhancement of the $\bar{g}$ state is also evident from Figure 4.2.) This indicates that our parent chains are richer in the more compact conformations, and one would expect them to appear somewhat "collapsed" in comparison to unperturbed chains. These conformational differences might be due to the initial guess generation procedure, in which consideration of long-range interactions causes parent chain conformational probabilities to depart from the RIS values (section 2.3.1.) During the subsequent energy minimization a large proportion (approx. 36%) of skeletal bonds "flips" (i.e. changes state), and these flips tend to restore the bond angle distribution towards the RIS values. The fully relaxed structures still show some differences from the state populations in a RIS model, however.

Table 4.1

Model System Bond Angle Distribution
Compared to Rotational Isomeric State Model Predictions
for Unperturbed Chains

State	ϕ-interval	State frequency obtained from 15 model systems	State a priori probability from R.I.S. model
$\bar{g}$	$-148° < \phi < -60°$	0.128 ± 0.039	0.0137 ± 0.0002
t	$-18° < \phi < 30°$	0.444 ± 0.055	0.5939 ± 0.0028
t*	$30° < \phi < 59°$	0.110 ± 0.026	0.0474 ± 0.0013
g*	$59° < \phi < 89°$	0.086 ± 0.022	0.0225 ± 0.0002
g	$89° < \phi < 135°$	0.230 ± 0.038	0.3224 ± 0.0016

4.2.3. Measures of Chain Size and Shape

The size of the parent chains was assessed by determining the ensemble-averaged rms end-to-end distance $\langle r^2 \rangle^{1/2}$, and the ensemble-averaged radius of gyration $\langle s^2 \rangle^{1/2}$, displayed in Table 4.2. The corresponding unperturbed chain values, computed by exact generator matrix methods [26] from 100 Bernoullian configurations with x = 76 and w_m = 0.48 (see above) are also shown in Table 4.2. The average expansion factor of our parent chains, calculated from $\langle r^2 \rangle^{1/2}$, is 0.85 ± 0.07. The calculation of $\langle s^2 \rangle^{1/2}$, however, indicates an expansion factor of 0.92 ± 0.06; since this value is based on a larger statistical sample than the end-to-end distance (all skeletal carbon atoms are considered for obtaining $\langle s^2 \rangle^{1/2}$), it is also less prone to errors due to limited

sample size than $\langle r^2 \rangle^{1/2}$. The dimensions of the parent chains are barely distinguishable from those of unperturbed chains; they are slightly smaller. Vacatello et al. [69] have reported size and conformation measures obtained from their model of liquid triacontane. It is interesting to note that their chains, too, appear to be somewhat collapsed in comparison to the RIS model predictions.

To explore the shape of the parent chains we computed, for each one of them, the eigenvalues $\overline{X^2}$, $\overline{Y^2}$, $\overline{Z^2}$ of the radius of gyration tensor ([54], [67]). These were used to calculate the shape asphericity [67]

$$b = \overline{X^2} - \frac{1}{2} (\overline{Y^2} + \overline{Z^2}) , \qquad (4.14)$$

the acylindricity [67]

$$c = \overline{Y^2} - \overline{Z^2} \qquad (4.15)$$

and the relative shape anisotropy [67]

$$\kappa^2 = (b^2 + 3c^2/4) / s^4 \qquad (4.16)$$

Values of the reduced measures

$$\frac{\langle \overline{X^2} \rangle}{\langle \overline{Z^2} \rangle} , \quad \frac{\langle \overline{Y^2} \rangle}{\langle \overline{Z^2} \rangle} , \quad \frac{\langle b \rangle}{\langle s^2 \rangle} , \quad \frac{\langle c \rangle}{\langle s^2 \rangle} \quad \text{and} \quad \langle \kappa^2 \rangle ,$$

obtained by averaging over the ensemble of 15 parent chains, are shown in table 4.2. The same measures were computed by Monte-Carlo generation of 2000 unperturbed chains (configurations and conformations, see Appendix B) with x=76 and w_m=0.48; they are also displayed in Table 4.2. Excellent agreement between the bulk results and the RIS model predictions is observed; the shape of the parent chains is indistinguishable from that of unperturbed coils.

Table 4.2

Shape and Size Characteristics of Parent Chains
(Mean Values ± Standard Deviation of the Mean)

Measure	Average value from 15 parent chains	R.I.S. value
$\langle r^2 \rangle^{1/2}$, Å	40.12 ± 3.18	47.00 ± 0.10[a]
$\langle s^2 \rangle^{1/2}$, Å	17.20 ± 1.06	18.76 ± 0.05[a]
$\frac{\langle r^2 \rangle}{\langle s^2 \rangle}$	5.44 ± 1.09	6.28 ± 0.04[a]
$\frac{\langle \bar{X}^2 \rangle}{\langle \bar{Z}^2 \rangle}$	15.24 ± 2.55	14.84 ± 0.25[b]
$\frac{\langle \bar{Y}^2 \rangle}{\langle \bar{Z}^2 \rangle}$	3.01 ± 0.47	3.13 ± 0.05[b]
$\frac{\langle b \rangle}{\langle s^2 \rangle}$	0.687 ± 0.141	0.674 ± 0.013[b]
$\frac{\langle c \rangle}{\langle s^2 \rangle}$	0.104 ± 0.093	0.112 ± 0.002[b]
$\langle \kappa^2 \rangle$	0.444 ± 0.057	0.431 ± 0.004[b]

a) By exact generator matrix method.

b) By Monte Carlo estimation.

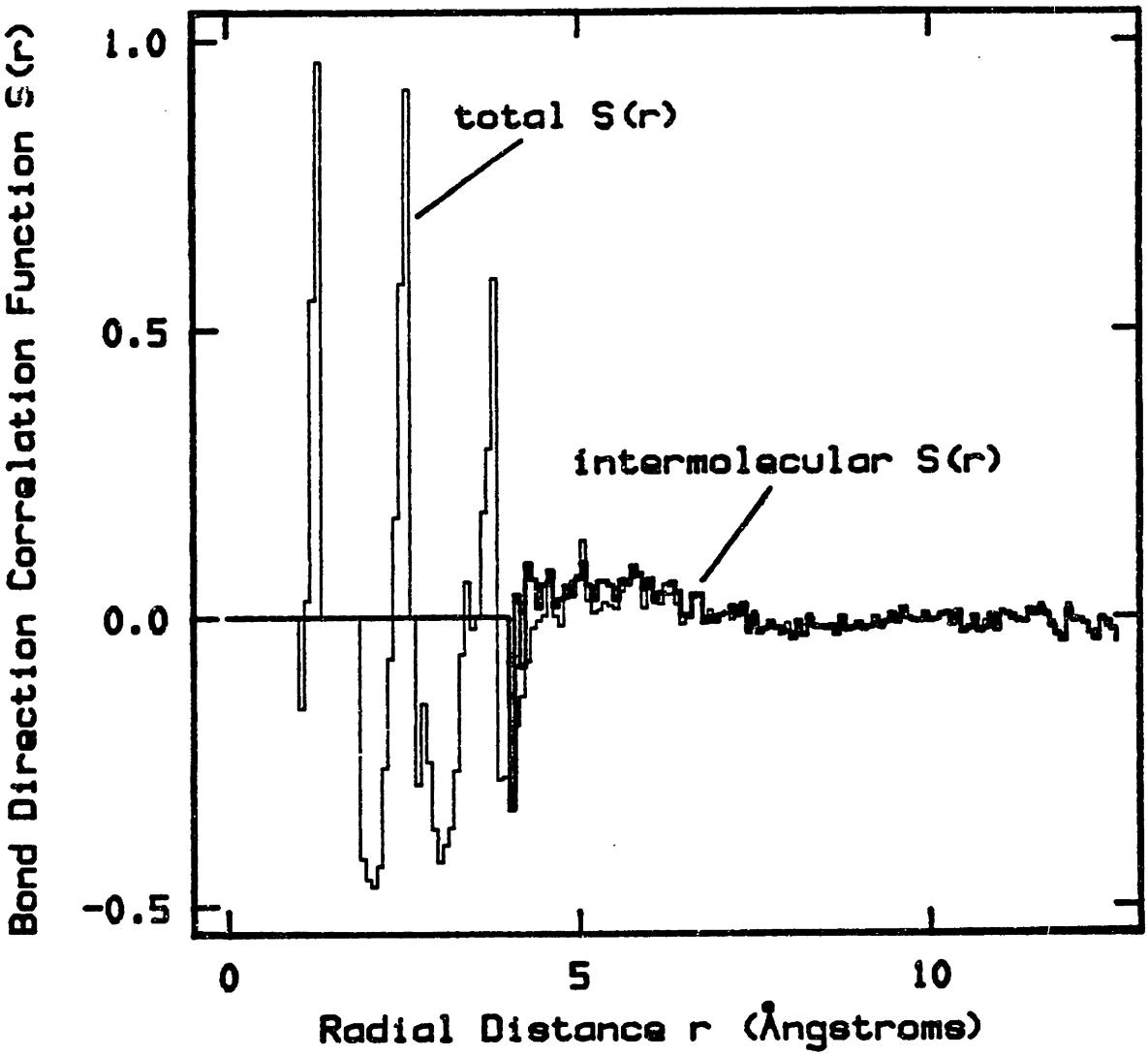

Figure 4.3

Bond direction correlation function S(r) between skeletal chords in the fifteen undeformed model systems, plotted against the distance r between chord centers.

4.3. THE STRUCTURE OF THE GLASSY POLYMERIC BULK

4.3.1. Bond Direction Correlation

The model systems obtained in this work provide us with detailed information not only on intra-molecular structure, but also on inter-molecular aspects, i.e. the relative arrangement of chains in the bulk.

The bond direction correlation function S(r), derived from eqn. (4.13) by averaging over chord pairs with given distance r between the chord midpoints, is plotted in Figure 4.3 as a thin line. The purely intermolecular part of S(r), obtained by considering those chord pairs only that belong to different images of the parent chain, is also displayed (bold line). The fact that S(r) goes to 0 at large distances proves that there is no long-range correlation, i.e. our model cubes are truly amorphous systems. The sharp correlation pattern observed at short distances is completely intramolecular, i.e. caused by connectivity and conformation along the parent chain. For example, the three maxima at 1.3, 2.5, and 3.8 Å are attributable to t, tt, and ttt conformations.

At the shortest possible intermolecular distances there is a tendency for perpendicular arrangements (perhaps due to the "rough" surface of the chains); at slightly larger distances there is a very weak trend towards parallelism.

4.3.2. Pair Distribution Functions

The pair distribution functions $g_{\alpha\beta}$ (α, $\beta \in \{H, C, R\}$) for all six species pairs in our systems are shown as bold lines in Figure 4.4 (a-f). If V is the volume of a model cube, the

function $g_{\alpha\beta}(r)$ is defined so that the quantity

$$\frac{1}{V} \; 4\pi r^2 \, g_{\alpha\beta}(r) \, dr$$

is equal to the probability of finding an α center and a β center at a distance of r to r+dr from each other. The method of obtaining g(r) from the model structures, with proper consideration of the periodic geometry, is discussed in [66]. Only pairs whose separation is conformation-dependent have been included in Figures 4.4. Contributions from pairs whose distance is fixed due to connectivity would appear as "Dirac pulses" on the plots. The locations and magnitudes of these pulses are listed in Appendix D (a). The distributions of inter-group distances were also calculated for the parent chains, and subtracted from the total to obtain the purely <u>intermolecular</u> part of the pair distribution functions, $g_{\alpha\beta}^{inter}(r)$. The function $g_{\alpha\beta}^{inter}(r)$ is such that the quantity

$$\frac{1}{V} \; 4\pi r^2 \, g_{\alpha\beta}^{inter}(r) \, dr$$

is equal to the probability of finding an α center and a β center <u>not</u> belonging to the same chain, and separated by a distance in the interval r to r+dr. In Figures 4.4 (a-f) the intermolecular parts of the pair distribution functions are displayed as thin lines.

At long distances all pair distribution functions approach unity, indicating that no long-range structure exists (as one would expect from a purely amorphous system). The intermolecular functions $g_{\alpha\beta}^{inter}$ rise more or less smoothly with increasing distance towards an asymptotic value of one. The sharp correlations observed at small distances in $g_{\alpha\beta}(r)$ are almost entirely intramolecular. The intermolecular pair distribution functions display some subtle structural features, but beyond 10 Å there is essentially no intermolecular correlation; only the HH, HR and RR (i.e., the substitu-

ent-substituent) distributions display a well-defined maximum at a distance roughly equal to the sum of the Van der Waals radii of the species involved. This "first coordination shell" appears particularly pronounced in the RR case. (The high noise level in this case is due to the small number of methyl substituents in the system.) Skeletal carbons of different chains are kept apart by the substituents surrounding them, so that the principal feature of the carbon-carbon intermolecular distribution is a broad hump in the vicinity of 6.3 Å. Broad humps of intermolecular origin at distances beyond 5 Å can also be discerned in the H-C and H-R distributions.

Note that the pair distribution functions have been calculated from a static ensemble of structures. In reality thermal motion will tend to broaden the peaks and to reduce their height.

Vacatello et al. [69] present a methylene-methylene pair distribution function, based on their model triacontane, which is qualitatively very similar to our skeletal carbon-carbon distribution (Figure 4.4d). The location and interpretation of the three first intramolecular maxima in our systems is practically identical to theirs, and our g_{CC}^{inter} confirms the presence of some intermolecular contribution in the region around 6.30 Å.

In reality there are no R groups, but only H and C atoms, whose spatial arrangement is characterized by the three element pair distribution functions g_{HH}^{el} , g_{HC}^{el} , g_{CC}^{el} . To obtain these, we "resolved" each of the methyl groups into a carbon, at the end of the carbon-methyl bond, and three hydrogens, symmetrically bonded to this carbon by bonds of length ℓ_H = 1.10 Å at an angle of 110° with the methyl stem. All methyls were taken in a staggered conformation with respect to the backbone. The element pair distributions

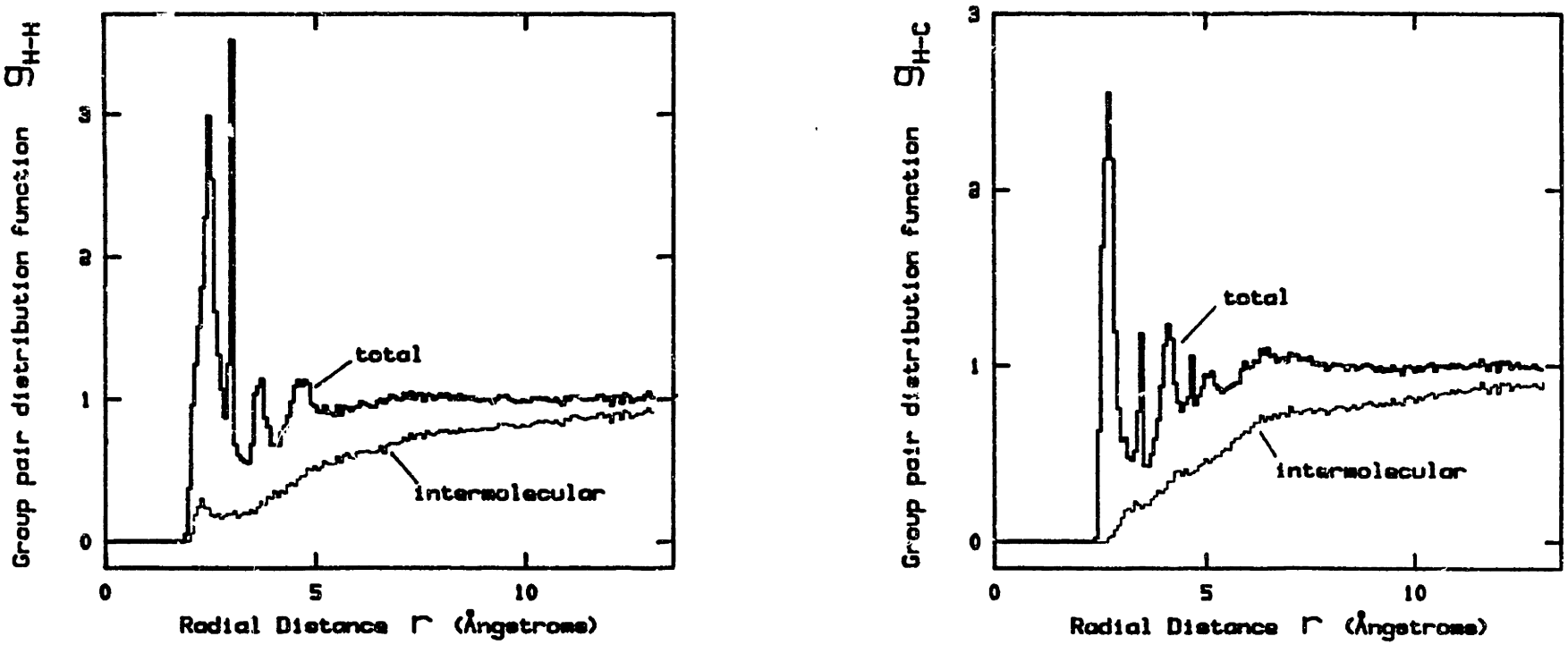

Figure 4.4 (a,b)

Group pair distribution functions for the species pairs HH, HC (from groups C=skeletal carbon, H=main chain hydrogen) in our fifteen undeformed model structures. Total and intermolecular component shown.

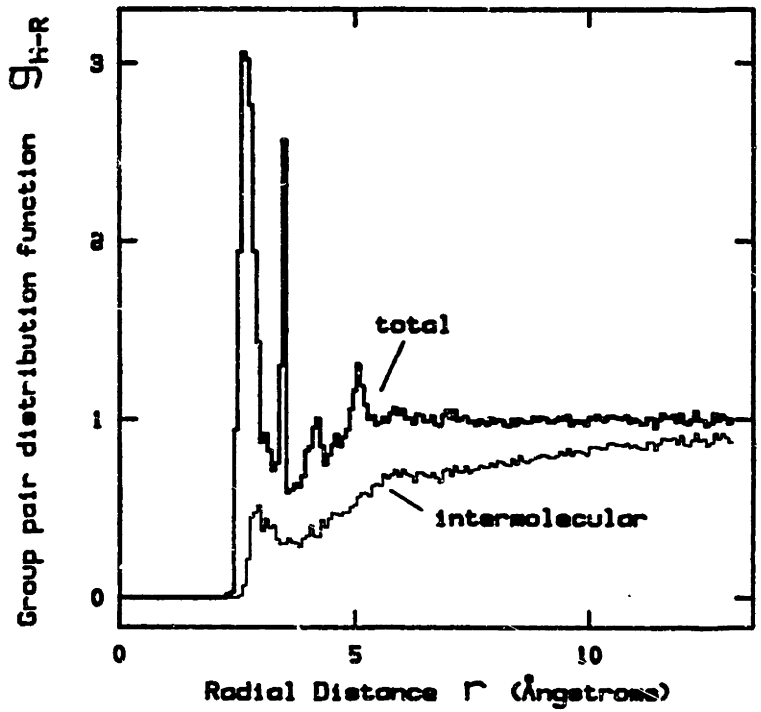

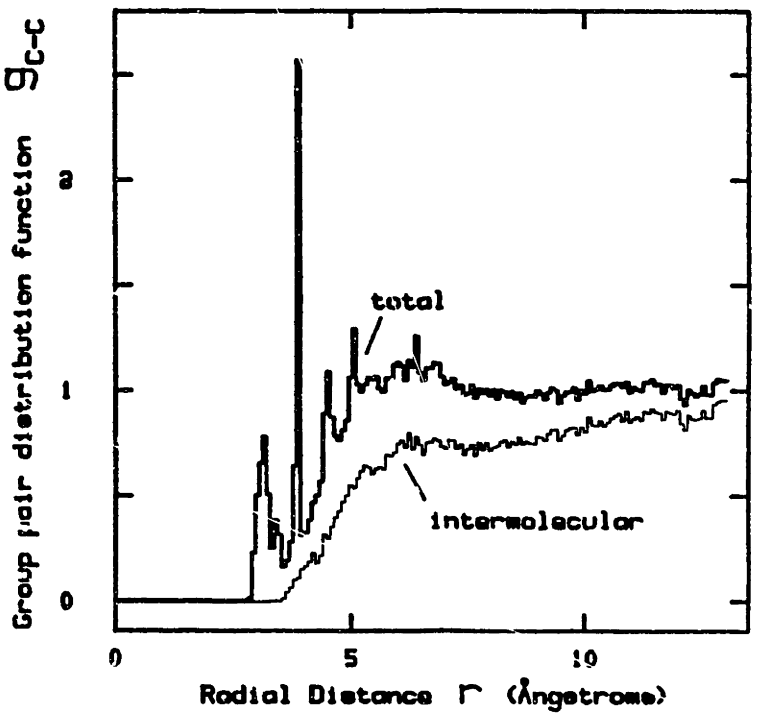

Figure 4.4 (c,d)

Group pair distribution functions for the species pairs HR, CC (from groups R=methyl, C=skeletal carbon, H=main chain hydrogen) in our fifteen undeformed model structures. Total and intermolecular component shown.

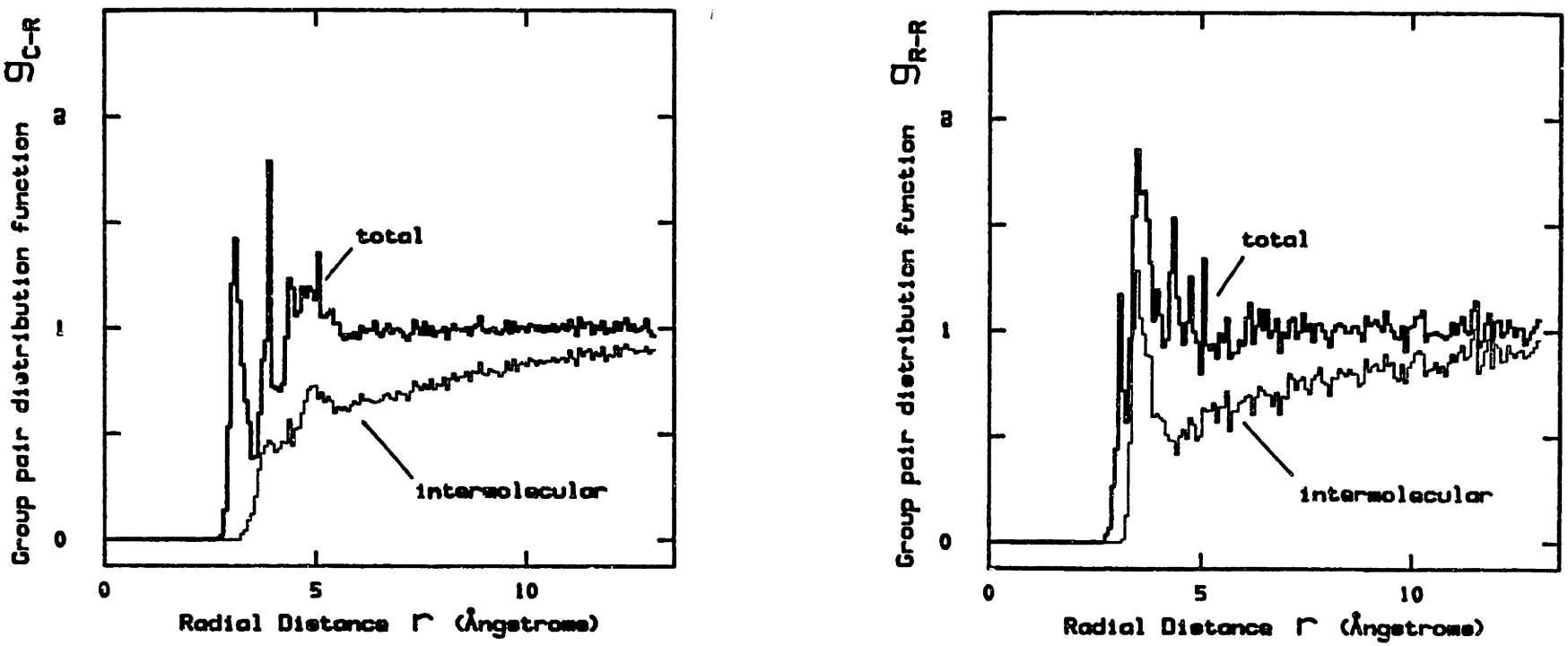

Figure 4.4 (e,f)

Group pair distribution functions for the species pairs CR, RR (from groups R=methyl, C=skeletal carbon) in our fifteen undeformed model structures. Total and intermolecular component shown.

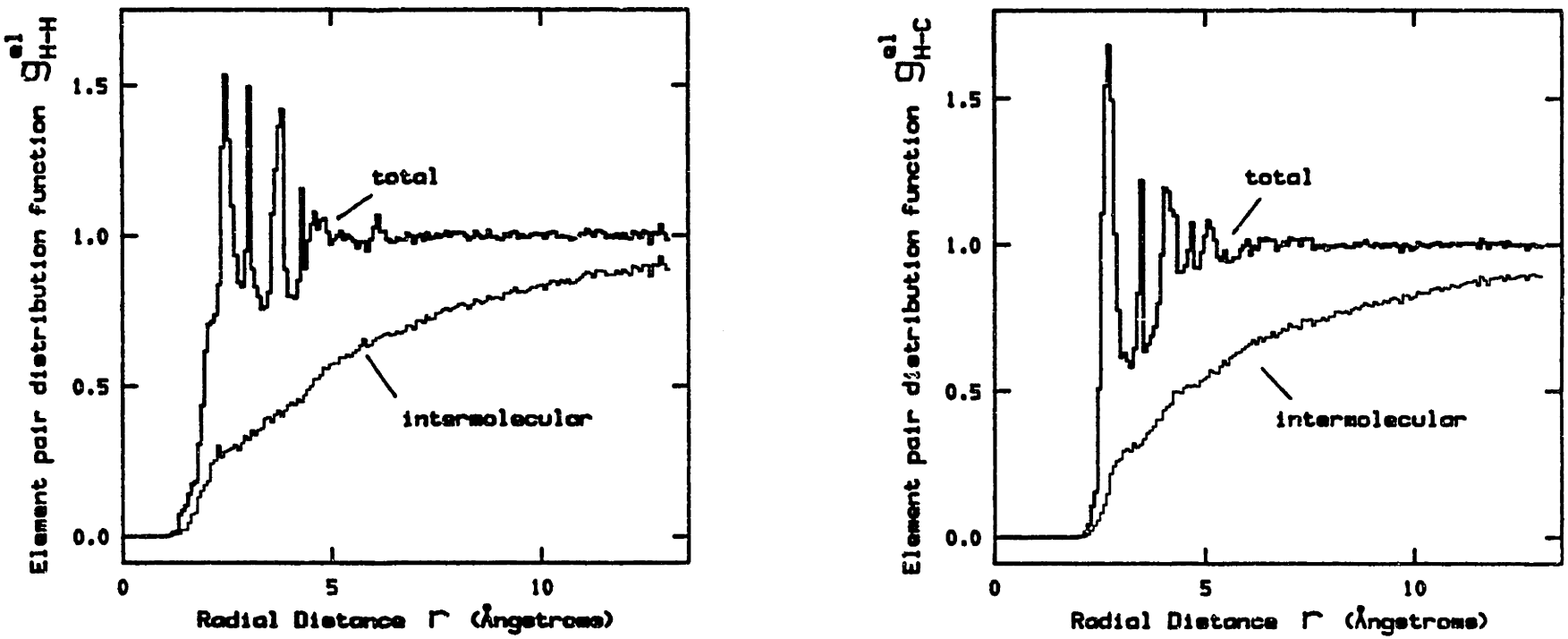

Figure 4.5 (a,b)

Element pair distribution functions for the element pairs HH, HC (from atoms C=skeletal carbon, H=main chain hydrogen) in our fifteen undeformed model structures. Total and intermolecular component shown.

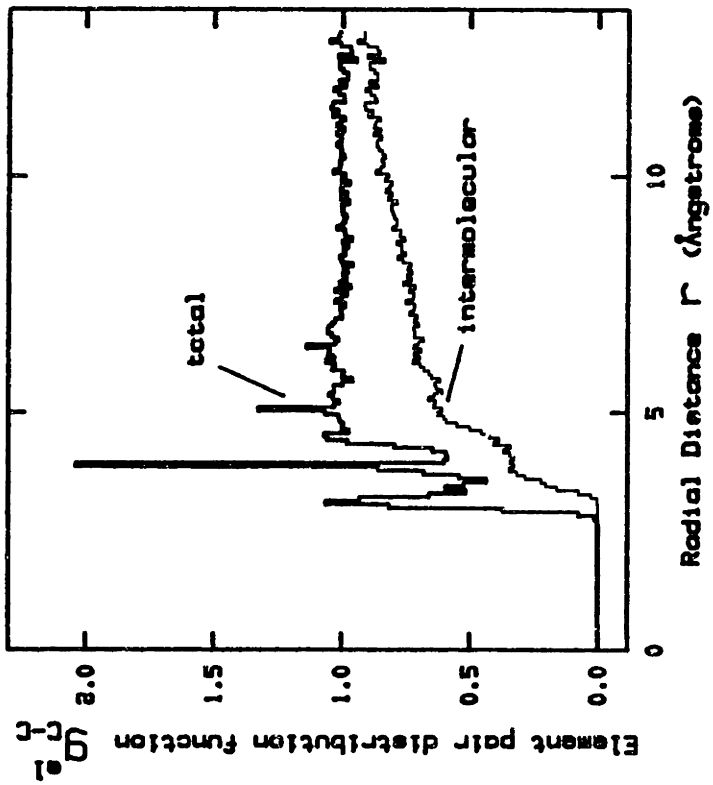

Figure 4.5 (c)

Element pair distribution function for the element pair CC (from atoms C=skeletal carbons) in our fifteen undeformed model structures.
Total and intermolecular component shown.

were computed in exactly the same way as the group pair distributions presented above, and are displayed as bold lines in Figures 4.5 (a-c). Also shown are the purely intermolecular contributions (thin lines). Again chain connectivity introduces additional "Dirac spikes"; their locations and magnitudes are listed in Appendix D(b).

4.4. X - RAY AND NEUTRON DIFFRACTION PATTERNS

Experimentally, information on molecular structure can be obtained by scattering. Our detailed atomistic model can be used to calculate scattering patterns theoretically; this calculation was carried out as described in Section 4.4.1 below. In parallel, an experimental program was undertaken to measure the actual X-ray and neutron diffraction patterns of glassy atactic polypropylene; experimental details are provided in Chapter 7. The direct comparison of theoretical against experimental diffraction results constitutes a useful check for the structural predictions of the model, and is presented in Section 4.4.2 below.

4.4.1. Method of Prediction

Consider a beam of radiation (X-rays, neutrons, electrons) of wavelength λ_s, whose direction is defined by the unit vector $\hat{k}_{s_o}$, falling on a specimen of matter. The radiation will interact with the particles in the specimen, under exchange of momentum and energy. If the wavelength of the radiation is comparable to interatomic distances, the momentum exchange, and the resulting interference of scattered radia-

tion in various directions, gives rise to a diffraction pattern, which contains information about the structure of the specimen. The energy exchange, which can provide useful information on dynamic phenomena, will not be considered here, i.e. the discussion will be confined to scattering under zero energy exchange, or <u>elastic</u> scattering. The scattered radiation we observe along a direction defined by the unit vector $\hat{k}_s$, forming an angle $2\theta_s$ with the direction of the incident beam. We define the "diffraction vector" $\underset{\sim}{Q}$ ([36], p.7; [4], p.74) by:

$$\underset{\sim}{Q} = \frac{2\pi}{\lambda_s} \left(\hat{k}_s - \hat{k}_{s_o} \right) \tag{4.17}$$

and denote its magnitude by

$$Q = |\underset{\sim}{Q}| = \frac{4\pi}{\lambda_s} \sin\theta_s \tag{4.18}$$

The scattered wave is related to the spatial distribution of scattering particles through a Fourier transformation. The scattered intensity can be expressed in terms of interatomic distances $\underset{\sim}{r}_{jk}$ as ([36], p.65):

$$\frac{I_{tot}(\underset{\sim}{Q})}{C_s} = \sum_j \sum_k f_j(Q)\, f_k(Q) \exp\left(i\, \underset{\sim}{r}_{jk} \cdot \underset{\sim}{Q}\right) \tag{4.19}$$

In eqn. (4.19) each of the indices j and k runs over all atoms in the system; C_s is a constant, depending on the incident intensity and the nature of the radiation, as described below; and $f_j(Q)$ is an "atomic scattering factor," characterizing the interaction of radiation with an isolated atom of the species to which atom j belongs.

In the system we are modelling, an atom may belong to one of two elemental species (H, C). The distribution of interatomic vectors within each species pair is characterized by the appropriate pair distribution function (compare Section 4.3.) Separating out terms with j=k, and introducing the pair

distribution functions $g_{\alpha\beta}^{el,tot}(\underline{r})$, we can rewrite equation (4.19) as:

$$\frac{I_{tot}(\underline{Q})}{C_s} = \sum_{\alpha} N_{\alpha} f_{\alpha}^2(Q) + \tag{4.20}$$

$$+ \frac{2}{V} \sum_{\alpha\beta} N_{\alpha\beta} f_{\alpha}(Q) f_{\beta}(Q) \int d^3\underline{r} \; g_{\alpha\beta}^{el,tot}(\underline{r}) \cos(\underline{r}\cdot\underline{Q})$$

The first summation in (4.20) runs over all species (α = H, C) while the second summation runs over all species pairs ($\alpha\beta$ = HH, HC, CC). N_{α} and $N_{\alpha\beta}$ stand for the total number of atoms of atoms of type α, and the total number of atomic pairs of type $\alpha\beta$, respectively, both known from the stoichiometry of our polymer (see Section 3.2.)

Adding and subtracting from $g_{\alpha\beta}^{el,tot}(\underline{r})$ its limiting value of unity (which corresponds to the average, macroscopic density for $\alpha\beta$ pairs):

$$\frac{I_{tot}(\underline{Q})}{C_s} = \sum_{\alpha} N_{\alpha} f_{\alpha}^2(Q) +$$

$$+ \frac{2}{V} \sum_{\alpha\beta} N_{\alpha\beta} f_{\alpha}(Q) f_{\beta}(Q) \left\{ \int d^3\underline{r} \; \cos(\underline{r}\cdot\underline{Q}) + \right.$$

$$\left. + \int d^3\underline{r} \left[g_{\alpha\beta}^{el,tot}(\underline{r}) - 1 \right] \cos(\underline{r}\cdot\underline{Q}) \right\} \tag{4.21}$$

The first term in the curly brackets of eqn. (4.21) contributes a delta function to $I(\underline{Q})$. It is nonzero only for $\underline{Q} = \underline{0}$, hence it is termed "forward scattering" ([4], [31]). The second term in the curly brackets incorporates the interference of waves scattered from different atoms; it is from this term that structural information about the material can be

extracted. Confining ourselves to isotropic systems, in which $g_{\alpha\beta}^{el,tot}$ is a function only of the magnitude of $\underset{\sim}{r}$, and not of orientation (this has been assumed in Section 4.3), we further write eqn. (4.21) as:

$$\frac{I_{tot}(Q)}{C_s} = \sum_{\alpha} N_{\alpha} f_{\alpha}^2(Q) + \frac{2}{V} \left\{ \sum_{\alpha\beta} N_{\alpha\beta} f_{\alpha}(Q) f_{\beta}(Q) \right\} V \delta(Q) +$$

$$+ \frac{2}{V} \sum_{\alpha\beta} N_{\alpha\beta} f_{\alpha}(Q) f_{\beta}(Q) \int_0^{2\pi} d\phi' \int_0^{\pi} \sin\theta' d\theta' \int_0^{\infty} r^2 dr \left[g_{\alpha\beta}^{el,tot}(r) - 1 \right] \cos(rQ\cos\theta'$$

$$= \sum_{\alpha} N_{\alpha} f_{\alpha}^2(Q) + \underbrace{\frac{2}{V} \left\{ \sum_{\alpha\beta} N_{\alpha\beta} f_{\alpha}(Q) f_{\beta}(Q) \right\} V \delta(Q)}_{\text{forward scattering, } I_{forw}(Q)} +$$

$$+ \frac{2}{V} \sum_{\alpha\beta} N_{\alpha\beta} f_{\alpha}(Q) f_{\beta}(Q) 4\pi \int_0^{\infty} r^2 \left[g_{\alpha\beta}^{el,tot}(r) - 1 \right] \frac{\sin(rQ)}{rQ} dr \qquad (4.22)$$

Following the usual convention [31], I will neglect the forward scattering term in the following, and focus on

$$I(Q) = I_{tot}(Q) - I_{forw}(Q) \qquad (4.23)$$

The theoretical prediction of the scattered intensity I(Q) requires knowledge of the pair distribution functions $g_{\alpha\beta}^{el,tot}$. In Section 4.3 I presented plots of the nonbonded element pair distribution function functions, $g_{\alpha\beta}^{el}(r)$. Furthermore, bonded contributions are described by the Dirac pulses $A_{b,k}^{\alpha\beta} \delta(r - r_{b,k}^{\alpha\beta})$, listed for each element pair in Appendix D(b). The total element pair distribution functions to be used in eqn. (4.22) are then equal to:

$$g_{\alpha\beta}^{el,tot}(r) = g_{\alpha\beta}^{el}(r) + \sum_{k} A_{b,k}^{\alpha\beta} \delta(r - r_{b,k}^{\alpha\beta}) \qquad (4.24)$$

There arises, however, the following problem: Our model structures are completely static; in deriving the pair

distribution functions, which appear on the right hand side of eqn.(4.24), we have assumed all atoms to be at rest in their average equilibrium positions. In reality, atoms are displaced from their equilibrium positions at any instant, due to thermal motion. It is the time-averaged domains swept by atoms in the course of their motion, rather than the single equilibrium points, that determine the elastic scattering pattern. Thus, our atom locations have to be "smeared out," to account for thermal motion, and this will lead to a broadening of the diffraction peaks.

To account for thermal motion in our model, we chose to assume that atoms may depart from their equilibrium positions by the same displacement in all directions ("thermal sphere" approximation.) Displacements are assumed to follow a Gaussian distribution centered at zero, with the root mean squared displacement equal to Δ. This, of course, is only an approximation. In reality thermal displacements may be very anisotropic, due to the presence of bonds, and differ among different atomic species. We chose the "thermal sphere" approximation because it is analytically simple, and introduces only one additional parameter (Δ). An appropriate value of the mean squared displacement for polymeric systems at room temperature, according to Vainshtein ([70], p.212) is $\Delta = 0.3$ to 0.4 Å.

Fluctuations in all <u>interatomic distances</u> will also follow a Gaussian distribution ([70], p.203 et seq.). To correctly account for these fluctuations in calculating the diffraction pattern, we must use, instead of $g_{\alpha\beta}^{el,tot}$ (see eqn. 4.22), the <u>convolution</u> of $g_{\alpha\beta}^{el,tot}$ with the probability density distribution of interatomic distance fluctuations. By Fourier transforming this convolution, one can readily reach the following equation for the scattered intensity (excluding forward scattering):

$$\frac{I(Q)}{C_s} = \sum_{\alpha} N_{\alpha} f_{\alpha}^2(Q) +$$

$$+ \frac{2}{V} \sum_{\alpha\beta} N_{\alpha\beta} f_{\alpha}(Q) f_{\beta}(Q) e^{-Q^2\Delta^2} 4\pi \int_0^{\infty} r^2 [g_{\alpha\beta}^{el,tot}(r) - 1] \frac{\sin(rQ)}{rQ} dr \qquad (4.25)$$

The broadening due to thermal motion appears as a simple exponential factor, multiplying the Fourier transform of the pair distribution function; in the literature of crystallography it is termed the "Debye-Waller factor" ([4], p.101). Equation (4.25) forms the basis for all diffraction pattern predictions described below.

I define the <u>elastic structure factor</u> S(Q,0) by:

$$S(Q,0) = \frac{I(Q)}{C_s \sum_{\alpha} N_{\alpha} f_{\alpha}^2 (Q)} \qquad (4.26)$$

This is to be distinguished from the "dynamic structure factor" S(Q,ω) ([46], [15]), which incorporates both momentum and energy transfer information, and is obtained from dynamic scattering; S(Q,0) refers to zero energy transfer. It is also to be distinguished from the "static structure factor" ([31]) $S(Q) = \int S(Q,\omega)\, d\omega$, which is an integral over all energy transfers. The denominator in eqn. (4.26) is equal to the intensity we would get in a hypothetical case whereby all atoms in our system form an "ideal gas," completely devoid of pair correlations. When the atomic scattering factors are Q-dependent, the function S(Q,0) may display structural features more clearly than I(Q) (see below.) Also, it has the convenient limiting property [compare eqns (4.25) and (4.26)]:

$$\lim_{Q \to \infty} S(Q,0) = 1 \qquad (4.27)$$

X - ray Diffraction Pattern

X-ray electromagnetic radiation is scattered by the electrons in matter. Atomic scattering factors for this radiation are dimensionless; they are decreasing functions of Q, their maximum value being equal to the total number of electrons in an atom.

$$f_\alpha \downarrow \text{ as } Q \uparrow, \quad \lim_{Q \to 0} f_C(Q) = 6, \quad \lim_{Q \to 0} f_H(Q) = 1 \qquad (4.28)$$

Detailed tables of the functions $f_C(Q)$ and $f_H(Q)$ are available in [37]. For unpolarized X-rays, the constant C_s, appearing in eqn. (4.25), is equal to ([36], [4]):

$$C_s = I_o \left(\frac{\mu_o}{4\pi} \right)^2 \left(\frac{e^4}{m_e^2 d^2} \right) \left[\frac{1 + \cos^2(2\theta_s)}{2} \right] \qquad (4.29)$$

where I_o is the incident intensity, d the distance of the point at which we detect the scattered radiation from the sample, $e = 1.6 \cdot 10^{-19}$ Cb is the electronic charge, $m_e = 9.16 \cdot 10^{-31}$ kg the electronic mass, and $\mu_o = 4\pi \cdot 10^{-7} \frac{V\ s}{A\ m}$ the permeability of free space. Observe the dependence of C_s on the diffraction angle.

The scattered intensity I(Q) was calculated by equations (4.24) and (4.25), employing the element pair distribution function results described in Section 4.3 and Appendix D(b). No smoothing was applied to pair distribution functions prior to Fourier transformation. For the purpose of calculating the Fourier integrals appearing in eqn. (4.25), the "tails" of the distribution functions were truncated at 10 Å, i.e. it was assumed that $g_{\alpha\beta}^{el,tot}(r) = 1$ for $r > r_{cutoff} = 10$ Å (compare Figs. 4.5.) Long-range density fluctuations are thus not taken into account, and as a consequence the predicted scattering patterns are not reliable below Q values of approximately $\frac{2\pi}{r_{cutoff}}$. In the following, we plot scattering

curves for values of $Q > 0.65$ Å. The shape of the plotted portion of the curves has been confirmed to be insensitive to the exact point of truncation.

Figure 4.6 depicts the predicted X-ray scattered intensity for a wide range of Q. Results are presented for four different values of the mean squared amplitude of thermal motion, Δ. I(Q) has been normalized by division by the total scattered intensity at zero angle (including forward scattering) $I_{tot}(0)$, computed by [compare eqns (4.19) and (4.22)]:

$$I_{tot}(0) = C_s \left[\sum_{\alpha} N_\alpha f_\alpha(Q) \right]^2 \qquad (4.30)$$

The predicted pattern exhibits weak, broad maxima, characteristic of an amorphous solid. The locations of the peaks are better seen in Figure 4.7 which depicts the elastic structure factor S(Q,0), computed according to eqn. (4.26). Thermal fluctuations severely dampen all maxima beyond the first two or three. As can be judged from the relative magnitude of f_C and f_H, X-ray diffraction is dictated predominantly by carbon-carbon correlations in the system. The first and highest peak, centered at 1.17 $Å^{-1}$, is the most interesting structural feature in the pattern; it contains a heavy intermolecular contribution, from neighboring carbon pairs that belong to different chains. The second peak, at approximately 2.96 $Å^{-1}$, is primarily intramolecular; it is due to pairs of carbon atoms tetrahedrally bonded to the same carbon ($C\diagup^{C}\diagdown C$ bonded sequence.) The third peak, at approx. 5.34 $Å^{-1}$, comes from carbon atoms directly bonded within a chain (C - C bonded sequence.)

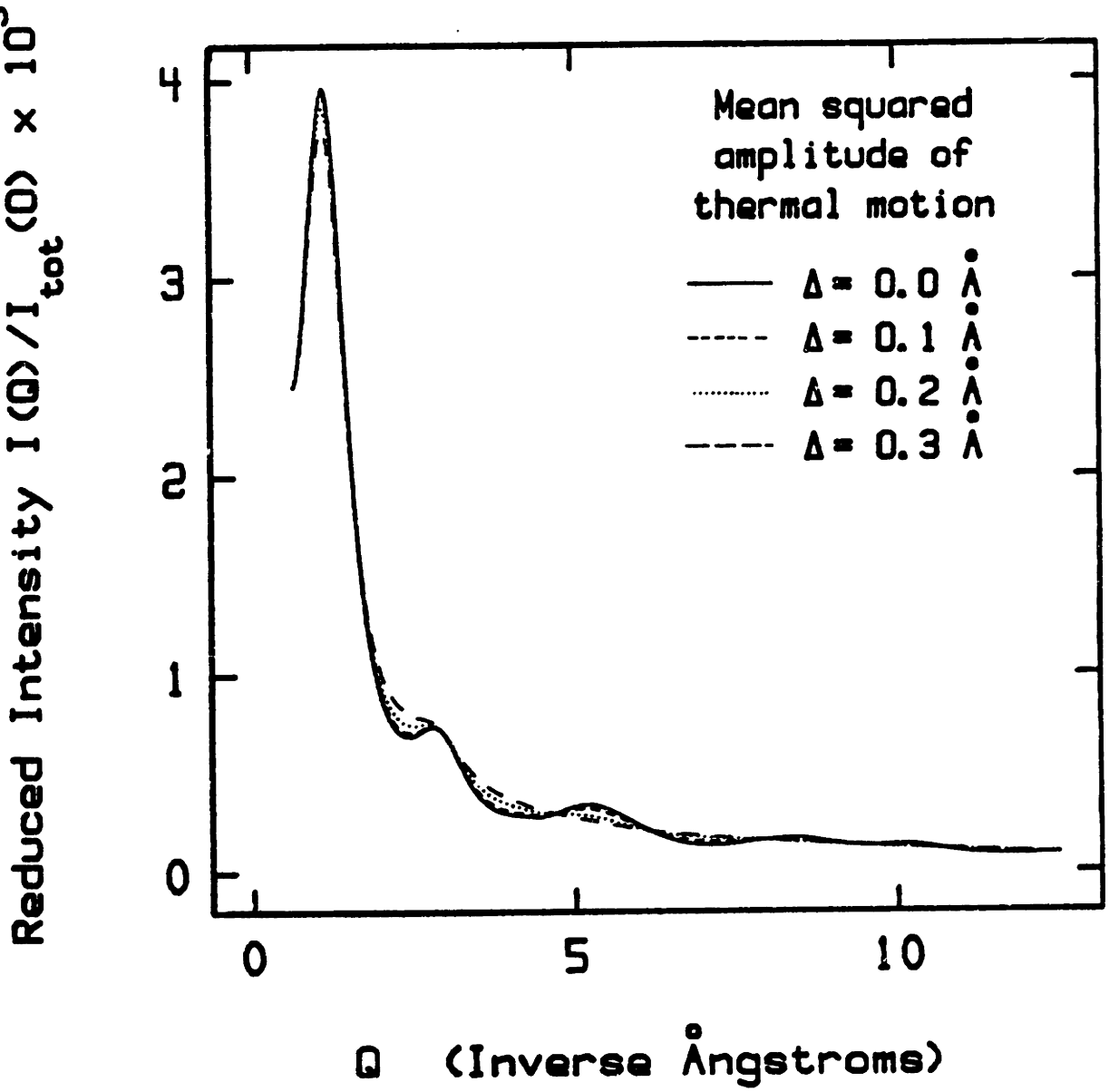

Figure 4.6

Predicted intensity of X-rays diffracted from atactic polypropylene as a function of the magnitude of the diffraction vector, Q, for various values of the thermal amplitude Δ.

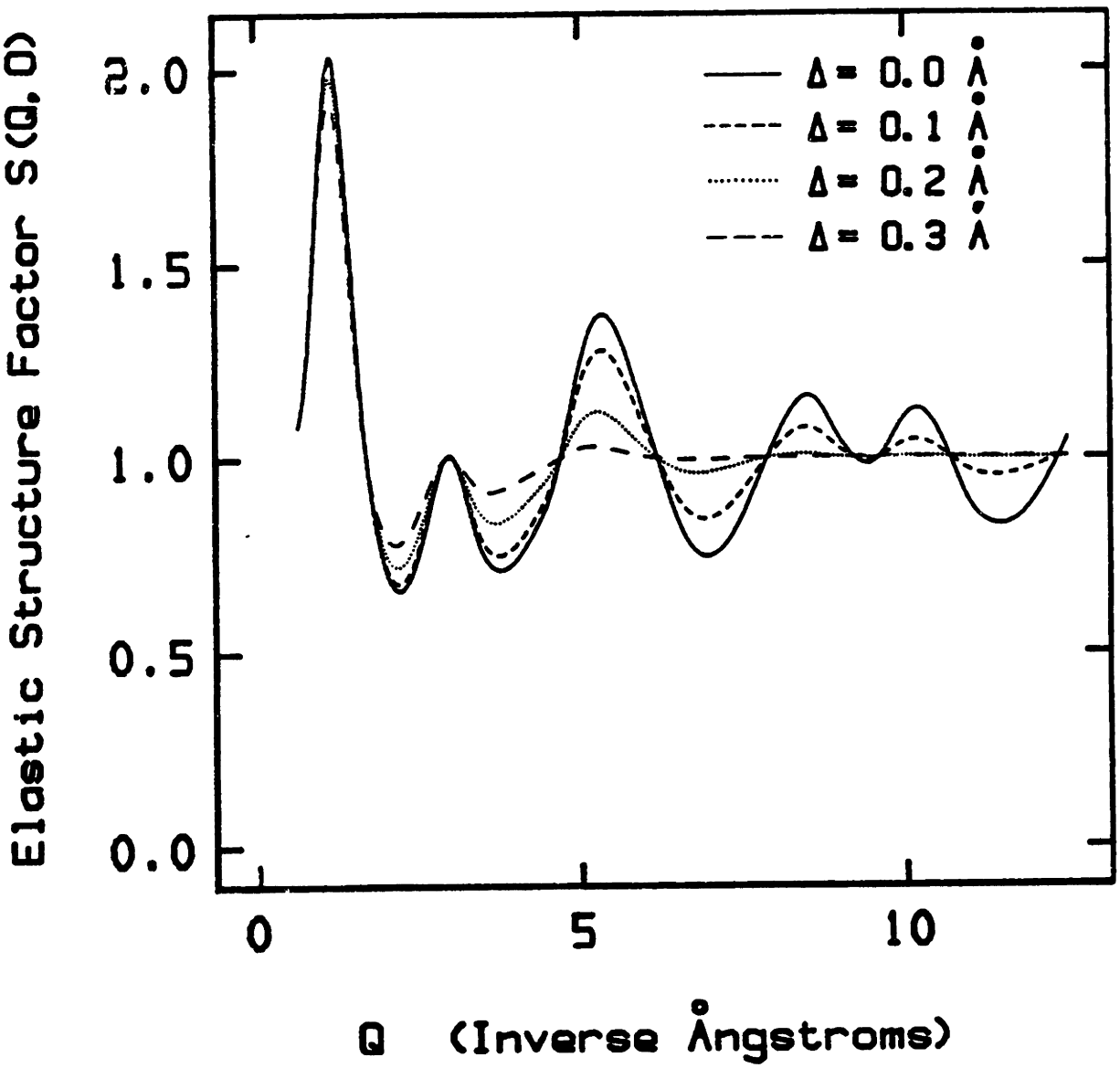

Figure 4.7

Predicted elastic structure factor for the diffraction of X-rays from atactic polypropylene as a function of the magnitude of the diffraction vector, Q, for various values of the thermal amplitude Δ.

Neutron Diffraction Pattern

Neutron scattering results from an extremely short-range interaction of thermal neutrons with atomic nuclei. The intensity $I(\underset{\sim}{Q})$ has the meaning of a differential coherent elastic scattering cross section ([15], [76]):

$$I(Q) = \frac{\text{number of neutrons/time scattered coherently and elastically, with momentum change } (\underset{\sim}{u}_n - \underset{\sim}{u}_{o,n})\, m_n / \hbar = \underset{\sim}{Q}}{\text{flux density of incident neutrons}} \qquad (4.31)$$

$I(\underset{\sim}{Q})$ is measured in units of area. The atomic scattering factors f_α are constant, independent of $\underset{\sim}{Q}$; they are known as "coherent scattering amplitudes," or "scattering lengths," and are measured in units of length. The most frequently employed unit is the Fermi (1 Fermi = 10^{-15} m). The quantities $4\pi f_\alpha^2$ are known as "coherent scattering cross sections," and are measured in barns (1 barn = 10^{-28} m^2/atom.) Table 4.3 summarizes the scattering amplitudes and cross-sections for the atomic species of interest in this work.

Observe the negative value of f_H, which indicates that coherent scattering by hydrogen is accompanied by a phase inversion of the neutron wave. Incoherent scattering refers to a situation whereby there is no interference between waves scattered by different atoms of the same species. Therefore, it amounts to a featureless background, that can bear no information on structure. Of the elements listed in Table 4.3, hydrogen exhibits a very large incoherent scattering cross-section. The value of this cross-section actually depends on the binding state, varying from a maximum of 80 barns (listed value) for completely bonded to a minimum of 20 barns for completely free hydrogen; moreover, the incoherent scattering cross-section shows a dependence on Q, falling off at high Q values.

For neutron scattering, the constant C_s appearing in eqn. (4.25) is taken equal to unity.

Table 4.3.

Neutron Scattering Amplitudes and Cross-sections ([46], [76])

Species α	Coherent Scattering Amplitude, f_α (Fermis)	Scattering Cross-section Coherent, $4\pi f_\alpha^2$ (barns)	Incoherent (barns)
Hydrogen (H)	-3.74	1.8	79.7
Carbon (C)	6.65	5.6	0.0
Deuterium (D)	6.67	5.6	2.0

Neutron diffraction patterns for the (protonated) polymer were calculated from our element pair distribution functions by a procedure analogous to that used in the case of X-rays. Normalized intensities $I(Q)/I_{tot}(0)$ and elastic structure factors $S(Q,0)$ are presented in Figures 4.8 and 4.9, for Q ranging from 0.6 to 12.5 Å^{-1}, and for four different values of the thermal amplitude, Δ. The shapes of the intensity and structure factor curves are identical in this case, due to the constancy of the atomic scattering factors.

A first observation from Figure 4.9 is that the predicted scattering is very weak, especially at low Q. According to the prediction, the elastically scattered intensity exhibits a minimum of practically zero at approx. 0.56 Å^{-1}. The reason for this weak scattering lies in the difference in sign between the scattering amplitudes of H and C; the relative proportion of these elements in polypropylene is such that they almost cancel each other. For example, calculating

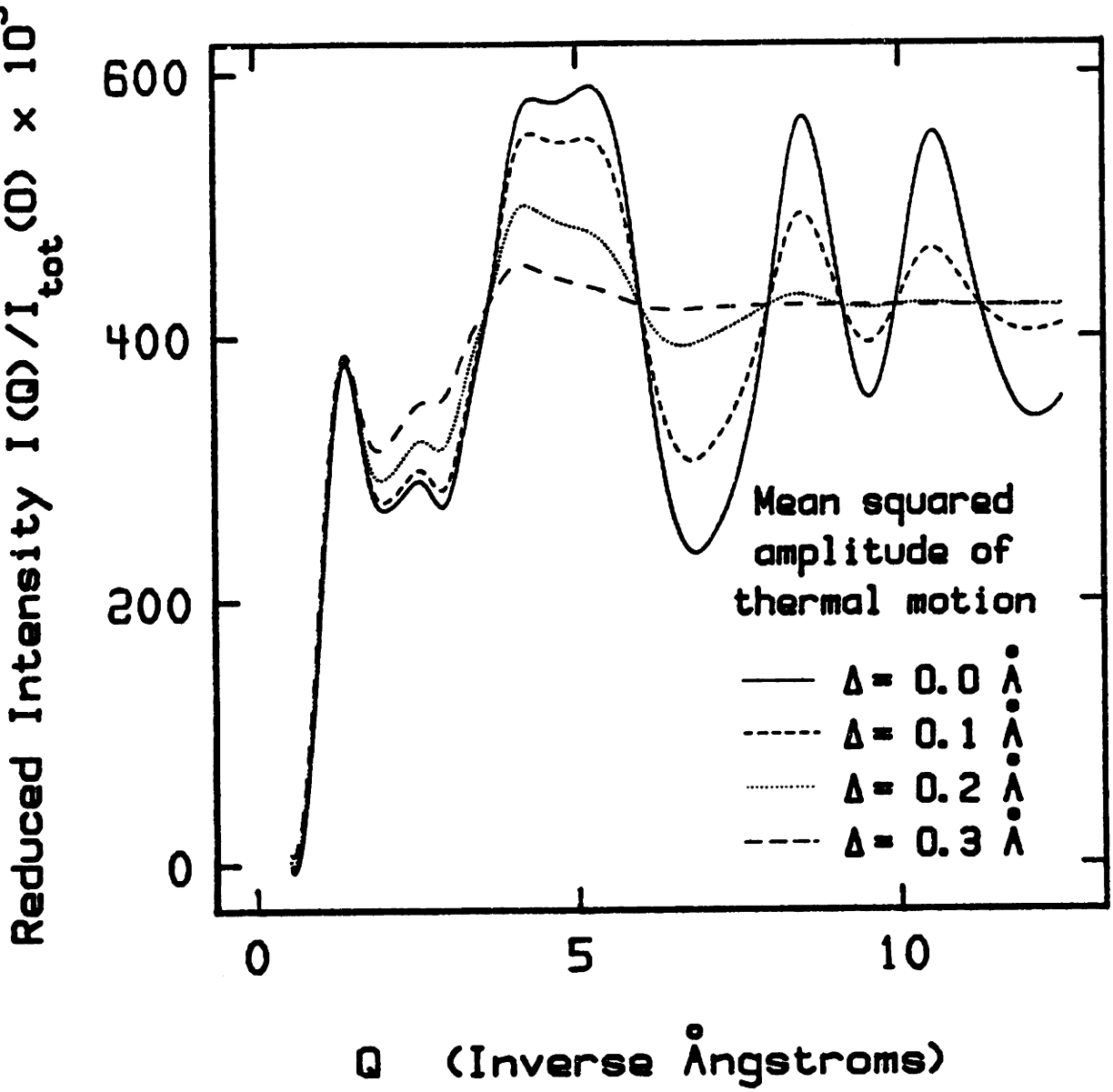

Figure 4.8

Predicted intensity of thermal neutrons diffracted from atactic polypropylene as a function of the magnitude of the diffraction vector, Q, for various values of the thermal amplitude Δ.

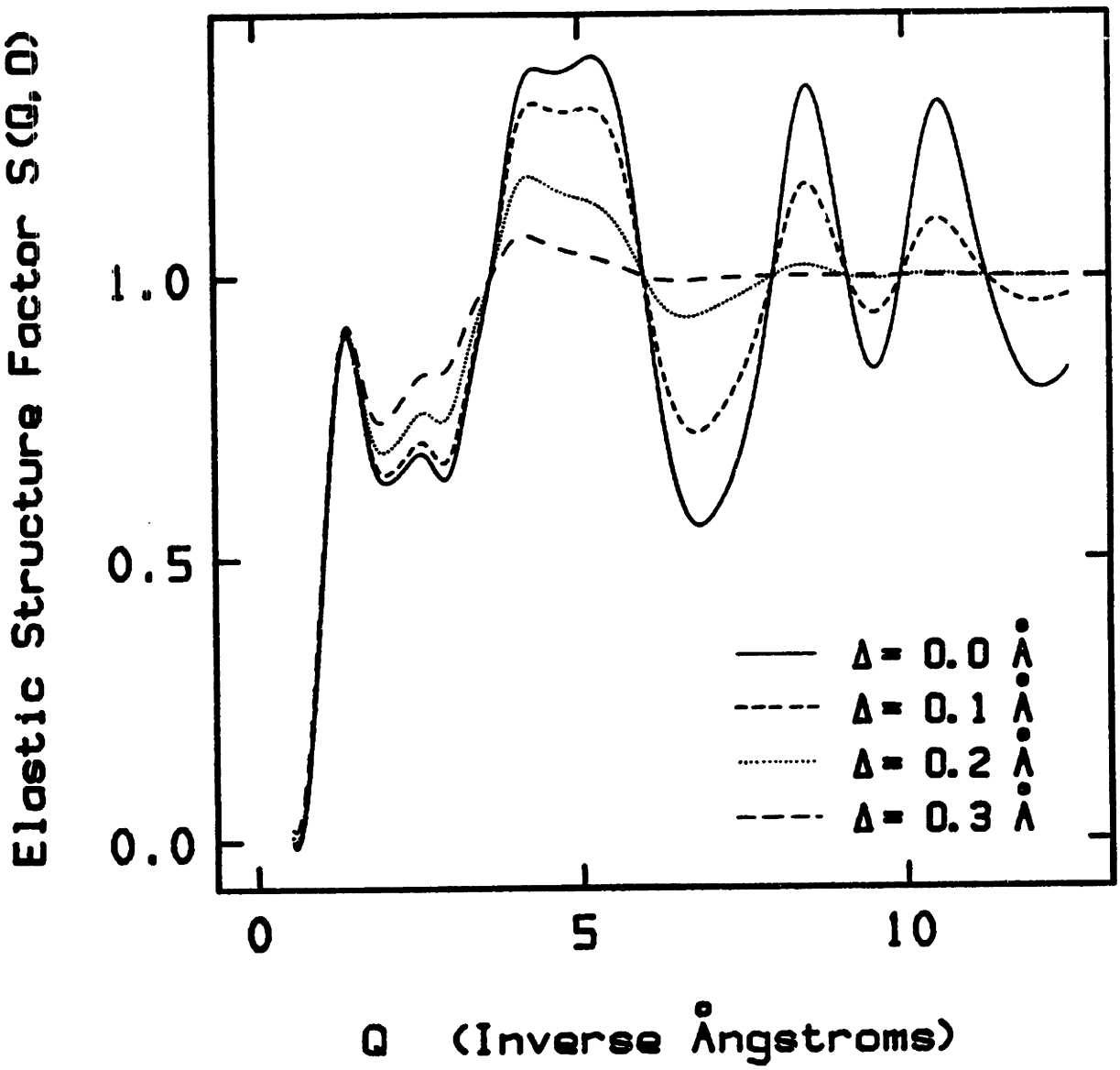

Figure 4.9

Predicted elastic structure factor for the diffraction of thermal neutrons from atactic polypropylene as a function of the magnitude of the diffraction vector, Q, for various values of the thermal amplitude Δ.

the effective scattering amplitude of one unit of the chain, (a representation in terms of units can be used in place of our detailed atomistic representation at low Q values, where scattering is governed by long-distance correlations) we find:

$$f_{C_3H_6} = 3\, f_C + 6\, f_H = 19.95 - 22.44 = -2.49 \qquad (4.32)$$

The shape of the pattern in Figs 4.8 and 4.9 is rather unconventional. It rises steeply with increasing Q to a first maximum at approx. 1.4 Å^{-1}, it passes through a second, lower maximum at approx. 2.5 Å^{-1}, and through a third at approx. 4.1 Å^{-1}. The structural features predicted at higher Q values in the Δ=0 case are washed out by thermal motion.

4.4.2. Comparison with Experiment

X - ray Diffraction Patterns

Experimental X-ray diffraction intensities were obtained from samples of equilibrium epimerized atactic polypropylene for a range of Q values from 0 to 3.4 Å^{-1}, and at temperatures of -82°C and 50°C. Details of the experimental measurement are provided in Section 7.3. The raw experimental data, after subtraction of the lines of the metal support, are plotted in Figures 4.10(a) and (c). The diffaction patterns differ only slightly between the two temperatures, confirming the structural similarity between the glass (a) and the "equilibrium" amorphous polymer (c).

The corresponding model predictions for the diffracted intensity have been plotted for the same Q-range, and for two different values of the mean squared amplitude of thermal motion, Δ = 0.0 Å (static case), and Δ = 0.30 Å, in Figures

4.10(b) and (d). (These plots simply redisplay a portion of the curves presented in Fig. 4.6.)

In the experimental curves one clearly discerns two maxima, centered at 1.20 Å^{-1} and 2.79 Å^{-1}. The locations of these maxima are predicted very accurately by the model (see Section 4.4.1 for theoretical prediction and interpretation of the peaks.) The fact that the intermolecular peak is well predicted is particularly encouraging, because it indicates that chain-chain correlations are realistically represented in our model of the bulk polymer. The relative heights of the maxima in the prediction are also in good agreement with experiment. As far as the shape of the pattern is concerned, peaks in the predicted patterns appear somewhat broader and more "diffuse"; this is especially true of the lower, bonded peak. The static predicted pattern (Δ= 0.0 Å) seems to reproduce more accurately the features of both experimental curves. The experimental curve at 2.79 Å^{-1} appears as a double hump, which indicates two distinct $C\diagup^{C}\diagdown C$ distances in the real polymer. This feature is not reproduced by the prediction, probably because of the simplified geometry used in the model (fixed bond lengths and bond angles, C - R bond taken equal to C - C bond.)

Neutron Diffraction Patterns

Neutron elastic scattering data were obtained from a sample of the (protonated) polymer for Q values ranging from 0.3 to 7 Å^{-1}, at -40°C (temperature of the model.) Details of the experiment are given in Section 7.4. The accuracy of the measurement is limited by the very large incoherent scattering cross-section of hydrogen (compare data in Table 4.3.) The weak coherent pattern is superposed on a very strong incoherent background. This background was assumed to vary linearly with Q [44], and was subtracted from the total count at each Q value, to obtain the pure coherent contribution. The latter

is displayed in Fig. 4.11(a). The magnitude of the error bars reflects the uncertainty due to background subtraction. A smooth curve has been passed through the data, to outline structural features. There is no structure beyond 5 $\mathring{A}^{-1}$. One can clearly discern a sharply rising pattern at low Q values, and three maxima at approx. 1.2, 2.1 and 3.8 $\mathring{A}^{-1}$. The predicted coherent elastic differential cross section is plotted in Fig. 4.11(b) for the same range of Q values. (This plot simply redisplays a portion of the curve presented in Fig. 4.8.) A value of $\Delta = 0.30$ $\mathring{A}$ has been used, as it is compatible with the absence of structure at high Q values. The predicted pattern is in good qualitative agreement with experiment. It exhibits the sharp rise at low Q, and the three maxima. The locations of the maxima agree satisfactorily with experiment (compare section 4.4.1.) The relative heights of the maxima, however, differ between Figs 4.11(a) and (b). This is probably partly due to the subtraction of the very high incoherent background in the experiment. It has been assumed that the incoherent contribution varies linearly with Q; in reality, however, it may show a more complicated Q-dependence.

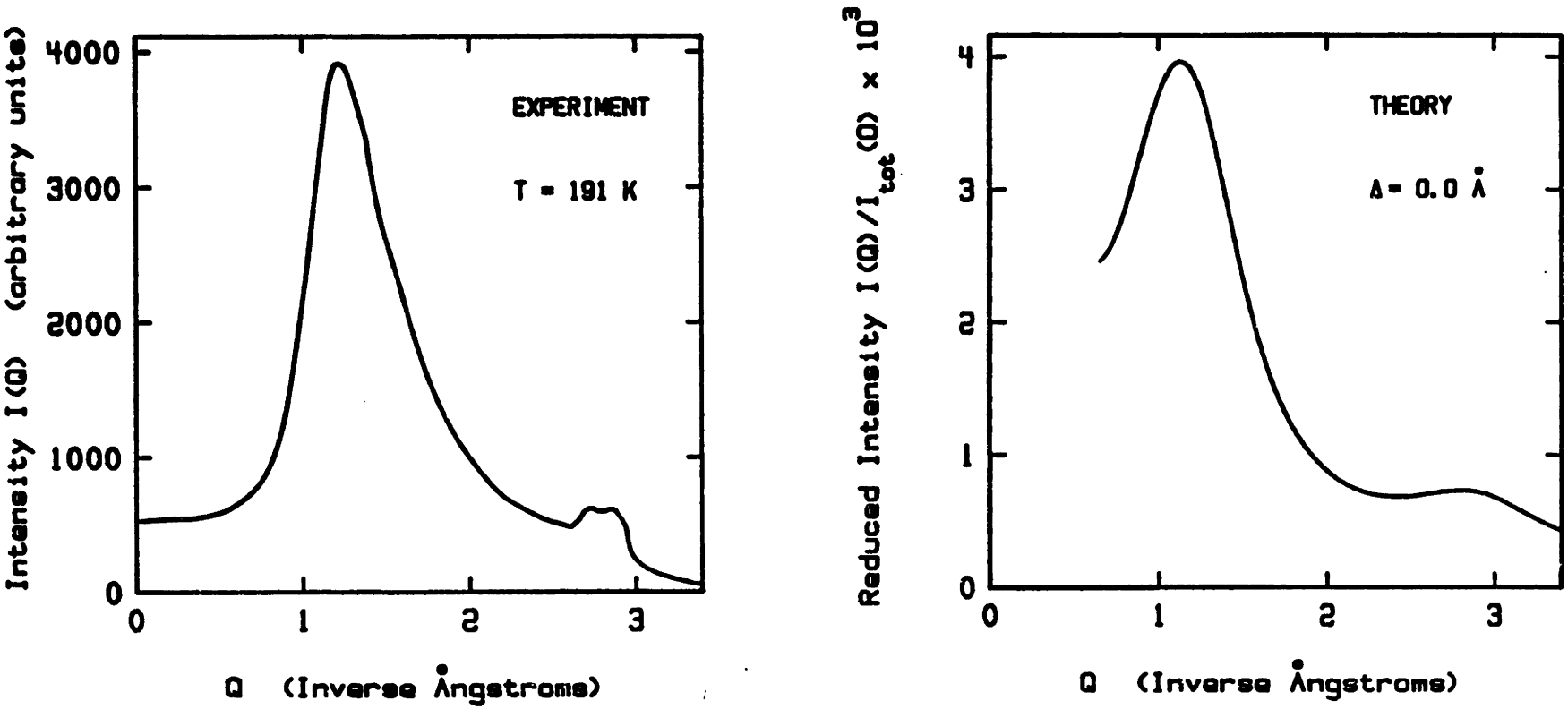

Figure 4.10 (a,b)

Comparison of experimental and predicted X-ray diffraction patterns of atactic polypropylene

(a) Experiment, Glassy Atactic Polypropylene at -82°C

(b) Theory, Amplitude of Thermal Motion A = 0.0 Å

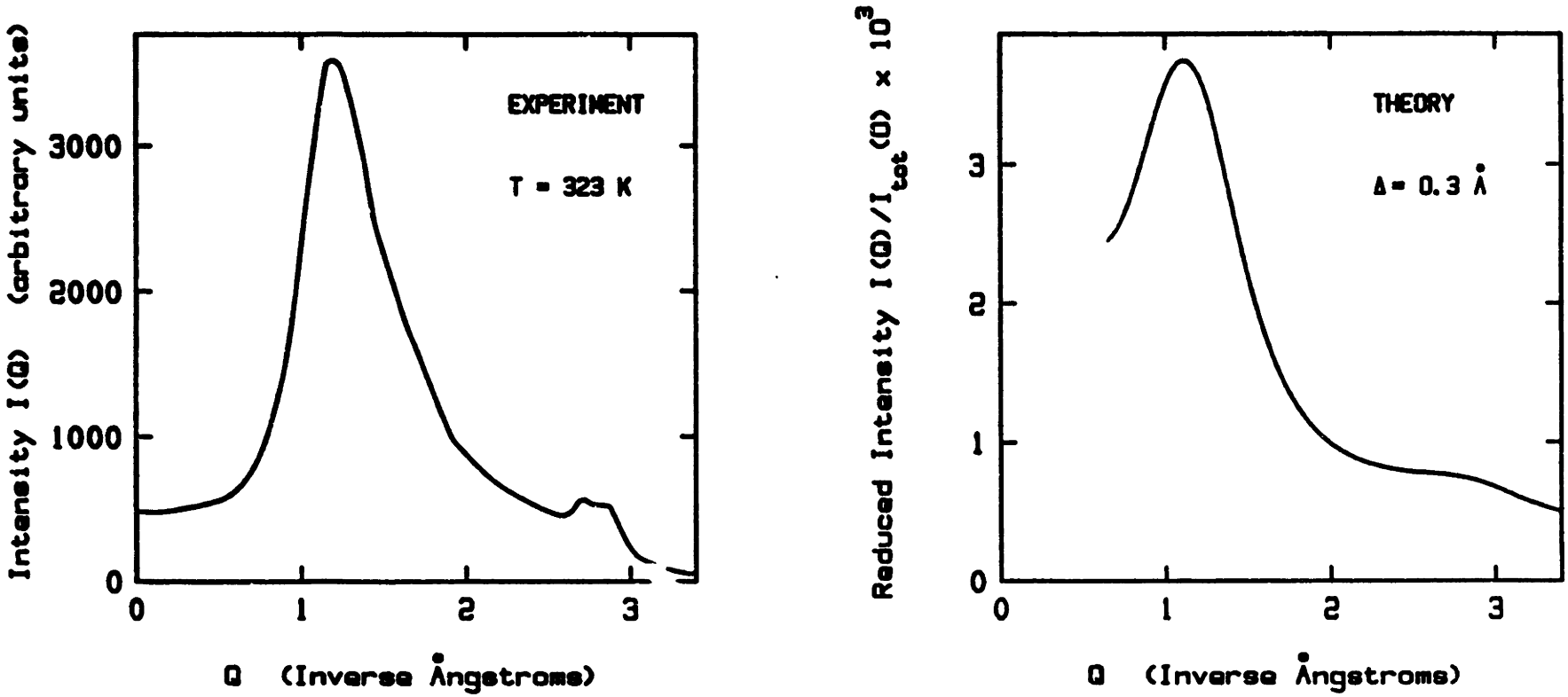

Figure 4.10 (c,d)

Comparison of experimental and predicted X-ray diffraction patterns of atactic polypropylene

(c) Experiment, Atactic Polypropylene at 50°C

(d) Theory, Amplitude of Thermal Motion Δ = 0.3 Å

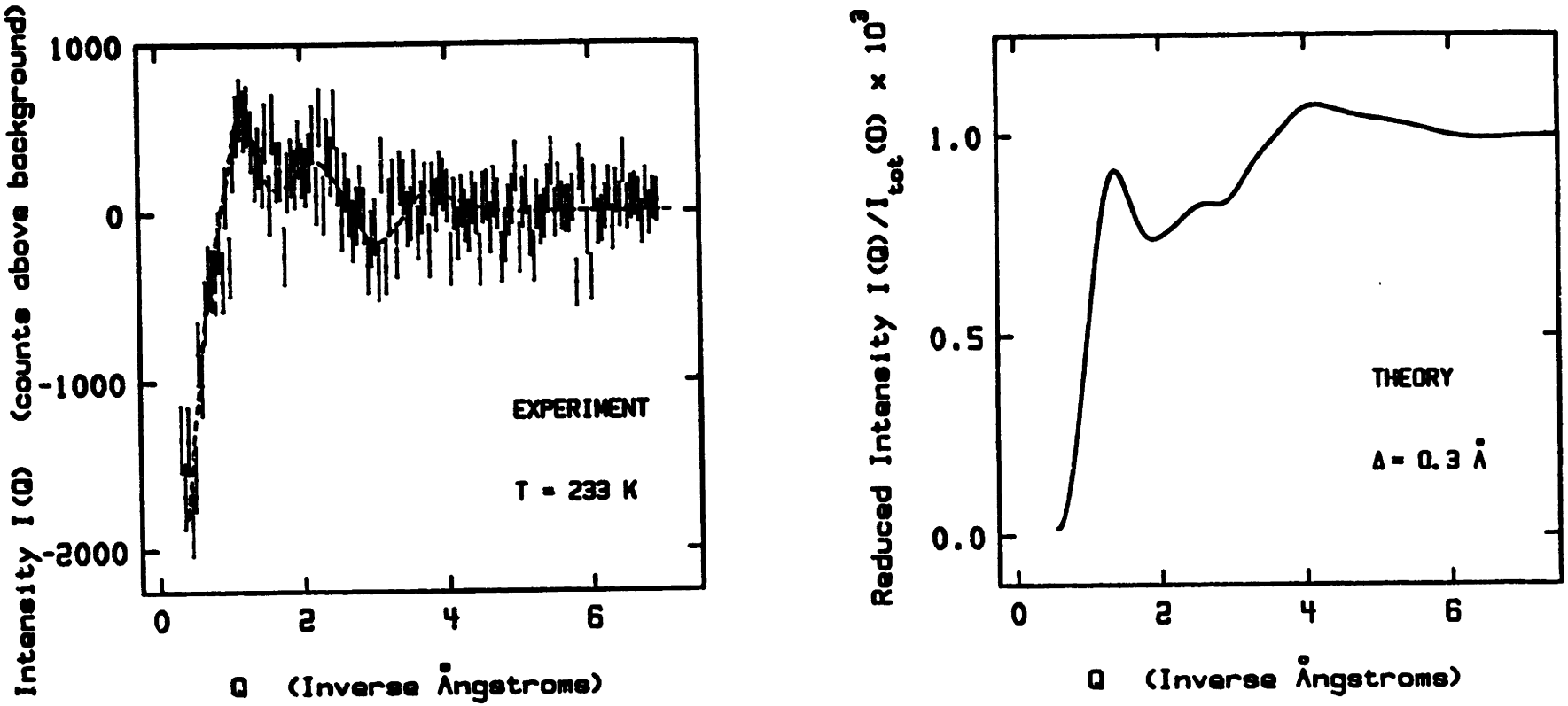

Figure 4.11

Comparison of experimental and predicted neutron diffraction patterns of glassy atactic polypropylene

5. PREDICTION OF MECHANICAL PROPERTIES

5.1. METHOD FOR THE MODELLING OF DEFORMATION

The theoretical framework underlying the prediction of mechanical properties has been set in Chapter 2, and the basic assumptions to be used in this prediction have been introduced in Section 3.1. We have to model the structural changes, on the atomistic level, brought about by various forms and degrees of deformation. From the functional dependence of the total potential energy on externally imposed small-strain deformations we will obtain the elastic constants.

Thus, there arises the following fundamental problem: how is a given macroscopic deformation to be interpreted on the molecular level? In other words, how will each microscopic degree of freedom respond when we impose a change on the external boundaries of the system? A frequently used assumption is that of "affine," or "homogeneous" ([75], p.9) or "quasicontinuum" ([73]) deformation, whereby all atom coordinates are transformed by a simple linear rule:

$$\underline{r}^{affine} = \underline{\underline{A}}\,\underline{r}_o + \underline{b} \qquad (5.1)$$

whence, using eqn. (2.1),

$$\underline{\underline{\varepsilon}}^{affine} = \frac{1}{2}\left(\underline{\underline{A}}^T\,\underline{\underline{A}} - \underline{\underline{I}}\right) = \frac{1}{2}\left(\underline{\underline{A}}^T + \underline{\underline{A}}\right) - \underline{\underline{I}} \qquad (5.2)$$

Such an affine transformation is impossible in our model systems, because it would entail distortion of bond lengths and bond angles, contrary to the requirements of Assumption C. Moreover, the result of an affine transformation will not, in general, satisfy the requirement of detailed mechanical equilibrium, imposed by Assumption B (Section 3.1.) Thus,

deformation in our systems has to be introduced in a subtler way.

The method developed in this thesis for simulating deformation consists of the following steps:

1. Start with an undeformed structure in detailed mechanical equilibrium. The continuation geometry in the undeformed state is cubic, i.e., continuation vectors $\underset{\sim}{a}_{x_o}$, $\underset{\sim}{a}_{y_o}$, $\underset{\sim}{a}_{z_o}$ are mutually perpendicular and equal in magnitude. The starting structure is a member of the ensemble of 15 structures discussed in Chapter 4, and satisfies the condition:

$$U^{pot}(\Psi, \Phi; \underset{\sim}{a}_{x_o}, \underset{\sim}{a}_{y_o}, \underset{\sim}{a}_{z_o}) = \min \qquad (5.3)$$

2. Choose the type of deformation to be imposed. Choose a small degree of deformation ε, such that $|\varepsilon| << 1$.

3. Modify the location of the cube origin $\underset{\sim}{Q}$ and the continuation vectors $\underset{\sim}{a}_x$, $\underset{\sim}{a}_y$ and $\underset{\sim}{a}_z$, so that they correspond to the chosen deformation. For the simple deformations studied in this work, initial system quantities ($\underset{\sim}{Q}_o$, $\underset{\sim}{a}_{x_o}$, $\underset{\sim}{a}_{y_o}$, $\underset{\sim}{a}_{z_o}$) are transformed to give the deformed system quantities ($\underset{\sim}{Q}$, $\underset{\sim}{a}_x$, $\underset{\sim}{a}_y$, $\underset{\sim}{a}_z$) as follows:

<u>Uniform Hydrostatic Compression</u>

$$\begin{aligned}
\underset{\sim}{Q} &= \underset{\sim}{Q}_o + \frac{1 - (1-\varepsilon)^{1/3}}{2} \left[\underset{\sim}{a}_{x_o} + \underset{\sim}{a}_{y_o} + \underset{\sim}{a}_{z_o} \right] \\
\underset{\sim}{a}_x &= (1-\varepsilon)^{1/3} \underset{\sim}{a}_{x_o} \\
\underset{\sim}{a}_y &= (1-\varepsilon)^{1/3} \underset{\sim}{a}_{y_o} \\
\underset{\sim}{a}_z &= (1-\varepsilon)^{1/3} \underset{\sim}{a}_{z_o}
\end{aligned} \qquad (5.4)$$

Pure Shear (perpendicular to z, along x)

$$\begin{aligned} \underset{\sim}{Q} &= \underset{\sim}{Q}_o - \frac{1}{2} \cdot \varepsilon \; \underset{\sim}{a}_{x_o} \\ \underset{\sim}{a}_x &= \underset{\sim}{a}_{x_o} \\ \underset{\sim}{a}_y &= \underset{\sim}{a}_{y_o} \\ \underset{\sim}{a}_z &= \underset{\sim}{a}_{z_o} + \varepsilon \; \underset{\sim}{a}_{x_o} \end{aligned} \qquad (5.5)$$

Pure Uniaxial Tension (along x)

$$\begin{aligned} \underset{\sim}{Q} &= \underset{\sim}{Q}_o - \frac{1}{2} \cdot \varepsilon \; \underset{\sim}{a}_{x_o} \\ \underset{\sim}{a}_x &= (1+\varepsilon) \; \underset{\sim}{a}_{x_o} \\ \underset{\sim}{a}_y &= \underset{\sim}{a}_{y_o} \\ \underset{\sim}{a}_z &= \underset{\sim}{a}_{z_o} \end{aligned} \qquad (5.6)$$

In eqns (5.4) to (5.6) $\underset{\sim}{Q}$ has been chosen so that the cube center remains the same before and after deformation. The transformations for other modes of shear and tension are obtained from (5.5), (5.6) by cyclic permutation. The undeformed system degrees of freedom (ψ , ϕ), together with the deformed continuation vectors $\underset{\sim}{a}_x$, $\underset{\sim}{a}_y$, $\underset{\sim}{a}_z$, define a new initial guess structure, which is <u>not</u> in detailed mechanical equilibrium.

4. Starting from this initial guess structure, minimize the total potential energy with respect to the 2x+1 microscopic degrees of freedom (ψ, ϕ), keeping the continuation vectors equal to their deformed values:

$$U^{pot}(\psi , \phi ; \underset{\sim}{a}_x , \underset{\sim}{a}_y , \underset{\sim}{a}_z) = \min \qquad (5.7)$$

The resulting structure again satisfies the conditions of detailed mechanical equilibrium, but under the

continuation geometry dictated by the mode and degree of deformation chosen in Step 2. [compare eqns (5.3), (5.7)]; it is a "deformed model structure." The minimization (5.7) is again performed using the BFGS quasi-Newton algorithm, using the analytical gradient developed in Appendix C. Computationally, the minimization problem [eqn. (5.7)] is identical to the relaxation problem discussed in Section 3.2. Since we want to realistically reproduce the elastic response of a glassy structure to small deformations, the "full" nonbonded interaction and torsional potential functions are used throughout the minimization (compare Section 3.2.) The computation time for an energy and gradient evaluation on the MIT Honeywell DPS 8/70 computer is, again, 77 seconds. Reaching a minimum energy deformed model structure for $|\varepsilon| = 0.001$ typically requires 300 to 450 function evaluations.

5. To study different degrees of deformation, change ε and go back to step 3.

Step 4 in the above procedure requires large amounts of computer time. We thus developed a computational expedient, which consists of a preliminary "approximately affine" deformation. It was carried out between Steps 3 and 4, as follows:

3a. Bring the cube interior as close as possible to an affine deformation. This is done by minimizing the sum of squares of the differences between actual and affinely deformed coordinates:

$$\sum_{i=1}^{6x-1} \{\underline{r}_i(\underline{r}_{C_o}, \Psi, \Phi; \underline{a}_x, \underline{a}_y, \underline{a}_z) - \underline{r}_i^{affine}(\underline{r}_{o,i}, \underline{0}_o, \underline{a}_{x_o}, \underline{a}_{y_o}, \underline{a}_{z_o}, \varepsilon)\}^2 = \text{minimum} \qquad (5.8)$$

During this minimization the continuation vectors $\underset{\sim}{a}_x$, $\underset{\sim}{a}_y$, $\underset{\sim}{a}_z$ are fixed at their deformed values. Also, the continuation coefficients (see appendix C) of each atom are kept equal to their values in the undeformed state. Minimization is performed with respect to the $2x+4 = 156$ variables $(\underset{\sim}{r}_{C_o}, \Psi, \Phi)$ using the undeformed state values $(\underset{\sim}{r}_{C_{o,o}}, \Psi_o, \Phi_o)$ as an initial guess.

The constants $\underset{\sim}{r}_i^{affine}$ for each type of deformation are determined as follows:

Uniform Hydrostatic Compression

$$\underset{\sim}{r}^{affine} = \underset{\sim}{0}_o + \frac{1 - (1-\varepsilon)^{1/3}}{2} \{\underset{\sim}{a}_{x_o} + \underset{\sim}{a}_{y_o} + \underset{\sim}{a}_{z_o}\} + (\underset{\sim}{r}_o - \underset{\sim}{0}_o)(1-\varepsilon)^{1/3} \tag{5.9}$$

Pure Shear (perpendicular to z, along x)

$$\underset{\sim}{r}^{affine} = \underset{\sim}{r}_o + \varepsilon \left\{ \frac{(\underset{\sim}{r}_o - \underset{\sim}{0}_o)\cdot(\underset{\sim}{a}_{x_o} \times \underset{\sim}{a}_{y_o})}{\underset{\sim}{a}_{z_o} \cdot (\underset{\sim}{a}_{x_o} \times \underset{\sim}{a}_{y_o})} - \frac{1}{2} \right\} \underset{\sim}{a}_{x_o} \tag{5.10}$$

Pure Uniaxial Tension (along x)

$$\underset{\sim}{r}^{affine} = \underset{\sim}{r}_o + \varepsilon \left\{ \frac{(\underset{\sim}{r}_o - \underset{\sim}{0}_o)\cdot(\underset{\sim}{a}_{y_o} \times \underset{\sim}{a}_{z_o})}{\underset{\sim}{a}_{x_o} \cdot (\underset{\sim}{a}_{y_o} \times \underset{\sim}{a}_{z_o})} - \frac{1}{2} \right\} \underset{\sim}{a}_{x_o} \tag{5.11}$$

Equations (5.9), (5.10) and (5.11) are of the general form (5.1). One can easily verify that they are the affine transformation equations corresponding to the boundary displacements of eqns (5.4), (5.5) and (5.6), and that they leave the cube center unchanged. Affine equations for other shears and tensions are obtained from eqns (5.10) and (5.11) by cyclic permutation. Approximately 300 objective function and gradient evaluations are typically needed to reach the minimum of

eqn. (5.8). The CPU time per function and gradient evaluation at the MIT Honeywell DPS 8/70 is less than 2 seconds. The sum, over all 455 atoms, of the squared deviations from affine displacement at the minimum is typically about $0.5 \cdot 10^{-3}$ Å^2 in the case of shear, about $0.1 \cdot 10^{-2}$ Å^2 in the case of compression, and about $0.2 \cdot 10^{-2}$ Å^2 in the case of uniaxial tension. Use of Step 3a typically reduces the number of function evaluations in Step 4 by ca 100; it reduces the overall computing effort by roughly 30%.

It must be emphasized again that Step 3a, i.e. the step of approximately affine deformation, is merely a computational expedient. Its purpose is to bring the structure closer to the deformed minimum energy configuration. Its utility lies in the fact that the minimization [eqn. (5.8)] is much less time consuming than the minimization [eqn. (5.7)]. If we omit Step 3a, we obtain <u>the same</u> deformed model structure, but at greater expense in computer time.

An observation worth mentioning is that, if one starts from a deformed model structure, as determined in Step 5, reverses the deformation by changing the continuation vectors $\underset{\sim}{a}_x$, $\underset{\sim}{a}_y$, $\underset{\sim}{a}_z$ back to $\underset{\sim}{a}_{x_o}$, $\underset{\sim}{a}_{y_o}$, $\underset{\sim}{a}_{z_o}$, and minimizes $U^{pot}(\psi, \phi; \underset{\sim}{a}_{x_o}, \underset{\sim}{a}_{y_o}, \underset{\sim}{a}_{z_o})$, one recovers the undeformed model structure (ψ_o, ϕ_o). In other words, within the strain range studied (ε of the order 10^{-3}) the model system's response to deformation is completely reversible, or "elastic," as demanded by assumption F (Section 3.1.)

The above observations support the idea that the detailed mechanical equilibrium requirement $U^{pot}(\psi, \phi; \varepsilon) = \text{min.}$ has a <u>unique</u> solution (ψ, ϕ) around the undeformed state (ψ_o, ϕ_o) within the range of degrees of deformation (ε) studied. This uniqueness characteristic may cease to hold for considerably larger values of ε. A bifurcation in the minimum potential

energy trajectory in configuration space might be indicative of the onset of flow.

Steps 3 and 4 constitute a new, perfectly general algorithm for the imposition of deformation in any periodic model system, which is of wider applicability and more rigorous than previous approaches (compare [75], Chapter 4.) Deformation is modelled as a progressive change in the periodic continuation conditions. Changes in the interior of the cube come as a consequence of displacements in its surroundings. The unconstrained minimization requirement [eqn. (5.7)] ensures that no artificial external forces are imposed on the interior of the modelled infinite continuum. Our scheme is totally free of preconceived assumptions (such as affine deformation.) In the case of a simple lattice, where all atoms are equivalent, the sequence of steps 3. and 4. would naturally lead to an affinely deformed state; thus, our method contains affine deformation as a special case.

The outcome from performing the loop of steps 3 to 5 many times is a sequence of deformed structures, corresponding to various degrees of deformation. Such a sequence, obtained from a series of hydrostatic compression-tension runs, is plotted in Fig. 5.1 as total potential energy U^{pot} (including tail corrections) versus fractional increase in volume. The point representative of the undeformed state lies at the center. On either side of it lie points representative of fractional compressions ±0.001, ±0.002, ±0.004, and ±0.008. All nine points fall on a smooth curve. For predicting the microscopic mechanical properties we require the slope and the curvature around the undeformed state [compare eqns (2.45), (2.46)]. We thus choose to confine ourselves to degrees of deformation of +0.001 and -0.001. These two points, together with the undeformed system point, provide all the information necessary.

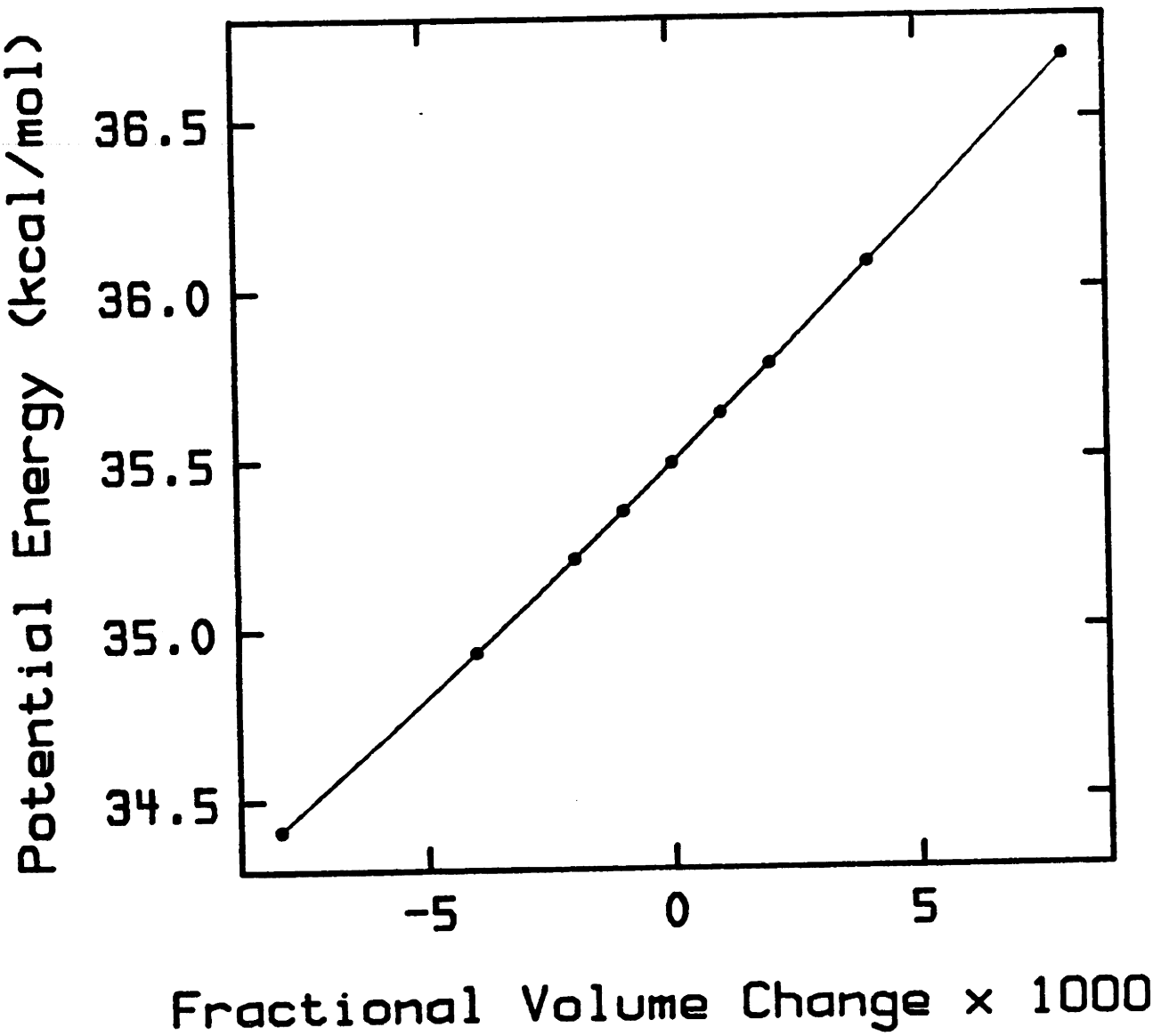

Figure 5.1

Total potential energy as a function of fractional increase in volume, for one model structure subjected to hydrostatic compression-tension experiments.

Each undeformed structure is studied in the following 14 modes and degrees of deformation:

1. Uniform Hydrostatic Compression, $\varepsilon = \pm 0.001$

   As seen from eqns. (5.4) and (5.9), the degree of deformation ε is defined as a fractional decrease in volume. From eqns (2.1) and (5.9), the strain tensor for this deformation is

$$\underline{\underline{\varepsilon}} = \begin{bmatrix} -\varepsilon/3 & 0 & 0 \\ 0 & -\varepsilon/3 & 0 \\ 0 & 0 & -\varepsilon/3 \end{bmatrix}$$

   and the vector of 6 strain components [eqn. (2.3)] is

$$\underline{\varepsilon} = [\, -\varepsilon/3 \quad -\varepsilon/3 \quad -\varepsilon/3 \quad 0 \quad 0 \quad 0 \,]^T \qquad (5.12)$$

2. Pure Shear, $\varepsilon = \pm 0.001$

   a. Perpendicular to z, along x $\quad \varepsilon = \pm 0.001$

   b. Perpendicular to z, along y $\quad \varepsilon = \pm 0.001$

   c. Perpendicular to x, along y $\quad \varepsilon = \pm 0.001$

   The degree of deformation ε [eqns (5.5), (5.10)] is defined as a component of shear strain [eqn. (2.3)]. For the zx-shear transformation, for instance, the strain tensor [eqns (2.1), (5.10)] is:

$$\underline{\underline{\varepsilon}} = \begin{bmatrix} 0 & 0 & \varepsilon/2 \\ 0 & 0 & 0 \\ \varepsilon/2 & 0 & 0 \end{bmatrix}$$

   and the vector of 6 strain components is

$$\underline{\varepsilon} = [\, 0 \quad 0 \quad 0 \quad \varepsilon \quad 0 \,]^T \qquad (5.13)$$

   and similarly for the zy- and xy- shears. In addition to the shear modes listed above, we performed some computer experiments in shear perpendicular to x and parallel

to z, to check our computations for consistency. The properties of a xz- sheared minimum energy structure are identical to those of the corresponding zx- sheared minimum energy structure, as expected from mechanics.

2. Pure Uniaxial Tension, $\varepsilon = \pm 0.001$

   a. Along x $\quad \varepsilon = \pm 0.001$

   b. Along y $\quad \varepsilon = \pm 0.001$

   c. Along z $\quad \varepsilon = \pm 0.001$

   In the case of tension, the degree of deformation ε [eqns. (5.6), (5.11)] is defined as a tensile strain. For example, in uniaxial tension along x the strain tensor [eqns (2.1), (5.11)] is:

$$\underline{\underline{\varepsilon}} = \begin{bmatrix} \varepsilon & 0 & 0 \\ 0 & 0 & 0 \\ 0 & 0 & 0 \end{bmatrix}$$ and the vector of 6 strain components is

$$\underline{\varepsilon} = [\, \varepsilon \quad 0 \quad 0 \quad 0 \quad 0 \,]^T \tag{5.14}$$

The above 14 deformations allow ample room for consistency checking.

5.2. CALCULATION OF THE INTERNAL STRESS AND THE ELASTIC COEFFICIENTS

Eight of the fifteen undeformed model structures, generated as described in Chapter 3, and discussed in Chapter 4, have been studied in the deformations described above. Hence, eight sets of structures, each consisting of one undeformed and 14 deformed states, were obtained. From each such set of

structures estimates of the mechanical properties were deduced by three methods, described below.

5.2.1. Energy Approach

This approach rests on a Taylor expansion of the total potential energy, U^{pot}_{min}, with respect to the degree of deformation, ε, around the undeformed state.

By virtue of equations (2.45) and (2.46), expanding the function U^{pot}_{min} in a manner entirely analogous to eqn. (2.11), we obtain

$$U^{min}_{pot} = U^{pot}_{min,o} + V_o \sum_{LM} \left[\tau_{LM} + \rho_o c_\varepsilon T \gamma_{LM} \right] \varepsilon_{LM} + \frac{1}{2} V_o \sum_{LM} \sum_{NK} C_{LMNK} \varepsilon_{LM} \varepsilon_{NK} \qquad (5.15)$$

where the tensor appearing in the first order term is the "internal stress" [eqn. (2.12)] and C_{LMNK} is an element of the fourth order tensor of isothermal elastic coefficients. Substituting the expressions (5.12), (5.13) and (5.14) for the strain tensor, and converting to condensed notation, we get from (5.15) the following special forms for the particular deformations studied:

Uniform Hydrostatic Compression

$$U^{min}_{pot} = U^{pot}_{min,o} - V_o \frac{1}{3} Tr \left(\underline{\underline{I}} + \rho_o c_\varepsilon T \underline{\underline{\gamma}} \right)_o \varepsilon +$$

$$+ \frac{1}{2} V_o \left(C_{1111} + C_{1122} + C_{1133} + C_{2211} + C_{2222} + \right.$$

$$+ C_{2233} + C_{3311} + C_{3322} + C_{3333}) \frac{\varepsilon^2}{9} =$$

$$= U^{pot}_{min,o} \underbrace{- V \left(-P + \frac{\alpha_p T}{\kappa_T}\right)_o \varepsilon}_{\frac{\partial U^{pot}_{min}}{\partial \varepsilon}} + \frac{1}{2} \underbrace{V_o B}_{\frac{\partial^2 U^{pot}_{min}}{\partial \varepsilon^2}} \varepsilon^2$$

(5.16)

Pure Shear (perpendicular to z, along x)

$$U^{min}_{pot} = U^{pot}_{min,o} + V_o \left[\tau_{13} + \tau_{31} + \rho_o c_\varepsilon T (\gamma_{13} + \gamma_{31})\right]_o \varepsilon/2 +$$

$$+ \frac{1}{2} V_o (C_{1313} + C_{1331} + C_{3113} + C_{3131}) (\varepsilon/2)^2 =$$

$$= U^{pot}_{min,o} \underbrace{+ V_o (\tau_5 + \rho_o c_\varepsilon T \gamma_5)_o \varepsilon}_{\frac{\partial U^{pot}_{min}}{\partial \varepsilon}} + \frac{1}{2} \underbrace{V_o C_{55}}_{\frac{\partial^2 U^{pot}_{min}}{\partial \varepsilon^2}} \varepsilon^2$$

(5.17)

Pure Uniaxial Tension (along x)

$$U^{min}_{pot} = U^{pot}_{min,o} + V_o (\tau_{11} + \rho_o c_\varepsilon T \gamma_{11})_o \varepsilon + \frac{1}{2} V_o C_{1111} \varepsilon^2 =$$

$$= U^{pot}_{min,o} \underbrace{+ V_o (\tau_1 + \rho_o c_\varepsilon T \gamma_1)_o \varepsilon}_{\frac{\partial U^{pot}_{min}}{\partial \varepsilon}} + \frac{1}{2} \underbrace{V_o C_{11}}_{\frac{\partial^2 U^{pot}_{min}}{\partial \varepsilon^2}} \varepsilon^2$$

(5.18)

The slopes $\frac{\partial U^{pot}_{min}}{\partial \varepsilon}$ and curvatures $\frac{\partial^2 U^{pot}_{min}}{\partial \varepsilon^2}$ were estimated from the results of our deformation simulations by three-point finite-difference formulae.

$$\frac{\partial U^{pot}_{min}}{\partial \varepsilon} \simeq \frac{U^{pot}_{min}(+0.001) - U^{pot}_{min}(-0.001)}{0.002} \tag{5.19}$$

$$\frac{\partial^2 U^{pot}_{min}}{\partial \varepsilon^2} \simeq \frac{U^{pot}_{min}(+0.001) + U^{pot}_{min}(-0.001) - 2\, U^{pot}_{min,o}}{(0.001)^2}$$

Contributions from "potential tails" are taken into account for compression and tension, since these do not preserve the system volume. The tail contribution is inversely proportional to system volume, and has the form [compare eqn. (4.4)]

$$\Delta U^{pot}_{tails} = \Delta U^{pot}_{tails,o} \left(\frac{V_o}{V} \right) \tag{5.20}$$

where

$$\Delta U^{pot}_{tails,o} = -84.76 \ \frac{kcal}{mol\ structures}$$

A test for internal consistency is provided by the fact that the "internal pressure," $-P + \alpha_P T / \kappa_T$, from eqn. (5.16) must be equal to

$\frac{1}{3} \sum_{i=1}^{3} (\tau_i + \rho_o c_\varepsilon T \gamma_i)_o = \frac{1}{3} Tr(\underline{\underline{g}}_o)$, obtained from eqn. (5.18) and the two equivalent forms for tension along y and z. In our calculations they were always found to be equal.

In summary, as first derivative information from the <u>energy approach</u> we obtain (in the case of compression) the internal pressure, $(-P + \alpha_P T / \kappa_T)_o$, and (in the case of shear and tension) the internal stress tensor, $\underline{\underline{g}}_o$. All first

derivative information pertains to the undeformed state only. As second derivative information we obtain (in the case of compression) the bulk modulus, B, and (in the case of shear and tension) the diagonal elements of the 6x6 matrix of isothermal elastic coefficients.

4.2.2. Force Approach

Another approach for obtaining estimates of the mechanical properties rests on a solution of the detailed force and torque balance equations for all atoms and bonds of each structure.

Force and torque balances in our model system are somewhat unconventional, because of the presence of bonds. According to our assumptions C,D (Section 3.1) and to our choice of potentials (Section 3.2), bonds are pictured as rigid "sticks" which are capable of exerting on the atoms attached to them:

- Forces of any magnitude and direction
- Torques of any magnitude in directions perpendicular to their axes
- Torques along their axes whose magnitude is determined by the intrinsic torsional potential function.

The last statement refers to skeletal bonds which, although rigid and rigidly attached to the carbons they connect, can yield to rotation around their axis.

Thus, atoms (or groups) in our system experience, as shown schematically in Figure 5.2:

- Nonbonded forces These are central, and their magnitude is a function of interatomic distance, dictated by the

nonbonded interaction potential. For the nonbonded force on atom i due to atom j,

$$\underline{F}_{ij}^{NB} = \left.\frac{dU_{ij}^{NB}}{dr}\right|_{r = |\underline{r}_i - \underline{r}_j|} \frac{\underline{r}_j - \underline{r}_i}{|\underline{r}_j - \underline{r}_i|} \qquad (5.21)$$

One need not consider non-bonded forces between atom pairs whose separation is fixed by connectivity.

- Bonded Forces These are, in general, non-central. Their magnitude and direction is determined by the balance conditions. The bonded force exerted on atom i from atom j through bond ij is symbolized as $\underline{F}_{ij}^{B}$.

- Bonded Torques These are exerted on skeletal carbons through either pendant or skeletal bonds. We symbolize by $\underline{\underline{T}}_{ij}^{B}$ the torque exerted on atom i due to atom j through the bond ij. If the bond is skeletal, characterized by a torsion (dihedral) angle ϕ_k, then the component of the torque $\underline{\underline{T}}_{ij}^{B}$ that is exerted along the axis of the bond is dictated by the intrinsic torsional potential function:

$$\underline{\underline{T}}_{ij}^{B} \cdot \frac{\underline{r}_j - \underline{r}_i}{|\underline{r}_j - \underline{r}_i|} = \left.\frac{dU_\phi}{d\phi}\right|_{\phi = \phi_k} \qquad (5.22)$$

The requirement of detailed mechanical equilibrium can be formulated as a problem in statics, as follows:

$$\left.\begin{aligned} \sum \underline{F} &= \underline{0} \\ \sum \underline{\underline{T}} &= \underline{0} \end{aligned}\right\} \begin{array}{l} \text{All atoms} \\ \text{All bonds} \end{array} \qquad (5.23)$$

The set of detailed force and torque balances (5.23) is equivalent to the requirements (5.3), (5.7) for minimum potential energy. Thus, our static undeformed and deformed structures constitute solutions to the problem (5.23). Since, for each of these structures, we know in advance the values of the

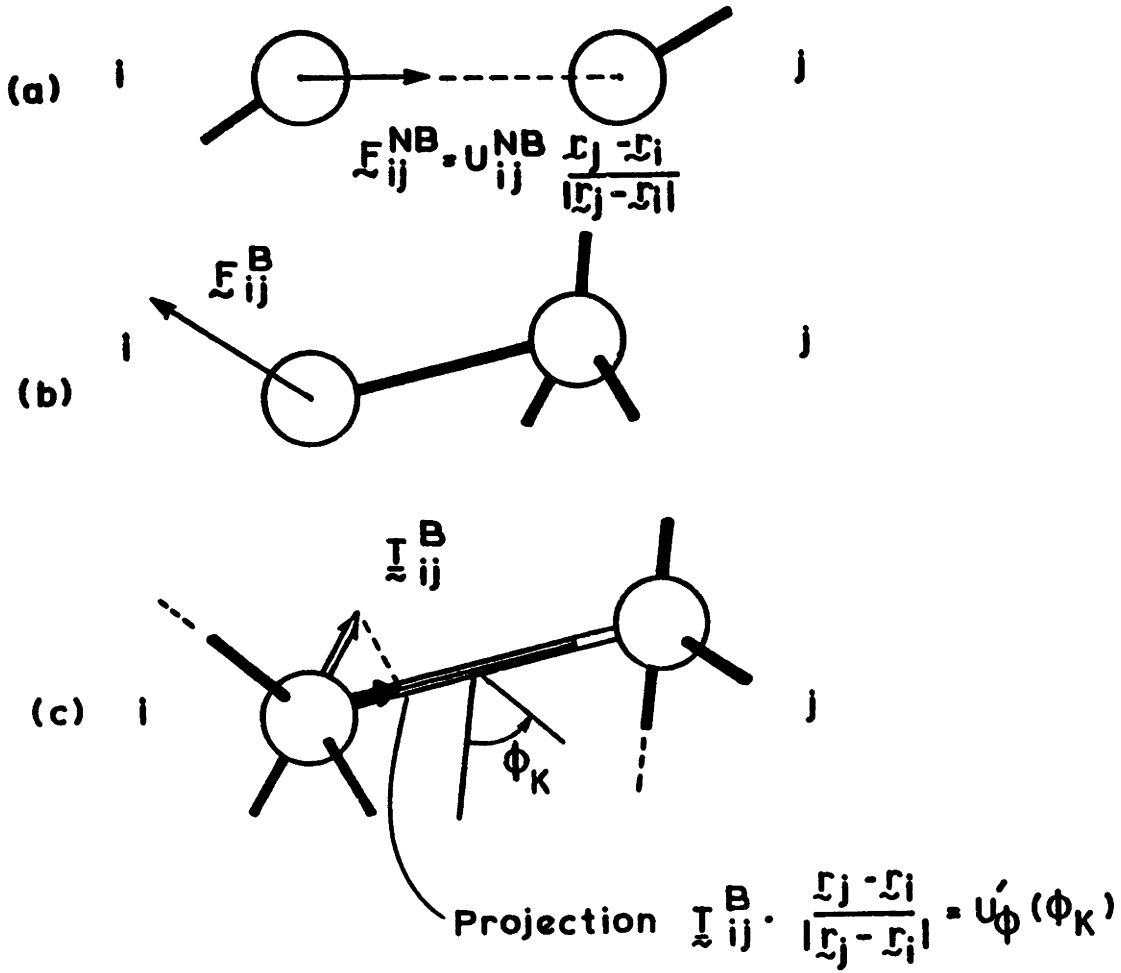

Figure 5.2 : Interatomic forces and torques
(a) nonbonded forces
(b) bonded forces
(c) bonded torques

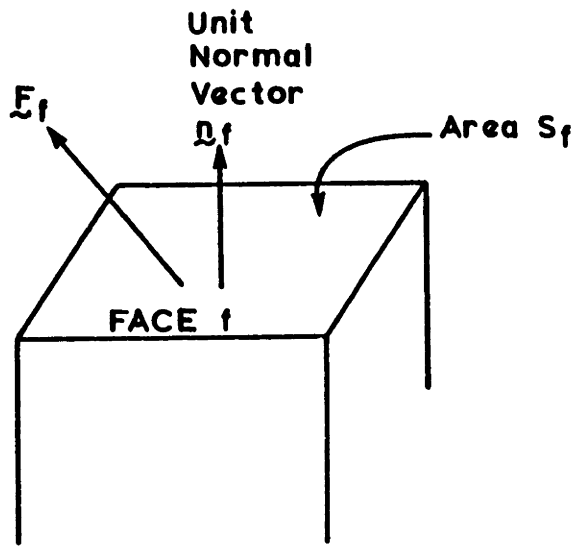

Figure 5.3 : Face force $\underset{\sim}{F}_f$, face area S_f, and face normal $\underset{\sim}{n}_f$

microscopic degrees of freedom ($\underline{\psi}$, $\underline{\phi}$), from having solved the minimization problem (5.3), the set of equations (5.23) is overdetermined. Thus, it allows us to perform (2x+1) = 153 consistency tests per structure, to check the accuracy of our minimizations.

A program was developed to solve the balance equations (5.23) in a segment-by-segment fashion along a parent chain, and thus determine all forces and all torques exerted on each atom and each bond of each of our structures. The precise form of equations (5.23), as well as the solution procedure, are described in Appendix E. Performing the abovementioned consistency tests we discovered that in all (undeformed and deformed) systems our balances close with a relative error less than 10^{-5} (see Appendix E.)

Having all atomic forces and torques at our disposal, we can now proceed to calculate the total forces $\underline{F}_f$ exerted on the interior of the model "box" from its surroundings, through each of its faces,f. This is done by simply summing individual forces (bonded and nonbonded) and torques exerted on interior atoms from surrounding atoms through each face. Face forces $\underline{F}_f$ exerted on opposite faces of the box are, of course, opposite, due to the periodicity of the system.

The internal stress tensor $\underline{\sigma}$ is simply related to the face forces $\underline{F}_f$ through the equations [compare eqn. (2.2)]:

$$\underline{F}_f = \underline{\sigma}^T \cdot \underline{n}_f \; S_f \qquad (5.24)$$

where $\underline{n}_f$ and S_f are the unit normal vector perpendicular to face f and the area of face f, as indicated in Figure 5.3. The nine independent equations (5.24) are solved for the nine elements of $\underline{\sigma}$. The resulting $\underline{\sigma}$ tensors turn out to be symmetric to an excellent approximation; this is an additional indication of closure of the balance equations.

Thus, from the force approach we obtain, by direct calculation, the internal stress tensor $\underline{\sigma}$ in the undeformed and in all deformed states. Notice that calculation of the undeformed state tensor, $\underline{\sigma}_o$, with this approach requires no information from the deformed states, unlike the corresponding calculation with the energy approach. Furthermore, eqn. (5.15) indicates that the isothermal elastic coefficients can be obtained from the first derivatives of the components of internal stress with respect to strain. From the slopes $\frac{\partial \sigma_{LM}}{\partial \varepsilon}$ in tension and in shear we can thus calculate the full 6 x 6 matrix $\underline{C}$ of elastic coefficients. A single tension experiment provides one of the first three columns of the $\underline{C}$ matrix; a single shear experiment provides one of the last three columns. Since we perform a couple of computer experiments in each mode of deformation ($\varepsilon = \pm 0.001$) we actually have two estimates for each element of the $\underline{C}$ matrix. These estimates, as a rule, agree very well with each other, indicating that changes upon deformation are symmetric around the undeformed state (harmonic behavior.) Theoretical estimates of the $\underline{C}$ matrix are symmetric to a very good approximation, which constitutes an additional confirmation of consistency.

The force approach yields more information than the energy approach, because it is more detailed. Those quantities ($\underline{\sigma}_o$ and the diagonal elements of $\underline{C}$) that can be obtained by both approaches turn out to be practically identical, as is theoretically expected.

5.2.3. Virial Theorem

The Virial Theorem approach constitutes an alternative formulation of the force approach. The Virial Theorem of

Statistical Mechanics [60] gives the stress tensor $\underline{\underline{\tau}}$ in a macroscopic, bounded system in terms of the atomic momenta p_i , masses m_i, coordinates $\underline{r}_i$ and interatomic forces $\underline{F}_{ij}$ as:

$$\tau_{LM} = - \frac{1}{V} \left\langle \sum_i \frac{p_{i,L}\, p_{i,M}}{m_i} \right\rangle - \\ - \frac{1}{2V} \left\langle \sum_i \sum_{j \neq i} (r_{i,L} - r_{j,L})\, F_{ij,M} \right\rangle \tag{5.25}$$

In our static, unbounded, periodic model structures the appropriate form of (5.25) can be shown to be:

$$\sigma_{LM} = - \frac{1}{2V} \left\langle \sum_i \sum_{j \neq i} (r_{i,L} - r_{j,L})_{min}\, F^{min}_{ij,M} \right\rangle \tag{5.26}$$

where "min" denotes distances and forces between minimum image (hence interacting) pairs of atoms. Both bonded and nonbonded forces are included in $\underline{F}_{ij}$, i.e.

$$\underline{F}_{ij} = \underline{F}^{B}_{ij} + \underline{F}^{NB}_{ij} \tag{5.27}$$

Equation (5.26) provides a means of directly calculating the internal stress tensor from interatomic forces, which are computed from the detailed force and torque balances as discussed in Appendix E. Since only minimum image pairs are involved, it is evident that $\underline{\underline{\sigma}}$ is invariant to translations of the cube borders.

The $\underline{\underline{\sigma}}$ tensor obtained by applying eqn. (5.26) to each of undeformed and deformed structures is identical to the one obtained by the force approach, described above. Results are treated in the same way to arrive at estimates of the elastic coefficients. The actual mathematical equivalence between the force approach and the virial theorem approach is proved in Appendix F.

5.3. RESULTS: ELASTIC CONSTANTS

5.3.1. Predicted Values

Values of the diagonal elastic coefficients and of the bulk modulus, obtained by the energy approach from the 8 structures studied in deformation are listed below. Mean values ± standard deviations of the mean over all structures are reported.

$$\underline{\underline{C}} = \begin{bmatrix} 4777\pm497 & & & & & \\ & 5871\pm774 & & & & \\ & & 3507\pm495 & & & \\ & & & 896\pm439 & & \\ & & & & 1230\pm136 & \\ & & & & & 1230\pm326 \end{bmatrix} \text{ MPa} \qquad (5.28)$$

$$B = 3270 \pm 415 \text{ MPa} \qquad (5.29)$$

Our estimate of the 6x6 matrix of elastic coefficients based on the force (or virial theorem) approach is presented below, in the same form.

$$\underline{\underline{C}} = \begin{bmatrix} 4773\pm498 & 3244\pm542 & 2047\pm355 & 93\pm242 & -243\pm274 & 51\pm231 \\ 3244\pm542 & 5871\pm774 & 2943\pm557 & 777\pm707 & -162\pm167 & 502\pm384 \\ 2047\pm355 & 2943\pm557 & 3492\pm497 & 695\pm497 & -367\pm191 & -31\pm158 \\ 93\pm242 & 777\pm707 & 695\pm497 & 858\pm472 & 8\pm64 & -696\pm477 \\ -243\pm274 & -162\pm167 & -367\pm191 & 8\pm64 & 1230\pm135 & 176\pm179 \\ 51\pm231 & 502\pm384 & -31\pm158 & -696\pm477 & 176\pm179 & 1221\pm333 \end{bmatrix} \text{ MPa} \qquad (5.30)$$

The diagonal elements of eqn. (5.30) are in excellent agreement with eqn. (5.28). For a macroscopic, isotropic

material the $\underline{C}$ matrix [eqn.(5.30)] should assume the form of eqn. (2.7). In practice, the small size of our model systems induces considerable fluctuations of the properties in different directions within a given structure. In addition, there are considerable fluctuations from structure to structure for the same property in the given direction. Nevertheless, it is obvious that the nonzero elements of (2.7) are dominant in eqn. (5.29), and that all elements deviate from the values suggested by eqn. (2.7) by less than two standard deviations.

To obtain estimates of the elastic constants and compare with experiment we proceed as follows:

Energy Approach

There is no physical reason for differentiating between x, y and z directions in our model. Thus, we choose to average our tension and shear computer results over all structures and over all directions. Mean values and standard deviations of the mean thus obtained are listed below. Observe that each value comes from 24 independent contributions, whereas each entry of eqn. (5.28) represented an average of 8 numbers. Also, the estimate of B from hydrostatic compression [compare eqn. (5.29)] is given, in which directional averaging is implicit.

$$\begin{aligned}
&\text{(Tension)} && \tfrac{1}{3}\left(C_{11} + C_{22} + C_{33} \right) = 4718 \pm 389 \text{ MPa} = 2\mu+\lambda \\
&\text{(Shear)} && \tfrac{1}{3}\left(C_{44} + C_{55} + C_{66} \right) = 1119 \pm 182 \text{ MPa} = \mu \\
&\text{(Compression)} && B = 3270 \pm 415 \text{ MPa} = \lambda+\tfrac{2}{3}\mu
\end{aligned} \qquad (5.31)$$

According to equations (2.7) and (2.8), the three numbers listed in eqn. (5.31) must be simple functions of only two independent parameters, λ and μ. Indeed, obtaining λ and μ from any two of the three entries in (5.31) and checking

against the third confirms that our three model estimates are consistent within 1%. Thus, our model ensemble's response to small deformations has the characteristics expected of an isotropic solid.

The values of λ and μ that best describe the results (5.31), together with the values of the elastic constants obtained from them through eqns (2.8), are listed in the third column of Table 5.1.

Force Approach

Averaging our theoretical estimates of elastic coefficients from the force approach over all structures and all orientations [compare eqn. (5.30)] we obtain:

$$\text{(Tension)} \quad \frac{1}{3}\left(C_{11} + C_{22} + C_{33} \right) = 4712 \pm 390 \text{ MPa} = 2\mu+\lambda$$

$$\text{(Tension)} \quad \frac{1}{3}\left(C_{12} + C_{23} + C_{31} \right) = 2745 \pm 292 \text{ MPa} = \lambda$$

$$\text{(Shear)} \quad \frac{1}{3}\left(C_{44} + C_{55} + C_{66} \right) = 1103 \pm 192 \text{ MPa} = \mu \qquad (5.32)$$

The three values (5.32) are consistent in λ and μ within 5%. The best values of λ and μ that describe the results, together with the elastic constants obtained through eqn. (2.8), are listed in the fifth column of Table 5.1.

5.3.2. Comparison with Experiment

Experimental data on the mechanical properties of glassy atactic polypropylene are somewhat difficult to find (most reported data refer to the much more abundant commercial isotactic form.) Direct measurements of the Young's modulus of elasticity, E, on atactic polypropylene in the glassy region

have been performed by Sauer et al. [50]. At a temperature of $-40^{o}C$, by mechanical testing at audio frequencies on atactic polypropylene of molecular weight $3 \cdot 10^5$ and 0% crystallinity they find:

$$\text{Experiment: } E = 2650 \text{ MPa} \tag{5.33}$$

An experimental value of B = 3500 MPa for the bulk modulus is reported in [71], p.271, but it probably refers to the isotactic, semicrystalline form of the polymer and to room temperature. A better value is obtained from the correlation presented in [71], p.267: for atactic polypropylene at $-40^{o}C$, a bulk modulus of

$$\text{Experiment: } B = 3340 \text{ MPa} \tag{5.34}$$

is most plausible. Values (5.33) and (5.34) are taken as the most reliable experimental values of mechanical properties for our polymer. These values, together with the constants λ, μ, G, ν obtained from them, are listed in the first column of Table 5.1. Observe that G is very near the typical "glassy" value of 1000 MPa, and ν obeys, to a good approximation, the rule of thumb that all glassy polymers have a Poisson ratio of approximately 1/3 ([77], p.111). The experimental values listed in Table 5.1 are thought to be accurate to within 15%.

Relative deviations between the theoretical estimates and the corresponding experimental values are listed in the fourth and sixth columns of Table 5.1., for the energy and the force approach, respectively. One must reiterate here that the model has no adjustable parameters. Also, there is an uncertainty associated with the theoretical values, an estimate of which is provided by the standard deviations in eqns (5.31) and (5.32). The energy approach predicts all elastic constants with a relative error of less than 15%. Estimates obtained by the force approach are in even better agreement with experiment. We can conclude that our methods are remarkably successful in estimating elastic constants.

Table 5.1

Comparison of Experimental and Predicted Values of the Elastic Constants

	Property	Experiment[a] Value	Theory: Energy Approach Value	Theory: Energy Approach Deviation from Experiment %	Theory: Force Approach Value	Theory: Force Approach Deviation from Experiment %
Lamé Constants	λ, MPa	2690	2520	- 6.3	2700	+0.4
	μ, MPa	970	1110	+14.4	1020	+5.2
	G, MPa	970	1110	+14.3	1020	+5.2
	E, MPa	2650	2990	+12.8	2790	+5.3
	B, MPa	3340	3250	- 2.6	3390	+1.5
	ν	0.37	0.35	- 5.4	0.36	-2.7

[a]References [50], [71]; see text for details.

5.4. RESULTS: THERMAL EXPANSION COEFFICIENT

5.4.1. Predicted Values

The ensemble averaged internal stress tensor in the undeformed state, $\underline{\underline{g}}_o$, obtained from our 15 model structures by the force approach, assumes the form (mean values ± standard deviations of the mean):

$$\underline{\underline{g}}_o = \begin{bmatrix} 82.4 \pm 26.6 & -17.9 \pm 12.4 & -0.2 \pm 12.3 \\ -17.9 \pm 12.4 & 67.3 \pm 40.2 & -7.2 \pm 11.0 \\ -0.2 \pm 12.3 & -7.2 \pm 11.0 & 96.9 \pm 22.9 \end{bmatrix} \text{ MPa} \tag{5.35}$$

Within the framework of our static model it is not possible to separate the external stress ($\underline{\underline{I}}_o$) from the Grüneisen tensor contribution ($\rho_o c_\varepsilon T \underline{\underline{\gamma}}_o$) to the internal stress tensor $\underline{\underline{g}}_o$. For ordinary external loads, however (an external pressure of 1 atm has been assumed in specifying the density of the undeformed system in Section 3.2) the Grüneisen tensor contribution, which is a measure of cohesive forces in the polymeric solid, is clearly dominant. For an isotropic, macroscopic material $\underline{\underline{g}}_o$ must then be diagonal, with all diagonal elements equal. [compare eqn. (2.10)]. The model estimates do not strictly satisfy this requirement, because of limited sample size, but all off-diagonal elements are zero within two standard deviations, and the diagonal elements are equal within the same limits.

From the trace of the $\underline{\underline{g}}_o$ tensor we obtain an estimate of the ratio of thermal expansion coefficient to compressibility:

$$\frac{\alpha_P}{\kappa_T} = \frac{1}{3\,T}\,\mathrm{Tr}(\underline{\underline{g}}_o) + \frac{P}{T} \tag{5.36}$$

Using P = 1 atm, T = 233 K, we obtain $\frac{\alpha_P}{\kappa_T} = 0.35 \pm 0.06 \frac{MPa}{K}$

Combining with our model value of the bulk modulus [eqn. (5.29)] we arrive at a theoretical estimate of the thermal expansion coefficient:

$$\alpha_p = (1.08 \pm 0.23) \cdot 10^{-4} \ K^{-1} \qquad (5.37)$$

5.4.2. Comparison with Experiment

Zakin and Simha [81] have carried out measurements of the thermal expansion of an isotactic polypropylene (18% crystalline). Their value for $-40^{o}C$ is $2.51 \cdot 10^{-4} \ K^{-1}$. An experimental curve of specific volume versus temperature for atactic polypropylene is given in [40], p.294. From it the thermal expansion coefficient of the glassy polymer at -40^{o} is $2.7 \cdot 10^{-4} \ K^{-1}$. Experimental values given in [71], p.60, on the other hand, lead to a value of $2.0 \cdot 10^{-4} \ K^{-1}$. We accept here as representative value

$$\text{Experiment: } \alpha_p = 2.5 \cdot 10^{-4} \ K^{-1} \qquad (5.38)$$

Compared with this, the theoretical estimate [eqn. (5.37)] is by 57% too low. An analysis of the sensitivity of computer estimates to perturbations in the potential parameters used showed that our estimate of the thermal expansion coefficient, unlike those of the elastic constants and the solubility parameter, can change significantly with small changes of the Van der Waals radii (see Appendix G.) Thus, a slightly inappropriate choice of the Van der Waals radii may be responsible for the discrepancy between equations (5.37) and (5.38).

5.5. INTRA- VS. INTERMOLECULAR CONTRIBUTIONS TO ELASTIC RESPONSE

It is an interesting question to separate between intra- and intermolecular energy contributions to the elastic response, and to assess the role of each. Some considerations regarding this question are presented in [79], [80].

Intramolecular contributions to $\underline{\underline{g}}_o$ and $\underline{\underline{C}}$ are computed from changes in the parent chain energy with deformation. Equations (5.16) to (5.18) are used, where now the role of U_{min}^{pot} is played by the total potential energy of an isolated parent chain, computed with the full Lennard-Jones potential function. Intermolecular contributions are determined as the difference of the intramolecular quantities from the corresponding total quantities. They, too, can be regarded as being determined by eqns. (5.16) to (5.18) if U_{min}^{pot} is replaced by the cohesive energy of a structure (see section 4.1).

Inter- versus intramolecular contributions to the three first diagonal elements of the $\underline{\underline{C}}$ matrix (C_{11}, C_{22}, C_{33}), obtained from the eight structures studied in deformation, are plotted in Figure 5.4. There is a total of 24 points. Each point comes from a pair of uniaxial tension "experiments." Points from the same structure have been plotted with the same symbol. The broken line corresponds to the equation (compare Table 5.1):

$$C_{II}^{inter} + C_{II}^{intra} = 2\mu + \lambda = 4740 \text{ MPa}, \quad I = 1,2,3 \qquad (5.39)$$

One clearly observes a strong negative correlation between the inter- and intramolecular contributions to the C_{II}'s. Each of these contributions may vary widely, but their sum is approximately constant. The same conclusion is reached by comparing

inter- and intramolecular shear moduli, or compressibility. The wide variation in the intramolecular elastic coefficients probably reflects the high multiplicity of single chain conformations within the polymer. The intermolecular interactions between different chains strongly dampen the effects of individual chain idiosyncrasy, however. The relationship between inter- and intramolecular contributions is therefore not synergistic, but antagonistic.

The intramolecular part of the internal stress tensor, averaged over the 8 structures studied in deformation, assumes the form

$$\underline{\underline{\sigma}}_{intra} = \begin{bmatrix} -146.7 \pm 38.5 & 11.2 \pm 24.0 & 11.2 \pm 11.0 \\ 11.2 \pm 24.0 & -203.8 \pm 57.6 & 32.4 \pm 46.9 \\ 11.2 \pm 11.0 & 32.4 \pm 46.9 & -150.4 \pm 29.8 \end{bmatrix} \text{ MPa} \qquad (5.40)$$

All diagonal elements in this intramolecular tensor are negative, in marked contrast to those of the total tensor [eqn. (5.35)]. The energy of an isolated parent chain would decrease if the chain were allowed to expand. In other words, single chains in the polymer bulk are under compression by their neighbors. Coexistence in the bulk counteracts the tendency of individual chains to expand due to "excluded volume" effects. This, of course, is only a restatement of Flory's "random coil" hypothesis ([25], p.602), for which our model provides computer experimental proof.

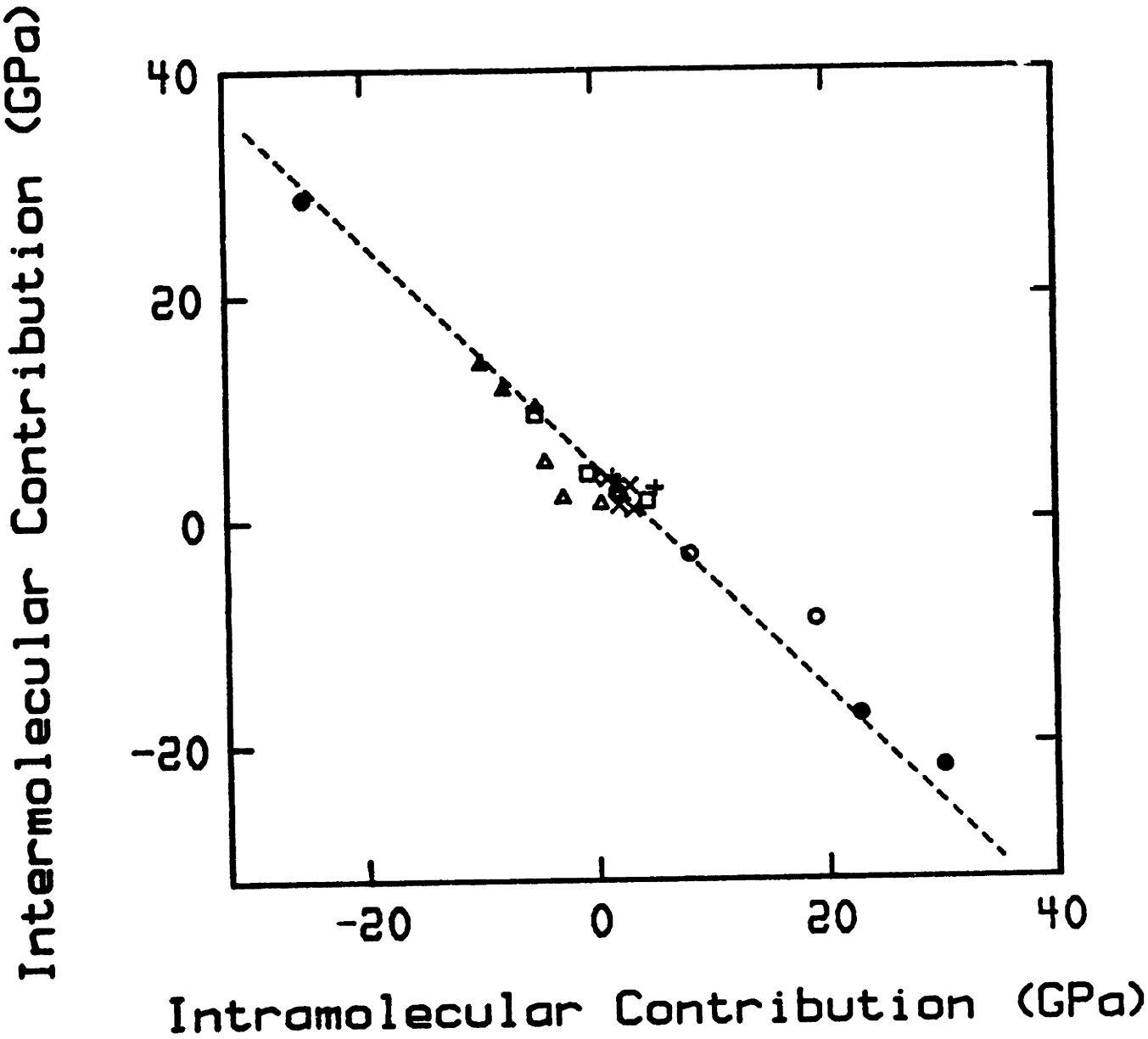

Figure 5.4 : Inter- and intramolecular contributions to the three first diagonal elements of the 6 x 6 matrix of isothermal elastic coefficients

5.6. MICROSCOPIC VS. MACROSCOPIC STABILITY

As we mentioned in Section 3.1., the fact that each of our microstructures is in detailed mechanical equilibrium does not imply that our model glass is in stable thermodynamic equilibrium. Here we further elucidate this distinction, using results from our model deformations.

The condition for stable mechanical equilibrium in a microscopic structure is (section 3.2)

$$\underline{\underline{H}} \text{ : positive definite} \qquad (5.41)$$

where $\underline{\underline{H}}$ is the Hessian matrix of the total potential energy with respect to the microscopic degrees of freedom. The thermodynamic criterion of stability for an elastic solid is ([11], chapter 13)

$$\underline{\underline{C}} \text{ : positive definite} \qquad (5.42)$$

where $\underline{\underline{C}}$ is the 6x6 matrix of isothermal elastic coefficients. All our model structures satisfy the microscopic criterion [eqn. (5.41)], by construction. However, application of the thermodynamic criterion [eqn. (5.42)] to the individual microstructures led to the conclusion that two of the eight structures studied in deformation are not stable thermodynamically. For these structures modes of deformation exist, in which the total energy is concave with respect to an externally imposed macroscopic strain. Our model deformations thus provide direct proof of the fact that criteria [eqns (5.41) and (5.42)] need not be simultaneously fulfilled. Although the ensemble averaged matrix [eqn. (5.30)] is positive definite, the existence of microstructures whose response to deformation does not satisfy criterion [eqn. (5.42)] may shed some light on the inherent "instability" of real polymeric glasses.

6. LOCAL TOPOLOGY AND THE MECHANISM OF RESPONSE TO ELASTIC DEFORMATION

Apart from serving as a starting point for the prediction of macroscopically observable properties, our model provides detailed atomistic information, which is not accessible by experiment. Some of this information we present below. The purpose of this chapter is:

- To characterize the local topology (i.e. the distribution of local environments experienced by each atomic species) in the polymeric glass.

- To probe the mechanism of small-strain elastic deformation on an atomistic level, by examining the structural changes brought about by the imposition of deformation.

6.1. ATOMIC LEVEL STRESSES

6.1.1. Theoretical Development

Local structure in amorphous solids is a fascinating problem, central to the understanding of properties of these materials [82]. Various methods have been developed for the partial characterization of local structure in the neighborhood of an atom. Concepts invoked include pair distribution functions, coordination numbers, symmetry coefficients [22], Voronoi polyhedra [43], and free volume ([13],[30]).

The concept of atomic level stresses can serve as a concise and meaningful basis for characterizing local

structure. A brief history of this concept , which dates back to Born and Huang (1954), and has been used in the study of defects in crystalline solids, is given in [22]. Egami, Maeda and Vitek [22] first applied atomic level stresses to glasses, using them on an atomistic model of amorphous iron. The concept was subsequently used in a study of plastic deformation in a metallic glass.

Nonbonded Systems

Up to now, the concept of atomic level stresses has been applied exclusively to nonbonded systems with central interatomic forces. In such systems we define the atomic level stress tensor for atom i (following [24], with slight modifications) by:

$$\sigma_{i,LM} = -\frac{1}{2V_i} \sum_{j \neq i} \left(r_{i,L} - r_{j,L} \right)_{min} F^{min}_{ij,M} \qquad (6.1)$$

where $\underline{r}_i$ and $\underline{r}_j$ are the position vectors of atoms i and j, $\underline{F}_{ij}$ is the force of interatomic interaction on atom i due to atom j, and V is a volume assigned to atom i, such that summing over all atoms gives the total volume of the system, V:

$$\sum_i V_i = V \qquad (6.2)$$

The indices L and M, standing for the three coordinate directions in a Cartesian system, assume the values 1,2,3. The subscript/superscript "min" signifies that interatomic distances and forces are calculated according to the minimum image convention.

For a system in detailed mechanical equilibrium, summing all atomic level stresses $\underline{\sigma}_i$, multiplied by the respective atomic volumes V_i, one recovers the macroscopic "internal stress tensor", $\underline{\sigma}$. This is a restatement of the Virial Theorem, eqn. (5.26).

$$\sigma_{LM} = \frac{1}{V} \sum_i V_i \, \sigma_{i,LM} \tag{6.3}$$

The way in which atomic volumes V_i are assigned is not very crucial to the physical significance of the atomic stress tensor. A partitioning into Voronoi polyhedra could be used. Since this is a laborious process, we choose here, following previous work [24], to assign the volumes V_i in direct proportion to the Van der Waals volumes of atoms:

$$V_i = V \frac{(r_i^o)^3}{\sum_i (r_i^o)^3} \tag{6.4}$$

so that all atoms belonging to the same species have the same V_i. This definition of V_i is used throughout.

Central, nonbonded interatomic forces can be directly substituted in terms of the potential of nonbonded interatomic interactions, $U_{ij}^{NB}(r)$, according to eqn. (5.21). It follows that the atomic level stress tensor, as defined by eqn. (6.1), is symmetric in the central force case (see Appendix H).

By its definition [eqn. (6.1)], the internal stress tensor is tied to the energetics of deformation as follows. Imagine our system subjected to a <u>small homogeneous</u> (or affine, or quasicontinuum) deformation, characterized by a strain tensor $\underline{\underline{\varepsilon}}$ ($| \varepsilon_{LM} | << 1$). Atom locations in the deformed state are then given in terms of the corresponding undeformed locations by eqn. (5.1), and the strain at any point, equal to the macroscopic strain, is described by eqn. (5.2). The corresponding increase in total potential energy can be written [55] as a sum of terms associated with the individual atoms:

$$\Delta U^{pot} = \sum_i \Delta U_i^{pot} \tag{6.5}$$

where, to first order in strain,

$$\Delta U_i^{pot} = V_i \sum_{LM} \sigma_{i,LM}\, \epsilon_{LM} + O(\epsilon_{LM}^2) \qquad (6.6)$$

Thus, the atomic level stress tensor $\underline{\sigma}_i$ can be defined from the coefficients of the first order term in an expansion of the potential energy associated with atom i with respect to strain, for a small homogeneous deformation of the material.

Following Egami and Vitek ([22], [24], [55]), we introduce two invariants of the atomic level stress tensor for characterizing local structure. These are:

. The "atomic level hydrostatic pressure", p_i, defined by:

$$p_i = \frac{1}{3}\, Tr(\underline{\sigma}_i) = \frac{\sigma_{i,ii} + \sigma_{i,22} + \sigma_{i,33}}{3} = \frac{I_1}{3} \qquad (6.7)$$

. The "atomic Von Mises shear stress" [64], τ_i, defined by:

$$\tau_i^2 = \frac{1}{6}\left\{(\sigma_{i,11} - \sigma_{i,22})^2 + (\sigma_{i,22} - \sigma_{i,33})^2 + (\sigma_{i,33} - \sigma_{i,11})^2\right\} + \sigma_{i,12}^2 + \sigma_{i,23}^2 + \sigma_{i,31}^2 = \frac{I_1^2}{3} - I_2 \qquad (6.8)$$

(I_1 and I_2 stand for the first and second invariants of the tensor $\underline{\sigma}_i$, respectively)

Although p_i is termed a "pressure", it is really a tension or negative pressure, as is obvious from the definition (6.9). The quantity p_i is a measure of <u>local density fluctuations</u> in the material. A high positive value of p_i is associated with a high coordination number around atom i, and with a lower than

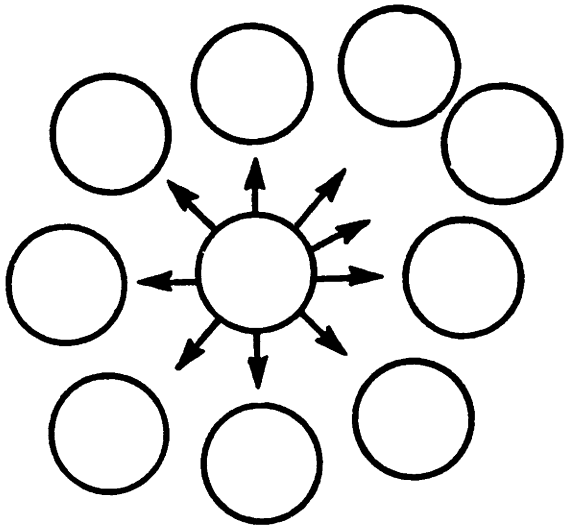

Local Density Low
Coordination Number High

$p_i > 0$

(Tension)

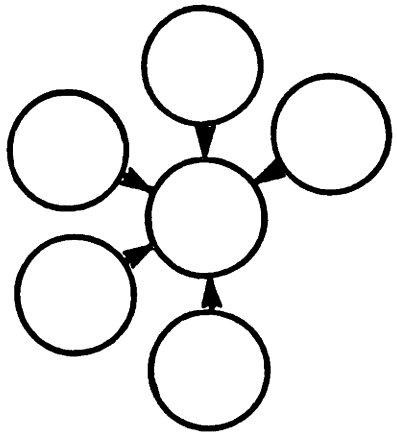

Local Density High
Coordination Number Low

$p_i < 0$

(Compression)

Figure 6.1 : Physical meaning of the atomic-level hydrostatic pressure, p_i, in a nonbonded system

average atomic density. A low negative value of p_i is associated with a low coordination number and with higher than average local atomic density [23]. This is schematically illustrated in Figure 6.1.

The quantity τ_i reflects the degree of asymmetry of the local environment around atom i.

Systems with Rigid Bonds

In this work we wish to extend the concept of atomic level stresses to bonded systems with rigid bon. lengths and bond angles. Our computer model structures of a glassy amorphous vinyl polymer, in which molecular rearrangement can occur only through torsion around skeletal bonds, provide an instance of such systems. The imposition of rigid constraints complicates the picture introduced above considerably.

Forces in bonded systems are no longer central. In addition to the nonbonded interactions $\underline{F}_{ij}^{NB}$, given by (5.21), there are bonded forces $\underline{F}_{ij}^{B}$, which may have arbitrary magnitude and direction [compare eqn. (5.27)]. Also, there are torques $\underline{\underline{T}}_{ij}^{B}$, exerted through the bonds (see section 5.2.2.) The definition (6.1) for the atomic level stresses can no longer be applied. Indeed, if one uses eqn. (6.1), with $\underline{F}_{ij}$ as the total (bonded + nonbonded) force, the resulting tensor $\underline{\underline{\sigma}}_i$ is, in general, not symmetric, due to the non-central character of the bonded forces (see Appendix H.) Omission of the bonded contribution to $\underline{F}_{ij}$ (i.e. defining $\underline{\underline{\sigma}}_i$ through eqn. (6.1), using $\underline{F}_{ij}^{NB}$ only in place of $\underline{F}_{ij}$) would lead to a symmetric $\underline{\underline{\sigma}}_i$, but would not be meaningful, and equation (6.3) would no longer be satisfied.

For defining a meaningful atomic level stress tensor in a bonded system we use eqn. (6.6). We imagine our system being subjected to an infinitesimal affine deformation described by

a strain tensor $\underline{\underline{\varepsilon}}$, defined as in eqn. (5.2). (Note that this is a thought experiment in the limit of infinitesimal displacements; finite-strain affine deformations are incompatible with the requirement of fixed bond lengths and bond angles, as discussed in section 5.1.) On each atom i acts a total (bonded and nonbonded) force $\sum_{j \neq i} \underline{F}_{ij}$, and a total torque $\sum_{j \neq i} \underline{\underline{T}}^{B}_{ij}$. In the course of the imposed infinitesimal deformation, atom i will be displaced by a vector $d\underline{r}_i = \underline{r}_i^{affine} - \underline{r}_{o,i}$ and rotated by a differential angle $\frac{1}{2} (\underline{\nabla} \times d\underline{r})_i$. The total work done by the system during the deformation, equal to the work of all forces and all torques exerted on all atoms, is:

$$dW = \underbrace{\sum_i \left(\sum_{j \neq i} \underline{F}_{ij} \right) \cdot d\underline{r}_i}_{\substack{\text{work of forces} \\ \text{(displacement of atoms)}}} + \underbrace{\sum_i \left(\sum_{j \neq i} \underline{\underline{T}}^{B}_{ij} \right) \cdot \frac{1}{2} \left(\underline{\nabla} \times d\underline{r} \right)_i}_{\substack{\text{work of torques} \\ \text{(rotation of bonds)}}} \quad (6.9)$$

Using eqn. (5.2) we obtain:

$$\begin{aligned} dr_{i,M} &= \left(A_{ML} - \delta_{ML} \right) r_{i,L} + b_M \\ (\nabla \times d\underline{r})_{i,K} &= \sum_L \sum_M e_{LMK} \left(A_{ML} - \delta_{ML} \right) \end{aligned} \quad (6.10)$$

where e_{KLM} is the alternating tensor [39].

Consequently,

$$dW = \sum_L \sum_M \left\{ \sum_i \sum_{j \neq i} F_{ij,M} \; r_{i,L} \right\} \left(A_{ML} - \delta_{ML} \right) + \sum_M \left\{ \sum_{j \neq i} F_{ij,M} \right\} b_M +$$

$$+ \frac{1}{2} \sum_L \left\{ \sum_i \sum_{j \neq i} e_{LMK} \, \underline{\underline{T}}^{B}_{ij,K} \right\} \left(A_{ML} - \delta_{ML} \right) \quad (6.11)$$

By virtue of the reciprocity of interatomic interactions, bonded or nonbonded, we have:

$$\sum_i \sum_{j\neq i} F_{ij,M} = \frac{1}{2} \sum_L \{ \sum_i \sum_{j\neq i} F_{ij,M} + \sum_j \sum_{i\neq j} F_{ji,M} \} =$$

$$= \frac{1}{2} \sum_i \sum_{j\neq i} (F_{ij,M} + F_{ji,M}) = 0 \qquad (6.12)$$

Furthermore,

$$\sum_i \sum_{j\neq i} F_{ij,M}\, r_{i,L} = \frac{1}{2} \{ \sum_i \sum_{j\neq i} F_{ij,M}\, r_{i,L} + \sum_j \sum_{i\neq j} F_{ji,M}\, r_{j,L} \}$$

$$= \sum_i \sum_{j\neq i} \{ \frac{1}{2} F_{ij,M} (r_{i,L} - r_{j,L}) \} \qquad (6.13)$$

and

$$\sum_i \sum_{j\neq i} e_{KLM}\, \underline{T}^B_{ij,K} = \frac{1}{2} \{ \sum_i \sum_{j\neq i} e_{KLM}\, \underline{T}^B_{ij,K} + \sum_j \sum_{i\neq j} e_{KLM}\, \underline{T}^B_{ji,K} \}$$

$$= \sum_i \sum_{j\neq i} \{ e_{LMK} \frac{\underline{T}^B_{ij,K} + \underline{T}^B_{ji,K}}{2} \} \qquad (6.14)$$

From eqns (6.11) to (6.14) we obtain:

$$dW = \sum_L \sum_M \sum_i \{ \sum_{j\neq i} \frac{1}{2} [(r_{i,L} - r_{j,L}) F_{ij,M} +$$

$$+ \sum_K e_{LMK} (\frac{\underline{T}_{ij,K} + \underline{T}_{ji,K}}{2})] \} (A_{ML} - \delta_{ML}) =$$

$$= \sum_L \sum_M \sum_i w_{i,LM} (A_{ML} - \delta_{ML}) \qquad (6.15)$$

The tensor within the curly brackets in eqn. (6.15), $\underline{w}_i$, is <u>symmetric</u> (see Appendix H), therefore:

$$dW = \sum_L \sum_M \sum_i w_{i,LM} (A_{ML} - \delta_{ML}) = \frac{1}{2} \sum_L \sum_M \{ \sum_i w_{i,LM} (A_{ML} - \delta_{ML}) +$$

$$+ \sum_i w_{i,ML} (A_{LM} - \delta_{LM}) \} = \sum_L \sum_M \sum_i w_{i,LM} \{ \frac{1}{2} (A_{ML} + A_{LM}) - \delta_{LM} \}$$

$$= \sum_L \sum_M \sum_i w_{i,LM} \varepsilon_{LM} \qquad (6.16)$$

(Equation (5.2) has been used to arrive at the last result.)

The change in total potential energy, associated with the imposed dofferential deformation is, if thermal motion is ignored:

$$dU^{pot} = - dW = \sum_L \sum_M \sum_i (- w_{i,LM}) \varepsilon_{LM} \qquad (6.17)$$

Comparing eqns (6.6) and (6.17) we conclude that the correct definition of the atomic level stress tensor in our bonded system is:

$$\sigma_{i,LM} = - \frac{1}{V_i} w_{i,LM} =$$

$$(6.18)$$

$$= - \frac{1}{2V_i} \sum_{j \neq i} \{ (r_{i,L} - r_{j,L})_{min} F^{min}_{ij,M} + \sum_K e_{LMK} (\frac{\underline{T}^B_{ij,K} + \underline{T}^B_{ji,K}}{2}) \}$$

(The minimum image convention has been introduced in the last expression.) Bonded forces and bonded torques play their role, together with the nonbonded forces, in shaping the atomic level stress tensor. For a system in detailed mechanical equilibrium the atomic stresses defined in eqn. (6.18) fulfil eqn. (6.3). This follows directly from the torque balances around each atom and the proof presented in Appendix F. In the case of a nonbonded system eqn. (6.18) correctly reduces to the less general form (6.1). By virtue of the torque balance

around atom i ($\sum_{j \neq i} \underline{\underline{T}}^{B}_{ij} = \underline{0}$) eqn. (6.16) can immediately be simplified to:

$$\sigma_{i,LM} = - \frac{1}{2 V_i} \sum_{j \neq i} \{ (r_{i,L} - r_{j,L})_{min} F^{min}_{ij,M} + \sum_{K} e_{LMK} \frac{T^{B}_{ji,K}}{2} \} \qquad (6.19)$$

6.1.2. Distribution of Atomic Level Stresses in the Polymer Glass

The theoretical principles developed above were applied to our ensemble of 15 model structures, representing the glassy polymer in the undeformed state. Atomic level stresses were calculated using eqn. (6.19) for each atom of each structure. To compensate for the use of finite-range potential energy functions, a value of +98.4 MPa (from the direct integration of potential "tails") was added to the diagonal elements of $\underline{\underline{\sigma}}_i$. The characteristic quantities p_i and τ_i were calculated according to eqns (6.7) and (6.8). The distributions of p and τ were accumulated separately for each type of center (H, C, R=CH_3) present in our system. These distributions are plotted in Figures 6.2 and 6.3, respectively. The means and standard deviations of the distributions are given in Table 6.1.

Table 6.1 : Characteristic Quantities of the Atomic Level Stress Distributions, Depicted in Figures 6.2 and 6.3

Species	$\langle p \rangle$, GPa	$\langle p^2 - \langle p \rangle^2 \rangle^{\frac{1}{2}}$, GPa	$\langle \tau \rangle$, GPa	$\langle \tau^2 - \langle \tau \rangle^2 \rangle^{\frac{1}{2}}$, GPa
Hydrogen, H	-3.756	2.211	4.804	2.488
Carbon, C	3.870	1.413	6.476	2.754
Methyl, R	-2.209	1.214	3.091	1.459

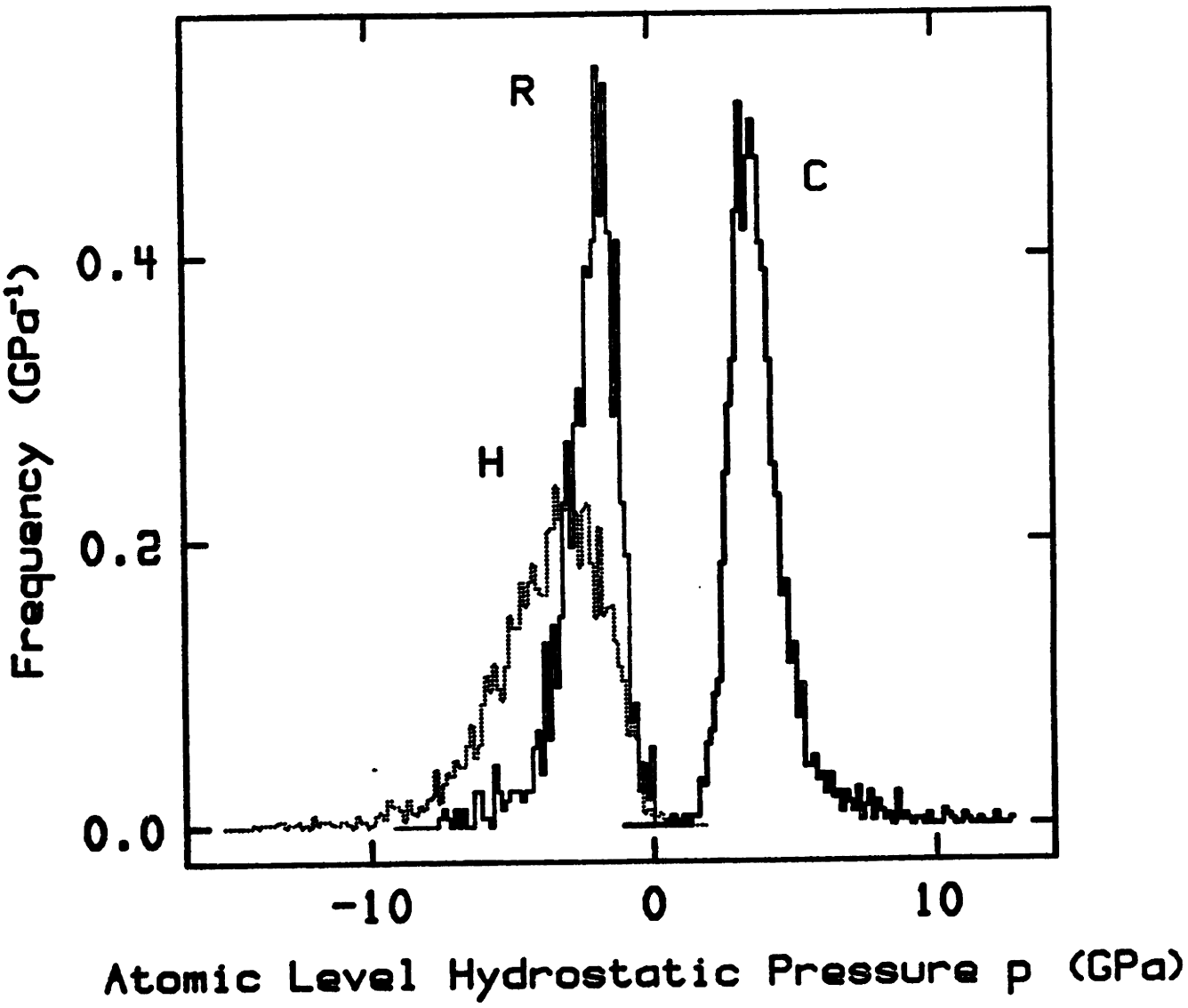

Figure 6.2

Distribution of the atomic-level hydrostatic pressure (p) for the three types of centers present in the model glass, atactic polypropylene (H=hydrogen, C=carbon, R=methyl).
The distributions are based on 15 undeformed structures.

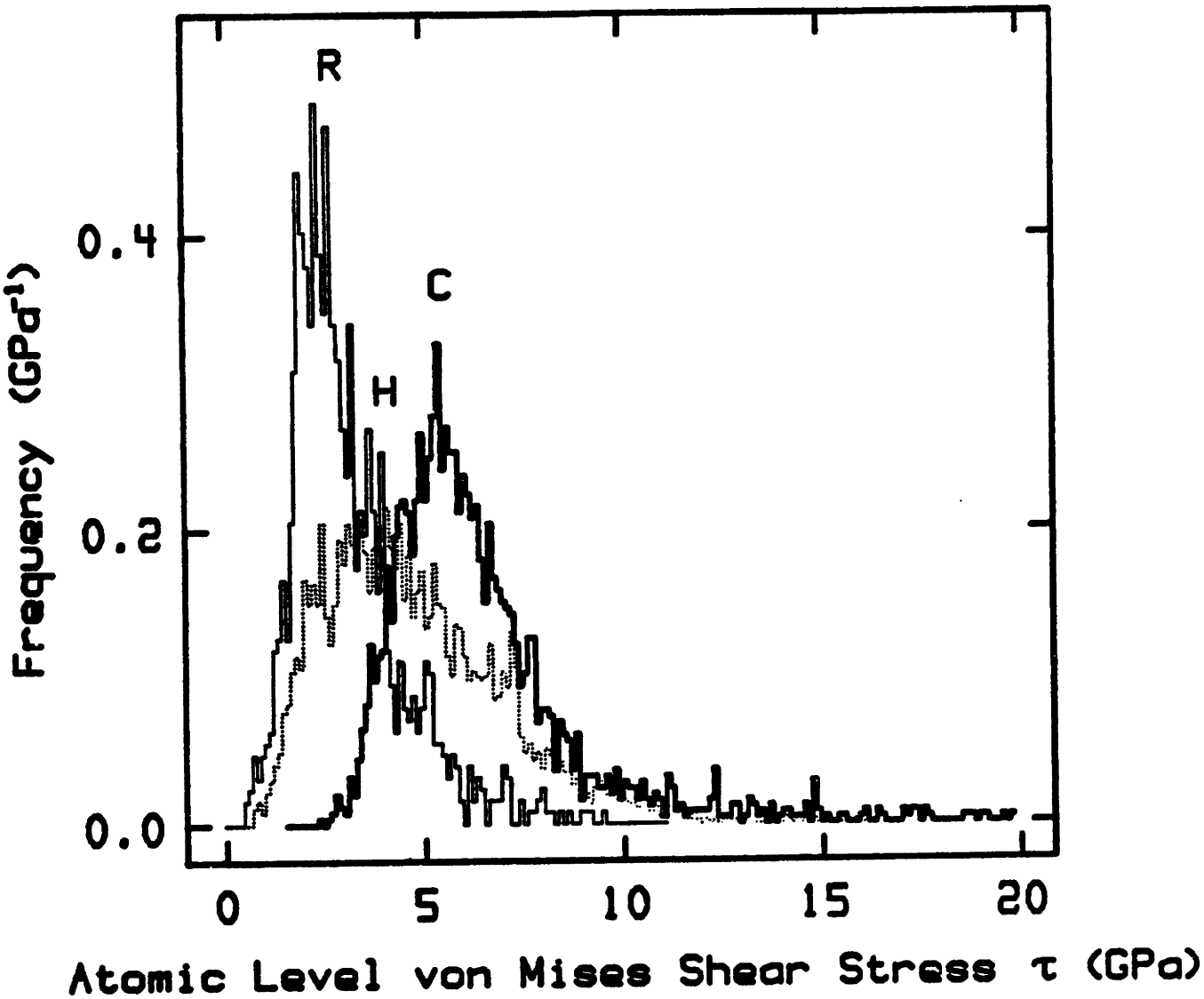

Figure 6.3

Distribution of the atomic Von Mises shear stress (τ) for the three species present in the model glass, atactic polypropylene (H=hydrogen, C=carbon, R=methyl). The distributions are based on 15 undeformed structures.

A striking feature, evident from Figs 6.2 and 6.3 and from Table 6.1, is the disparity in order of magnitude between atomic level stresses $\underline{\underline{\sigma}}_i$ and the overall macroscopic internal stress $\underline{\underline{\sigma}}$. The average diagonal element of the internal stress tensor, $\underline{\underline{\sigma}}$, is equal to 82.2 MPa [compare eqn. (5.35)]. A typical atomic stress (Table 6.1) is at least 30 times larger, the tails of the distributions in Figs 6.2 and 6.3 reaching out to 20 GPa. In other words, there is a strong compensation effect in the superposition (6.3) of atomic-level stresses to form the overall stress. The large magnitude of atomic level stresses has been pointed out by Egami, Maeda and Vitek [22] in the case of an atomic, nonbonded system. Plots of their p- and τ-distributions are presented in [55]. In their model of a metallic glass consisting of a single type of atoms, with central interactions described by a modified Johnson potential [23] they observe p-values ranging from -32 to +28 GPa, and τ-values ranging from 2 to 36 GPa. Their atomic stresses are thus of the same order of magnitude as ours, although somewhat larger, due to the fundamentally different type of interaction in their system.

Figure 6.2 reveals a distinct difference in the shape and position of the p-distribution between skeletal carbons on the one hand, and substituents (H, R) on the other. Hydrogens and methyls are under "compression" ($p < 0$), with p-distributions skewed to the left. Carbons are under "tension" ($p > 0$), with a p-distribution skewed to the right. This segregation proves that the concept of atomic-level stresses is sensitive to the topological role of each atomic species along the chain. For comparison, the nonbonded, single-species work of Srolovitz, Vitek and Egami [55] rendered a single p-distribution, centered around zero and skewed to the left, of shape similar to that of our H and R distributions in Figure 6.2.

A detailed examination of the forces experienced by each atomic species in our model systems was undertaken, to better understand the implications of our p-distributions. This examination revealed the following:

- Short-range nonbonded interactions (i.e. nonbonded interactions between atoms 3 or 4 bonds apart) are predominantly repulsive.

- Long-range nonbonded interactions (i.e. interactions between atoms more than 4 bonds apart, or belonging to different chains) are predominantly attractive, and weaker than short-range interactions.

- Bonded forces between skeletal carbon atoms are almost always attractive, and stronger than carbon-substituent bonded forces, or nonbonded forces.

- Methine carbon-methyl substituent bonded forces are attractive.
  Methylene carbon-pendant hydrogen bonded forces are mainly attractive.
  Methine carbon-pendant hydrogen bonded forces are frequently repulsive.

Based on these observations, the stress situation created in the neighborhood of each atomic species is summarized schematically in Figure 6.4. The compressive stress field ($p < 0$) seen in the case of substituents is mainly due to the repulsive short-range nonbonded forces. The tensile field ($p > 0$) experienced by the carbon atoms originates mainly in the strong skeletal carbon-carbon bonded forces. Let it be noted that the purely nonbonded contribution to p is compressive, and follows a distribution skewed to the left for all three atomic species considered. This confirms that carbons

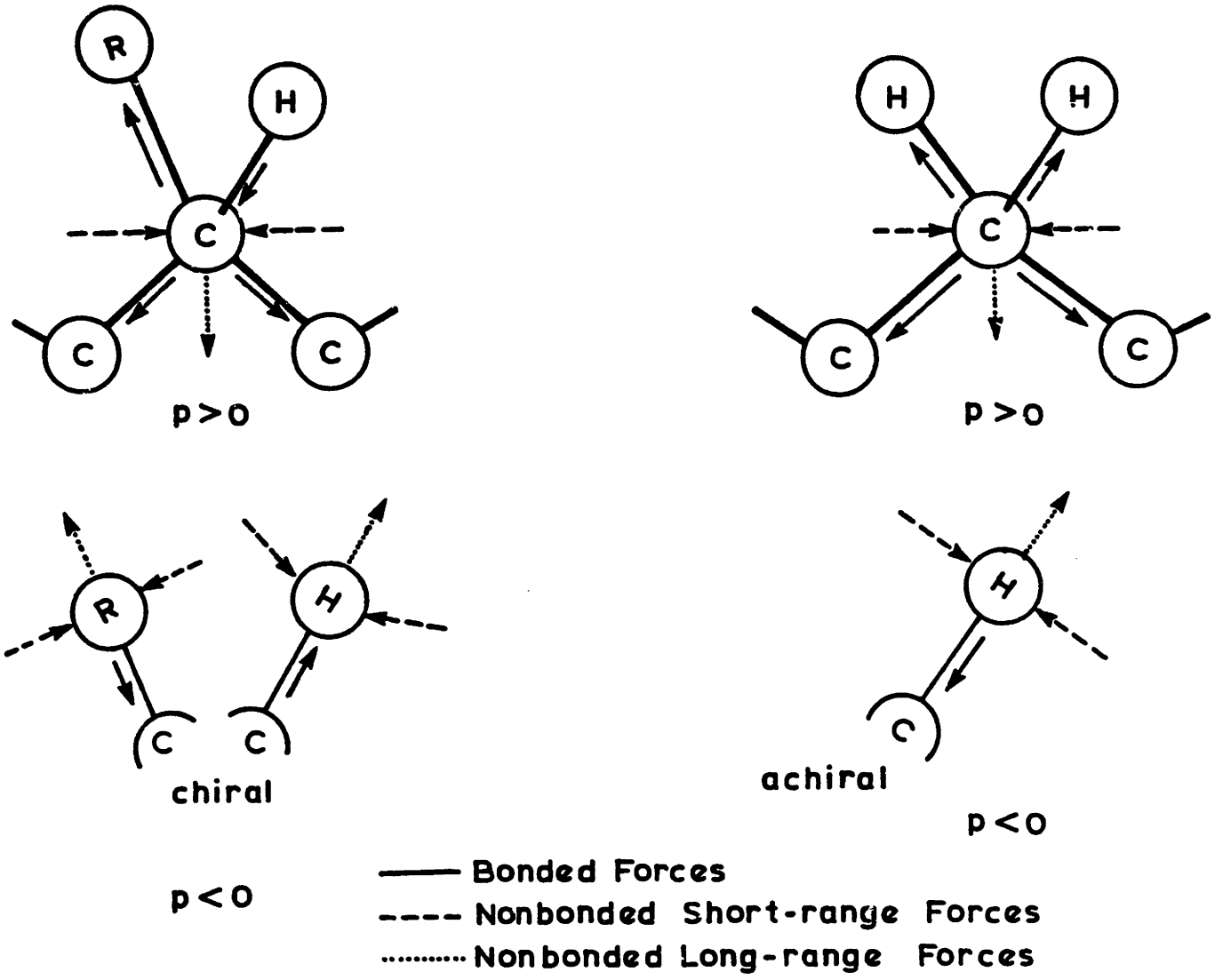

Figure 6.4 : Stress situation in the neighborhood of each "atomic" species in the model systems. Bonded forces are pictured as central, for simplicity.

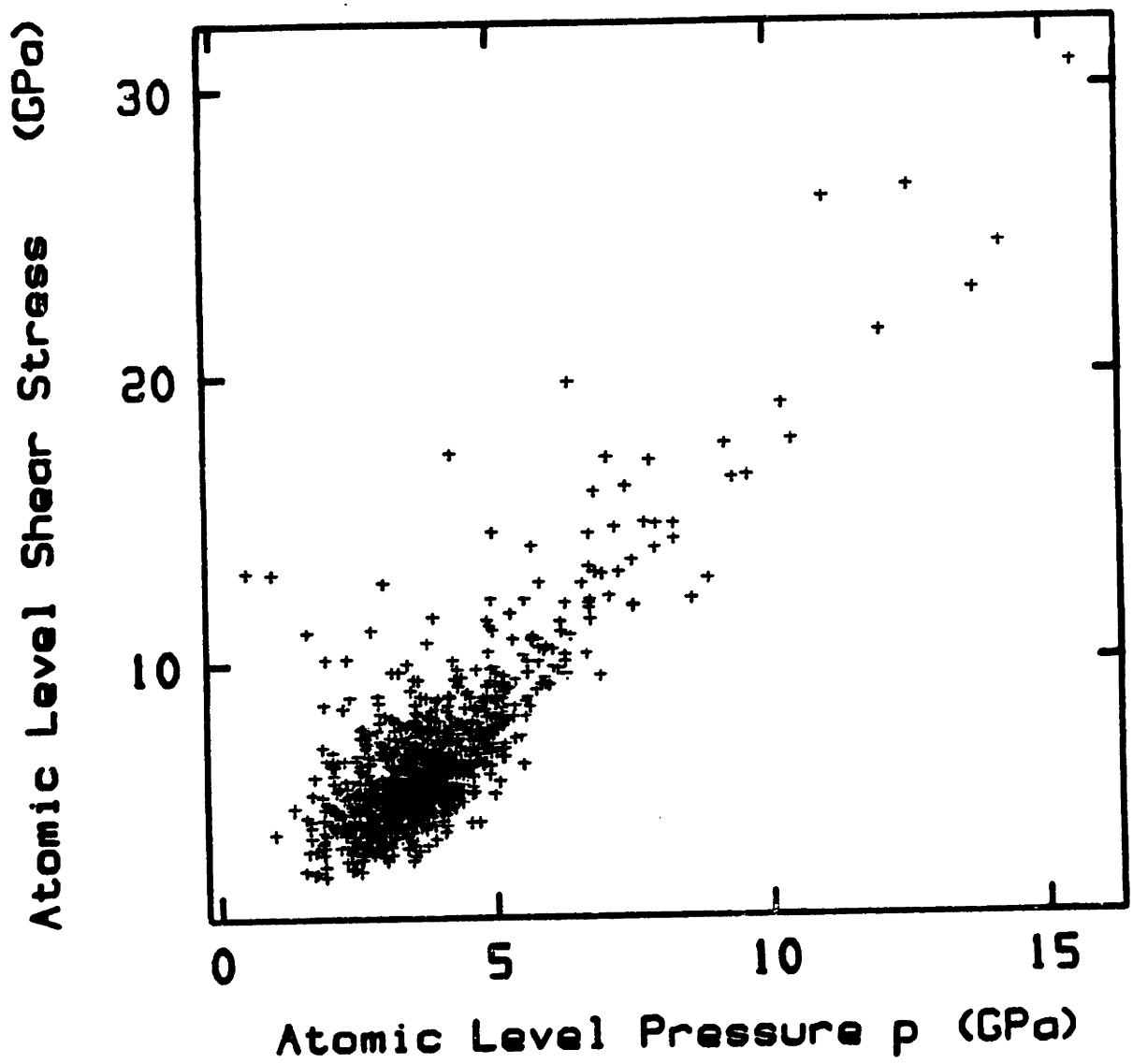

Figure 6.5

Correlation between atomic-level pressure and atomic-level shear stress (carbon atoms, 8 undeformed structures)

are differentiated from substituents in Figure 6.2 as a result of the special bonded forces they experience.

The spread of the p-distribution reflects the variation in density of the local environments experienced by each atomic species. The p-distribution for hydrogens is considerably wider than that of carbons and methyls (Table 6.1.) This probably originates in the fact that hydrogens come topologically in two classes, those connected to methine, and those bound to methylene carbon atoms (compare Fig. 6.4.) No trace of bimodality can be discerned in the distribution, however.

The atomic shear stress distributions (Fig. 6.3) are all skewed to the right (this is the shape observed by Srolovitz, Vitek and Egami.) The means and standard deviations listed in Table 6.1 indicate that skeletal carbons experience a greater asymmetry of local environments. This is probably due to the strong skeletal bonded forces pulling on each carbon atom from both sides (compare Fig. 6.4.)

Figure 6.5 contains a correlation plot of the p- and τ-values experienced by carbon atoms in all model structures. Each point corresponds to a single carbon atom. A strong positive correlation is evident; large values od p are accompanied by large values of τ, and vice versa. Similar correlations are also observed in the case of the other two species studied (not displayed here.) We can conclude that the "stress ellipsoids" experienced by all atoms belonging to a certain species are roughly similar to each other in the undeformed state.

6.2. STRUCTURAL CHANGES UPON DEFORMATION

To model the elastic response to small strain mechanical deformation (chapter 5), each one of eight undeformed structures was subjected to a "hydrostatic" compression, a "hydrostatic" tension, six shear deformations (±zx, ±zy, ±xy), and six uniaxial tension-compression deformations (±x, ±y, ±z). In this section we will concentrate on the shear and uniaxial compression-tension deformations only. Thus, for each undeformed model structure, we will be considering 12 deformed model structures, forming 6 pairs of exactly opposite macroscopic deformations. The degree of deformation, ε, defined in chapter 5, is always ±0.001.

By direct comparison of the structural features of the deformed structures with those of the undeformed structures from which they were obtained, conclusions can be drawn about the microscopic mechanism to deformation.

6.2.1. Rotation Angle Changes

The torsion angles of the skeletal bonds constitute the internal microscopic degrees of freedom of our model polymer chains. The rotation angle change for bond i upon deformation is simply defined as:

$$\Delta\phi_i = \phi_i - \phi_{o,i} = \phi_i^{\text{deformed}} - \phi_i^{\text{undeformed}}, \quad 2 \leq i \leq 2x-1 \tag{6.20}$$

The distribution of $\Delta\phi$ upon shear was accumulated from all shear "experiments" on all deformed model structures. A distribution of $\Delta\phi$ upon tension was similarly accumulated from

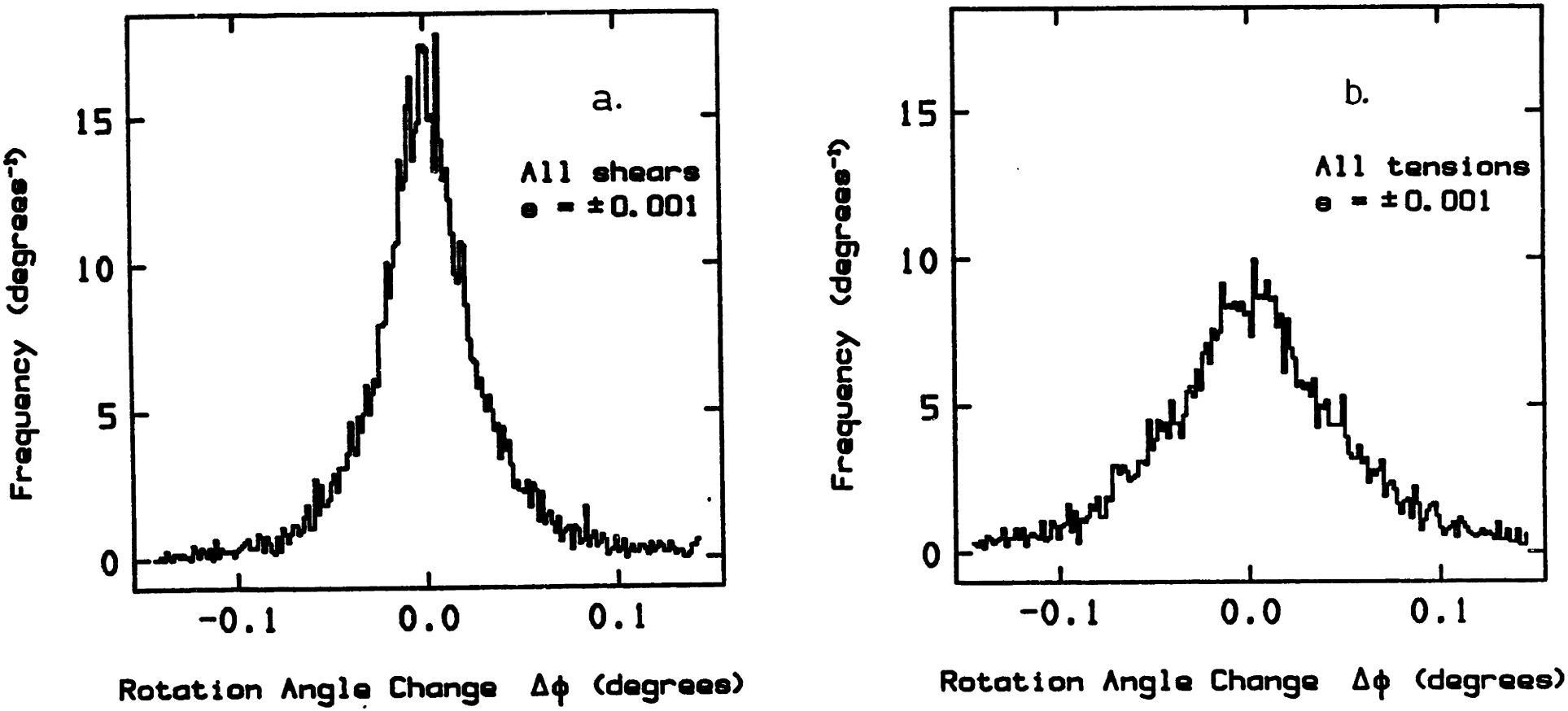

Figure 6.6: a. Distribution of rotation angle changes upon shear (8 structures, 6 shear experiments per structure)

b. Distribution of rotation angle changes upon tension (8 structures, 6 tension experiments per structure)

all tension experiments. These distributions are displayed in Figs 6.6(a) and (b). Characteristic quantities are also given in Table 6.2.

The $\Delta\phi$ - distributions are symmetric, with average values of practically 0. It should be emphasized that the symmetry observed in Figs 6.6(a) and (b) is not related to the fact that pairs of opposite deformations were used for constructing them. The $\Delta\phi$ - distribution for each individual deformation is symmetric, indicating that, at least for the small deformations studied here, torsion angles have, on the average, equal probabilities of changing in either direction. Superposition of many deformations is used, here and in the following, only to reduce the statistical noise associated with a limited sample size.

The standard deviation of the distribution of torsion angle changes upon shear is entirely comparable in order of magnitude to the macroscopic shear angle imposed on the model system during the shearing deformation (Table 6.2.) The standard deviation of the $\Delta\phi$-distribution in tension is greater than that that in shear by approximately 30%. This indicates that, for the same value of ε, more drastic structural changes accompany tension than shear. The reason probably lies in that shear is a volume-preserving transformation, whereas tension is not, so it requires more drastic topological changes in order to occur.

6.2.2. Atomic Displacements

Perhaps the most direct evidence of changes brought about by deformation is provided by the individual atom displacements. The atomic displacements reflect not only local topological changes in the material, but also the macroscopic,

externally imposed strain field. For example, the total displacements of atoms in the vicinity of two opposite faces of the "periodic box" would appear correlated during shear, simply because of the parallelity of the faces. To study strictly local, microscopic rearrangements, we subtract the affine contribution from all displacements.

We define the "inhomogeneous displacement vector" of atom i as the difference:

$$\Delta \underset{\sim}{r}_i = \underset{\sim}{r}_i^{\text{deformed}} - \underset{\sim}{r}_i^{\text{affine}} \qquad (6.21)$$

where $\underset{\sim}{r}_i^{\text{deformed}}$ is the position vector of this atom in the deformed system, and $\underset{\sim}{r}_i^{\text{affine}}$ is the position that this atom would have if we subjected the undeformed system to a hypothetical strictly affine [eqn. (5.1)] deformation, characterized by the same macroscopic strain tensor as the actual deformation, and such that the centers of mass of the hypothetical affinely deformed and of the actual deformed system coincide.

As discussed in Chapter 5, strictly affine deformations in our system are impossible, because of the constraints imposed by fixed bond lengths and bond angles. The magnitude of $\Delta \underset{\sim}{r}_i$ is a direct measure of deviation from affine behavior, sensitive to the local topological rearrangements in the vicinity of atom i. The distributions of this "inhomogeneous displacement length" were accumulated for each type of center from all shear and all tension deformations considered. The distributions for hydrogen atoms are presented in Figures 6.7(a) and (b). The distributions for carbon atoms and methyl groups are entirely analogous. The characteristic quantities of all distributions are summarized in Table 6.2. All $|\Delta \underset{\sim}{r}|$ distributions are skewed to the right. Displacements tend to be largest for methyl groups. Hydrogens follow, while carbon atoms experience the smallest displacements. This can readily

be understood if we view the motion of substituents as a rotation about the chain backbone, superposed on the displacement of skeletal carbons; C-R bonds are longer than C-H bonds, so that methyl groups move about a longer moment arm, which explains their larger $\langle|\Delta\underset{\sim}{r}|\rangle$ in comparison with hydrogens. Within a given species, the average inhomogeneous displacement in tension is larger than that in shear by approximetely 45%. This again suggests more drastic topological changes.

The average affine displacement length corresponding to the studied deformations can be obtained by simple geometrical considerations. For a cube of edgelength a, sheared to a strain ε perpendicular to axis z, so that its center remains unchanged,

$$\langle|\Delta\underset{\sim}{r}^{affine}|\rangle \equiv \langle \underset{\sim}{t}^{affine} \rangle = \frac{1}{\frac{a^3}{2}} \int_0^{a/2} (\varepsilon z)\, a^2\, dz = \varepsilon \frac{a}{4} \tag{6.22}$$

For the same cube, extended uniaxially to a strain ε along axis x, in a transformation that leaves its center unchanged,

$$\langle|\Delta\underset{\sim}{r}^{affine}|\rangle \equiv \langle \underset{\sim}{t}^{affine} \rangle = \frac{1}{\frac{a^3}{2}} \int_0^{a/2} (\varepsilon x)\, a^2\, dx = \varepsilon \frac{a}{4} \tag{6.23}$$

Using our cube edgelength a = 18.15 Å, and an extent of deformation ε = 0.001, we arrive at a value of $\langle|\Delta\underset{\sim}{r}^{affine}|\rangle = 4.54\ 10^{-3}$ Å. Comparing with the $\langle|\Delta\underset{\sim}{r}|\rangle$ values listed in Table 6.2 we conclude that, the average displacement length is entirely comparable, and actually larger than the average affine displacement length corresponding to the same deformation. In other words, there is a strong nonaffine component to the deformation of a polymeric glass.

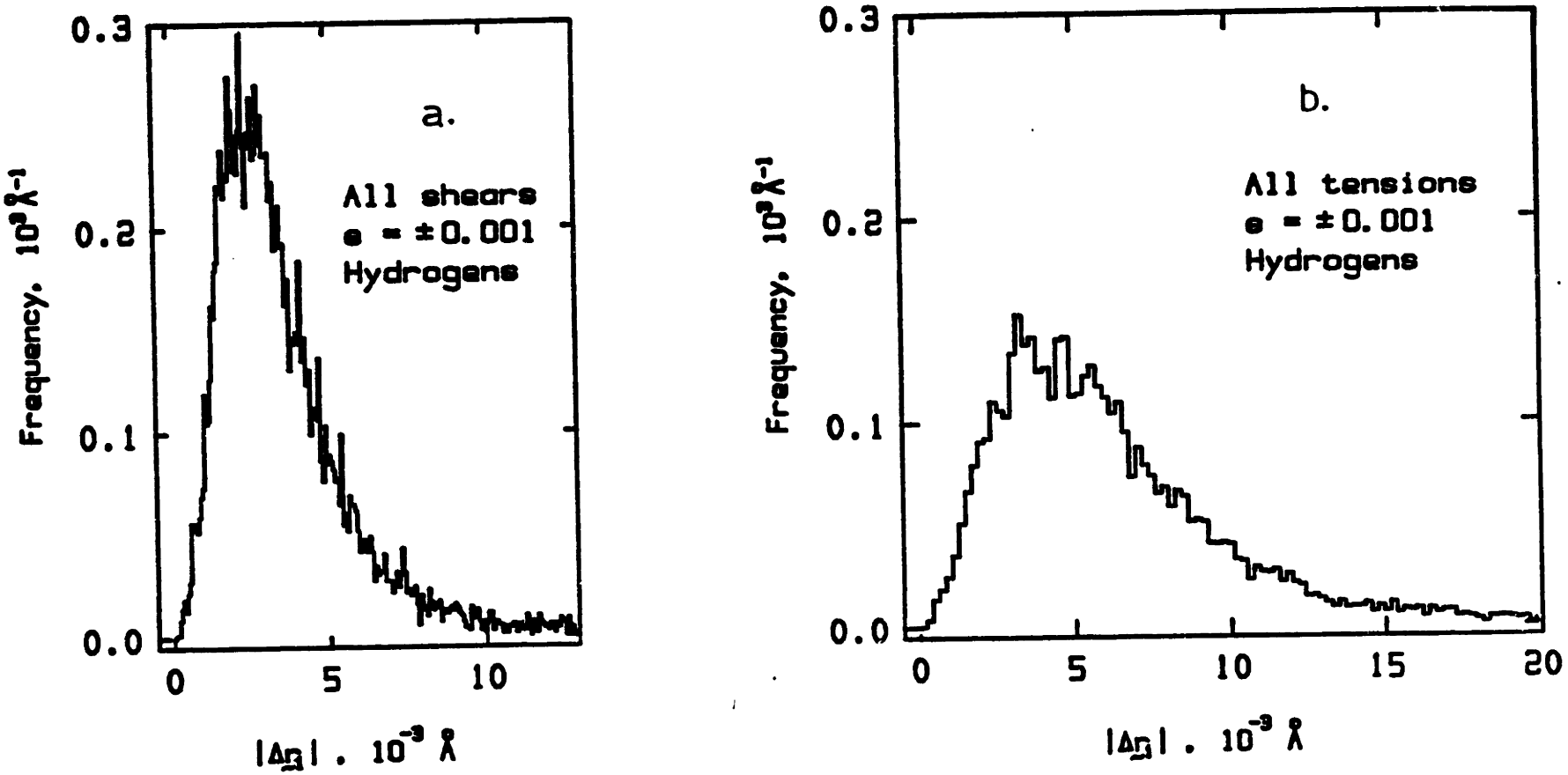

Figure 6.7 : a. Distribution of inhomogeneous displacement lengths of hydrogen atoms upon shear (8 structures, 6 shear experiments per structure)

b. Distribution of inhomogeneous displacement lengths of hydrogen atoms upon tension (8 structures, 6 tension experiments per structure)

In order to investigate the motion of atoms relative to each other, we define the relative inhomogeneous displacement vector for a pair of atoms (i,j) as the difference $(\Delta\underline{r}_i - \Delta\underline{r}_j)$. We would expect the length of this vector to be a function of interatomic separation. Neighboring atoms would tend to move together, and so would give a low value of $|\Delta\underline{r}_i - \Delta\underline{r}_j|$. The relative inhomogeneous displacement length should increase continuously with interatomic distance, approaching a limit corresponding to completely uncorrelated motion of the atoms considered. Indeed, such a behavior is observed. In Figures 6.8(a) and (b) I present $|\Delta\underline{r}_i - \Delta\underline{r}_j|$ as a function of $|\underline{r}_i - \underline{r}_j|$ for hydrogen atoms, in all shears and tensions performed. (The minimum image convention is always used in determining interatomic separations.) The corresponding plots for carbons and methyls (not shown here) are very similar. The asymptotic values reached in the limit of high interatomic separations are listed in Table 6.2 , and are compared with the average inhomogeneous displacement length $\langle|\Delta\underline{r}|\rangle$. If the vectors $\Delta\underline{r}_i$ and $\Delta\underline{r}_j$ consisted of completely uncorrelated Gaussianly distributed components, then the ratio

$$\frac{\langle|\Delta\underline{r}_i - \Delta\underline{r}_j|\rangle}{\langle|\Delta\underline{r}_i|\rangle}$$

would assume a value of $2^{1/2}$. From Table 6.2 we see that this ratio is observed, within the limits of statistical noise, for high interatomic separations. The displacements of atoms lying as close as ca. 10 Å are completely independent.

6.2.3. Directional Correlation of Displacements

To quantitatively characterize the directional correlation of displacements, we consider the angle

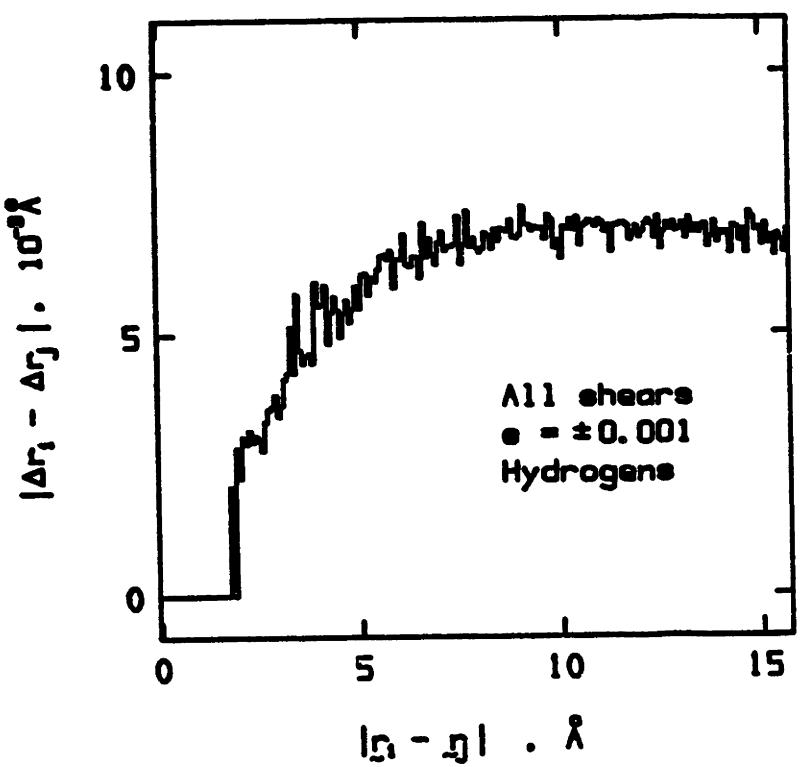

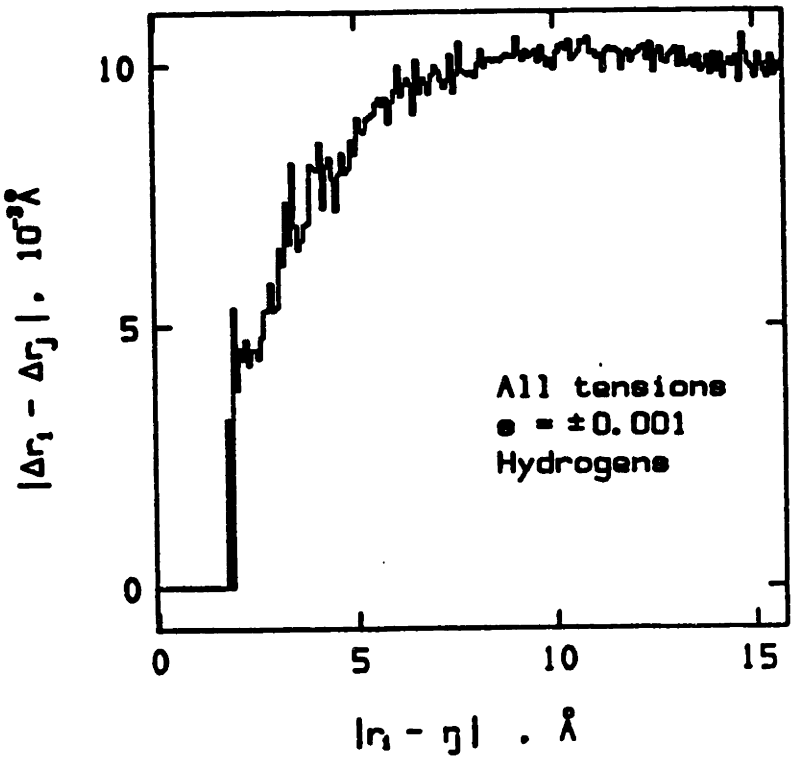

Figure 6.8:

a. Relative inhomogeneous displacement length as a function of interatomic distance, for hydrogen atoms in all shear deformations studied (8 structures, 6 shear experiments per structure)

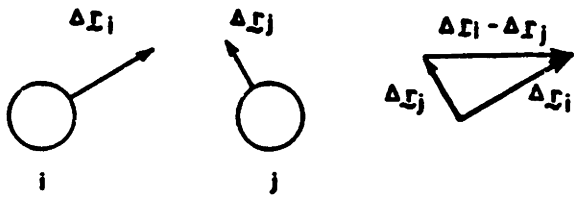

b. Relative inhomogeneous displacement length as a function of interatomic distance, for hydrogen atoms in all tension deformations studied (8 structures, 6 shear experiments per structure)

Table 6.2 : Structural Changes Upon Deformation

	Shear	Tension
Average rotation angle Change $\langle\Delta\phi\rangle$, 10^{-3} degrees	-0.12	-0.03
Stand. dev. of distribution of rotation angle changes, $\left[\langle(\Delta\phi)^2\rangle - \langle\Delta\phi\rangle^2\right]^{1/2}$, 10^{-3} degrees	70.6	90.3
Macroscopically imposed shear angle $\tan^{-1}(\varepsilon)$, 10^{-3} degrees	57.3	

	Atomic Species			Atomic Species		
	H	C	R	H	C	R
Average inhomogeneous displacement length, $\langle\lvert\Delta\underline{r}\rvert\rangle$, 10^{-3} Å	4.73	4.41	5.27	6.85	6.37	7.80
Standard deviation of the distribution of inhomogeneous displacement lengths, $\left[\langle\lvert\Delta\underline{r}\rvert^2\rangle - \langle\lvert\Delta\underline{r}\rvert\rangle^2\right]^{1/2}$, 10^{-3} Å	6.05	5.75	7.09	5.73	5.33	6.80
Average affine displacement length corresponding to the same deformation, $\langle\lvert\Delta\underline{r}^{affine}\rvert\rangle$, 10^{-3} Å	4.54	4.54	4.54	4.54	4.54	4.54
Relative atomic displacement length in the limit of large distances $\lim_{\lvert\underline{r}_i-\underline{r}_j\rvert\to\infty} \lvert\Delta\underline{r}_i - \Delta\underline{r}_j\rvert$, 10^{-3} Å	7.09	6.67	7.89	9.93	9.31	11.14
Ratio $\dfrac{\lim_{\lvert\underline{r}_i-\underline{r}_j\rvert\to\infty} \lvert\Delta\underline{r}_i-\Delta\underline{r}_j\rvert}{\langle\lvert\Delta\underline{r}\rvert\rangle}$	1.49	1.51	1.49	1.45	1.46	1.43

$$\theta = \cos^{-1}\left[\frac{\Delta\underset{\sim}{r}_i \cdot \Delta\underset{\sim}{r}_j}{|\Delta\underset{\sim}{r}_i|\,|\Delta\underset{\sim}{r}_j|} \right]$$

between the inhomogeneous displacement vectors of each pair of atoms, and form the function:

$$S(r) = \frac{1}{2}\{ 3 \langle\cos^2\theta(r)\rangle - 1 \} \qquad (6.24)$$

where the average is taken over all atom pairs at a distance $|\underset{\sim}{r}_i - \underset{\sim}{r}_j| = r$ from each other. Plots of S(r) for hydrogens are presented in Figures 6.9(a) and (b). One sees strong directional correlation (tendency for parallelity) between neighboring atoms, which drops quasiexponentially with increasing distance. Again, there is no correlation at large distances. (The fact that the asymptotic value reached at large distances deviates somewhat from 0 in Figure 6.9 is due to the way the $\Delta\underset{\sim}{r}$'s are normalized, and is not significant.) We also accumulated the purely intermolecular direction correlation function, from atom pairs belonging to different images of the parent chain only. The intermolecular S(r) is a measure of how deformation "hops" ([79],[80]) from chain to chain in the bulk. It, too, displays some correlation at short distances (Fig. 6.9), which, however, is considerably weaker than the total.

The directional correlation of the inhomogeneous displacements of atoms belonging to the same chain is examined in Figures 6.10(a) and (b). Again, only plots for hydrogens are shown, but the behavior for the other two atomic species is very similar. The angle θ between displacement vectors is considered, and the quantity

$$S_k = \frac{1}{2}\{ 3 \langle\cos^2\theta_k\rangle - 1 \} \qquad (6.27)$$

formed, where the ensemble average is taken over all atom

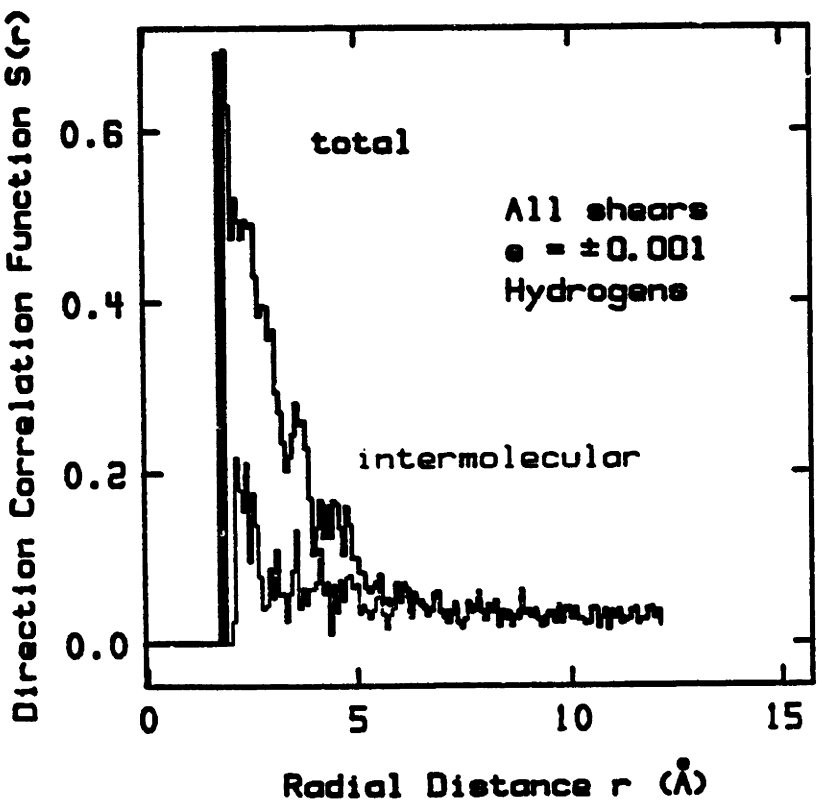

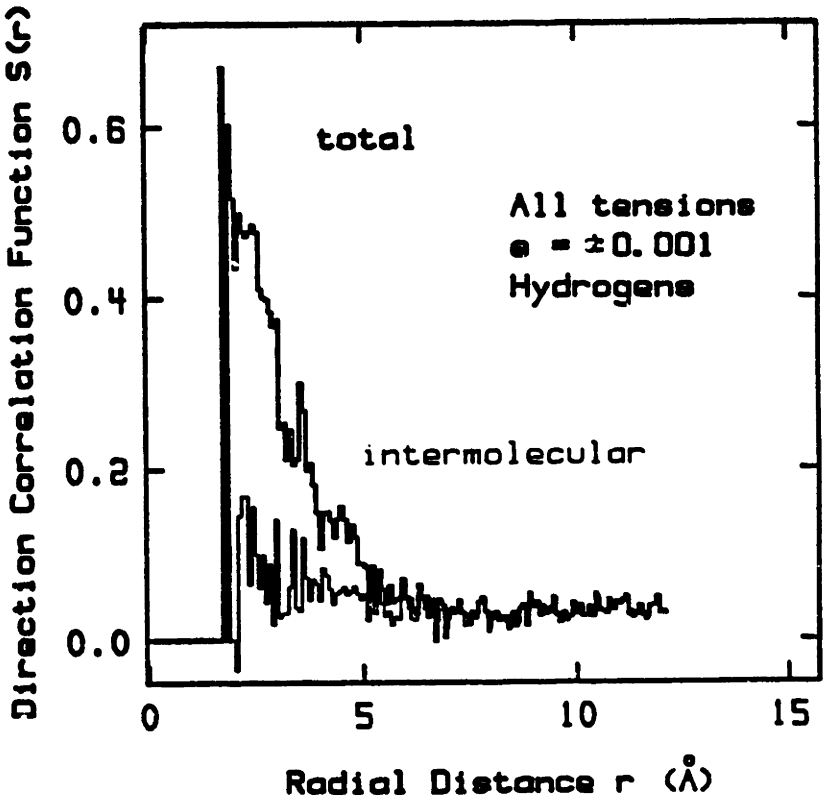

Figure 6.9 : Directional correlation of inhomogeneous displacements as a function of interatomic distance in the bulk, for hydrogen atoms.

(a) all shear deformations studied (8 structures, 6 shear experiments per structure)

(b) all tension deformations studied 8 structures, 6 tension experiments per structure)

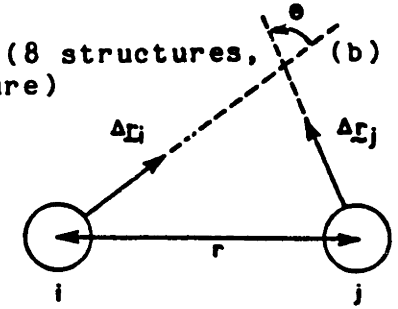

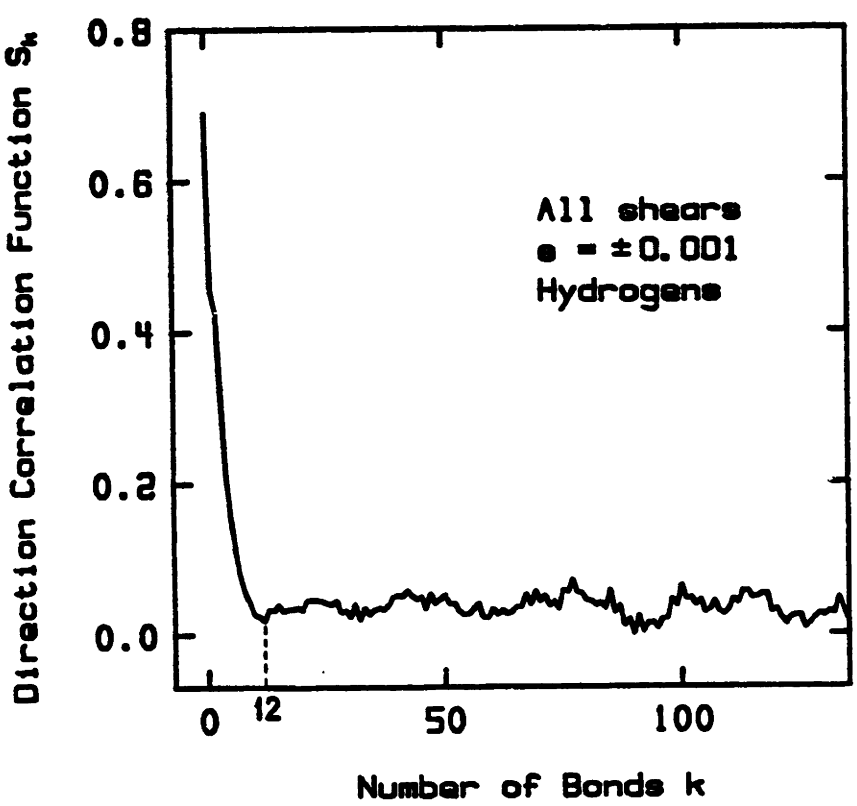

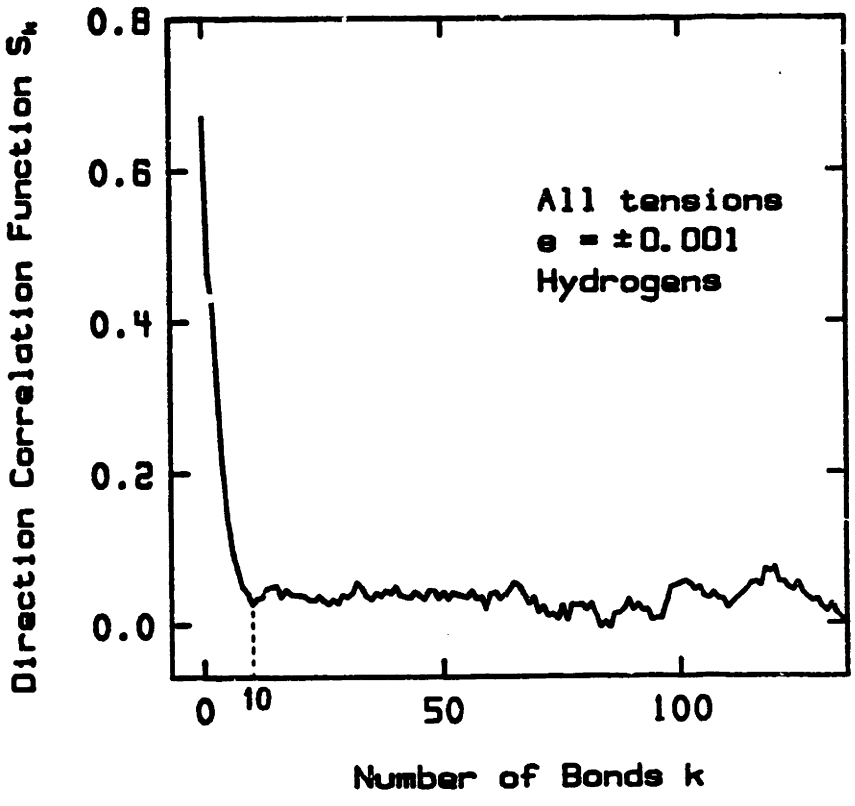

Figure 6.10: Directional correlation of inhomogeneous displacements of hydrogen atoms belonging to the same parent chain, as a function of the number of skeletal bonds (k) between the segments to which the atoms are attached.

(a) all shear deformations studied (8 structures, 6 shear experiments per structure)

(b) all tension deformations studied (8 structures, 6 tension experiments per structure)

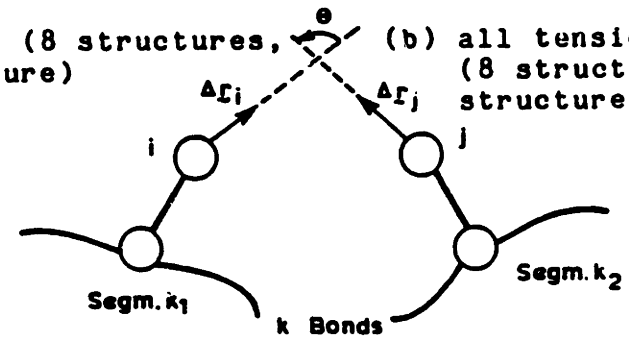

pairs attached to segments (k_1, k_2) belonging to the same chain and separated by a fixed number of bonds $|k_1 - k_2| = k$. This intramolecular S_k is plotted against the number of intervening bonds, k. We see strong directional correlation at small separations, which, however, drops quickly to a value of practically 0; 12 bonds in the case of shear, and 10 bonds in the case of tension suffice. Thus, our model results indicate that deformation in the glass is accompanied by coordinated displacement of chain segments approximately 10 bonds long.

6.2.4. Changes in Atomic Level Stresses upon Deformation

Atomic level stresses reflect the topological characteristics of the local environment around each atom. Hence, the changes

$$\Delta p_i = p_i^{\text{deformed}} - p_i^{\text{undeformed}}$$

and (6.26)

$$\Delta \tau_i = \tau_i^{\text{deformed}} - \tau_i^{\text{undeformed}}$$

are direct quantitative measures of topological changes brought about by deformation.

In Figure 6.11 Δp is plotted against $\Delta \tau$ for all carbon atoms of a typical model structure subjected to shear deformations. We observe a pronounced positive correlation between Δp and $\Delta \tau$, and conclude that large changes in local density upon elastic deformation occur under retention of the shape of the atomic stress ellipsoids (compare Fig. 6.5.)

A remarkable feature of the pattern displayed in Fig. 6.11 is its almost perfect central symmetry. The points in this pattern have been obtained from three pairs of opposite

($\varepsilon = \pm 0.001$) shearing deformations ($\pm zx$, $\pm zy$, $\pm xy$). The symmetry observed indicates tnat, within the range of deformations considered, for a "normal" structure (see below), opposite macroscopic deformations induce exactly opposite microscopic changes in local atomic environment. Indeed, it has been confirmed that the displacement vectors of any atom are strictly opposite for such pairs of deformations, although they strongly deviate from affine behavior.

It has been mentioned (section 5.6) that two of our eight model structures exhibit thermodynamic instability. ($\underline{C}$ - matrix of isothermal elastic coefficients non-positive definite) when subjected to deformation. One of these structures is strongly "abnormal", in that it gives negative shear moduli in two of the three modes of shearing examined. In Fig. 6.12 we plot Δp vs. $\Delta \tau$ for this structure; this plot is completely analogous to Fig. 6.11. Two observations can be made immediately:

(a) The magnitude of atomic-level stress changes in this unstable structure is at least five times that in a "normal" structure.

(b) The pattern is no longer symmetric, especially near its fringes. The excessive topological rearrangement and the lack of microscopic symmetry, laid bare by Fig. 6.12, is observed only in this single unstable structure. Furthermore, it stems solely from the two "abnormal" modes of shearing deformation. The contribution of the third shear mode, which is mainly responsible for the cluster of points at the center of the pattern, is symmetric and of ordinary magnitude, resembling Fig. 6.11. Closer examination has revealed that a particular portion of the parent chain undergoes vigorous motion (relative to the small magnitude of

the strains) when an "abnormal" shear is imposed, with displacements that change in magnitude by more than a factor of two when the direction of shear is reversed.

In their study of plastic deformation in an amorphous metal, Srolovitz, Vitek and Egami [55] observed well-defined localized deformation events. Collective, two-dimensional sliding motions of groups involving approximately 8 atoms, as well as circular, three-dimensional motions of groups of approximately 14 atoms were seen, and large τ-values ("τ-defects") were found to be associated with deformation sites. The present study, carried out in a range of strains much smaller than theirs (within the elastic regime), did not reveal <u>any</u> significant correlation between τ (or p) and atomic displacements. Such correlations might, however, appear at larger strains, where plastic deformation becomes important.

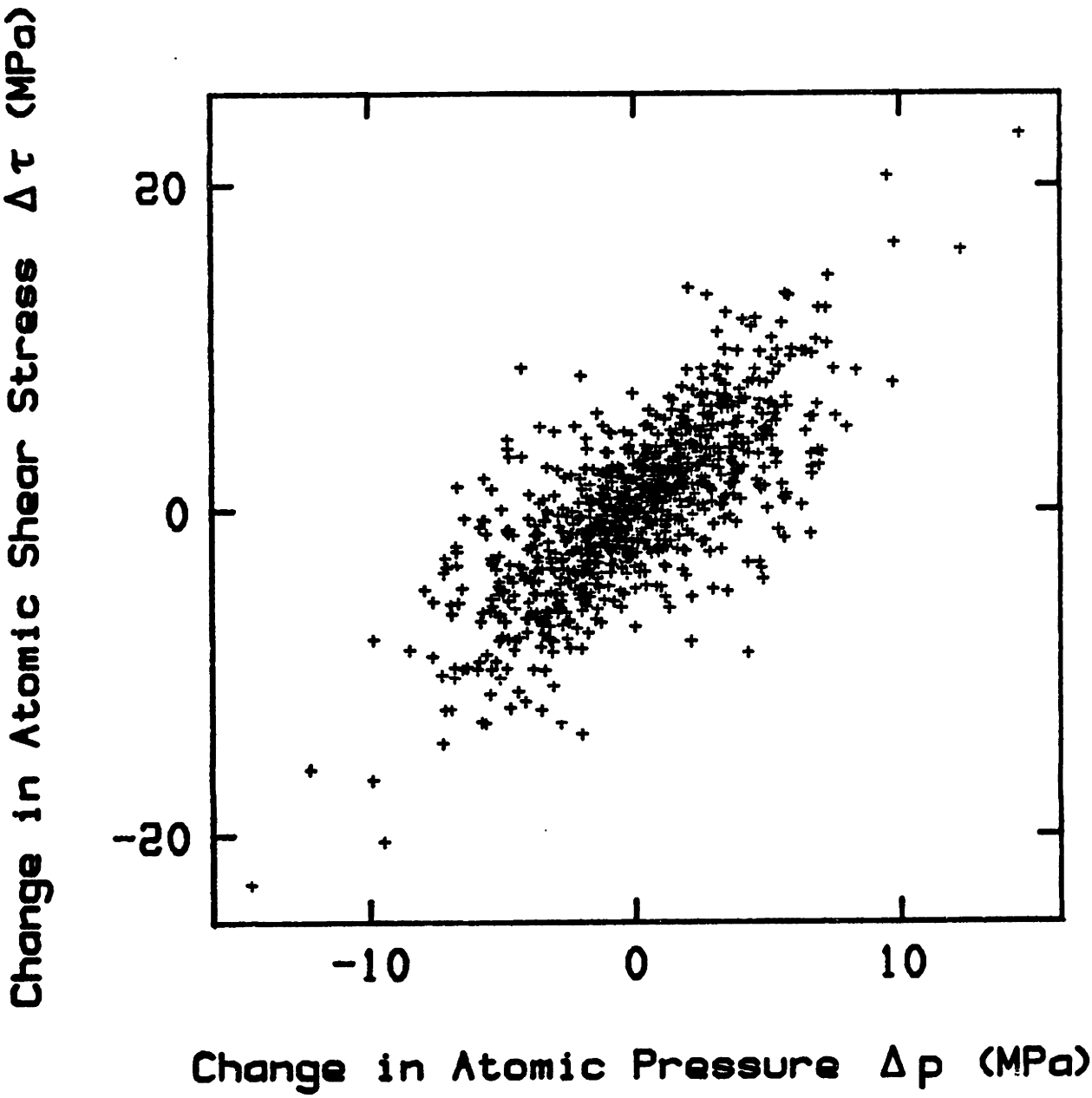

Figure 6.11: Changes in the atomic-level hydrostatic pressure (p) plotted against changes in the atomic-level shear stress (τ), for carbon atoms in a typical model structure subjected to shear. The plotted points are from 6 shear deformations on a single structure.

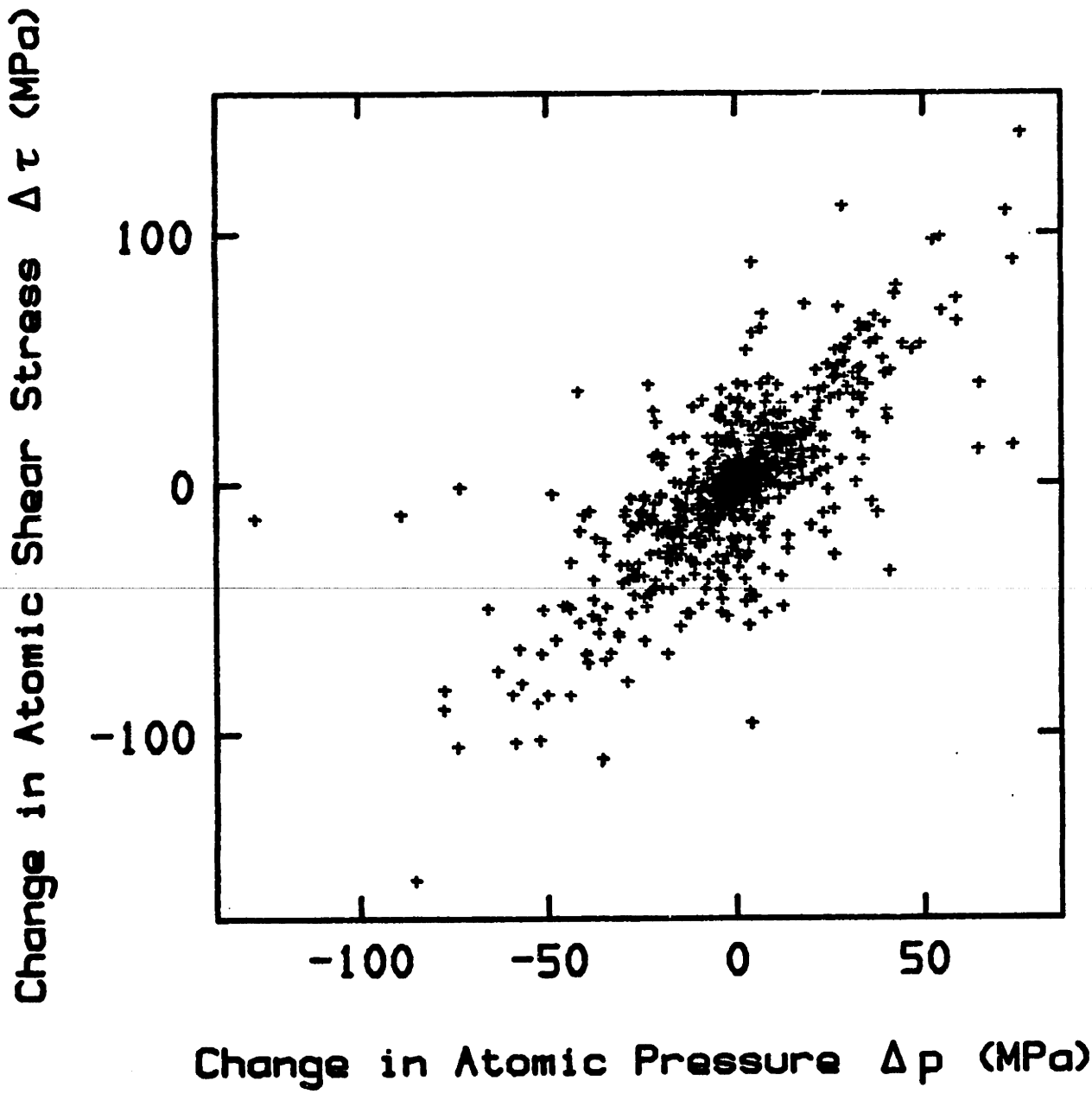

Figure 6.12: Changes in the atomic-level hydrostatic pressure (p) plotted against changes in the atomic-level shear stress (τ), for carbon atoms in a model structure exhibiting thermodynamic instability when subjected to shear. The plotted points are from 6 shear deformations on a single structure.

7. EXPERIMENTAL

The purpose of the experimental part of this thesis was:

- To produce well-characterized samples of the modelled polymer, atactic polypropylene.

- To study the molecular structure of these samples by X-ray and neutron diffraction, and to compare against model predictions.

7.1. PRODUCTION OF EQUILIBRIUM EPIMERIZED ATACTIC POLYPROPYLENE

7.1.1. Reaction

Atactic polypropylene is obtained from the isotactic form of the polymer, by catalytic epimerization at 250°C, under a pressure of 13.2 atmospheres of hydrogen, using a Palladium catalyst supported on activated alumina:

$$\text{PP-it} \xrightarrow[Pd/Al_2O_3]{250^{\circ}C\ ,\ p_{H_2} = 13.2\ \text{Atm}} \text{PP-at} \qquad (7.1)$$

The epimerization reaction has been extensively studied by Suter [56], and by Suter and Neuenschwander ([59]). Industrial interest in various variants of polypropylene epimerization is obvious from the patents issued on the subject [34]. It has been shown ([59]) that a stereochemical equilibrium is established. The tacticity of the polymer at equilibrium is well approximated by Bernoullian statistics, with a fraction of meso-dyads equal to $w_m = 48\%$. Equilibrium atactic polypro-

pylene is thus a polymer with very well-defined tacticity,and this is one of the reasons why it was chosen for our modelling work (see Section 3.1.) Some considerations on the mechanism of the catalytic reaction (7.1) are presented in [56].

The highly isotactic polypropylene PRO-FAX PD-701, produced by Hercules, Inc. by Ziegler-Natta polymerization, was used as a starting material for the epimerizations carried out in this thesis. The catalyst (Palladium on activated aluminum oxide 10% w/w, hydrogenation catalyst) was obtained from Fluka AG. Hydrogen of 99.99% purity, provided by Matheson Gas Products, was used in the gaseous phase.

A schematic of the apparatus built for carrying out the epimerization is given in Figure 7.1. The reactor is a steel autoclave of internal volume 160 cm^3. It is kept in a well-insulated casing. A pair of semicylindrical heating units (Lindberg Laboratory Heat Systems, Model 150312) is used for maintaining the desired reaction temperature. Temperature control is accomplished using a Love Controls, Model 49 proportioning controller; the sensor is a Chromel-Alumel Type K thermocouple (Omega Engineering), attached to the external surface of the autoclave, for avoiding long time lags in the response. There is an additional thermocouple, immersed in the reacting mixture, and connected to a digital indicator (Omega Engineering, Model 199), which directly displays the reaction temperature at all times. The temperature was maintained constant at 250 ± 2^{o}C. The reactor operation is batch. A reaction time of 30 days was used, to reach equilibrium.

To start an epimerization reaction, ca. 25 g. of isotactic polypropylene pellets were frozen in liquid nitrogen, and subsequently broken in a press, to reduce particle size. The polymer was then thoroughly mixed with an equal weight of

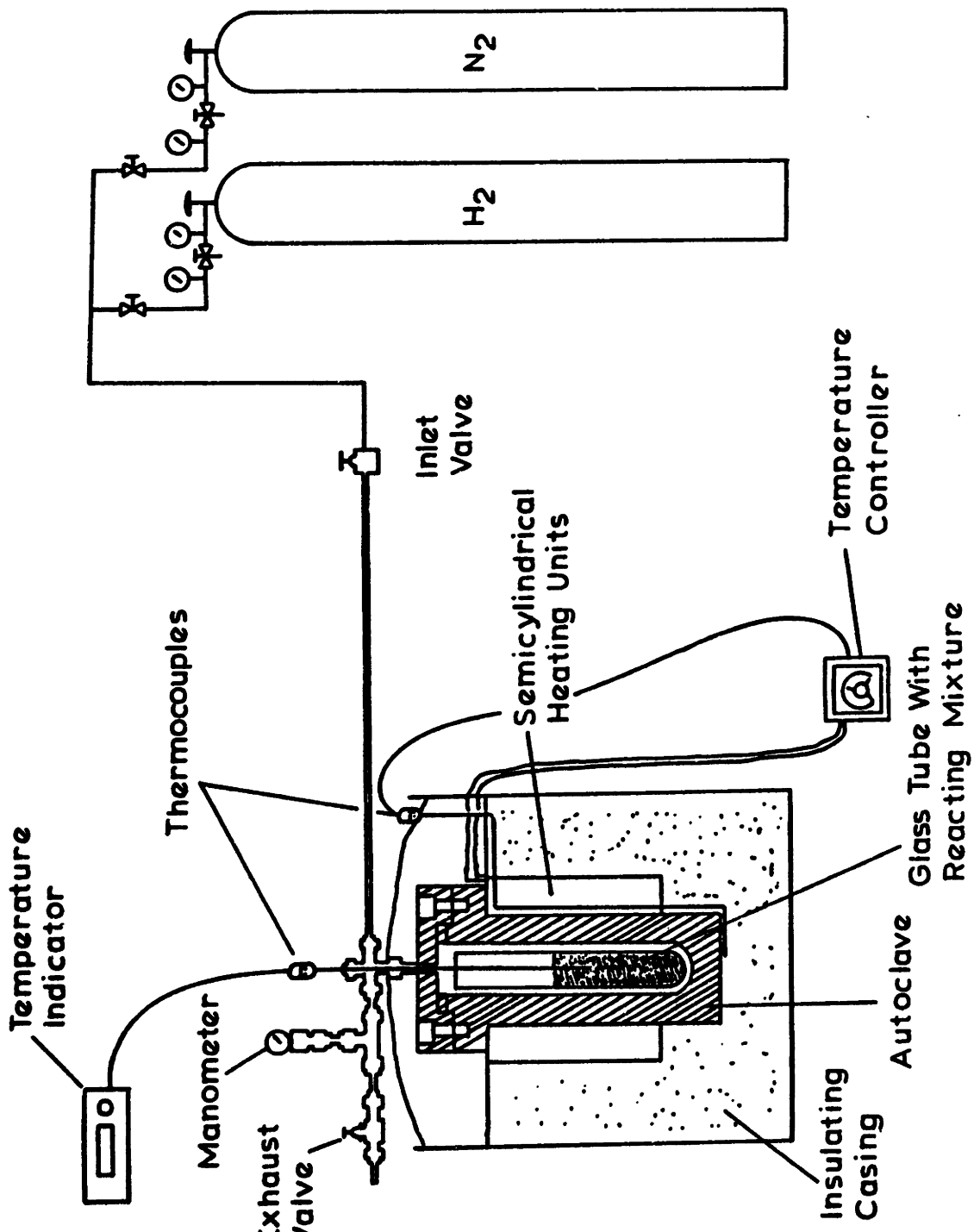

Figure 7.1 : Apparatus used for the epimerization reaction of isotactic polypropylene to equilibrium atactic polypropylene

catalyst, and put in a glass tube. The tube was placed in the autoclave and the reactor was sealed and purged with nitrogen, to remove atmospheric oxygen. Hydrogen was then introduced and heating was commenced, to reach the desired temperature and pressure operating conditions. The system was maintained at these conditions for the entire reaction time. To stop the reaction, the autoclave was depressurized, purged with nitrogen, removed from its casing and quenched in ice. The reaction obviously took place in a melt of bulk polypropylene, bearing catalyst particles in suspension, and saturated with hydrogen gas. The product mixture was recovered from the reactor as a rubbery substance of black color (due to the presence of the catalyst.)

7.1.2. Product Separation and Purification

Atactic polypropylene was separated from the catalyst by extraction in diethyl ether. "Kumagawa extractors" [56] were used for this purpose. The Kumagawa extractor, depicted in Figure 7.2, is similar in construction to a Soxhlet extractor, but is designed so that the tube containing the sample under extraction is directly exposed to the vapor of the solvent; thus, the extraction always takes place at the solvent boiling temperature. An extraction time of 3 days was typically used. The entire polymer goes into solution. This is an indication of epimerization: atactic polypropylene readily dissolves in ether (solubility parameter 15.4 $(J/cm^3)^{1/2}$ according to [71],p.144); on the contrary, the starting isotactic material was completely insoluble in ether, and only dissolved in boiling xylene (solubility parameter ,according to [71],p.144, equal to 17.9 $(J/cm^3)^{1/2}$). The catalyst was recovered completely pure as the residue, and was recycled. The extract (solution of polypropylene in ether) was filtered, and subsequently precipitated in an excess of methanol.

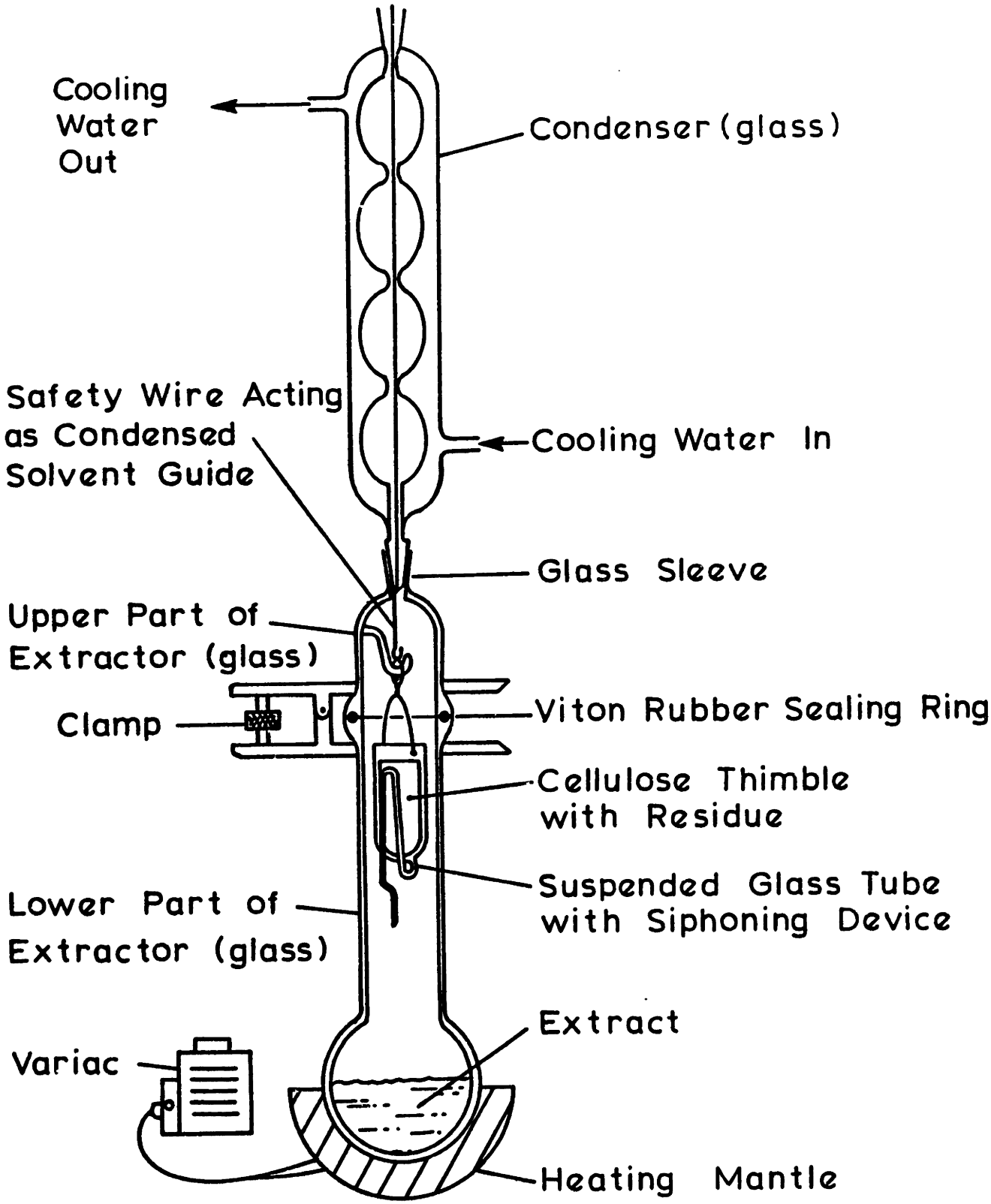

Figure 7.2 : The Kumagawa extractor

A tendency to form colloidal suspensions in methanol can be completely eliminated by vigorous stirring. The precipitated polymer was collected and dried in a vacuum oven at 60°C. The overall yield, from isotactic to pure atactic polymer, was always better than 80%.

Pure atactic polypropylene has an appearance pronouncedly different from that of the isotactic form. Whereas the isotactic polymer is white and opaque, the atactic is perfectly transparent and colorless, due to complete absence of crystallinity. At room temperature it is a leathery, sticky substance, which flows very slowly under its own weight.

7.1.3. Product Characterization

Tacticity

The tacticity of the product polymer was determined by nuclear magnetic resonance spectroscopy. 270 MHz ^{1}H - NMR spectra were taken in 12% w/w solutions of the polymer in o-dichlorobenzene-d_4 (99.5% atom D, Chemical Dynamics Corp.) at 423 K. A typical ^{1}H - NMR spectrum is presented in Figure 7.3(a). Also, some 67.9 MHz ^{13}C - NMR spectra were taken in C_6D_6 solutions at 383 K. A ^{13}C - NMR spectrum is presented in Figure 7.3(b). The assignment of peaks follows [59]. Epimerization is evident from the signal due to methylene protons belonging to racemic dyads in the ^{1}H - NMR spectrum, as well as from the shape of the methyl signal in the ^{13}C - NMR spectrum (compare with spectra of the isotactic polymer in [59].) Both spectra in Fig.7.3 display features practically identical to the ones reported in [59] for equilibrium atactic PP. The five individual peaks of the ^{1}H - NMR spectrum, due to methyl, m-methylene, r-methylene, m-methylene and methine protons [Fig. 7.3(a); order of increasing chemical shift] were resolved and integrated by cutting and weighing.

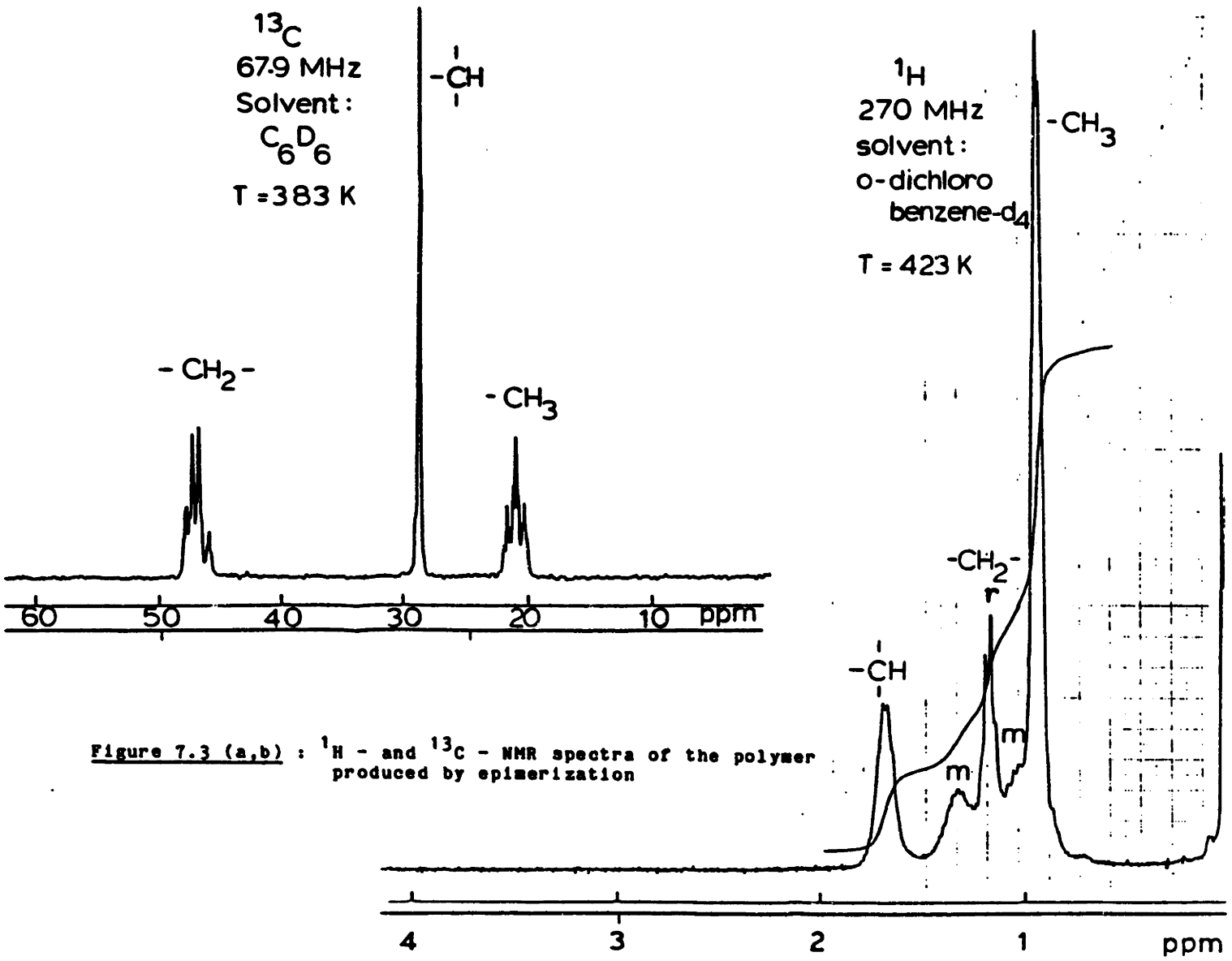

Figure 7.3 (a,b) : ^1H - and ^{13}C - NMR spectra of the polymer produced by epimerization

The areas of these peaks are related as 3 : w_m : 2(1 - w_m) : w_m : 1 , and thus permit a quantitative assessment of the tacticity. Within the accuracy of the integration, w_m was found to be indistinguishable from the value of 0.48, reported in [59] for stereochemical equilibrium. Thus, NMR spectroscopy confirms that we have indeed produced equilibrium atactic polypropylene, of a configuration identical to the one we use in our modelling work.

Molecular Weight

The epimerization reaction (7.1) is accompanied by some degradation; an equilibrium average molecular weight is reached under given temperature and catalyst conditions [59]. The viscosity average molecular weight of our samples was determined in cyclohexane and in benzene at 30°C, using simple Ostwald-Fenske viscometers. Mark-Houwink parameter values were taken from [59] and [16]. The determined molecular weight was $\bar{M}_v$ = 30000 ± 3000.
This is considerably lower than the equilibrium molecular weight reported in [59], probably because of the different epimerization reaction conditions used there.

7.2. PRODUCTION OF DEUTERATED EQUILIBRIUM EPIMERIZED ATACTIC POLYPROPYLENE

7.2.1. Deuteration Reaction

The experimental problems encountered in neutron scattering due to the very high incoherent scattering cross-section of hydrogen (see Section 4.4.2) triggered our interest in producing a fully deuterated form of atactic polypropylene.

Since the incoherent scattering cross-section of deuterium is much smaller than that of hydrogen (table 4.3), the experimental information obtained from neutron scattering using deuterated samples is more conclusive.

The catalytic epimerization reaction (7.1) involves exchange of hydrogen atoms between the polymer and the gaseous phase. Similarly, if deuterium is introduced in the gas phase, we would expect it to partition itself chemically between the gas and the polymer. By analogy to reaction (7.1) we developed the following direct exchange scheme for the deuteration of atactic polypropylene:

$$\text{PP-at} \xrightarrow[Pd/Al_2O_3]{250^{\circ}C\ ,\ p_{D_2} = 13.2\ \text{Atm}} \text{deuterated PP-at} \qquad (7.2)$$

An excess of deuterium must be used to drive the exchange equilibrium towards the deuterated polymer.

The following procedure was used to implement scheme (7.2) in practice: A small amount of epimerized atactic polypropylene [the product from reaction (7.1)], mixed with an equal weight of catalyst, was placed in the reactor, and the reactor was pressurized with gaseous D_2 (Deuterium C.P., 99.5% mol/mol purity, Matheson Gas Products) and brought to reaction conditions, as described in section 7.1. At intervals of 24 hrs the reactor was emptied of its contents (down to atmospheric pressure) and refilled with D_2.

Let:

M = the initial mass of (protonated) polypropylene placed in the reactor

w_H = the hydrogen content of polypropylene, measured in moles H_2 / g PP ($w_H = \frac{3 \text{ moles}}{42 \text{ g}}$)

v_o = the quantity of gas remaining in the reactor after emptying (in moles)

v = the quantity of D_2 introduced in the reactor upon filling (in moles)

y_D = the purity of the D_2 gas used (mol/mol)

n = the number of fillings (including the initial filling)

x_n = the degree of deuteration of the polymer immediately before the (n+1)th filling

If one assumes that:

- the exchange reaction is fast enough, so that equilibrium is established within 24 hours (in the interval between successive fillings)
- there is no preference for H or for D, i.e. the chemical roles of these two atomic species are completely equivalent, and exchange equilibrium implies an identical ratio of H to D in the gaseous and polymer phases,

then a recursive relation for x_n can be arrived at by a simple deuterium mass balance:

$$M\,w_H\,x_{n-1} + v_o\,x_{n-1} + v\,y_D = (v + v_o)\,x_n + M\,w_H\,x_n$$

$M\,w_H\,x_{n-1}$	$v_o\,x_{n-1}$	$v\,y_D$	$(v + v_o)\,x_n$	$M\,w_H\,x_n$
moles D_2 in polymer from previous reaction	moles D_2 remaining in gas from previous filling	D_2 input	moles D_2 in gas after attaining equilibrium following n^{th} filling	moles D_2 in polymer after attaining equilibrium following n^{th} filling

$$\text{or} \quad x_n = \frac{M\,w_H + v_o}{M\,w_H + v_o + v}\,x_{n-1} + \frac{v}{M\,w_H + v_o + v}\,y_D\,,$$

which can be solved to yield:

$$x_n = y_D \left[1 - \left(\frac{M w_H + v_o}{M w_H + v_o + v} \right)^n \right] \qquad (7.3)$$

According to this simple model of hydrogen-deuterium exchange, therefore, the degree of deuteration varies exponentially with the number of fillings, asymptotically tending to the purity of the D_2 gas used.

A trial deuteration experiment involved an atactic polypropylene sample of initial mass M = 4.3626 g.
The volume occupied by the sample and the glass tube in the reactor was 29 cm^3, so the volume of the reactor accessible to gas was (160 - 29) cm^3 = 131 cm^3.
The quantity of gas remaining in the reactor after purging to atmospheric pressure at the reaction temperature is then:

$$v_o = \frac{(1 \text{ atm})\ (131 \text{ cm}^3)}{(0.082 \cdot 10^3 \ \frac{\text{cm}^3 \text{ atm}}{\text{mol K}})\ (523 \text{ K})} = 3.05 \cdot 10^{-3} \text{ mol}$$

The quantity of gas introduced upon refilling to the operation pressure of 13.2 atm is

$$v = \frac{(13.2 \text{ atm})\ (131 \text{ cm}^3)}{(0.082 \cdot 10^3 \ \frac{\text{cm}^3 \text{ atm}}{\text{mol K}})\ (523 \text{ K})} - v_o = 37.2 \cdot 10^{-3} \text{mol}$$

A total of 17 refillings was used, hence n = 18.
With $w_H = \frac{1}{14} \ \frac{\text{mol}}{\text{g}}$ and $y_D = 0.995$, the degree of deuteration predicted by eqn. (7.3) is:

$$x_D^{calc} = x_{18} = 0.995 \left[1 - (0.894)^{18} \right] = 86\% \text{ mol/mol} \qquad (7.4)$$

The exchange reaction is discontinued and the deuterated product purified exactly as described in Section 7.1 for the epimerization reaction. The recovered deuterated polymer is

similar in appearance to the equilibrium epimerized protonated polymer; at room temperature it is considerably stickier and more liquidlike (faster flowing) than the protonated form.

7.2.2. Product Characterization

270 MHz ^1H - NMR spectra of the deuterated polymer were obtained in solution in o-dichlorobenzene-d_4 at 423 K. Although the intensity of the entire spectrum is much weaker, due to deuteration, its appearance is similar to that of the protonated polymer spectrum. This indicates that all hydrogens in polypropylene are exchanged to the same extent, i.e. the catalytic deuteration reaction (7.2) shows no selectivity between methyl, methylene and methine hydrogens.

The degree of deuteration was determined by quantitative ^1H - NMR spectroscopy, using naphthalene as an internal standard. Accurately weighed amounts of deuterated polymer and of naphthalene were dissolved in o-dichlorobenzene-d_4 and the relative amounts of hydrogen contained in each were determined by integration of the respective ^1H - NMR peaks (Naphthalene gave a double signal at 7.31 and 7.67 ppm, which is clearly discerned from that of polypropylene.) The absolute amount of hydrogen contained in the polymer was thus determined on the basis of the internal standard. The degree of deuteration, for the particular trial run described in section 7.2.1, was found to be:

$$x_D^{exp} = 79 \text{ \% mol/mol} \qquad (7.5)$$

Comparison of eqns (7.4) and (7.5) shows that our simple theoretical calculation of deuteration, based on establishment of equilibrium, is not unreasonable.

After the trial run, described above, confirmed that the deuteration reaction (7.2) is feasible, runs with longer reaction time were carried out. Our longest deuteration experiment rendered a batch whose degree of deuteration, determined by ^1H - NMR, is $x_D = 88$ % mol/mol (7.6)

7.3. X - RAY DIFFRACTION MEASUREMENTS

Samples of equilibrium epimerized atactic polypropylene (Section 7.1) were prepared in the shape of flat films of area 50.8 x 50.8 mm^2 and thickness 0.8 mm. The thickness was chosen on the basis of a calculation of the mass absorption coefficient of polypropylene for X - rays [37], so as to avoid significant absorption of the incident radiation by the sample.

Forming the samples proved to be a nontrivial problem, because of the sticky nature of the material at room temperature. Molds in the shape of square pans, of base area equal to the desired film area, were constructed out of Teflon, to which atactic polypropylene adheres only weakly at room temperature. To prepare a sample, a carefully weighed amount of pure atactic polymer was placed in the mold and allowed to flow under its own weight at a temperature of 60 to 80 ^oC in a vacuum oven, until it acquired the desired shape. To remove a sample, its mold was frozen in liquid nitrogen, and the glassified polypropylene film detached and transferred to the sample holder of the diffractometer. There it was allowed to slowly heat and equilibrate to ambient conditions. Low-temperature handling required a moisture-free environment, to avoid condensation of ice on the sample.

The diffraction experiments were performed in the laboratory of Professor T. Egami, Department of Materials Science and Engineering and Laboratory for Research on the Structure of Matter, University of Pennsylvania. A reflection geometry was used. The diffraction angle θ_s was kept constant at 4^o, and the photon energy E_X varied from 0 to 48 keV. The magnitude of the diffraction vector, Q, is therefore obtained from the photon energy as:

$$Q = \frac{4\pi}{\lambda_s} \sin\theta_s = \left(\frac{2}{\hbar c} \sin\theta_s \right) E_X = 0.07065\ E_X \qquad (7.7)$$

where E_X is measured in keV, and Q in Å^{-1}. The experimental X - ray diffraction patterns have been presented in Figure 4.10(a),(c).

7.4. NEUTRON DIFFRACTION MEASUREMENTS

Samples for neutron scattering were prepared in the shape of small cylinders, of height 25.4 mm and diameter 9.5 mm. Again, Teflon molds were constructed. The sample was placed in a cylindrical bore in the mold, and allowed to sit in a vacuum oven at 60 to 80^oC, until it acquired the shape of a solid, bubble-free cylinder. For the measurement, the mold was opened after freezing in liquid nitrogen, and the sample removed and placed in a cylindrical sample holder made of vanadium (this metal is practically transparent to neutrons.)

The neutron diffraction pattern of the protonated polymer, depicted in Figure 4.11(a), was obtained under the guidance of Dr. H. Mook, using the HB-2 spectrometer facility at the High Flux Isotope Reactor of the Oak Ridge National Laboratory. An especially high incident neutron flux is available in this

spectrometer [10^7 neutrons/(cm^2 s)], which makes it most appropriate for our weakly scattering samples. Technical data on the facility are provided in [45]. Thermal neutrons of energy E_n = 56 meV were used for the particular measurement. The wavelength of the incident beam is:

$$\lambda_s = \frac{2\pi\hbar}{m_n^{1/2}} \frac{1}{E_n^{1/2}} = \frac{0.286}{E_n^{1/2}} \qquad (7.8)$$

with E_n in eV and λ_s in Å, and, for our measurements,

$$\lambda_s = 1.209 \text{ Å} \qquad (7.9)$$

The polypropylene sample was cooled to -40°C at a rate of -1.3 K/min, and a scan was performed over a range of diffraction angles $2\theta_s$ from 3.2 to 84.5 degrees. The magnitude of the diffraction vector Q is related to the diffraction angle through equation (4.18). The scanned diffraction angle was varied by computer control in Q - increments of 0.05 $Å^{-1}$. The count time at each position was 3.7 min. Only the elastic component of the scattered radiation was picked up, using the spectrometer's analyzer crystal. However, no separation can be made between coherent and incoherent scattering, i.e. the total (coherent + incoherent) elastic scattering was counted. An identical scan was performed with the empty sample holder, and the two scans subtracted, to obtain the pattern of the sample. This is presented in Figure 4.11. The problem of incoherent scattering has already been discussed in Section 4.4.1.

Samples of our 88% deuterated polymer, obtained as described in Section 7.2, have been sent to the HFIR ar ORNL, for additional neutron scattering measurements. With this degree of deuteration we expect the incoherent scattering problem to be much less serious. Results will be reported in a future publication.

8. CLOSING REMARKS

8.1. CONCLUSIONS AND SIGNIFICANCE

We summarize here some of the most important conclusions reached in this thesis.

- A thermodynamic analysis showed that the elastic response to deformation in a glassy amorphous polymer is governed by potential energy, rather than by entropic effects. A statistical mechanical analysis showed that thermal vibrations associated with bond length and bond angle variations can safely be neglected in predicting the elastic constants.

- A new method has been developed for the detailed atomistic computer simulation of a glassy vinyl polymer (glassy atactic polypropylene.) The polymer is pictured as an ensemble of static model structures in detailed mechanical equilibrium. Each structure is arrived at by Monte Carlo generation, using the Rotational Isomeric State Theory, followed by total potential energy minimization with respect to all microscopic degrees of freedom. The modelling approach involves no adjustable parameters.

- Model estimates of thermodynamic properties, such as the cohesive energy and Hildebrand's solubility parameter, are in very good agreement with reported experimental values.

- The conformation of chains in the bulk polymer model structures is essentially unperturbed, in agreement with

Flory's "random coil hypothesis." Structural features are predominantly intramolecular, and long-range order is completely absent.

- Well-characterized samples of equilibrium epimerized atactic polypropylene (the modelled polymer) were prepared by catalytic epimerization of isotactic polypropylene, and their molecular structure was studied by X - ray and neutron diffraction. Theoretical diffraction patterns, computed directly from the model, are consistent with experiment.

- A method has been developed for predicting the elastic constants, by simulating small-strain mechanical deformations of the model structures. Theoretical elastic constants are within 15% of the reported experimental values.

- The model was used to explore local topology in the polymer glass, and to probe the mechanism of deformation on an atomistic level. Deformation was found to have a strongly nonaffine character, and coordinated displacement of chain segments approx. 10 bonds long was observed.

On the basis of the above results we make the following general statement: Detailed atomistic simulations of bulk polymeric systems can be computationally manageable, and at the same time serve as powerful tools for understanding and predicting macroscopic properties on the basis of molecular structure.

8.2. POSSIBLE EXTENSIONS

A variety of interesting problems, associated with the amorphous polymer bulk, can be attacked along the lines developed in this thesis:

- Our methodology is quite general, and can readily be applied to other vinyl polymers, such as poly(vinyl chloride), which offers the opportunity of studying the effects of polar groups. Extension of our modelling approach to a non-vinyl glass, such as polycarbonate, would be another step towards generalization.

- The deformation simulation method we developed can be used to look at much larger strains, in order to elucidate the mechanisms of plastic deformation in a polymeric glass.

- The effects of chain orientation, on the molecular level, on mechanical properties could be explored by imposing a certain degree of chain alignment in the model structures, and examining the resulting changes in elastic constants.

- The existence of well-defined "filled" and "void" spaces in the model glass permits quantification of the so often used, but somewhat hazy, concept of "free volume." Its spatial distribution, as well as its redistribution under various forms and degrees of deformation, can be studied. Another key concept that can be similarly quantified is the concept of "chain entanglements."

- Chain dynamics in the bulk constitute a rich and intriguing topic. A problem in doing molecular dynamics simulations in a multichain system is that the approach to equilibrium is very slow; thus, if one starts from an

unrealistic structure, and due to the very limited time span covered by the molecular dynamics simulation, one ends up exploring the wrong region of phase space. Our static relaxed structures can serve as excellent initial configurations for a molecular dynamics simulation, to explore dynamic characteristics in the glass, or in the melt, using structures generated at lower densities. Performing molecular dynamics simulations at a variety of temperatures could shed some light on the phenomenon of glass transition.

- Experimentally, a detailed study of the amorphous polymer bulk by X - ray and neutron scattering, at various temperatures above and below the glass transition temperature, would provide valuable molecular information on the structural changes accompanying the glass transition.

- The diffusion of gaseous species in the amorphous polymer bulk can be studied, and a prediction of diffusion coefficients attempted on the basis of force fields experienced by a penetrant molecule in the model structure. The phenomenon of plasticization may be similarly studied by the introduction of plasticizer molecules.

- The onset of crazing may be detectable in model structures, such as ours, as a phase separation into void and dense spaces under very large stresses.

The author hopes to be able to explore some of these, and related problems in the future. He also hopes that working on them will be as stimulating and rewarding as working on this thesis has been.

REFERENCES

[1] Abramowitz, M.; Stegun, I.A. "Handbook of Mathematical Functions"; 10th Printing; National Bureau of Standards: Washington, D.C., 1972.

[2] Alexandrowitz, Z.; Accad, Y. "Monte Carlo of Chains with Excluded Volume: Distribution of Intersegmental Distances" J. Chem. Phys. 1971, 54, 5338-5345.

[3] Allen, G.; Petrie, S.E.B. (Editors) "Physical Structure of the Amorphous State"; Marcel Dekker: New York, 1977.

[4] Azároff, L.V.; Kaplow, R.; Kato, N.; Weiss, R.J.; Wilson, A.J.C.; Young, R.A. "X-ray Diffraction"; McGraw-Hill: New York, 1974.

[5] Ballard, D.G.; Wignall, G.D.; Schelten, J. "Measurement of Molecular Dimensions of Polystyrene Chains in the Bulk Polymer by Low Angle Neutron Diffraction" Europ. Polymer J. 1973, 9, 965-969.

[6] Bishop, M.; Ceperley, D.; Frisch, H.L.; Kalos, M.H. "Investigation of Static Properties of Model Bulk Polymer Fluids" J. Chem. Phys. 1980, 72, 3228-3235.

[7] Bondi, A. "Physical Properties of Molecular Crystals, Liquids and Glasses"; John Wiley: New York, 1968.

[8] Born, M.; Huang, K. "Dynamical Theory of Crystal Lattices"; Clarendon Press: Oxford, 1954; Chapter II.

[9] Bovey, F.A.; Winslow, F.H. (Editors) "Macromolecules: an Introduction to Polymer Science"; Academic Press: New York, 1979.

[10] Brandrup, J.; Immergut, E.H. (Editors) "Polymer Handbook"; 2nd Edition; Wiley Interscience: New York, 1975.

[11] Callen, H.B. "Thermodynamics"; John Wiley: New York, 1960.

[12] Cohen, M.H.; Grest, G.S. "A New Free Volume Theory of the Glass Transition", in O'Reilley, J.M.; Goldstein, M. (Editors) "Structure and Mobility in Molecular and Atomic Glasses"; Annals of the New York Academy of Sciences, Vol. 371: New York, 1981; p 199-209.

[13] Cohen, M.H.; Grest, G.S. "Liquid-Glass Transition, a Free Volume Approach" Phys. Rev. B 1979, 20, 1077-1098.

[14] Cotton, J.P.; Farnoux, B.; Jannink, G.; Mous, J.; Picot, C. "Observation de la conformation de la chaîne polymérique dans le solide amorphe par diffusion des neutrons aux pétits angles" C. R. Acad. Sci. (Série C) 1972, 275, 175-178.

[15] Dachs, H. (Editor) "Neutron Diffraction"; Springer Verlag: Berlin, 1978.

[16] Danusso, F.; Moraglio, G. "On the Behavior of Isotactic and Atactic Polypropylene in Solution" Makromol. Chem. 1958, 28, 250-252.

[17] Dennis, J.E.; More, J.J. "Quasi-Newton Methods, Motivation and Theory" SIAM Review 1977, 19, 46-89.

[18] de Santis, R.; Zachmann, H.G. "Study of the Conformations of the Molecules in Amorphous Polymers by Computer Simulation I. Non-Equilibrium State Obtained by Introducing Chains in a Primitive Cubic Lattice" Colloid and Polymer Sci. 1977, 225, 729-734.

[19] de Santis, R.; Zachmann, H.G. "Study of the Conformations of the Molecules in Amorphous Polymers by Computer Simulation II. Approach to Equilibrium in a Primitive Cubic Lattice by Simulation of Thermal Motion" Progr. Colloid and Polymer Sci. 1978, 64, 281-285.

[20] De Vos, E.; Bellemans, A. "Concentration Dependence of the Mean Dimension of a Polymer Chain" Macromolecules 1974, 7, 812-814.

[21] Dill, K.A.; Flory, P.J. "Interphases of Chain Molecules: Monolayers and Lipid Bilayer Membranes" Proc. Natl. Acad. USA 1980, 77, 3115-3119.

[22] Egami, T.; Maeda, K.; Vitek, V. "Structural Defects in Amorphous Solids: A Computer Simulation Study" Phil. Mag. A 1980, 41, 883-901.

[23] Egami, T.; Vitek, V. "Local Structural Fluctuations and Properties of Amorphous Metals", in Proceedings of Symposium on Amorphous Materials: Modeling of Structure and Properties, AIME, Oct. 25-26, 1982.

[24] Egami, T.; Vitek, V. "Local Structural Fluctuations and Defects in Metallic Solids" J. Non-Cryst. Solids 1984, 61-62, 499-510.

[25] Flory, P.J. "Principles of Polymer Chemistry"; Cornell University Press: Ithaca, N.Y., 1953.

[26] Flory, P.J. "Statistical Mechanics of Chain Molecules"; John Wiley Interscience: New York, 1969.

[27] Flory, P.J. "Molecular Configuration in Bulk Polymers", reprinted from Macromolecular Chemistry-8, IUPAC International Symposium, Helsinki, Finland, 1972.

[28] Flory, P.J. "Foundations of the Rotational Isomeric State Theory and General Methods for Generating Configurational Averages" Macromolecules 1974, 7, 381-392.

[29] Gō, N.; Scheraga, H.A. "On the Use of Classical Statistical Mechanics in the Treatment of Polymer Chain Conformation" Macromolecules 1976, 9, 535-542.

[30] Grest, G.S.; Cohen, M.H. Adv. Chem. Phys. 1981, 48, 455-525.

[31] Hansen, J.P.; Mc Donald, I.R. "Theory of Simple Liquids" Academic Press: New York, 1976.

[32] Haward, R.N.; MacCallum, J.R. "The Relationship between Volume and Elasticity in Polymer Glasses" Polymer 1971, 12, 189-193.

[33] Hayashi, H.; Flory, P.J. "Configuration of the Polyiisobutylene Chain according to Neutron and X-ray Scattering" Macromolecules 1983, 16, 1328-1335

[34] HERCULES, Inc. (Déposant) "Demande de brevet d' invention No 7730100", Institut National de la Propriété Industrielle, Paris, France, 1977.

[35] Hillstrom, K. "Nonlinear Optimization Routines in AMDLIB", Technical Memorandum No 297, Argonne National Laboratory, Applied Mathematics Division, 1976; Subroutine GQBFGS in AMDLIB, 1976, Argonne, Ill.

[36] Hukins, D.W.L. "X-ray Diffraction by Disordered and Ordered Systems"; Pergamon Press: Oxford, 1981.

[37] International Union of Crystallography "International Tables of X-ray Crystallography"; Kynoch Press: Birmingham, England, 1952-1962; Vol. III: Physical and Chemical Tables.

[38] Jagodic, F.; Borštnik, B,; Ažman, A. "Model Calculation of the Gas Diffusion through the Polymer Bulk" Makromol. Chem. 1973, 173, 221-231.

[39] Jeffreys, H. "Cartesian Tensors"; Cambridge University Press: Cambridge, England, 1969.

[40] Kaufmann, H.S.; Falcetta, J.J. "Introduction to Polymer Science and Technology"; J.Wiley: New York, 1977.

[41] Kirste, R.G.; Kruse, W.A.; Schelten, J. "Die Bestimmung des Trägheitsradius von Polymethylmethakrylat im Glaszustand durch Neutronenbeugung" Makromol. Chem. 1973, 162, 299-303.

[42] Koppelmann, J.; Leder, H.; Royer, F. "Relaxations-spektroskopie amorpher hochpolymerer Stoffe II. Mechanische Untersuchungen im linearen Bereich" Colloid and Polymer Sci. 1979, 257, 673-688.

[43] Maeda, K.; Takeuchi, S. "Atomistic Process of Plastic Deformation in a Model Amorphous Metal" Phil. Mag. A 1981, 44, 643-656.

[44] Dr. H. A. Mook, personal communication.

[45] "Neutron Scattering at the High Flux Isotope Reactor", brochure published by the Solid State Division of the Oak Ridge National Laboratories, June 1981.

[46] Page, D.I. "The Structure of Liquids by Neutron Scattering", in Willis, B.T.M. (Editor) "Chemical Applications of Thermal Neutron Scattering"; Oxford University Press: Oxford, 1973; p 173-200.

[47] Pastine, D.J. "P,V,T Equation of State for Polyethylene" J. Chem. Phys. 1968, 49, 3012-3022.

[48] Pechhold, W.; Liska, E.; Grossman, H.P.; Hägele, P.C. "On Present Theories of the Condensed Polymer State" Pure and Appl. Chem. 1976, 46, 127-134.

[49] Reichl, L.E. "A Modern Course in Statistical Physics"; University of Texas Press: Austin, 1980.

[50] Sauer, J.A; Wall, R.A.; Fuscillo, N.; Woodward, A.E. "Segmental Motion in Polypropylene" J. Appl. Phys. 1958, 29, 1385-1389.

[51] Simha, R.; Roe, J.M.; Nanda, V.S. "Low Temperature Equation of State for Amorphous Polymer Glasses" J. Appl. Phys. 1972, 43, 4312-4317.

[52] Skvortsov, A.M.; Sariban, A.A.; Birshtein, T.M. "'Machine' Experimental Study of the Structure of Amorphous Polymers" Vysokomol. Soyed. 1977, 5, 1014-1021.

[53] Slichter, W.P.; Mandell, E.R. "Molecular Motion in Polypropylene, Isotactic and Atactic" J. Appl. Phys. 1958, 29, 1438-1441.

[54] Šolc, K.; Stockmayer, W.H. "Shape of a Random Flight Chain" J. Chem. Phys. 1971, 54, 2756-2757; Šolc, K. "Shape of a Random Flight Chain" J. Chem. Phys. 1971, 55, 335-344.

[55] Srolovitz, D.; Vitek, V.; Egami, T. "An Atomistic Study of Deformation of Amorphous Metals" Acta Met. 1983, 31, 335-352.

[56] Suter, U.W. "Ueber die konformationellen Eigenschaften der diastereomeren 2,4,6,8-Tetramethylnonane und 2,4,6,8,10-Pentamethylundekane, Modellsubstanzen von Polypropylen", Ph.D. Dissertation Nr. 5133, ETH-Zürich, 1973.

[57] Suter, U.W.; Flory, P.J. "Conformational Energy and Configurational Statistics of Polypropylene" Macromolecules 1975, 8, 765-776.

[58] Suter, U.W. "Epimerization of Vinyl Polymers to Stereochemical Equilibrium 1. Theory" Macromolecules 1981, 14, 523-528.

[59] Suter, U.W.; Neuenschwander, P. "Epimerization of Vinyl Polymers to Stereochemical Equilibrium 2. Polypropylene" Macromolecules 1975, 8, 765-776.

[60] Swenson, R.J. "Comments on Virial Theorems for Bounded Systems" Am. J. Phys. 1983, 51, 940-942.

[61] Tadokoro, H. "Structure of Crystalline Polymers"; J. Wiley: New York, 1979.

[62] Tashiro, K.; Kobayashi, M.; Tadokoro, H. "Theoretical Elastic Moduli and Conformations of Polymer Chains" Macromolecules 1977, 10, 413-420.

[63] Tashiro, K,; Kobayashi, M.; Tadokoro, H. "Calculation of Three-Dimensional Elastic Constants of Polymer Crystals" Macromolecules 1978, 11, 908-913.

[64] Timoshenko, S.P.; Goodier, J.N. "Theory of Elasticity"; 3rd Edition; McGraw-Hill: New York, 1970; p.224.

[65] Theodorou, D.N., Doctoral Thesis Proposal, M.I.T., December 1983.

[66] Theodorou, D.N.; Suter, U.W. "Geometrical Considerations in Model Systems with Periodic Boundaries" J. Chem. Phys. 1985, 82, 955-966.

[67] Theodorou, D.N.; Suter, U.W. "The Shape of Unperturbed Linear Polymers; Polypropylene" Macromolecules 1985, 18, 000-000.

[68] Uhlmann, D.R.; Kreidl, N.J. (Editors) "Glass Science and Technology", Vol.I (Glass-Forming Systems); Academic Press: New York, 1983; p.6.

[69] Vacatello, M; Avitabile, G.; Corradini,P.; Tuzi, A. "A Computer Model of Molecular Arrangement in an n-Paraffinic Liquid" J. Chem. Phys. 1980, 73, 543-552.

[70] Vainshtein, B.K. "Diffraction of X-rays by Chain Molecules"; Elsevier: Amsterdam, 1966.

[71] Van Krevelen, D.W.; Hoftyzer, P.J. "Properties of Polymers - Their Estimation and Correlation with Chemical Structure"; Elsevier: Amsterdam, 1976.

[72] Wall, F.T.; Seitz, W.A. "Simulation of Polymers by Self-Avoiding, Nonintersecting Random Chains at Various Concentrations" J. Chem. Phys. 1977, 67, 3722-3726.

[73] Weaire, D.; Ashby, M.F.; Logan, J.; Weins, M.J. "On the Use of Pair Potentials to Calculate the Properties of Amorphous Metals" Acta Met. 1971, 19, 779-788

[74] Weber, T.A.; Helfand, E. "Molecular Dynamics Simulation of Polymers I. Structure" J. Chem. Phys. 1979, 71, 4760-4762.

[75] Weiner, J.H. "Statistical Mechanics of Elasticity"; John Wiley: New York, 1983.

[76] Windsor, C.G. "Basic Theory of Thermal Neutron Scattering by Condensed Matter", in Willis, B.T.M. (Editor) "Chemical Applications of Thermal Neutron Scattering"; Oxford University Press: Oxford, 1973; p 1-30.

[77] Yannas, I. V. "Introduction to Polymer Science and Engineering - A Set of Lecture Notes"; Part 2; M.I.T., 1981.

[78] Yannas, I.V. "Molecular Interpretation of Deformation in Glassy Polymers", in Mano (Editor) , "Proceedings of the International Symposium on Macromolecules", Rio de Janeiro, July 26-31"; Elsevier: Amsterdam, 1975.

[79] Yannas, I.V.; Luise, R.R. "Distinction Between Two Molecular Mechanisms for Deformation of Glassy Amorphous Polymers" J. Macromol. Sci. - Phys. 1982, B21(3), 443-474.

[80] Yannas, I.V.; Luise, R.R. "The Strophon Theory of Deformation of Glassy Amorphous Polymers: Application to Small Deformations", in Zachariades, A.E.; Porter, R.S. (Editors) "The Strength and Stiffness of Polymers"; Marcel Dekker: New York, 1983.

[81] Zakin, J.L.; Simha, R.; Hershey, C. "Low-Temperature Thermal Expansivities of Polyethylene, Polypropylene, and Polystyrene" J. Appl. Polymer Sci. 1966, 10, 1455-1473.

[82] Zallen, R. "The Physics of Amorphous Solids"; J. Wiley: New York, 1983.

NOTATION

		units
a	: edge length of model cube	Å
$\underline{a}$	: edge vector of model cube	Å
a_{ij}	: coefficient of r^{-12} repulsive term in monbonded interatomic interaction potential	(kcal/mol) Å^{12}
A	: Helmholtz energy	J
$A^{\alpha\beta}_{b,k}$	: area of k^{th} Dirac pulse appearing in the pair distribution function of species pair (α,β) at the bonded distance $r^{\alpha\beta}_{b,k}$, due to chain connectivity	Å
b	: shape asphericity of a polymer chain $b = \overline{X^2} - \frac{1}{2}(\overline{Y^2} + \overline{Z^2})$	Å^2
$\underline{b}$	: chain bond vector	Å
B	: bulk modulus of elasticity	MPa
c	: velocity of light; also,	m/s
c	: shape acylindricity of a polymer chain $c = \overline{Y^2} - \overline{Z^2}$	Å^2
c_{ij}	: coefficient of r^{-6} attractive term in nonbonded interatomic interaction potential	(kcal/mol) Å^6
c_ε	: specific heat at constant strain	J/(kg K)
C_{LMNK}	: element of fourth-order tensor of isothermal elastic coefficients	MPa
C_s	: constant in the expression [eqn.(4.19)] for the scattered intensity	
C_{vib}	: vibrational heat capacity	J/K
$\underline{\underline{C}}$	: 6 x 6 matrix of isothermal elastic coefficients	MPa
d	: distance of the point of detection of the scattered radiation from the scattering sample	m
$D(x)$	: Debye function [eqn.(2.44)]	

e : electronic charge — Cb

e_{KLM} : alternating tensor

E : Young's modulus of elasticity — MPa

E_{coh} : cohesive energy — J

E_n : neutron kinetic energy — meV

E_X : X-ray photon energy — keV

f_j : atomic scattering factor of atom j

$\underline{F}_{ij}$: force of interaction on atom i due to atom j — N

$\underline{F}_f$: force exerted on interior of model cube through face f — N

$\underline{\underline{F}}$: force matrix, defined in Appendix F — N

g : gauche rotational isomeric state

$\underline{g}$: gradient of the total potential energy wrt microscopic degrees of freedom — kcal/(mol degree)

$g_{\alpha\beta}(r)$: nonbonded pair distribution function, for group pair (α,β)

$g^{el}_{\alpha\beta}(r)$: nonbonded element pair distribution function, for element pair (α,β)

$g^{el,tot}_{\alpha\beta}(r)$: total element pair distribution function for element pair (α,β), including bonded contributions

G : shear modulus — MPa

$\underline{\underline{G}}$: Gō and Scheraga transformation matrix, defined in eqn. (2.25) — $kg^{-1}m^{-2}degree^2$

h : Planck's constant — J s

$\hbar$: $h/2\pi$

$\underline{\underline{H}}$: Hessian matrix of second derivatives of the potential energy wrt. microscopic degrees of freedom — kcal/(mol $degree^2$)

I_K : K^{th} invariant of a second order tensor ($K = 1,2,3$)

I_o : intensity of incident radiation

$I(Q)$: scattered intensity, excluding forward scattering

$I_{forw}(Q)$: intensity of forward scattering

$I_{tot}(Q)$: total scattered intensity, including forward scattering

k_B : Boltzmann constant J/(molecule K)

k_ϕ : intrinsic torsional potential barrier kcal/mol bonds

$\hat{k}_{s_o}$: unit vector defining direction of incident radiation

$\hat{k}_s$: unit vector defining direction of scattered radiation

ℓ : carbon-carbon bond length Å

ℓ_H : carbon-hydrogen bond length Å

ℓ_R : carbon-methyl bond length Å

m_e : rest mass of electron kg

m_i : mass of atom i kg

m_n : rest mass of neutron kg

M : mass of polypropylene placed in the reactor for deuteration g

M_α : atomic or molecular weight of species α g/mol

$\bar{M}_v$: viscosity average molecular weight of a polymer g/mol

n : number of fillings of deuteration reactor; also,

n : number of skeletal bonds of a chain

$\underline{n}_f$: unit vector normal to face f

N : total number of atoms (or groups) in the model system

$N_{e,\alpha}$: effective number of electrons of species α in Slater-Kirkwood formula

N_h : number of hard degrees of freedom

N_L : Avogadro's number

N_s : number of soft degrees of freedom

$\underline{Q}$: position vector of the cube origin — Å

p_i : atomic-level hydrostatic pressure of atom i — MPa

$\underline{p}_i$: momentum of atom i — kg m/s

$p_{\xi;i}$: a' priori probability for bond i to be in rotational state ξ

$p_{\zeta\xi;i}$: a' priori probability for bond i-1 to be in rotational state ζ, and bond i to be in state ξ

P : pressure — MPa

$q_{\zeta\xi;i}$: conditional probability for bond i to be in rotational state ξ, given that bond i-1 is in state ζ

$q'_{\zeta\xi;i}$: modified conditional probability, according to scheme [eqn.(3.10)].

$\underline{Q}$: diffraction vector — $Å^{-1}$

$$Q = |\underline{Q}| = \frac{4\pi}{\lambda_s} \sin\theta_s$$

r : distance; also, chain end-to-end distance — Å

$\underline{r}_i$: position vector of atom i — Å

r_i^o : van der Waals radius of atom i — Å

R : ideal gas constant; also, — J/(mol K)

R : interatomic potential range — Å

R_1 : radial distance beyond which quintic spline is used to approximate the interatomic potential — Å

s : chain radius of gyration — Å

S : entropy — J/K

S_f : surface area of face f — m^2

$\underline{\underline{S}}$: area matrix, defined in Appendix F — m^2

$S(r)$: direction correlation function (order parameter)

$S(Q)$: static structure factor

$S(Q,\omega)$: dynamic structure factor

$S(Q,0)$: elastic structure factor

t : <u>trans</u> rotational isomeric state

$\underline{t}_i$: displacement vector of atom i — Å

T : temperature — K

$\underline{\underline{T}}_i$: coordinate transformation matrix from reference frame of bond (i+1) to reference frame of bond i of parent chain (Appendix C)

$\underline{\underline{T}}_o$: coordinate transformation matrix from internal to external coordinates (Appendix C)

$\underline{\underline{T}}^B_{ij}$: bonded torque on atom i from atom j through bond ij — N m

u : velocity — m/s

u_{long} : longitudinal sound velocity — m/s

$\bar{u}_{Rao}$: Rao function, or molar sound velocity, eqn. (1.3) — $m^{10/3}/(s^{1/3}_{mol})$

U : internal energy — J

U^{pot} : total potential energy of a microscopic structure — kcal/mol structures

$U^{LJ}(r)$: Lennard-Jones potential function — kcal/mol pairs

$U^{NB}(r)$: nonbonded interatomic potential function — kcal/mol pairs

$U_\phi(\phi)$: intrinsic torsional potential function — kcal/mol bonds

$\underline{\underline{U}}'$, $\underline{\underline{U}}''$, $\tilde{\underline{\underline{U}}}_\xi$, $\tilde{\underline{\underline{U}}}'_{\zeta\xi}$, $\tilde{\underline{\underline{U}}}''_{\zeta\xi}$: R.I.S. theory statistical weight matrices, defined in Appendix B.

v	: quantity of Deuterium gas introduced in the deuteration reactor upon refilling	mol
v_o	: quantity of gas remaining in the reactor after emtying	mol
$\underline{v}^{(j)}$	: coordinate vector of a substituent in the reference frame of bond j	Å
$\underline{v}_{\psi_k}$	: unit vector associated with Eulerian angle ψ_k , defined in eqn. (C.7)	
V	: volume; molar volume	m^3; m^3/mol
w_H	: hydrogen content of polypropylene	mol/g PP
$\underline{\underline{w}}_i$	: tensor appearing in the formulation of atomic level stresses in bonded systems, eqn. (6.15)	J
w_m	: fraction of <u>meso</u> dyads in an atactic vinyl chain	
W	: work produced by the system upon deformation	J
x	: degree of polymerization of parent chain; also,	
x	: Cartesian coordinate	Å
x_n	: degree of deuteration before $(n+1)^{th}$ filling of reactor	
$\overline{X^2}$	: largest eigenvalue of the radius of gyration tensor of a chain	$Å^2$
y	: Cartesian coordinate	Å
y_D	: purity of D_2 gas	mol/mol
$\overline{Y^2}$	: intermediate eigenvalue of the radius of gyration tensor of a chain	$Å^2$
z	: Cartesian coordinate	Å
Z	: partition function	
Z_{cfm}	: conformational partition function	
$\overline{Z^2}$	: smallest eigenvalue of the radius of gyration tensor of a chain	$Å^2$

Greek Symbols

		units
α_i	: polarizability of atom i	Å^3
α_P	: thermal expansion coefficient	K^{-1}
$\underline{\alpha}$	: thermal expansion tensor	K^{-1}
β	: factor $1/(k_B\ T)$	$(J/molecule)^{-1}$
γ	: Grüneisen parameter	
$\underline{\gamma}$	: Grüneisen tensor	
δ	: Hildebrand solubility parameter	$(J/cm^3)^{1/2}$
$\delta(r)$	: Dirac delta function	
Δ	: dimensionless radial distance, over which quintic spline is used to approximate potential tail : $\Delta = (R-R_1)/\sigma$; also,	
Δ	: root mean squared amplitude of thermal motion	Å
$\Delta\underline{r}_i$	: inhomogeneous displacement vector of atom i	Å
ε	: characteristic energy of Lennard-Jones potential expression; also,	kcal/mol pairs
ε	: extent of deformation	
$\underline{\varepsilon}$	: strain tensor	
η	: R.I.S. model statistical weight (Table B.1)	
θ	: bond (valence) angle; angle between skeletal bond chords; angle between inhomogeneous atomic displacements	degrees
θ', θ'', θ'_H, θ''_H, θ''_R	: bond angles defined in Fig.3.2	degrees
θ_s	: half scattering angle	degrees
Θ	: characteristic temperature in Einstein or Debye model of thermal vibrations	K
κ_S	: adiabatic compressibility	MPa^{-1}
κ_T	: isothermal compressibility	MPa^{-1}

κ^2	: relative shape anisotropy of a chain $\kappa^2 = (b^2 + 3c^2/4)/s^4$	
λ	: Lame' constant	MPa
λ_i'	: continuation coefficient of atom i, corresponding to continuation vector $\underline{a}_x$	
λ_s	: wavelength of incident radiation in scattering experiments	Å
μ	: Lame' constant	MPa
μ_i'	: continuation coefficient of atom i, corresponding to continuation vector $\underline{a}_y$	
μ_o	: magnetic permeability of free space	V s/(A m)
ν	: Poisson ratio	
ν_i'	: continuation coefficient of atom i, corresponding to continuation vector $\underline{a}_z$	
ρ	: mass density	kg/m^3
σ	: characteristic length in Lennard-Jones potential expression	Å
$\underline{\sigma}$	: internal stress tensor	MPa
$\underline{\sigma}_i$	: atomic level stress tensor of atom i	MPa
τ	: R.I.S. model statistical weight (Table B.1)	
τ_i	: atomic level von Mises shear stress of atom i	MPa
$\underline{\tau}$	: stress tensor	MPa
ϕ	: bond torsion (dihedral) angle	degrees
ψ	: Eulerian angle	degrees
ω	: vibrational frequency; radiation frequency	s^{-1}
ω^*	: R.I.S. model statistical weight (Table B.1)	

Subscripts

b : bonded

cfm : conformational

C : skeletal carbon

C_o : chain start

D : Debye model of thermal vibrations

E : Einstein model of thermal vibrations

f : numbering index for cube faces

h : contribution from hard degrees of freedom

i : index for atoms and bonds

I : index for coordinate directions (I=1,2,3)

j : index for atoms and bonds

J : index for coordinate directions (J=1,2,3)

k : index for atoms and bonds

K : index for coordinate directions (K=1,2,3)

long : longitudinal

L : index for coordinate directions (L=1,2,3)

m : meso - dyad

m, min: minimum image convention

M : index for coordinate directions (M=1,2,3)

n : neutron

N : index for coordinate directions (N=1,2,3)

P : isobaric

parent: referring to parent chain

r : racemo - dyad

R : methyl substituent

s : contribution from soft degrees of freedom

S : adiabatic

T : isothermal

tails : contribution from potential tails

tot : total; for potential, including tail contributions; for scattering, including forward scattering

vib : vibrational

x : coordinate direction x

X : X-rays

y : coordinate direction y

z : coordinate direction z

α : index for atomic species (α=H,C,R)

β : index for atomic species (β=H,C,R)

ζ : index for rotational isomeric states

ξ : index for rotational isomeric states

o : undeformed state

~ : vector

= : second order tensor, or matrix

Superscripts

affine: corresponding to an affine (homogeneous, quasi-continuum) deformation

B : bonded

el : elemental

intra : intramolecular

inter : intermolecular

LJ : Lennard-Jones potential function

min : minimum image convention

NB : nonbonded

pot : potential energy contribution

tot : total; for pair distribution functions, including bonded contribution

T : matrix transpose

' : first derivative

" : second derivative

- : mean, over all chain atoms

^ : unit vector

~ : dimensionless

Special Symbols

$\langle \quad \rangle$: ensemble average

$\xi[j_1, j_2, \ldots]$: all quantities ξ_i kept constant, <u>except</u> $\xi_{j_1}, \xi_{j_2}, \ldots$

APPENDIX A : Criterion for the Significance of Entropic Effects in Elastic Deformation

We will derive criterion (2.16) from the less useful form (2.15). For an arbitrary thermodynamic quantity a, characteristic of an elastic solid, we may write:

$$a = a(T,\underline{\underline{\tau}}) = a(T, \underline{\underline{\tau}}\,(T,\underline{\underline{\varepsilon}})) \tag{A.1}$$

Then:

$$\left.\frac{\partial a}{\partial T}\right|_{\underline{\underline{\varepsilon}}} = \left.\frac{\partial a}{\partial T}\right|_{\underline{\underline{\tau}}} + \sum_{LM}\left[\left.\frac{\partial a}{\partial \tau_{LM}}\right|_{T,\tau[LM]} \left.\frac{\partial \tau_{LM}}{\partial T}\right|_{\underline{\underline{\varepsilon}}}\right] \tag{A.2}$$

Considering $\underline{\underline{\tau}} = \underline{\underline{\tau}}(T, \underline{\underline{\varepsilon}})$ we have:

$$d\tau_{LM} = \left.\frac{\partial \tau_{LM}}{\partial T}\right|_{\underline{\underline{\varepsilon}}} dT + \sum_{NK} \frac{\partial \tau_{LM}}{\partial \varepsilon_{NK}} d\varepsilon_{NK}$$

hence

$$\left.\frac{\partial \tau_{LM}}{\partial T}\right|_{\underline{\underline{\varepsilon}}} = -\sum_{NK} \frac{\partial \tau_{LM}}{\partial \varepsilon_{NK}} \left.\frac{\partial \varepsilon_{NK}}{\partial T}\right|_{\underline{\underline{\tau}}} = -\sum_{NK} C_{LMNK}\,\alpha_{NK} \tag{A.3}$$

where $\underline{\underline{\alpha}} = \left.\frac{\partial \underline{\underline{\varepsilon}}}{\partial T}\right|_{\underline{\underline{I}}}$ is the thermal expansion tensor (p. 33 of ref. [75]). Combining eqns. (A.1) and (A.3),

$$\left.\frac{\partial a}{\partial T}\right|_{\underline{\underline{\varepsilon}}} = \left.\frac{\partial a}{\partial T}\right|_{\underline{\underline{\tau}}} - \sum_{LM}\sum_{NK} C_{LMNK}\,\alpha_{NK} \left.\frac{\partial a}{\partial \tau_{LM}}\right|_{T,\tau[LM]} \tag{A.4}$$

For an <u>isotropic solid</u>, we have $\alpha_{NK} = \frac{\alpha_p}{3}\delta_{NK}$, and eqn. (A.4) gives:

$$\left.\frac{\partial a}{\partial T}\right|_{\underline{\underline{\varepsilon}}} = \left.\frac{\partial a}{\partial T}\right|_{\underline{\underline{\tau}}} - \alpha_p \sum_{LM} \frac{C_{LM11} + C_{LM22} + C_{LM33}}{3} \left.\frac{\partial a}{\partial \tau_{LM}}\right|_{T,\tau[LM]} \tag{A.5}$$

Furthermore, expressing all isothermal elastic coefficients as functions of the Lamé constants [eqn.(2.7)] we obtain:

$$\left.\frac{\partial a}{\partial T}\right|_{\underline{\underline{\varepsilon}}} = \left.\frac{\partial a}{\partial T}\right|_{\underline{\underline{\tau}}} - \alpha_p\left(\lambda + \frac{2}{3}\mu\right)\left\{\left.\frac{\partial a}{\partial \tau_{11}}\right|_{T,\tau[11]} + \left.\frac{\partial a}{\partial \tau_{22}}\right|_{T,\tau[22]} + \left.\frac{\partial a}{\partial \tau_{33}}\right|_{T,\tau[33]}\right\} \tag{A.6}$$

Assuming, in addition to the isotropy of the system, that the distribution of stress is isotropic, all three derivatives within the curly brackets are equal. Application of the differential stresses $d\tau_{11}$, $d\tau_{22}$, $d\tau_{33}$ on the system leads to a change in a equal to:

$$\left.da\right|_{T} = \left.\frac{\partial a}{\partial \tau_{11}}\right|_{T,\tau[11]} d\tau_{11} + \left.\frac{\partial a}{\partial \tau_{22}}\right|_{T,\tau[22]} d\tau_{22} + \left.\frac{\partial a}{\partial \tau_{33}}\right|_{T,\tau[33]} d\tau_{33} =$$

$$= \left.\frac{\partial a}{\partial \tau_{11}}\right|_{T,\tau[11]} \left(d\tau_{11} + d\tau_{22} + d\tau_{33}\right)$$

$$= -3 \left.\frac{\partial a}{\partial \tau_{11}}\right|_{T,\tau[11]} dP$$

Whence,

$$\left.\frac{\partial a}{\partial \tau_{11}}\right|_{T,\tau[11]} = \left.\frac{\partial a}{\partial \tau_{22}}\right|_{T,\tau[22]} = \left.\frac{\partial a}{\partial \tau_{33}}\right|_{T,\tau[33]} = -\frac{1}{3}\left.\frac{\partial a}{\partial P}\right|_{T} \tag{A.7}$$

Therefore, using eqn. (A.7) and eqn. (2.8), eqn. (A.6) becomes:

$$\left.\frac{\partial a}{\partial T}\right|_{\underline{\underline{\varepsilon}}} = \left.\frac{\partial a}{\partial T}\right|_{P} + \frac{\alpha_P}{\kappa_T}\left.\frac{\partial a}{\partial P}\right|_{T} \tag{A.8}$$

Application of eqn. (A.8) for $a = C_{LMNK}$ leads directly from the criterion (2.15) to criterion (2.16).

APPENDIX B : Monte-Carlo Generation of Unperturbed Chains Based on the Rotational Isomeric State Model

The conformational statistics of unperturbed single chains are described very accurately by rotational isomeric state models. We cannot give here a detailed description of the rotational isomeric state theory. Excellent overviews can be found in [26] and in [28]. In a few words:

- A rotational isomeric state model is based on a discretization conformation space. The rotational angles ϕ are considered as assuming a set of discrete values, instead of being allowed to vary continuously in the interval $(-\pi, \pi)$. Each of these values defines a "rotational isomeric state." A conformation of the whole chain is thus approximated as a sequence of rotational states.

- By detailed conformational analysis of the variation of the potential energy as a function of the rotation angles in a dyad of the polymer, statistical weights are attributed to all pairs of rotational isomeric states. Statistical weights are conveniently expressed in the form of matrices. In vinyl polymers, such as polypropylene, one defines two kinds of statistical weight matrices: $\underline{U}''$, incorporating both interdyad and intradyad (see Fig.3.2) first-order (three-bond) interactions, as well as intradyad second-order (four-bond) interactions, and $\underline{U}'$, incorporating interdyad second-order interactions. Furthermore, there are two $\underline{U}''$ matrices, depending on the tacticity (m- or r-) of the dyad considered.

- For an unperturbed chain conformational statistics are dictated exclusively by short-range interactions (i.e. interactions between atoms or groups less than 5 bonds apart, plus the intrinsic rotational potential.)

Consequently, the statistical weight matrices derived from consideration of simple dyads contain all the information necessary for the description of conformation-dependent quantities.

The five states proposed in the model of Suter and Flory [57] for polypropylene are listed in Table B.1, together with the statistical weight matrices of that model.

The statistical mechanics of a single chain is governed, according to Flory [26], by the "conformational partition function"

$$Z_{cfm} = \int \exp\left[-\beta\, U^{pot}(\phi)\right] d\phi \qquad (B.1)$$

(For a single chain U^{pot} does not depend on the Eulerian angles ψ, compare formulation in section 2.2.)
By virtue of the R.I.S. discretization, Z_{cfm} is approximated as a product of statistical weight matrices:

$$Z_{cfm} = \underline{U}_o \, \underline{U}_1^{(2)} \left(\prod_{k=2}^{x-2} \underline{U}_k^{(2)} \right) \underline{U}_{x-1}^{(2)} \, \underline{U}_x \qquad (B.2)$$

where

$$\underline{U}_k^{(2)} = \underline{U}' \, \underline{U}_k'' \quad (2 \le k \le x-2), \text{ with } \underline{U}_k'' = \begin{cases} \underline{U}_m'' & \text{if dyad } k \text{ is m-} \\ \underline{U}_r'' & \text{if dyad } k \text{ is r-} \end{cases}$$

$$\underline{U}_1^{(2)} = \underline{U}' \, \mathrm{diag}(1,1,1,\eta,1) \, \underline{U}_{(m \text{ or } r)}''$$

$$\underline{U}_{x-1}^{(2)} = \underline{U}' \, \underline{U}_{(m \text{ or } r)}'' \, \mathrm{diag}(1,1,1,\eta,1)$$

$$\underline{U}_o = [\,1\;0\;0\;0\;0\,], \quad \underline{U}_x = [\,1\;1\;1\;1\;1\,]^T$$

The <u>a'priori</u> probability for a particular bond to be in a particular state, or for a particular pair of bonds to assume a particular pair of states, can be obtained from eqn.(B.1).

Table B.1 : Parameters of the Rotational-Isomeric State Model of Polypropylene

State #	1	2	3	4	5
State Name	t	t*	g*	g	$\bar{g}$
State Angle	15°	50°	70°	105°	-115°

(State angle measured in the sense indicated by Newman projections)

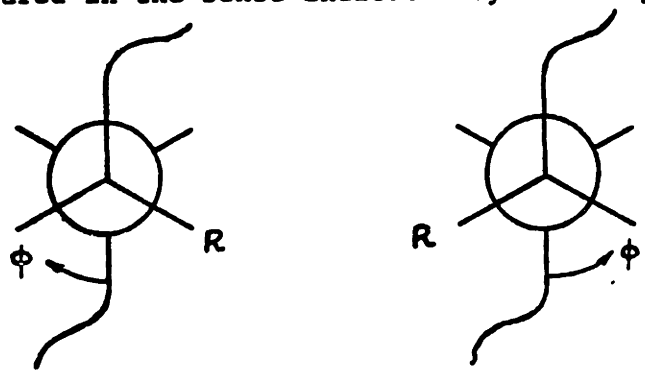

Statistical weight matrices:

$$\underline{U}' = \begin{bmatrix} 1 & 1 & 1 & 1 & 1 \\ 1 & 1 & 1 & 1 & 1 \\ 1 & 1 & 0 & 0 & 1 \\ 1 & 1 & 0 & 0 & 1 \\ 1 & 1 & 1 & 1 & 0 \end{bmatrix}$$

$$\underline{U}_m'' = \begin{bmatrix} 0 & \eta\omega^* & 0 & \eta & 0 \\ \eta\omega^* & 0 & 0 & 0 & \tau\omega^* \\ 0 & 0 & 0 & \omega^* & \tau\omega^* \\ \eta & 0 & \omega^* & 0 & 0 \\ 0 & \tau\omega^* & \tau\omega^* & 0 & 0 \end{bmatrix} \qquad \underline{U}_r'' = \begin{bmatrix} \eta^2 & 0 & \eta\omega^* & 0 & 0 \\ 0 & 0 & 0 & \omega^* & \tau\omega^* \\ \eta\omega^* & 0 & 0 & 0 & \tau\omega^* \\ 0 & \omega^* & 0 & 1 & 0 \\ 0 & \tau\omega^* & \tau\omega^* & 0 & 0 \end{bmatrix}$$

where $\eta = 1.0 \exp\left(-\frac{60}{RT}\right)$

$\tau = 0.4 \exp\left(-\frac{500}{RT}\right)$

$\omega^* = 0.9 \exp\left(-\frac{1600}{RT}\right)$

R = gas constant in $\frac{\text{cal}}{\text{mole}}$

T = absolute temperature in K

Thus, the a' priori probability for bond 2 to be in state ξ is:

$$p_{\xi;2} = Z_{cfm}^{-1} \underline{U}_o \tilde{\underline{U}}_\xi' \mathrm{diag}(1,1,1,\eta,1) \underline{U}_1'' \left[\prod_{k=2}^{x-2} \underline{U}_k^{(2)}\right] \underline{U}_{x-1}^{(2)} \underline{U}_x \qquad (B.3)$$

where $\tilde{\underline{U}}_\xi'$ symbolizes the matrix obtained from $\underline{U}'$ by replacing all of its elements, except those of column ξ, by zeros.

The a'priori probabilities $p_{\zeta\xi;i}$ that bond i-1 be in state ζ and bond i be in state ξ $(3 \le i \le 2x-1)$ are given by:

$$p_{\zeta\xi;3} = Z_{cfm}^{-1} \underline{U}_o \underline{U}' \mathrm{diag}(1,1,1,\eta,1) \tilde{\underline{U}}''_{\zeta\xi;1} \left(\prod_{k=2}^{x-2} \underline{U}_k^{(2)}\right) \underline{U}_{x-1}^{(2)} \underline{U}_x$$

$$p_{\zeta\xi;4} = Z_{cfm}^{-1} \underline{U}_o \underline{U}_1^{(2)} \tilde{\underline{U}}'_{\zeta\xi} \underline{U}_2'' \left(\prod_{k=3}^{x-2} \underline{U}_k^{(2)}\right) \underline{U}_{x-1}^{(2)} \underline{U}_x$$

$$p_{\zeta\xi;5} = Z_{cfm}^{-1} \underline{U}_o \underline{U}_1^{(2)} \underline{U}' \tilde{\underline{U}}_{\zeta\xi;2} \left(\prod_{k=3}^{x-2} \underline{U}_k^{(2)}\right) \underline{U}_{x-1}^{(2)} \underline{U}_x$$

$$p_{\zeta\xi;2h} = Z_{cfm}^{-1} \underline{U}_o \underline{U}_1^{(2)} \left(\prod_{k=2}^{h-1} \underline{U}_k^{(2)}\right) \tilde{\underline{U}}'_{\zeta\xi} \underline{U}_h'' \left(\prod_{k=h+1}^{x-2} \underline{U}_k^{(2)}\right) \underline{U}_{x-1}^{(2)} \underline{U}_x \quad (3 \le h \le x-3)$$

$$p_{\zeta\xi;2h+1} = Z_{cfm}^{-1} \underline{U}_o \underline{U}_1^{(2)} \left(\prod_{k=2}^{h-1} \underline{U}_k^{(2)}\right) \underline{U}' \tilde{\underline{U}}''_{\zeta\xi;h} \left(\prod_{k=h+1}^{x-2} \underline{U}_k^{(2)}\right) \underline{U}_{x-1}^{(2)} \underline{U}_x \quad (3 \le h \le x-3)$$

$$p_{\zeta\xi;2x-4} = Z_{cfm}^{-1} \underline{U}_o \underline{U}_1^{(2)} \left(\prod_{k=2}^{x-3} \underline{U}_k^{(2)}\right) \tilde{\underline{U}}'_{\zeta\xi} \underline{U}_{x-2}'' \underline{U}_{x-1}^{(2)} \underline{U}_x$$

$$p_{\zeta\xi;2x-3} = Z_{cfm}^{-1} \underline{U}_o \underline{U}_1^{(2)} \left(\prod_{k=2}^{x-3} \underline{U}_k^{(2)}\right) \underline{U}' \tilde{\underline{U}}''_{\zeta\xi;x-2} \underline{U}_{x-1}^{(2)} \underline{U}_x$$

$$p_{\zeta\xi;2x-2} = Z_{cfm}^{-1} \underline{U}_o \underline{U}_1^{(2)} \left(\prod_{k=2}^{x-2} \underline{U}_k^{(2)}\right) \tilde{\underline{U}}'_{\zeta\xi} \underline{U}_{x-1}'' \mathrm{diag}(1,1,1,\eta,1) \underline{U}_x$$

$$p_{\zeta\xi;2x-1} = Z_{cfm}^{-1} \underline{U}_o \underline{U}_1^{(2)} \left(\prod_{k=2}^{x-2} \underline{U}_k^{(2)}\right) \underline{U}' \tilde{\underline{U}}''_{\zeta\xi;x-1} \mathrm{diag}(1,1,1,\eta,1) \underline{U}_x \qquad (B.4)$$

where $\tilde{\underline{U}}'_{\zeta\xi}$ (respectively, $\tilde{\underline{U}}''_{\zeta\xi;k}$) symbolizes the matrix obtained

from $\underline{U}'$ (respectively, $\underline{U}''_k$) by replacing all of its elements, except the one lying at the intersection of row ζ and column ξ, by zeros.

The conditional probability $q_{\zeta\xi;i}$ that bond i be in state ξ, given that bond i-1 is in state ζ ($3 \leq i \leq 2x-1$) is obtained directly from eqns (B.4) as:

$$q_{\zeta\xi;i} = \frac{p_{\zeta\xi;i}}{p_{\zeta;i-1}} = \frac{p_{\zeta\xi;i}}{\sum_{\varepsilon} p_{\varepsilon\zeta;i-1}} \qquad (B.5)$$

Equations (B.2) to (B.5) define an "equivalent Markov model" that can be used to generate correctly weighed conformations (i.e., sequences of rotational isomeric states) by Monte Carlo simulation. Notice that the conformational statistics of macromolecules are actually not Markovian ([26], p.89), since the state of a bond depends not only on the bonds that precede it, but also on the bonds that follow it along the chain. This is reflected in the fact that probabilities (B.3), (B.4) depend on the entire chain. Although formulated in terms of unidirectional conditional probabilities, the stochastic model [eqns (B.2) to (B.5)] actually "looks ahead" along the chain, in order to decide on the state of a bond. This is an admirable aspect of the rotational isomeric state theory.

In practice, random number generation of an unperturbed chain proceeds as follows: A Bernoullian sequence of m- and r-dyads with a prescribed fraction of m-dyads, $w_m = 0.48$ (see section 3.3.1) is first generated by repeated trials, in order to fix the tacticity of the parent chain. The <u>a' priori</u> probabilities $p_{\xi;2}$ and the conditional probabilities $q_{\zeta\xi;i}$ are calculated for this tacticity by eqns (B.1), to (B.5). A rotational state is randomly chosen for bond 2 using $p_{\xi;2}$, and a sequence of states is generated for bonds $3,4,\ldots,2x-1$

using $q_{\zeta\xi;i}$. Absolute configurations are decided by randomly picking the configuration of the first asymmetric carbon in the chain. Individual atom coordinates are computed using the transform matrix technique discussed in Appendix C. Characteristic quantities (mean squared end-to-end distance, radius of gyration tensor, etc.) computed from randomly generated ensembles of unperturbed chains, using this method, agree very well with statistical mechanical averages obtained by generator matrix techniques ([26]).

A three-dimensional plot of an unperturbed chain of atactic polypropylene, generated by the stochastic scheme described above, is presented in Fig.B.1. The tacticity sequence is indicated above, and the conformation sequence below the chain.

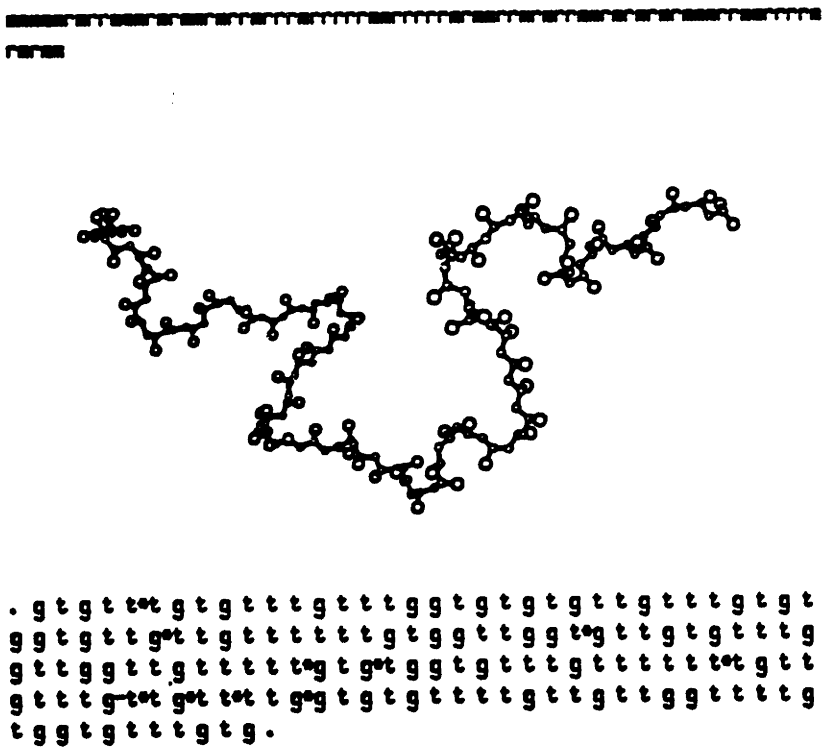

Figure B.1

Unperturbed chain of atactic polypropylene, generated by the stochastic scheme described in Appendix B, using the Rotational Isomeric State Model.

APPENDIX C : The Total Potential Energy Function and Its Derivatives

Consider the parent chain and number its skeletal groups from 0 to 2x. Groups 0 and 2x are the terminal methyls; groups 2i-1, $1 \leq i \leq x$, are of the type -CHR- , while groups 2i, $1 \leq i \leq x-1$, are of the type $-CH_2-$. Skeletal bonds are numbered from 1 to 2x, so that bond i connects groups i-1 and i. The bond rotation angle ϕ_i is the dihedral angle between the planes of bonds (i-1, i) and bonds (i, i+1), measured in a right-handed sense relative to trans [26].

Local reference frames are introduced at skeletal bonds following the conventions of Flory (p. 20 of [26]). The cube ("external") frame of reference, with respect to which all coordinates are ultimately expressed, is denoted as xyz. Eulerian angle ψ_1 is taken as the angle between the x-direction and the projection of bond 1 on the xy-plane; Eulerian angle ψ_2 is taken as the angle between the z-direction and bond 1; Eulerian angle ψ_3 is taken as the dihedral angle between the planes (z-direction, bond 1) and (bond 1, bond 2). The coordinates of an atom with respect to the cube frame of reference are denoted by $\underset{\sim}{r}$. The coordinates of the chain start (terminal methyl 0) are denoted by $\underset{\sim}{r}_{C_o}$. For any atom in the cube, let j symbolize the index of the skeletal group to which the parent image of this atom is connected. The notation is explained in Figures C.1 and C.2.

The position vector $\underset{\sim}{r}$ of an atom in the cube can be expressed in terms of the variables $(\underset{\sim}{r}_{C_o}, \psi_1, \psi_2, \psi_3, \phi_2, \ldots, \phi_{2X-1})$ as (in matrix-notation):

$$\underset{\sim}{r} = \underset{\sim}{r}_{Co} + \underline{T}_0 \underset{\sim}{\ell} + \underline{T}_0 \underline{T}_1 \underset{\sim}{\ell} + \ldots + \underline{T}_0 \underline{T}_1 \cdots \underline{T}_{j-1} \underset{\sim}{v}^{(j)} + \lambda' \underset{\sim}{a}_x + \mu' \underset{\sim}{a}_y + \nu' \underset{\sim}{a}_z \qquad (C.1)$$

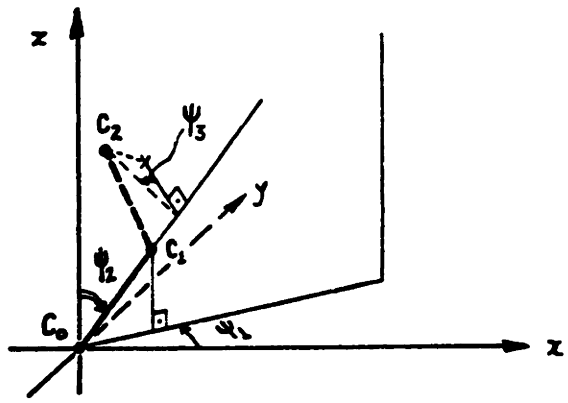

Figure C.1 : Definition of the Eulerian Angles ψ_1, ψ_2, ψ_3.

ψ_1 : angle between x-axis and projection of bond 1 on xy-plane

ψ_2 : angle between z-axis and bond 1

ψ_3 : dihedral angle between planes (z-axis, bond 1) and (bond 1, bond 2)

x, y, z : coordinate axis directions of a fixed Cartesian system (generally not centered at C_o)

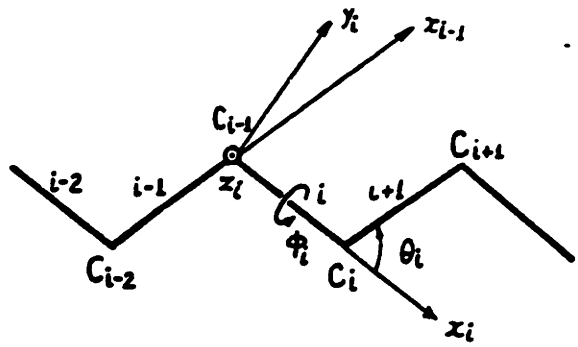

Figure C.2 : Reference frame of skeletal bond i of a chain, according to Flory [26]

ϕ_i : dihedral angle between planes (i-1,i) and (i,i+1)

$-\pi < \phi_i \leq \pi$

$\phi_i = 0$ for bond i = <u>trans</u>

$\phi_i > 0$ for right-handed rotation relative to <u>trans</u>

where

$$\underline{T}_o = \begin{bmatrix} \cos\psi_1 \sin\psi_2 & -\cos\psi_1 \cos\psi_2 \cos\psi_3 - \sin\psi_1 \sin\psi_3 & -\cos\psi_1 \cos\psi_2 \sin\psi_3 + \sin\psi_1 \sin\psi_3 \\ \sin\psi_1 \sin\psi_2 & -\sin\psi_1 \cos\psi_2 \cos\psi_3 + \cos\psi_1 \sin\psi_3 & -\sin\psi_1 \cos\psi_2 \sin\psi_3 - \cos\psi_1 \cos\psi_3 \\ \cos\psi_2 & \sin\psi_2 \cos\psi_3 & \sin\psi_2 \sin\psi_3 \end{bmatrix} \tag{C.2}$$

is the orthogonal transformation matrix of "internal" to "external" coordinates,

$$\underline{T}_i = \begin{bmatrix} \cos\theta_i & \sin\theta_i & 0 \\ \sin\theta_i \cos\phi_i & -\cos\theta_i \cos\phi_i & \sin\phi_i \\ \sin\theta_i \sin\phi_i & -\cos\theta_i \sin\phi_i & -\cos\phi_i \end{bmatrix} \quad (i = 1, 2, \ldots 2x-1) \tag{C.3}$$

is the orthogonal transformation matrix from the reference frame of bond (i + 1) to the reference frame of bond i (by definition, $\phi_1 = 0$), and (from here on we use <u>vector-notation</u>)

$$\underset{\sim}{\ell} = \ell \quad (1, 0, 0) \tag{C.4}$$

$\underset{\sim}{v}^{(j)}$ is the coordinate vector of the parent image in the reference frame of bond j. The possible values of $\underset{\sim}{v}^{(j)}$ are:

$$\underset{\sim}{v}^{(j)} = \ell(1, 0, 0) \tag{C.5a}$$

for a skeletal carbon;

$$\underset{\sim}{v}^{(j)} = \ell_H \left(-\cos\theta'_H, \cos\theta'_H \cot\frac{\theta'}{2}, \mp \sqrt{1 - \frac{\cos^2\theta'_H}{\sin^2\frac{\theta'}{2}}} \right) \tag{C.5b}$$

for a hydrogen attached to an achiral skeletal carbon (the $\mp$ sign distinguishes between the two hydrogen atoms in the methylene group);

$$\underset{\sim}{v}^{(j)} = \ell_H \left(-\cos\theta''_H, \cos\theta''_H \cot\frac{\theta''}{2}, \pm \sqrt{1 - \frac{\cos^2\theta''_H}{\sin^2\frac{\theta''}{2}}} \right) \tag{C.5c}$$

for a hydrogen attached to a chiral skeletal carbon (the $\pm$ sign denotes the chirality);

$$\underset{\sim}{v}^{(j)} = \ell_R \left(-\cos\theta''_R \, , \, \cos\theta''_R \cdot \cot\frac{\theta''}{2} \, , \, \mp \sqrt{1 - \frac{\cos^2\theta''_R}{\sin^2\frac{\theta''}{2}}} \right) \qquad (C.5d)$$

for a methyl substituent (the $\mp$ sign denotes the chirality).

The last three terms in equation (C.1) arise from the periodicity of the system: $\underset{\sim}{a}_x$, $\underset{\sim}{a}_y$, $\underset{\sim}{a}_z$ are the edge-vectors of the cube (hereafter called "continuation vectors") while the integers λ', μ', ν' (hereafter called "continuation coefficients") measure the magnitude of the translations required to reach the considered atom of the cube from its image belonging to the parent chain starting at $\underset{\sim}{r}_{C_o}$.

By differentiation of equation (C.1) one obtains the derivatives of $\underset{\sim}{r}$ with respect to each of the 2x + 1 degrees of freedom:

$$\frac{\partial \underset{\sim}{r}}{\partial \psi} = \underset{\sim}{v}_\psi \times \left\{ \underset{\sim}{r} - \underset{\sim}{r}_{C_o} - \lambda' \underset{\sim}{a}_x - \mu' \underset{\sim}{a}_y - \nu' \underset{\sim}{a}_z \right\} \qquad (C.6)$$

where $\psi \in \{\psi_1, \psi_2, \psi_3\}$ and

$$\text{for } \psi = \psi_1 \qquad \underset{\sim}{v}_\psi = (0, 0, 1) \qquad (C.7a)$$

$$\psi = \psi_2 \qquad \underset{\sim}{v}_\psi = (-\sin\psi_1, \cos\psi_1, 0) \qquad (C.7b)$$

$$\psi = \psi_3 \qquad \underset{\sim}{v}_\psi = (-\cos\psi_1 \sin\psi_2, -\sin\psi_1 \sin\psi_2, -\cos\psi_2) \qquad (C.7c)$$

$$\frac{\partial \underset{\sim}{r}}{\partial \phi_i} = \begin{cases} \underset{\sim}{0} \, , \text{ if } j<i & (C.8a) \\ \frac{1}{\ell}\left[\underset{\sim}{r}_{C_i} - \underset{\sim}{r}_{C_{i-1}} - \left(\lambda'_{C_i} - \lambda'_{C_{i-1}}\right)\underset{\sim}{a}_x - \left(\mu'_{C_i} - \mu'_{C_{i-1}}\right)\underset{\sim}{a}_y - \left(\nu'_{C_i} - \nu'_{C_{i-1}}\right)\underset{\sim}{a}_z\right] \times \\ \quad \times \left[\underset{\sim}{r} - \underset{\sim}{r}_{C_i} - \left(\lambda' - \lambda'_{C_i}\right)\underset{\sim}{a}_x - \left(\mu' - \mu'_{C_i}\right)\underset{\sim}{a}_y - \left(\nu' - \nu'_{C_i}\right)\underset{\sim}{a}_z\right], \text{ if } i \le j & (C.8b) \end{cases}$$

The derivatives of all interatomic distances can now be found. In particular, for the distance $|\underset{\sim}{r}_1-\underset{\sim}{r}_{2,m}|$ between an atom, 1, and the image of another atom, 2, that lies closest to 1, one obtains:

$$\frac{\partial\left(|\underset{\sim}{r}_1-\underset{\sim}{r}_{2,m}|\right)}{\partial\psi} = -\underset{\sim}{v}_{\psi}\cdot\left\{(\lambda'_1-\lambda'_{2,m})\underset{\sim}{a}_x+(\mu'_1-\mu'_{2,m})\underset{\sim}{a}_y+(\nu'_1-\nu'_{2,m})\underset{\sim}{a}_z\right\}\times\frac{\underset{\sim}{r}_1-\underset{\sim}{r}_{2,m}}{|\underset{\sim}{r}_1-\underset{\sim}{r}_{2,m}|} \tag{C.9}$$

and

$$\frac{\partial}{\partial\phi_i}|\underset{\sim}{r}_1-\underset{\sim}{r}_{2,m}| = \begin{cases} = 0 & \text{for } j_1<i \quad \text{(C.10a)} \\ = -\dfrac{\left[\underset{\sim}{r}_{c_i}-\underset{\sim}{r}_{c_{i-1}}-\left(\lambda'_{c_i}-\lambda'_{c_{i-1}}\right)\underset{\sim}{a}_x-\left(\mu'_{c_i}-\mu'_{c_{i-1}}\right)\underset{\sim}{a}_y-\left(\nu'_{c_i}-\nu'_{c_{i-1}}\right)\underset{\sim}{a}_z\right]}{|\underset{\sim}{r}_1-\underset{\sim}{r}_{2,m}|\ \ell}\cdot\left(\underset{\sim}{r}_1-\underset{\sim}{r}_{2,m}\right)\times \\ \quad\times\left[\underset{\sim}{r}_1-\underset{\sim}{r}_{c_i}-\left(\lambda'_1-\lambda'_{c_i}\right)\underset{\sim}{a}_x-\left(\mu'_1-\mu'_{c_i}\right)\underset{\sim}{a}_y-\left(\nu'_1-\nu'_{c_i}\right)\underset{\sim}{a}_z\right]\cdot \\ \quad \text{for } j_2<i\leq j_1 \quad \text{(C.10b)} \\ = -\dfrac{\left[\underset{\sim}{r}_{c_i}-\underset{\sim}{r}_{c_{i-1}}-\left(\lambda'_{c_i}-\lambda'_{c_{i-1}}\right)\underset{\sim}{a}_x-\left(\mu'_{c_i}-\mu'_{c_{i-1}}\right)\underset{\sim}{a}_y-\left(\nu'_{c_i}-\nu'_{c_{i-1}}\right)\underset{\sim}{a}_z\right]}{|\underset{\sim}{r}_1-\underset{\sim}{r}_{2,m}|\ \ell}\cdot\left(\underset{\sim}{r}_1-\underset{\sim}{r}_{2,m}\right)\times \\ \quad\times\left[\left(\lambda'_{2,m}-\lambda'_1\right)\underset{\sim}{a}_x+\left(\mu'_{2,m}-\mu'_1\right)\underset{\sim}{a}_y+\left(\nu'_{2,m}-\nu'_1\right)\underset{\sim}{a}_z\right]\cdot \\ \quad \text{for } i\leq j_2 \quad \text{(C.10c)} \end{cases}$$

The total potential energy function is the sum:

$$U^{prot}(\underline{\psi},\underline{\phi}) = \sum_{\substack{i,\ \text{bonds of}\\ \text{parent chain}\\ 2\le i\le 2x-1}} U_\phi(\phi_i) + \sum_{\substack{1,\ \text{atoms}\\ \text{in cube}\\ j_1>0}} \sum_{\substack{2,\ \text{atoms}\\ \text{in cube}\\ 0\le j_2<j_1}} U^{NB}(|\underline{r}_1-\underline{r}_{2,m}|) \qquad (C.11)$$

where the functions $U_\phi(\phi)$ and $U^{NB}(r)$ have been introduced in the main text. The double summation runs over atom pairs whose parent images are at least three bonds apart, so that their distance is conformation-dependent. The derivatives of U^{prot} with respect to the degrees of freedom are obtained by direct differentiation of eq. (C.11) and use of eq. (C.9) and eq. (C.10).

Introducing the abbreviated notations:

$$\underline{b}_i = \underline{r}_{c_i}-\underline{r}_{c_{i-1}} - \left(\lambda'_{c_i}-\lambda'_{c_{i-1}}\right)\underline{a}_x - \left(\mu'_{c_i}-\mu'_{c_{i-1}}\right)\underline{a}_y - \left(\nu'_{c_i}-\nu'_{c_{i-1}}\right)\underline{a}_z \qquad (C.12a)$$

$$\underline{r}_{1i} = \underline{r}_1-\underline{r}_{c_i} - \left(\lambda'_1-\lambda'_{c_i}\right)\underline{a}_x - \left(\mu'_1-\mu'_{c_i}\right)\underline{a}_y - \left(\nu'_1-\nu'_{c_i}\right)\underline{a}_z \qquad (C.12b)$$

$$\underline{r}_{12} = \underline{r}_1-\underline{r}_2 - \left(\lambda'_1-\lambda'_2\right)\underline{a}_x - \left(\mu'_1-\mu'_2\right)\underline{a}_y - \left(\nu'_1-\nu'_2\right)\underline{a}_z \qquad (C.12c)$$

$$\underline{r}_m = \underline{r}_1-\underline{r}_{2,m} \quad ; \quad r_m = |\underline{r}_m| \qquad (C.12d)$$

$$\underline{a}_{12} = \left(\lambda'_{2,m}-\lambda'_1\right)\underline{a}_x + \left(\mu'_{2,m}-\mu'_1\right)\underline{a}_y + \left(\nu'_{2,m}-\nu'_1\right)\underline{a}_z = \underline{r}_{12}-\underline{r}_m \qquad (C.12e)$$

$$\underline{r}_{2i,m} = \underline{r}_{2,m}-\underline{r}_{c_i} - \left(\lambda'_1-\lambda'_{c_i}\right)\underline{a}_x - \left(\mu'_1-\mu'_{c_i}\right)\underline{a}_y - \left(\nu'_1-\nu'_{c_i}\right)\underline{a}_z = \underline{r}_{1i}-\underline{r}_m \qquad (C.12f)$$

$$U'_{12} = \left.\frac{\partial U^{NB}}{\partial r}\right|_{r=r_m} \quad ; \quad U''_{12} = \left.\frac{\partial^2 U^{NB}}{\partial r^2}\right|_{r=r_m} \quad ; \quad U'_\phi = \frac{\partial U_\phi}{\partial \phi} \quad ; \quad U''_\phi = \frac{\partial^2 U_\phi}{\partial \phi^2} \qquad (C.12g)$$

we obtain:

Gradient

$$\frac{\partial U^{pot}}{\partial \psi} = \sum_{\substack{1 \\ j_1>0}} \sum_{\substack{2 \\ 0\le j_2<j_1}} \frac{U'_{12}}{r_m} \underset{\sim}{v}_{\psi} \cdot (\underset{\sim}{a}_{12} x \underset{\sim}{r}_m) \qquad (C.13)$$

$$\frac{\partial U^{pot}}{\partial \phi_i} = U'_{\phi}(\phi_i) + \frac{1}{\ell}\left[\sum_{\substack{1 \\ j_1\ge i}} \sum_{\substack{2 \\ 0\le j_2<i}} \frac{U'_{12}}{r_m} \underset{\sim}{b}_i \cdot \left(\underset{\sim}{r}_{1i} x \underset{\sim}{r}_m\right) + \sum_{\substack{1 \\ j_1>i}} \sum_{\substack{2 \\ i\le j_2<j_1}} \frac{U'_{12}}{r_m} \underset{\sim}{b}_i \cdot \left(\underset{\sim}{a}_{12} x \underset{\sim}{r}_m\right)\right] \qquad (C.14)$$

Hessian

$$\frac{\partial^2 U^{pot}}{\partial \psi_i \partial \psi_k} = \frac{1}{\ell}\left[\sum_{\substack{1 \\ j_1\ge 0}} \sum_{\substack{2 \\ 0\le j_2<j_1}} \left\{\frac{1}{r_m^2}\left(U''_{12} - \frac{U'_{12}}{r_m}\right)\left[\underset{\sim}{v}_{\psi_k} \cdot \left(\underset{\sim}{a}_{12} x \underset{\sim}{r}_m\right)\right]\left[\underset{\sim}{v}_{\psi_i} \cdot \left(\underset{\sim}{a}_{12} x \underset{\sim}{r}_m\right)\right] + \frac{U'_{12}}{r_m}\left[\left(\underset{\sim}{v}_{\psi_k} \cdot \underset{\sim}{v}_{\psi_i}\right)\left(\underset{\sim}{r}_{12} \cdot \underset{\sim}{a}_{12}\right) - \left(\underset{\sim}{v}_{\psi_k} \cdot \underset{\sim}{r}_{12}\right)\left(\underset{\sim}{v}_{\psi_i} \cdot \underset{\sim}{a}_{12}\right)\right]\right\}\right]$$

$$\text{with } (i,k) \in \{1,2,3\}^2 \ , \ i \ge k \qquad (C.15)$$

$$\frac{\partial^2 U^{pot}}{\partial\psi\partial\phi_i} = \frac{1}{\ell}\left[\sum_{\substack{1\\ j_1\geq i}}\sum_{\substack{2\\ 0\leq j_2<i}}\left\{\frac{1}{r_m^2}\left[U''_{12}-\frac{U'_{12}}{r_m}\right]\left[\underset{\sim}{v}_\psi\cdot\left[\underset{\sim}{a}_{12}\times\underset{\sim}{r}_m\right]\right]\left[\underset{\sim}{b}_i\cdot\left[\underset{\sim}{r}_{1i}\times\underset{\sim}{r}_m\right]\right]+\right.\right.$$

$$\left.+\frac{U'_{12}}{r_m}\left[\left(\underset{\sim}{b}_i\cdot\underset{\sim}{v}_\psi\right)\left(\underset{\sim}{r}_{1i}\cdot\underset{\sim}{a}_{12}\right)-\left(\underset{\sim}{v}_\psi\cdot\underset{\sim}{r}_{1i}\right)\left(\underset{\sim}{b}_i\cdot\underset{\sim}{a}_{12}\right)\right]\right\}+$$

$$+\sum_{\substack{1\\ j_1\geq i}}\sum_{\substack{2\\ i\leq j_2<j_1}}\left\{\frac{1}{r_m^2}\left[U''_{12}-\frac{U'_{12}}{r_m}\right]\left[\underset{\sim}{v}_\psi\cdot\left[\underset{\sim}{a}_{12}\times\underset{\sim}{r}_m\right]\right]\left[\underset{\sim}{b}_i\cdot\left[\underset{\sim}{a}_{12}\times\underset{\sim}{r}_m\right]\right]+\right.$$

$$\left.\left.+\frac{U'_{12}}{r_m}\left[\left(\underset{\sim}{b}_i\cdot\underset{\sim}{v}_\psi\right)\left(\underset{\sim}{r}_{12}\cdot\underset{\sim}{a}_{12}\right)-\left(\underset{\sim}{b}_i\cdot\underset{\sim}{a}_{12}\right)\left(\underset{\sim}{v}_\psi\cdot\underset{\sim}{r}_{12}\right)\right]\right\}\right] \qquad (C.16)$$

$$\frac{\partial^2 U^{pot}}{\partial\phi_i\partial\phi_k} = \delta_{ik}U''_\phi\left(\phi_i\right)+$$

$$+\frac{1}{\ell}\left[\sum_{\substack{1\\ j_1\geq i}}\sum_{\substack{2\\ 0\leq j_2<k}}\left\{\frac{1}{r_m^2}\left[U''_{12}-\frac{U'_{12}}{r_m}\right]\left[\underset{\sim}{b}_k\cdot\left[\underset{\sim}{r}_{1k}\times\underset{\sim}{r}_m\right]\right]\left[\underset{\sim}{b}_i\cdot\left[\underset{\sim}{r}_{1i}\times\underset{\sim}{r}_m\right]\right]+\right.\right.$$

$$\left.+\frac{U'_{12}}{r_m}\left[\left(\underset{\sim}{b}_i\cdot\underset{\sim}{b}_k\right)\left(\underset{\sim}{r}_{1i}\cdot\underset{\sim}{r}_{2k,m}\right)-\left(\underset{\sim}{b}_i\cdot\underset{\sim}{r}_{2k,m}\right)\left(\underset{\sim}{b}_k\cdot\underset{\sim}{r}_{1i}\right)\right]\right\}+$$

$$+\sum_{\substack{1\\ j_1\geq i}}\sum_{\substack{2\\ k\leq j_2<i}}\left\{\frac{1}{r_m^2}\left[U''_{12}-\frac{U'_{12}}{r_m}\right]\left[\underset{\sim}{b}_k\cdot\left[\underset{\sim}{a}_{12}\times\underset{\sim}{r}_m\right]\right]\left[\underset{\sim}{b}_i\cdot\left[\underset{\sim}{r}_{1i}\times\underset{\sim}{r}_m\right]\right]+\right.$$

$$\left.+\frac{U'_{12}}{r_m}\left[\left(\underset{\sim}{b}_i\cdot\underset{\sim}{b}_k\right)\left(\underset{\sim}{r}_{1i}\cdot\underset{\sim}{a}_{12}\right)-\left(\underset{\sim}{b}_i\cdot\underset{\sim}{a}_{12}\right)\left(\underset{\sim}{b}_k\cdot\underset{\sim}{r}_{1i}\right)\right]\right\}+$$

$$+\sum_{\substack{1\\ j_1>i}}\sum_{\substack{2\\ i\le j_2<j_1}}\left\{\frac{1}{r_m^2}\left[U''_{12}-\frac{U'_{12}}{r_m}\right]\left[\underline{b}_k\cdot\left(\underline{a}_{12}x\underline{r}_m\right)\right]\left[\underline{b}_i\cdot\left(\underline{a}_{12}x\underline{r}_m\right)\right]+\right.$$

$$\left.+\frac{U'_{12}}{r_m}\left[\left(\underline{b}_i\cdot\underline{b}_k\right)\left(\underline{r}_{12}\cdot\underline{a}_{12}\right)-\left(\underline{b}_i\cdot\underline{a}_{12}\right)\left(\underline{b}_k\cdot\underline{r}_{12}\right)\right]\right\}\Bigg] \qquad (C.17)$$

with $i\ge k$

and δ_{ik} is the Kronecker delta function.

The analytical development described above was implemented in a routine which calculates, for given values of the degrees of freedom, the total potential energy and its derivatives. This calculation is the heart of the energy minimization program, which drives the system to mechanical equilibrium (see Appendix J.) Discussion here focuses mainly on a routine written for the computation of the objective function U^{pot} and the gradient g by the exact analytical eqns (C.11) to (C.14). A variant of this routine was written for the calculation of the objective function, gradient and Hessian, $\underline{H}$, by incorporating eqns (C.15) to (C.17).

The tasks of the objective function and derivative calculating routine are:

. to determine the structure for a given (ψ, ϕ), i.e. to calculate position vectors and continuation coefficients for every atom or group in the cube.

. To select significant interactions by performing a double loop over all atoms and groups in the system, employing the geometrical screening algorithm mentioned in section 3.2.

. to accumulate, for all significantly interacting pairs, contributions to the total energy and its derivatives.

. to accumulate, for all skeletal angles in the system, contributions from the intrinsic rotational potential.

Some data on the time allocation among these tasks are given in table C.1. From this table one can conclude that:

- The actual calculation of interatomic energies and forces constitutes only a very small fraction of the total computation time. Energy and force "tabulation" schemes, frequently used in molecular dynamics simulations, are thus not appropriate in this problem.

- Most of the computational effort goes to forming the gradient, by accumulating contributions from all interacting pairs of groups [eqns (C.13), (C.14)]. This is to be expected, since gradient calculation involves a triple loop over the degrees of freedom of the system, as described above. It is remarkable, however, that use of the analytical formulae, in addition to giving exact values for the derivatives, is much more efficient, as regards computer time, than a finite-difference estimation of the gradient. For a finite difference estimation one would have

to use 154 function evaluations, hence one would need approximately

$$154 \times (2.0 + 1.3 + 7.7 + 0.1)\% = 1700\ \%$$

of the times listed in Table 3.3.; i.e. use of the analytical formulae [eqns (C.13), (C.14)], as opposed to numerical differentiation, makes the program 17 times more efficient.

Table C.1

Computation of the Total Potential Energy U^{pot} and of the gradient g : Time Allocation to Various Tasks (Full potential, LABTECH70)

Task	Percent of total CPU time
. Initializations, Input/Output	3.0
. Atom coordinate calculation	2.0
. Interatomic energy and force calculation	1.3
. Topological screening (including calculation of minimum image distance)	7.7
. Energy updating	0.1
. Gradient Updating	85.9
Total	100.0

APPENDIX D : Bonded Contributions to the Pair Distribution Functions

r_b symbolizes the location of each "Dirac pulse" on the r-axis, in $\mathring{A}$.

A_b symbolizes the area of the "Dirac pulse" in a g(r) plot, in $\mathring{A}$.

V is the cube volume, in $\mathring{A}^3$.

D(a) : Group Pair Distribution Functions

Pair Species αβ	Distance r_b (Å)	Fraction of total number of αβ pairs separated by r_b due to connectivity, $\frac{4\pi r_b^2}{V} \cdot A_b$
C - C	1.53	$\frac{2x-2}{(2x-1)(x-1)} = 0.01325$
	2.537	$\frac{x-2}{(2x-1)(x-1)} = 0.00653$
	2.566	$\frac{x-1}{(2x-1)(x-1)} = 0.00662$
C - H	1.10	$\frac{1}{2x-1} = 0.00662$
	2.127	$\frac{2(x-1)}{(3x-2)(2x-1)} = 0.00440$
	2.156	$\frac{4(x-1)}{(3x-2)(2x-1)} = 0.00879$
C - R	1.53	$\frac{1}{2x-1} = 0.00662$
	2.537	$\frac{2x}{(2x-1)(x+2)} = 0.01291$
H - H	1.764	$\frac{2}{3(3x-2)} = 0.00295$
H - R	2.127	$\frac{1}{3x-2} = 0.00442$
R - R	2.537	$\frac{4}{(x+2)(x+1)} = 0.00067$

D(b) : Element Pair Distribution Functions

Element Pair Species αβ	Distance r_b (Å)	Fraction of αβ pairs separated by r_b due to connectivity, $\frac{4\pi r_b^2}{V} \cdot A_b$
C - C	1.53	$\frac{2}{3x+1}$ = 0.00873
	2.537	$\frac{2}{3x+1}$ = 0.00873
	2.566	$\frac{2(x-1)}{3x(3x+1)}$ = 0.00287
C - H	1.10	$\frac{1}{3x+1}$ = 0.00437
	2.127	$\frac{3x}{(3x+1)(6x+4)}$ = 0.00216
	2.156	$\frac{4(x-1)}{(3x+1)(6x+4)}$ = 0.00285
	2.168	$\frac{3(x+2)}{(3x+1)(6x+4)}$ = 0.00222
	2.759	$\frac{2(x+2)}{(3x+1)(6x+4)}$ = 0.00148
	2.813	$\frac{2(x+2)}{(3x+1)(6x+4)}$ = 0.00148
	3.486	$\frac{2(x+2)}{(3x+1)(6x+4)}$ = 0.00148
H - H	1.764	$\frac{x-1}{(6x+3)(3x+2)}$ = 0.00071
	1.790	$\frac{3(x+2)}{(6x+3)(3x+2)}$ = 0.00222
	2.457	$\frac{2(x+2)}{(6x+3)(3x+2)}$ = 0.00148
	2.524	$\frac{2}{(6x+3)(3x+2)}$ = 0.00002

(continued)

Element Pair Distribution Functions (continued)

Element Pair	Distance r_b (Å)	Fraction of αβ pairs separated by r_b due to connectivity, $\frac{4\pi r_b^2}{y} \cdot A_b$
H - H	2.643	$\frac{2}{(6x+3)(3x+2)} = 0.00002$
	3.050	$\frac{x+2}{(6x+3)(3x+2)} = 0.00074$
	3.143	$\frac{4}{(6x+3)(3x+2)} = 0.00004$
	3.755	$\frac{4}{(6x+3)(3x+2)} = 0.00004$
	3.822	$\frac{4}{(6x+3)(3x+2)} = 0.00004$
	4.315	$\frac{2}{(6x+3)(3x+2)} = 0.00002$

APPENDIX E : Force and Torque Balance Equations

Consider a parent chain, $CH_3 - CHR - (CH_2-CHR)_{x-1} - CH_3$, immersed in a sea of its neighbors. Following Flory we number its skeletal bonds from 1 to 2x and its skeletal atoms from 0 to 2x. Furthermore, we number its atoms from 1 to 6x-1 as follows (compare Fig.E.1):

- Atoms 1 and 6x-1 are the terminal CH_3-substituents
- Atoms 3k-1, $1 \leq k \leq 2x-1$ are skeletal carbons; they are chiral if k is odd, and achiral if k is even
- Atoms 3k, $1 \leq k \leq 2x-1$ are pendant hydrogens.
- Atoms 3k+1, $1 \leq k \leq 2x-1$ are pendant hydrogens (if k is even) or R-substituents (if k is odd).

We call "skeletal segment" a skeletal atom and all its substituents. Skeletal segment 0 consists of the terminal atom 1. Skeletal segment 2x consists of the terminal atom 6x-1. Skeletal segment k ($1 \leq k \leq 2x-1$) consists of the carbon 3k-1 and the substituents 3k and 3k+1. Bond k connects skeletal segments k-1 and k.

With this nomenclature, and with the notation introduced in the discussion of the force approach in the main text, the detailed force and torque balance equations assume the form:

Segment 0

Force balance on atom 1: $$\underset{\sim}{F}^{B}_{12} = \sum_{j \neq 1} \underset{\sim}{F}^{NB}_{1j} \qquad (E.1)$$

Torque balance on atom 1: $$\underset{\sim}{T}^{B}_{12} = \underset{\sim}{0} \qquad (E.2)$$

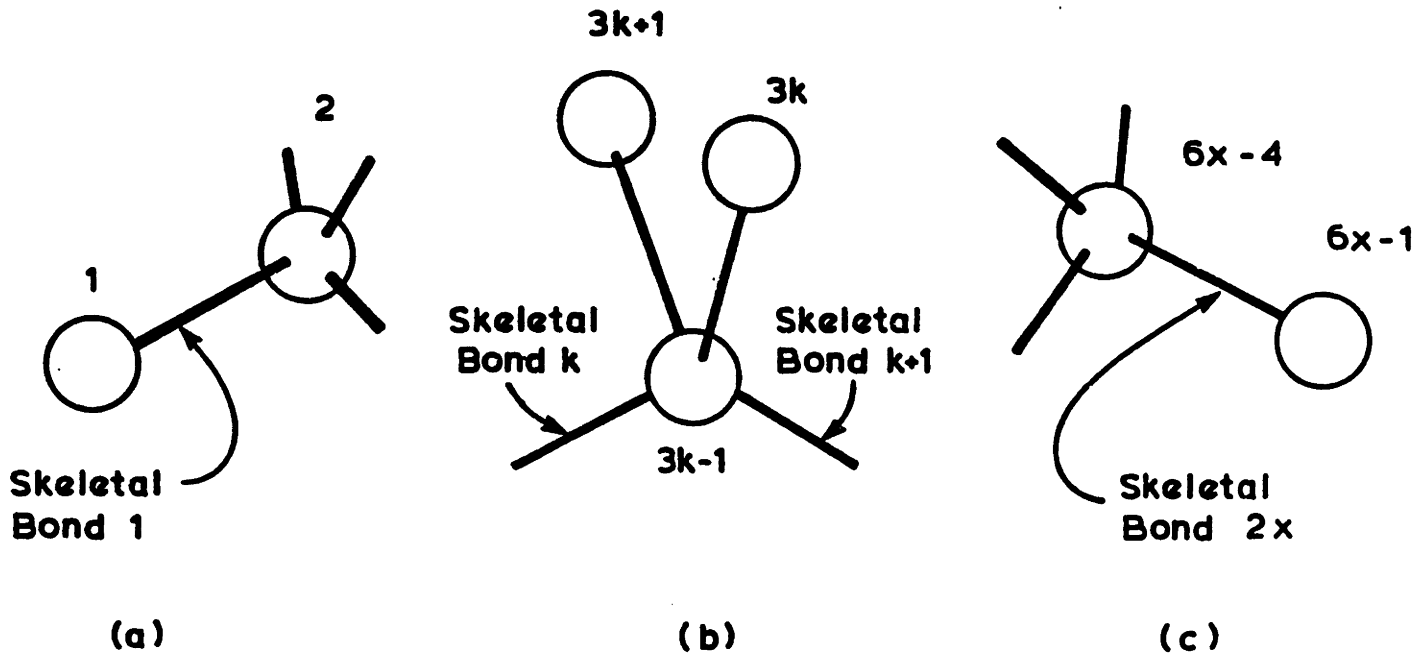

Figure E.1 : Notation used in formulating the detailed force and torque balance equations

(a) first segment

(b) intermediate segment

(c) last segment

Force balance on bond 1: $\left(-\underset{\sim}{F}^{B}_{12}\right)+\left(-\underset{\sim}{F}^{B}_{21}\right)=\underset{\sim}{0}$ and $\underset{\sim}{F}^{B}_{21}=-\underset{\sim}{F}^{B}_{12}$ (E.3)

Torque balance on bond 1: $\left(-\underset{\approx}{T}^{B}_{12}\right)+\left(\underset{\sim}{r}_1-\underset{\sim}{r}_2\right)\times\left(-\underset{\sim}{F}^{B}_{12}\right)+\left(\underset{\approx}{T}^{B}_{21}\right)=0$

or $\underset{\approx}{T}^{B}_{21}=\underset{\approx}{T}^{B}_{12}-(\underset{\sim}{r}_1-\underset{\sim}{r}_2)\times\underset{\sim}{F}^{B}_{12}$ (E.4)

Segment k, $1\leq k\leq 2x-1$

Force balance on pendant atom 3k: $\underset{\sim}{F}^{B}_{3k,3k-1}=-\sum_{j\neq 3k}\underset{\sim}{F}^{NB}_{3k,j}$ (E.5)

Torque balance on pendant atom 3k: $\underset{\approx}{T}^{B}_{3k,3k-1}=\underset{\sim}{0}$ (E.6)

Force balance on pendant atom 3k+1: $\underset{\sim}{F}^{B}_{3k+1,3k-1}=\sum_{j\neq 3k+1}\underset{\sim}{F}^{NB}_{3k+1,j}$ (E.7)

Torque balance on pendant atom 3k+1: $\underset{\approx}{T}^{B}_{3k+1,3k-1}=\underset{\sim}{0}$ (E.8)

Force balance on pendant bond (3k-1,3k): $\underset{\sim}{F}^{B}_{3k-1,3k}=-\underset{\sim}{F}^{B}_{3k,3k-1}$ (E.9)

Torque balance on pendant bond (3k-1,3k):

$$\left(-\underset{\approx}{T}^{B}_{3k,3k-1}\right)+\left(\underset{\sim}{r}_{3k}-\underset{\sim}{r}_{3k-1}\right)\times\left(-\underset{\sim}{F}^{B}_{3k,3k-1}\right)+\left(-\underset{\approx}{T}^{B}_{3k-1,3k}\right)=\underset{\sim}{0}$$

and $$\underset{\approx}{T}^{B}_{3k-1,3k}=-\underset{\approx}{T}^{B}_{3k,3k-1}-\left(\underset{\sim}{r}_{3k}-\underset{\sim}{r}_{3k-1}\right)\times\underset{\sim}{F}^{B}_{3k,3k-1}$$ (E.10)

Force balance on pendant bond (3k-1,3k+1): $\underset{\sim}{F}^{B}_{3k-1,3k+1}=-\underset{\sim}{F}^{B}_{3k+1,3k-1}$ (E.11)

Torque balance on pendant bond (3k-1,3k+1):

$$\left(-\underline{\underline{T}}^{B}_{3k+1,3k-1}\right) + \left(\underline{r}_{3k+1}-\underline{r}_{3k-1}\right) \times \left(-\underline{F}^{B}_{3k+1,3k-1}\right) + \left(-\underline{\underline{T}}^{B}_{3k-1,3k+1}\right) = \underline{0}$$

and $$\underline{\underline{T}}^{B}_{3k-1,3k+1} = -\underline{\underline{T}}^{B}_{3k+1,3k-1} - \left(\underline{r}_{3k+1}-\underline{r}_{3k-1}\right) \times \underline{F}^{B}_{3k+1,3k-1} \qquad (E.12)$$

Force balance on skeletal atom 3k-1:

$$\underline{F}^{B}_{3k-1,3k+2} = -\left\{ \sum_{j\neq 3k-1} \underline{F}^{NB}_{3k-1,j} + \underline{F}^{B}_{3k-1,k_1} + \underline{F}^{B}_{3k-1,3k} + \underline{F}^{B}_{3k-1,3k+1} \right\}$$

where $$k_1 = \max\,(1,\ 3k-4) \qquad (E.13)$$

Torque balance as skeletal atom 3k-1:

$$\underline{\underline{T}}^{B}_{3k-1,3k+2} = -\left\{ \underline{\underline{T}}^{B}_{3k-1,k_1} + \underline{\underline{T}}^{B}_{3k-1,3k} + \underline{\underline{T}}^{B}_{3k-1,3k+1} \right\}$$

where $$k_1 = \max\,(1,\ 3k-4) \qquad (E.14)$$

Force balance on skeletal bond k+1: $$\underline{F}^{B}_{3k+2,3k-1} = -\underline{F}^{B}_{3k-1,3k+2} \qquad (E.15)$$

Torque balance on skeletal bond k+1:

$$\left(-\underline{\underline{T}}^{B}_{3k+2,3k-1}\right) + \left(\underline{r}_{3k-1}-\underline{r}_{3k+2}\right) \times \left(-\underline{F}^{B}_{3k-1,3k+2}\right) + \left(-\underline{\underline{T}}^{B}_{3k-1,3k+2}\right) = \underline{0}$$

or $$\underline{\underline{T}}^{B}_{3k+2,3k-1} = -\underline{\underline{T}}^{B}_{3k-1,3k+2} - \left(\underline{r}_{3k-1}-\underline{r}_{3k+2}\right) \times \underline{F}^{B}_{3k-1,3k+2} \qquad (E.16)$$

Axial torque balance along skeletal bond k+1 [see eqn. (5.22)]

$$\underline{\underline{T}}^{B}_{3k+2,3k-1} \cdot \frac{\underline{r}_{3k-1} - \underline{r}_{3k+2}}{\left|\underline{r}_{3k-1} - \underline{r}_{3k+2}\right|} = \frac{dU_{\phi}}{d\phi}\Bigg|_{\phi=\phi_{k+1}} \qquad (E.17)$$

For eqns. (E.5) to (E.16) the index k runs from 1 to 2x-1. For eqn. (E.17) it runs from 1 to 2x-2.

Segment 2x

Torque balance on atom 6x-1: $\underline{\underline{T}}^{B}_{6x-1,6x-4} = \underline{0}$ (E.18)

Nonbonded interatomic interaction forces are functions of interatomic distances. For any significantly interacting pair (i,j) we have, according to eqn. (5.21):

$$\underline{F}^{NB}_{ij} = \frac{dU^{NB}_{ij}}{dr}\bigg|_{r=|\underline{r}_i-\underline{r}_j|} \frac{\underline{r}_j-\underline{r}_i}{|\underline{r}_j-\underline{r}_i|} \qquad (E.19)$$

Moreover, as shown in Appendix C above, all interatomic distance vectors are analytically expressible in terms of the microscopic degrees of freedom. Symbolically,

$$\underline{r}_j-\underline{r}_i = f(\underline{\psi},\underline{\phi}\ ;\ \underline{a}_x,\ \underline{a}_y,\ \underline{a}_z) \qquad (E.20)$$

Equations (B.19) and (B.20) remain valid when the minimum image convention is imposed.

Equations (B.1) to (B.20) are a complete set of independent balance equations.

We use eqns. (E.19) and (E.20) to directly substitute all nonbonded forces $\underline{F}^{NB}_{ij}$ and interatomic distance vectors $\underline{r}_j-\underline{r}_i$ appearing in eqns. (E.1) to (E.18) in terms of the microscopic degrees of freedom $(\underline{\psi},\underline{\phi})$. Consider now the system of eqns. (E.1) to (E.18) after this substitution. A count of the unknowns appearing in this system yields

Components of bonded forced $\underline{F}^{B}_{ij}$	6(6x-2)
Components of bonded torques $\underline{\underline{T}}^{B}_{ij}$	6(6x-2)
Microscopic degrees of freedom $\underline{\psi},\underline{\phi}$	2x+1
Total number of unknowns	74x-23

A count of the number of equations gives

Balances (E.1) to (E.4)	12
Balances (E.5) to (E.16)	36(2x-1)
Projected torque balances (E.17)	2x-2
Balances (E.18)	3
Total number of equations	74x-23

The number of equations is thus equal to the number of unknowns and, in principle, the microscopic degrees of freedom $\underset{\sim}{\psi},\underset{\sim}{\phi}$ are determinable from the solution of this system. The minimum energy requirement [(3.11)]is obtained by elimination of the variables $\underset{\sim}{F}^B_{ij}$ and $\underset{\equiv}{T}^B_{ij}$ from the system of eqns. (E.1) to (E.18). It involves only 2x+1 variables, and is thus much preferable to solve in practice.

Once we know the microscopic degrees of freedom $\underset{\sim}{\psi}$ and $\underset{\sim}{\phi}$ (as we do for every one of the undeformed and deformed structures in this work), the system of deformed balance equations becomes overdetermined and (2x+1) of the equations can be used as consistency tests. As such we chose here to use the 2x-2 projected torque balances (E.17), together with the 3 torque balances on the last atom (E.18).

To obtain all forces and torques in a given structure we first compute all nonbonded forces (hence, the total nonbonded force on each atom) via eqn. (E.19). We then solve eqns. (E.1) to (E.16) sequentially, in the order they have been written above, to get all bonded forces and torques. In the course of this segment-by-segment solution of the balance equations we test for consistency via eqns. (E.17) and (E.18).

We found that the projected torques on the left hand side of eqns. (E.17) and (E.18) deviate from the derivatives $U'_\phi(\phi_{k+1})$ by a relative error of less than 10^{-5}, which confirms the excellent performance of the minimizations.

APPENDIX F : Equivalence of the Force and Virial Theorem Approaches for Calculating Mechanical Properties

The force approach rests on a calculation of the "face forces" $\underset{\sim}{F}_f$ exerted on the interior of the cube by its surroundings through each of its faces, f. We denote by f=1 the face parallel to the edge vectors $\underset{\sim}{a}_y$ and $\underset{\sim}{a}_z$ and containing the origin $\underset{\sim}{0}$; by f=3 the face parallel to the edge vectors $\underset{\sim}{a}_z$ and $\underset{\sim}{a}_x$ and containing the origin $\underset{\sim}{0}$; and by f=5 the face parallel to the edge vectors $\underset{\sim}{a}_x$ and $\underset{\sim}{a}_y$ and containing the origin $\underset{\sim}{0}$.

$$\underset{\sim}{n}_1 = -\frac{\underset{\sim}{a}_y \times \underset{\sim}{a}_z}{S_1} \quad , \quad S_1 = |\underset{\sim}{a}_y \times \underset{\sim}{a}_z|$$

$$\underset{\sim}{n}_2 = -\frac{\underset{\sim}{a}_z \times \underset{\sim}{a}_x}{S_2} \quad , \quad S_2 = |\underset{\sim}{a}_z \times \underset{\sim}{a}_x| \qquad (F.1)$$

$$\underset{\sim}{n}_3 = -\frac{\underset{\sim}{a}_x \times \underset{\sim}{a}_y}{S_3} \quad , \quad S_3 = |\underset{\sim}{a}_x \times \underset{\sim}{a}_y|$$

From eqn.(5.24), applied for the faces 1, 3 and 5, we have, in matrix notation (all vectors taken as column vectors):

$$\underline{\underline{F}} = \left[\underset{\sim}{F}_1 \;\; \underset{\sim}{F}_3 \;\; \underset{\sim}{F}_5\right] = \underline{\underline{\sigma}}^T \left[\underset{\sim}{n}_1 S_1 \;\; \underset{\sim}{n}_3 S_3 \;\; \underset{\sim}{n}_5 S_5\right] = \underline{\underline{\sigma}}^T \underline{\underline{S}}$$

and

$$\underline{\underline{\sigma}}^T = \underline{\underline{F}} \;\; \underline{\underline{S}}^{-1} \qquad (F.2)$$

Using eqns.(F.1) one can readily calculate $\underline{\underline{S}}^{-1}$ as:

$$\underline{\underline{S}}^{-1} = -\frac{1}{V}\begin{bmatrix} \underset{\sim}{a}_x^T \\ \underset{\sim}{a}_y^T \\ \underset{\sim}{a}_z^T \end{bmatrix} \qquad (F.3)$$

Therefore, from eqns. (F.2) and (F.3),

$$\underline{\underline{\sigma}} = -\frac{1}{V}\left[\underline{a}_x\ \underline{a}_y\ \underline{a}_z\right]\begin{bmatrix} \underline{F}_1^T \\ \underline{F}_2^T \\ \underline{F}_3^T \end{bmatrix} \tag{F.4}$$

or, equivalently,

$$\sigma_{LM} = -\frac{1}{V}\left(a_{x,L}\,F_{1,M} + a_{y,L}\,F_{3,M} + a_{z,L}\,F_{5,M}\right) \tag{F.5}$$

$\underline{F}_1$ is the sum of all forces exerted on cube atoms from images of other cube atoms that lie across face 1. Let $(\lambda_j', \mu_j', \nu_j')$ denote the continuation coefficients of an atom j of the cube (see Appendix C for the definition of these quantities). Let $j_{min}(i)$ be that image of atom j of the cube that lies closest to atom i (minimum image of j with respect to i). By the minimum image convention, only minimum image pairs interact. We have

$$\underline{F}_1 = \sum_i \sum_j \underline{F}_{ij}^{min} = \frac{1}{2}\left[\sum_i \sum_j \underline{F}_{ij}^{min} + \sum_j \sum_i \underline{F}_{ji}^{min}\right]$$

i,j in cube i and $j_{min}(i)$ lie across face 1	i,j in cube i and $j_{min}(i)$ lie across face 1	i,j in cube j and $i_{min}(j)$ lie across face 1

Now, if j and $i_{min}(j)$ lie across face 1, then $j_{min}(i)$ and i will lie across face 2, which is the face opposite to face 1. Then:

$$\underline{F}_1 = \frac{1}{2}\left[\sum_i \sum_j \underline{F}_{ij}^{min} - \sum_i \sum_j \underline{F}_{ij}^{min}\right] =$$

i,j in cube i and $j_{min}(i)$ lie across face 1	i,j in cube i and $j_{min}(i)$ lie across face 2

$$= \frac{1}{2}\left[\sum_i \sum_j \underset{\sim}{F}_{ij}^{min} - \sum_i \sum_j \underset{\sim}{F}_{ij}^{min}\right] =$$

i,j in cube j and $j_{min}(i)$ lie across face 1 — i,j in cube j and $j_{min}(i)$ lie across face 2

$$= \frac{1}{2}\left[\sum_i \sum_j \underset{\sim}{F}_{ij}^{min} - \sum_i \sum_j \underset{\sim}{F}_{ij}^{min}\right]$$

i,j in cube $\lambda'_j - \lambda'_{j_{min}(i)} = +1$ — i,j in cube $\lambda'_j - \lambda'_{j_{min}(i)} = -1$

and, since the possible values of the difference $\lambda'_j - \lambda'_{j_{min}(i)}$ are -1,0 and 1, we have:

$$\underset{\sim}{F}_1 = \frac{1}{2}\sum_i \sum_j \left[\lambda'_j - \lambda'_{j_{min}(i)}\right] \underset{\sim}{F}_{ij}^{min} \qquad (F.6)$$

and similarly for $\underset{\sim}{F}_3$ and $\underset{\sim}{F}_5$. Then, eqn. (F.5) assumes the form:

$$\sigma_{LM} = -\frac{1}{2V}\sum_i \sum_{j\neq i} \left[\left(\lambda'_j - \lambda'_{j_{min}(i)}\right) a_{x,L} + \left(\mu'_j - \mu'_{j_{min}(i)}\right) a_{y,L} + \left(\nu'_j - \nu'_{j_{min}(i)}\right) a_{z,L}\right] F_{ij,M}^{min}$$

$$= -\frac{1}{2V}\sum_i \sum_{j\neq i} \left(r_j - r_{j_{min}(i)}\right)_L F_{ij,M}^{min}$$

$$= -\frac{1}{2V}\sum_i \sum_{j\neq i} \left(r_{j,L} - r_{i,L}\right) F_{ij,M}^{min} - \frac{1}{2V}\sum_i \sum_{j\neq i} \left(r_{i,L} - r_{j,L}\right)_{min} F_{ij,M}^{min} \qquad (F.7)$$

The first term in eqn. (F.7) can further be written:

$$-\frac{1}{2V}\sum_i\sum_{j\neq i}(r_{j,L}-r_{i,L})\;F^{min}_{ij,M}=\frac{1}{2V}\sum_i\sum_{j\neq i}r_{j,L}\,F^{min}_{ji,M}+\frac{1}{2V}\sum_i\sum_{j\neq i}r_{i,L}\,F^{min}_{ij,M}$$

$$=\frac{1}{V}\sum_i\sum_{j\neq i}r_{i,L}\,F^{min}_{ij,M}=\frac{1}{V}\sum_i r_{i,L}\sum_{j\neq i}F^{min}_{ij,M} \qquad (F.8)$$

$$=0$$

because the condition of detailed mechanical equilibrium around atom i dictates that $\sum_{j\neq i}F^{min}_{ij,M}=0$.

We are thus left, from eqns. (F.7) and (F.8), with the expression:

$\sigma_{LM}=-\frac{1}{2V}\sum_i\sum_{j\neq i}\left(r_{i,L}-r_{j,L}\right)_{min}F^{min}_{ij,M}$, which is exactly the

Virial Theorem expression [eqn. (5.26)].

APPENDIX G : A Sensitivity Analysis

To test the sensitivity of the model estimates to the potential parameters employed, I subjected one of the undeformed structures to a new relaxation and to tension and shear deformations, using a slightly different set of Van der Waals radii. All computations presented in the main body of this thesis have been performed using the potential parameters listed in Table 3.2. The Van der Waals radii listed in that table we call the "Base Case" radii, and repeat in Table G.1. For the sensitivity analysis runs, values were changed to the ones suggested by Bondi ([7], p.2) and by Tadokoro ([61], p. 326). The two sets differ by 0.1 Å for H and C only, reflecting the small degree of uncertainty that exists regarding the potential parameters.

The particular structure examined in the sensitivity runs was somewhat anomalous, since it displayed a negative ratio α_p/κ_T , and considerably higher than average elastic coefficients. The influence of changing Van der Waals radii on the theoretical estimates of various properties is displayed in Table G.2. One sees that the solubility parameter and the elastic constants change relatively little, while the ratio α_p/κ_T (hence, our estimate of the thermal expansion coefficient) exhibits a very strong dependence on the atomic radii, jumping from its original negative value to a positive one (which actually is close to the experimental ratio α_p/κ_T for glassy atactic polypropylene under the modelled conditions).

Thus, small uncertainties in the potential parameters can well be tolerated in predicting the solubility and the elastic constants with our approach, but appear to render our estimate of the thermal expansion coefficient unreliable.

Table G.1. : Van der Waals radii, in Å

Species	H	C	R
I. Base Case	1.3	1.8	2.0
II. Perturbed Case	1.2	1.7	2.0

Table G.2.: Changes in Estimated Properties

Property	I. Value, Base Case	II. Value, Perturbed Case	Change %
Solubility Parameter, δ $(J/cm^3)^{1/2}$	14.6	15.6	+ 6.8
$\frac{1}{3}(C_{11}+C_{22}+C_{33})$ MPa	6524	5303	- 18.7
$\frac{1}{3}(C_{44}+C_{55}+C_{66})$ MPa	1278	1337	+ 4.6
$\frac{\alpha_P}{\kappa_T}$ MPa/K	-0.175	0.717	-509.7

APPENDIX H : Symmetry of the Atomic Level Stress Tensor

Systems with Exclusively Central Forces. In the case of a nonbonded system with central forces, the condition of symmetry of the tensor $\underline{\underline{\sigma}}_i$, defined by eqn.(6.1) becomes $\sigma_{i,LM} = \sigma_{i,ML}$, hence

$$\sum_{j\neq i} \left[(r_{i,L}-r_{j,L})_{min} F^{min}_{ij,M} - (r_{i,M}-r_{j,M})_{min} F^{min}_{ij,L} \right] = 0$$

$$\forall (L,M) \quad \{1,2,3\}^2$$

This is equivalent to the statement:

$$\sum_{j\neq i} (\underline{r}_j-\underline{r}_i)_{min} \times \underline{F}^{min}_{ij} = \underline{0} \qquad (H.1)$$

Since the central force $\underline{F}^{min}_{ij}$ is collinear with the vector $(\underline{r}_j-\underline{r}_i)_{min}$ [eqn. (5.21)], eqn. (H.1) is fulfilled, and tensor $\underline{\underline{\sigma}}_i$ is symmetric.

Bonded Systems. In the presence of noncentral bonded forces eqn. (H.1) is no longer true, and the tensor defined by eqn.(6.1) is no longer symmetric. We defined the atomic-level stress tensor by eqn.(6.18). The tensor $\underline{\underline{\sigma}}_i$ is symmetric if, and only if, the tensor $\underline{\underline{w}}_i$ [see eqn.(6.15)] is symmetric. Here we prove the symmetry of this tensor. Symmetry of $\underline{\underline{w}}_i$, i.e., $w_{i,LM} = w_{i,ML}$, is tantamount to

$$\sum_{j\neq i} \left\{ (r_{i,L}-r_{j,L})_{min} F^{min}_{ij,M} - (r_{i,M}-r_{j,M})_{min} F^{min}_{ij,L} + e_{LMK} \frac{\underline{T}^B_{ij,K} + \underline{T}^B_{ji,K}}{2} \right.$$

$$\left. - e_{MLK} \frac{\underline{T}^B_{ij,K} + \underline{T}^B_{ji,K}}{2} \right\} = 0$$

Since $e_{LMK} = -e_{MLK}$,

$$\sum_{j\neq i} \left\{ (r_{i,L}-r_{j,L})_{min} F^{min}_{ij,M} - (r_{i,M}-r_{j,M})_{min} F^{min}_{ij,L} + e_{LMK}\left(T^{B}_{ij,K} + T^{B}_{ji,K}\right)\right\} = 0$$

and

$$\sum_{K}\sum_{j\neq i} \left\{ \left[(\underset{\sim}{r}_i-\underset{\sim}{r}_j)_{min} \times \underset{\sim}{F}^{min}_{ij} \right]_K e_{LMK} + \left(\underset{\sim}{T}^{B}_{ij} + \underset{\sim}{T}^{B}_{ji} \right)_K e_{LMK} \right\} = 0$$

For this equation to hold $\forall$ (L,M) ε $\{1,2,3\}^2$ it is necessary and sufficient that

$$\sum_{j\neq i} \left[(\underset{\sim}{r}_i-\underset{\sim}{r}_j)_{min} \times \underset{\sim}{F}^{min}_{ij} + \underset{\approx}{T}^{B}_{ij} + \underset{\approx}{T}^{B}_{ji} \right] = \underset{\sim}{0}$$

Decomposing the force $\underset{\sim}{F}_{ij}$ into its bonded and nonbonded part, as in eqn. (5.27). and realizing that the nonbonded part is collinear with the interatomic vector [(5.21)] we obtain, equivalently:

$$\sum_{j\neq i} \left[(\underset{\sim}{r}_i-\underset{\sim}{r}_j)_{min} \times \underset{\sim}{F}^{B}_{ij} + \underset{\approx}{T}^{B}_{ij} + \underset{\approx}{T}^{B}_{ji} \right] = \underset{\sim}{0} \qquad \text{(H.2)}$$

If centers i and j are not connected by a bond, all terms in the bracket of equation (H.2) automatically vanish. In case atoms i and j are bonded to each other, the torque balance on bond ij (Appendix E) gives:

$$(\underset{\sim}{r}_i-\underset{\sim}{r}_j) \times (-\underset{\sim}{F}^{B}_{ij}) + (-\underset{\approx}{T}^{B}_{ij}) + (-\underset{\approx}{T}^{B}_{ji}) = \underset{\sim}{0}$$

or

$$(\underset{\sim}{r}_i-\underset{\sim}{r}_j)_{min} \times \underset{\sim}{F}^{B}_{ij} + \underset{\approx}{T}^{B}_{ij} + \underset{\approx}{T}^{B}_{ji} = \underset{\sim}{0}$$

and the contribution from bonded pair ij is again zero. Thus eqn. (H.2) is true, which proves the symmetry of tensors $\underset{\approx}{W}_i$ and $\underset{\approx}{\sigma}_i$.

APPENDIX I : Listing of the FORTRAN Program Used to Generate an Initial Guess Structure by the Modified Markov Scheme of Section 3.3.1

```
      PROGRAM GENERATE
C
C  ***************************************************************************
C  *                                                                         *
C  *                        DOROS N. THEODOROU                               *
C  *                                                                         *
C  *                Department of Chemical Engineering                       *
C  *                                                                         *
C  *              Massachusetts Institute of Technology                      *
C  *                                                                         *
C  *                             June 1985                                   *
C  *                                                                         *
C  ***************************************************************************
C
C  Monte-Carlo generation of a vinyl polymer chain of the type
C           H-(CH2-CHR)x-CH3
C  in a periodic box, with simultaneous computation of the system
C  potential energy, so as to avoid strong short- and long range
C  interactions.
C
      INTEGER*1 LAMDA(3000), MU(3000), NU(3000), ICHIR(500), KIND(3000),
     1          MODUL(3000), CONNECT(0:5,0:5), CONFORM(1000), TACTIC(500)
      INTEGER*2 IC(0:1000), ISEG(3000)
      INTEGER*4 SEED1,SEED2,SEED10
      REAL L, LH, LR, MW, MWUNIT, MWR
      CHARACTER CHAINNM*20, NAME(3)*4, CHIRNM(-1:1)*1, RISNM(5)*2,
     1          DYADNM(0:1)*1, FORM*19
      DIMENSION X(3000), Y(3000), Z(3000), PHI(1000), PHIO(5),
     1          AX(3), AY(3), AZ(3), AXCY(3), AYCZ(3), AZCX(3), ORIGIN(3),
     2          VC(3), VH1D(3), VH1L(3), VH2(3), VH3(3), VRD(3), VRL(3),
     3          TO(3,3), TP(3,3), TPP(3,3), TPROD(3,3),
     4          ALFA(3), EFFNE(3), VDWR(3), EPS(3,3), SIGMA(3,3),
     5          RANGE(3,3), RANGEX(3,3), RANGEY(3,3), RANGEZ(3,3), EPSIG(3,3),
     6          UM2(5,5), UR2(5,5), UO(5), UX(5), U(5,5), UP(5,5), UMPP(5,5),
     7          URPP(5,5), DIAG(5,5), VEC(5), Q(5), UPRODL(5,500),
     8          UPRODR(5,500)
C
      COMMON UP,UMPP,URPP,DIAG,UO,UX,UM2,UR2,Q
      COMMON /BLOCK1/ X, Y, Z
      COMMON /BLOCK2/ ICHIR, LAMDA, MU, NU, KIND, IC, ISEG, MODUL, CONNECT
      COMMON /BLOCK3/ NUNITS, NBONDS, NSEGMENTS, NATOMS, THETAP, THETAHP,
     1                THETAPP, THETAHPP, THETARPP, STHP, CSTHP, STHPP,
     2                CSTHPP, L, LH, LR, VC, VH1D, VH1L, VH2, VH3, VRD,
     3                VRL, TO, TP, TPP, TPROD
      COMMON /BLOCK4/ ALPHA, BETA, GAMMA, AX, AY, AZ, AXX, AYY, AZZ,
     1                AXCY, AYCZ, AZCX, ORIGIN, VOLUME
      COMMON /BLOCK5/ ALFA, EFFNE, VDWR, EPS, SIGMA, EPSIG, RANGE, RANGEX,
     1                RANGEY, RANGEZ, NAME, NNUC, RR1, RR2, DELRR, AU, BU,
     2                CU, AF, BF, CF, ROTBAR
      COMMON /BLOCK7/ N, N1, TEMP, PHIO, RISNM, CONFORM, TACTIC, PHI, IWRPR
      COMMON /BLOCK8/ UPRODL, UPRODR
C
      CALL GETTIME
C
      RKCAL=1.987E-03
      DYADNM(0)='m'
      DYADNM(1)='r'
      CHIRNM(-1)='L'
      CHIRNM(0)='*'
      CHIRNM(1)='D'
```

```
C
C  Enter chain type and size.
      READ(5,10) CHAINNM,MWR,NUNITS
   10 FORMAT(A20/F10.5/I5)
      NSEGMENTS=2*NUNITS+1
      NBONDS=2*NUNITS
      NDYADS=NUNITS-1
      NDF=NBONDS-2
      NDF1=NDF+1
      NATOMS=3*NDF+5
      MWUNIT=MWR+27.04621
      MW=16.04303+NUNITS*MWUNIT
      WRITE(6,20) CHAINNM,NUNITS,NATOMS,NBONDS,NDF,MW
   20 FORMAT(/////2X,'MOLECULE : ',A20/13X,13('-')//2X,'DEGREE OF ',
     1 'POLYMERIZATION : ',I5,5X,'(',I5,'  SKELETAL ATOMS, ',3X,I5,
     2 '  BONDS )'//2X,'NUMBER OF INTERNAL DEGREES OF FREEDOM : ',I5//
     3 2X,'MOLECULAR WEIGHT : ',E16.8/)
C
C  Enter bond lengths (Angstroms) and bond angles (degrees)
C  L        =  C-C bond length
C  LH       =  C-H bond length
C  LR       =  C-R bond length
C  THETAP   =  complement of intradyad C-C-C angle
C  THETAHP  =  complement of intradyad H-C-C angle
C  THETAHHP =  complement of intradyad H-C-H angle
C  THETAPP  =  complement of interdyad C-C-C angle
C  THETAHPP =  complement of interdyad H-C-C angle
C  THETARPP =  complement of interdyad R-C-C angle
C
      READ(5,30) L,LH,LR
      READ(5,30) THETAP,THETAHP
      READ(5,30) THETAPP,THETAHPP,THETARPP
   30 FORMAT(3F8.3)
      WRITE(6,25) L,LH,LR,THETAP,THETAPP,THETAHP,THETAHPP,THETARPP
   25 FORMAT(//2X,'BOND LENGTHS'/15X,'C - C  : ',F5.3,' ANGSTROMS'/
     115X,'C - H  : ',F5.3,' ANGSTROMS'/15X,'C - R  : ',F5.3,' ANGSTROMS'/
     215X,'(R=SUBSTITUENT)'//2X,'BOND ANGLES'/15X,'INTRADYAD C-C-C : ',
     3F8.3,' DEG'/15X,'INTERDYAD C-C-C : ',F8.3,' DEG'/15X,
     4'INTRADYAD H-C-C : ',F8.3,' DEG'/15X,'INTERDYAD H-C-C : ',F8.3,
     5' DEG'/15X,'INTERDYAD R-C-C : ',F8.3,' DEG'/)
C
C    Enter temperature (in K)
      READ (5,35) TEMP
   35 FORMAT(F10.4)
      WRITE(6,40) TEMP
   40 FORMAT(//2X,'TEMPERATURE OF CALCULATION : ',F6.2,'  K'/)
C
C  Read normalization frequency for Flory U-matrix multiplications
      READ(5,36) NNORM
   36 FORMAT(I4)
C
C    Enter rotational isomeric state number, names. angles and statistical
C    weight matrices.
C
      CALL RISDATA (N,TEMP,PHIO,RISNM)
C
      CALL MATMAT(UP,UMPP,UM2,5,5,5,N,N,N)
      CALL MATMAT(UP,URPP,UR2,5,5,5,N,N,N)
      UO(1)=1.
      UX(1)=1.
```

```
      DO 12 I=2,N
          UO(I)=0.0
   12     UX(I)=1.0
      N1=N-1
      WRITE(6,45)  (I,RISNM(I),PHIO(I), I=1,N)
   45 FORMAT(//2X,'ROTATIONAL ISOMERIC STATES :'//5X,'STATE No',4X,
     1'SYMBOL',6X,'ANGLE PHI(DEG) '//(8X, I3, 8X, A2, 10X, F8.2))
C
      FORM(1:3)='(( '
      FORM(5:6)='X,'
      FORM(8:19)='(F8.5,3X)/)) '
      IF(N.LT.5) FORM(3:3)='1'
      FORM(4:4)=CHAR(49+N)
      FORM(7:7)=CHAR(48+N)
      WRITE(6,46)
   46 FORMAT(///2X,'STATISTICAL WEIGHT MATRICES '//26X,'U'' '/26X,2('- '))
      WRITE(6,FORM)  ((UP(I,J),J=1,N),I=1,N)
      WRITE(6,47)
   47 FORMAT(//25X,'Um'' '/25X,3('- '))
      WRITE(6,FORM)  ((UMPP(I,J),J=1,N),I=1,N)
      WRITE(6,48)
   48 FORMAT(//25X,'Ur'' '/25X,3('- '))
      WRITE(6,FORM)  ((URPP(I,J),J=1,N),I=1,N)
C
C  Enter continuation vectors of cube (coordinates in Angstroms)
      READ(5,50)  (AX(I),I=1,3)
      READ(5,50)  (AY(I),I=1,3)
      READ(5,50)  (AZ(I),I=1,3)
   50 FORMAT(3E16.8)
      WRITE(6,55)  (AX(I),I=1,3),(AY(I),I=1,3),(AZ(I),I=1,3)
   55 FORMAT(//2X, 'CONTINUATION VECTORS FOR PERIODIC CUBE (COMPONENTS IN ',
     1'ANGSTROMS) :'//5X, 'AX :  ',3(E16.8, 5X)//5X,'AY :  ',3(E16.8,5X)//
     25X,'AZ :  ',3(E16.8,5X))
C
C  Calculate cross products Ax x Ay, Ay x Az, Az x Ax
      CALL VCROSSV(AX, AY, AXCY)
      CALL VCROSSV(AY, AZ, AYCZ)
      CALL VCROSSV(AZ, AX, AZCX)
C  Calculate cube volume, V=Ax.(Ay x Az)
      VOLUME=AX(1)*AYCZ(1)+AX(2)*AYCZ(2)+AX(3)*AYCZ(3)
      WRITE(6,60) VOLUME
   60 FORMAT(/2X,'CUBE VOLUME = ',E16.8, 2X, 'CUBIC ANGSTROMS'/)
C
C  Calculate density
      DENSITY=MW/VOLUME*1.6603022
      WRITE(6,72) DENSITY
   72 FORMAT(2X,'CUBE MASS DENSITY = ',E16.8,2X,' G/CM3')
C
C  Enter coordinates of cube origin
      READ(5,50)  (ORIGIN(I),I=1,3)
      WRITE(6,70)  (ORIGIN(I),I=1,3)
   70 FORMAT(/2X,'CUBE ORIGIN AT (',E16.8,',',E16.8,',',E16.8,')')
C
C    Specify tacticity. Read fraction of meso- dyads, WM.
C    Read tolerance for configuration generation
      READ (5,75) WM,TOLR
   75 FORMAT (F7.5,E15.8)
C
C  Read number of chains to be generated
      READ(5,78) NCHAINS
```

```
   78 FORMAT(I6)
C
C  Read seeds for Random Number Generation
      READ(5,80) SEED1,SEED2
   80 FORMAT(2I11)
      WRITE(6,85) WM,TOLR
   85 FORMAT(//2X,'TACTICITY SPECIFICATION'/2X,'FRACTION OF meso DYADS : ',
     1F7.5/2X,'TOLERANCE    :  ',E16.9)
C
      BLO=INT((1.-TOLR)*WM*NDYADS)
      BHI=INT((1.+TOLR)*WM*NDYADS)
      IF(INT(BHI).GE.BLO) GO TO 90
      WRITE(6,95)
   95 FORMAT(//2X,'TACTICITY RESTRICTION TOO STRICT : TRY LARGER TOLERANCE')
      GO TO 600
C
C    Fix position of three first skeletal carbon atoms.
C    X(1),Y(1),Z(1) = coordinates of first carbon atom (chain start)
C    ALPHA, BETA = polar angles determining orientation of first chain bond
C                  (ALPHA measured from direction of axis x on plane parallel
C                    to xy )
C                    BETA measured from direction of axis z )
C    GAMMA = dihedral angle between the planes (bond 1, axis z) and
C            (bond 1, bond 2)
C
C  Position of first skeletal carbon (terminal methyl)
   90 READ(5,50) X(1), Y(1), Z(1)
C
C  Flag for Eulerian angles:
C  . If IEULER=1, Eulerian angles read from input file
C  . If IEULER=0, Eulerian angles randomly generated using SEED1.
      READ(5,110) IEULER
C
      IF(IEULER.NE.1) GO TO 102
C
C  Angles specifying the orientation of first two bonds (in DEGREES)
      READ(5,100) ALPHA,BETA,GAMMA
  100 FORMAT(3E16.9)
C
C
C  Option input for creating an output file with the degrees of freedom
C  necessary to specify a chain (chirality sequence,position of first
C  skeletal atom, orientation of first two bonds and rotation angles
C  of bonds 2 through NBONDS-1)
C       IDF=1 : such an output file is to be created
C       IDF=0 : no such output file will be created
C
  102 READ(5,110) IDF
  110 FORMAT(I2)
C
      IF(IDF.EQ.0) GO TO 115
      CALL DELETEFILE('CHAIN.DF',8)
      OPEN(UNIT=20,FILE='CHAIN.DF')
C
  115 IF(IEULER.NE.1) GO TO 116
      WRITE(6,120) X(1),Y(1),Z(1),ALPHA,BETA,GAMMA
  120 FORMAT(///2X,'SPECIFICATION OF LOCATION OF THREE FIRST SKELETAL CARBONS'//
     1       2X,'. CARBON No 0 at ( ',E16.9,',',2X,E16.9,',',2X,E16.9,') '//2X,
     2       '. ANGLE BETW. x-AXIS AND PROJECTION OF BOND No 1 ON PLANE xy  ',
     3       'alpha = ',E16.9,'  DEG'//2X,'. ANGLE BETW. z-AXIS AND BOND No 1  '
```

```
     4       ,'beta = ',E16.9,'  DEG'//2X,'. DIHEDRAL ANGLE BETWEEN PLANES ',
     5       '(bond1, z-axis) AND (bond1, bond2)  gamma = ',E16.9,'  DEG'/)
      IF(IDF.NE.0) WRITE(20,105) X(1),Y(1),Z(1),ALPHA,BETA,GAMMA
  105 FORMAT(3E16.9/3E16.9)
C
C
C  Potential parameter initializations
C
C  Enter the left boundary and the width of the reduced radius interval
C  over which the Lennard-Jones potential will be approximated by a
C  quintic spline.
  116 READ(5,130) RR1,DELRR
  130 FORMAT(2F13.10)
C
C  Read option parameter for printing the potential parameters initialized
C  in POTINIT.
      READ(5,110)  IPRPOT
C
C  ISHRINK is a flag determining how the Lennard-Jones epsilons and sigmas
C  are to be initialized within the subroutine.
C  . If ISHRINK=0, Lennard-Jones sigmas and epsilons, and the rotational
C                  potential, are given their true values
C  . If ISHRINK=1, Lennard-Jones sigmas are scaled, using the scaling parameter
C                  SHRINKRAD, Lennard-Jones epsilons are scaled, using the
C                  scaling parameter SHRINKPOT, and rotational potentials
C                  are scaled, using the scaling parameter SHRINKROT.
      READ(5,110)  ISHRINK
      IF(ISHRINK.EQ.0) GO TO 140
      READ(5,150)  SHRINKRAD,SHRINKPOT,SHRINKROT
  150 FORMAT(3E15.8)
C
C  Option input for printing coordinates in output file
C       IWRCD=1 : Coordinates printed
C       IWRCD=0 : Coordinates not printed
  140 READ(5,110)  IWRCD
C
C  Option input for creating detailed printout of inrteractions
C       IDETAIL=1 : Detailed table of interaction energies created
C       IDETAIL=0 : Table of interaction energies not created
      READ(5,110)  IDETAIL
C
C  Option input for prointing the probabilities of the various rotational
C  isomeric states according to the Flory and the Metropolis scheme for
C  each bond.
      READ(5,110)  IWRPR
C
C  Convert valence bond angles and angles alpha, beta, gamma to radians
      DEGRAD=ASIN(1.)/90.
      THETAP=THETAP*DEGRAD
      THETAHP=THETAHP*DEGRAD
      THETAPP=THETAPP*DEGRAD
      THETAHPP=THETAHPP*DEGRAD
      THETARPP=THETARPP*DEGRAD
      IF(IEULER.NE.1) GO TO 117
      ALPHA=ALPHA*DEGRAD
      BETA=BETA*DEGRAD
      GAMMA=GAMMA*DEGRAD
C
C  Invoke initializations in potential calculating routines
  117 CALL POTINIT(ISHRINK,SHRINKRAD,SHRINKPOT,SHRINKROT,IPRPOT)
```

```
C
C  Check whether conditions for screening algorithm are fulfilled.
      RANGEXM=0.0
      RANGEYM=0.0
      RANGEZM=0.0
      DO 225 J=1,3
          DO 225 I=1,3
              IF(RANGEX(I,J).GT.RANGEXM) RANGEXM=RANGEX(I,J)
              IF(RANGEY(I,J).GT.RANGEYM) RANGEYM=RANGEY(I,J)
              IF(RANGEZ(I,J).GT.RANGEZM) RANGEZM=RANGEZ(I,J)
  225 CONTINUE
      IF(2.*RANGEXM.GT.AXX) GO TO 235
      IF(2.*RANGEYM.GT.AYY) GO TO 235
      IF(2.*RANGEZM.GT.AZZ) GO TO 235
      GO TO 230
  235 WRITE(6,245)
  245 FORMAT(//2X,'INTERATOMIC INTERACTION RANGE TOO LONG'/2X,'IN COMPARISON',
     1 ' WITH SIZE OF CONTINUATION VECTORS'//2X,'NECESSARY CRITERIA FOR ',
     2 'VALIDITY OF SCREENING ALGORITHM NOT FULFILLED'/)
      GO TO 600
C
C
  230 DO 700 ICHAIN=1,NCHAINS
C
C  TACTICITY CALCULATIONS
C  ----------------------
C    Array TACTIC keeps track of dyad tacticity. TACTIC(I)=0 or 1 if
C  dyad I is meso- or racemo- , respectively.
C    Index ICHIR(I) designates the absolute configuration of the chiral
C  skeletal carbon atom (6I-4).
C  A value of ICHIR = +1 indicates that the chiral center is D- in a
C  Fischer projection constructed so that the beginning of the chain
C  (atom C0) lies upwards.
C  A value of ICHIR = -1 indicates an L- configuration, based on the
C  same convention.
C
C    Generate absolute configuration of atom C1.
C
  160     WMGEN=0.0
          ICHIR(1)=1
          SEED10=SEED1
          IF(RANDS1(SEED1).LE.0.50) ICHIR(1)=-1
C
C    Generate dyad configurations using Bernoullian statistics with
C  specified tacticity.
C
          DO 145 I=2,NUNITS
              ICHIR(I)=ICHIR(I-1)
              ITAC=0
              IF(RANDS1(SEED1).LE.WM) GO TO 145
              ICHIR(I)=-ICHIR(I)
              ITAC=1
  145         TACTIC(I-1)=ITAC
          DO 155 I=1,NDYADS
  155         WMGEN=WMGEN+FLOAT(TACTIC(I))
          WMGEN=1.-WMGEN/FLOAT(NDYADS)
C
C  Compare the fraction of meso-dyads WMGEN in the randomly generated
C  configuration with the prespecified fraction, WM. If the fractional
C  deviation of WMGEN from WM is greater than TOLR, then discard
```

```
C  the chain and proceed to a new generation
          IF(ABS(WMGEN/WM-1.).LE.TOLR) GO TO 170
          GO TO 160
C
  170     WRITE(6,180) ICHAIN,SEED10,SEED2
  180     FORMAT(///2X,'CHAIN GENERATION No ',I6/2X,26('=')
     1           //2X,'SEEDS USED FOR R.N.G. :'/2X,'SEED1(tacticity) : ',I11,8X
     2           ,'SEED2(conformation) : ',I11)
C
          WRITE(6,190) (DYADNM(TACTIC(I)),I=1,NDYADS)
  190     FORMAT(///2X,'DYAD TACTICITY SEQUENCE'//(2X,70A1))
          WRITE(6,200) (CHIRNM(ICHIR(I)),I=1,NUNITS)
  200     FORMAT(//'SKELETAL CARBON CHIRALITY SEQUENCE'//3X,'* ',17(A1,' * ')/
     1           (5X,17(A1,' * ')))
C
C  Random generation of Eulerian angles, using SEED1.
          IF(IEULER.EQ.1) GO TO 104
          ALPHA=RANDS1(SEED1)*360.-180.
          BETA=RANDS1(SEED1)*180.
          GAMMA=RANDS1(SEED1)*360.-180.
          WRITE(6,120) X(1),Y(1),Z(1),ALPHA,BETA,GAMMA
          IF(IDF.NE.0) WRITE(20,105) X(1),Y(1),Z(1),ALPHA,BETA,GAMMA
          ALPHA=ALPHA*DEGRAD
          BETA=BETA*DEGRAD
          GAMMA=GAMMA*DEGRAD
  104     IF(IDF.NE.0) WRITE(20,220) (ICHIR(I),I=1,NUNITS)
  220     FORMAT(4012)
C
C  Form left-weight matrix products for all dyads.
C  -----------------------------------------------
C  UPRODL(*,K) contains the product U0.U2(1).U2(2).U2(3)...U2(K)
C
C  First dyad- initialization
  106 CALL VECMAT(U0, UP, VEC, 5, 5, N, N)
      CALL VECMAT(VEC, DIAG, VEC, 5, 5, N, N)
      IF(TACTIC(1).NE.0) GO TO 49
      CALL VECMAT(VEC,UMPP,VEC,5,5,N,N)
      GO TO 51
   49 CALL VECMAT(VEC,URPP,VEC,5,5,N,N)
   51 DO 52 I=1,N
   52     UPRODL(I,1)=VEC(I)
C  Calculation of products
      DO 53 K=2,NUNITS-2
          IF(TACTIC(K).NE.0) GO TO 54
          CALL VECMAT(VEC,UM2,VEC,5,5,N,N)
          GO TO 56
   54     CALL VECMAT(VEC,UR2,VEC,5,5,N,N)
C  Periodic normalization
   56     KRAT=K/NNORM
          IF(K-KRAT*NNORM.NE.0) GO TO 57
          CALL RENML(VEC,5,N,DUMMY)
   57     DO 58 I=1,N
   58         UPRODL(I,K)=VEC(I)
   53 CONTINUE
C
C  Form right weight matrix products for all dyads.
C  ------------------------------------------------
C  UPRODL(*,K) contains the product U2(K).U2(K+1)...U2(X-1).UX
C
C  Last dyad - initialization
```

```
      CALL MATVEC (DIAG, UX, VEC, 5, 5, N, N)
      IF(TACTIC(NUNITS-1).NE.0) GO TO 59
      CALL MATVEC(UM2,VEC,VEC,5,5,N,N)
      GO TO 61
   59 CALL MATVEC(UR2,VEC,VEC,5,5,N,N)
   61 DO 62 I=1,N
   62     UPRODR(I,NUNITS-1)=VEC(I)
C  Calculation of products
      DO 63 K1=2,NUNITS-2
          K=NUNITS-K1
          IF(TACTIC(K).NE.0) GO TO 64
          CALL MATVEC(UM2,VEC,VEC,5,5,N,N)
          GO TO 65
   64     CALL MATVEC(UR2,VEC,VEC,5,5,N,N)
C  Periodic normalization
   65     KRAT=K1/NNORM
          IF(K1-KRAT*NNORM.NE.0) GO TO 66
          CALL RENML(VEC,5,N,DUMMY)
   66     DO 67 I=1,N
   67         UPRODR(I,K)=VEC(I)
   63 CONTINUE
C
C  Initialize Coordinate Calculation (Initialize local position vectors
C  and transfer matrices; compute those atom coordinates which do not
C  depend on bond rotation angles).
C  Convert bond rotation angles to radians
C
          CALL CRDINIT(NDF)
C
C  Build the rest of the chain in a bond-by-bond fashion
          CALL METROP(SEED2,ETOTLJ,ETOTLR,ETOTSR,ETOTROT,ETOT,IDETAIL)
C
          IF(IDF.NE.0) WRITE(20,460)  (PHI(I),I=1,NBONDS-2)
  460     FORMAT(5E16.9)
C
          WRITE(6,470)  (RISNM(CONFORM(III)),III=2,NBONDS-1)
  470     FORMAT(///2X,'GENERATED SEQUENCE OF BOND ROTATIONAL ISOMERIC STATES'
     1           //2X,'* ',34A2/(2X,35A2))
C
          WRITE(6,480) NDF1,(PHI(I),I=1,NDF)
  480     FORMAT(////2X,'SEQUENCE OF ROTATION ANGLES OF BONDS 2 THROUGH ',I5,
     1           ' (DEGREES) '/2X,62('-')/(/2X,5(F10.5,6X)))
C
          IF(IWRCD.NE.0) CALL PRCD
C
          WRITE(6,490) ETOTSR,ETOTLR,ETOTLJ,ETOTROT,ETOT
  490     FORMAT(///2X,'SHORT RANGE INTERATOMIC INTERACTION ENERGY : ',4X,E16.9
     1    ,' KCAL/MOLE'//2X,'LONG RANGE INTERATOMIC INTERACTION ENERGY : ',5X,
     2    E16.9,' KCAL/MOLE'//2X,'TOTAL ENERGY DUE TO INTERATOMIC INTERACTIONS'
     3    ,' :    ',E16.9,' KCAL/MOLE'//2X,'TOTAL ENERGY DUE TO BOND ROTATIONAL'
     2    ,' BARRIERS :    ',E16.9,' KCAL/MOLE'//2X,'TOTAL ENERGY (SUM OF BOTH '
     3    ,'CONTRIBUTIONS) :   ',5X,E16.9,' KCAL/MOLE')
C
  700 CONTINUE
C
  600 CONTINUE
C
      CALL GETTIME
C
      END
```

```
      subroutine gettime
      integer*2 exep, i
      integer*1 argument(20), dqdecodetime, dummy
      character  dateandtime*16
         argument(1)=0
         argument(2)=0
         argument(3)=0
         argument(4)=0
         dummy=dqdecodetime (argument,exep)
         write (dateandtime,1) (argument(i),i=5,20)
         write (6,2) (dateandtime(i:i), i=1,8), (dateandtime(i:i),i=9,16)
    1 format (20a1)
    2 format (//'system date: ',8a1,',  system time: ',8a1//)
      return
      end



      subroutine deletefile(filename,namelength)
      integer*1 namelength, dqdelete, dummy, argument(81)
      integer*2 excep
      character*80 filename
      argument(1)=namelength
      do 1 i=1,namelength
    1     argument(i+1)=ichar(filename(i:i))
      dummy=dqdelete(argument, excep)
      return
      end



      SUBROUTINE METROP(SEED2,ETOTLJ,ETOTLR,ETOTSR,ETOTROT,ETOT,IDETAIL)
C
C  Quasi-Metropolis Monte Carlo algorithm for choosing a succession of
C  bond rotation angles so as to avoid excessive short- and long range
C  interactions.
C
      INTEGER*1 LAMDA(3000), MU(3000), NU(3000), ICHIR(500), KIND(3000),
     1          MODUL(3000), CONNECT(0:5,0:5), CONFORM(1000), TACTIC(500),
     2          LNEW(3,5), MNEW(3,5), NNEW(3,5)
      INTEGER*2 IC(0:1000), ISEG(3000)
      INTEGER*4 SEED2
      REAL L, LH, LR
      CHARACTER NAME(3)*4, RISNM(5)*2
      DIMENSION X(3000), Y(3000), Z(3000), PHI(1000), PHIO(5),
     1          AX(3), AY(3), AZ(3), AXCY(3), AYCZ(3), AZCX(3), ORIGIN(3),
     2          VC(3), VH1D(3), VH1L(3), VH2(3), VH3(3), VRD(3), VRL(3),
     3          TO(3,3), TP(3,3), TPP(3,3), TPROD(3,3), VECT(3),
     4          XNEW(3,5), YNEW(3,5), ZNEW(3,5), PHINEW(5), DENRGY(5),
     5          WEIGHT(5), DENLR(5), DENSR(5), DENROT(5), TTEMP(3,3),
     6          ALFA(3), EFFNE(3), VDWR(3), EPS(3,3), SIGMA(3,3),
     7          EPSIG(3,3), RANGE(3,3), RANGEX(3,3), RANGEY(3,3), RANGEZ(3,3),
     8          UP(5,5), UMPP(5,5), URPP(5,5), DIAG(5,5), UO(5), UX(5),
     9          UM2(5,5), UR2(5,5), Q(5)  ,PROB(5)
```

```
      COMMON UP, UMPP, URPP, DIAG, UO, UX, UM2, UR2, Q
      COMMON /BLOCK1/ X, Y, Z
      COMMON /BLOCK2/ ICHIR, LAMDA, MU, NU, KIND, IC, ISEG, MODUL, CONNECT
      COMMON /BLOCK3/ NUNITS, NBONDS, NSEGMENTS, NATOMS, THETAP, THETAHP,
     1                THETAPP, THETAHPP, THETARPP, STHP, CSTHP, STHPP,
     2                CSTHPP, L, LH, LR, VC, VH1D, VH1L, VH2, VH3, VRD,
     3                VRL, TO, TP, TPP, TPROD
      COMMON /BLOCK4/ ALPHA, BETA, GAMMA, AX, AY, AZ, AXX, AYY, AZZ,
     1                AXCY, AYCZ, AZCX, ORIGIN, VOLUME
      COMMON /BLOCK5/ ALFA, EFFNE, VDWR, EPS, SIGMA, EPSIG, RANGE, RANGEX,
     1                RANGEY, RANGEZ, NAME, NNUC, RR1, RR2, DELRR, AU, BU,
     2                CU, AF, BF, CF, ROTBAR
      COMMON /BLOCK6/ J1, J2CM, LAMJ1, MUJ1, NUJ1, X1, Y1, Z1
      COMMON /BLOCK7/ N, N1, TEMP, PHIO, RISNM, CONFORM, TACTIC, PHI, IWRPR
C
      RKCAL=1.987E-03
      N1=N-1
      DEGRAD=ATAN(1.)/45.
      ETOTLR=0.0
      ETOTSR=0.0
      ETOTROT=0.0
      DO 230 JRIS=1,N
  230     DENROT(JRIS)=ROTBAR/2.*(1.-COS(3.*DEGRAD*PHIO(JRIS)))
C
      DO 240 I=2,NBONDS-1
C
C  Compute all the rotation angles (Flory's sign convention) which the bond
C  may assume under the N possible rotational isomeric states.
          IF(MOD(I,2)) 250,260,250
  250     IMULT=-ICHIR((I+1)/2)
          GO TO 270
  260     IMULT=ICHIR(I/2)
  270     DO 280 JRIS=1,N
  280         PHINEW(JRIS)=IMULT*DEGRAD*PHIO(JRIS)
C
C  Compute all possible position vectors and continuation factors of the
C  substituents 3I and 3I+1, and of carbon 3I+2, under the various rotational
C  states of bond I.
          IREF=IC(I-1)
          XREF=X(IREF)
          YREF=Y(IREF)
          ZREF=Z(IREF)
          J2CM=-2
          IF(I.GE.4) J2CM=IC(I-4)
          DO 290 JRIS=1,N
              DO 290 IATOM=1,3
                  LNEW(IATOM,JRIS)=LAMDA(IREF)
                  MNEW(IATOM,JRIS)=MU(IREF)
                  NNEW(IATOM,JRIS)=NU(IREF)
  290     CONTINUE
C
          IF(MOD(I,2)) 300,310,300
  300     ICH=ICHIR((I+1)/2)
          DO 320 JRIS=1,N
              ANGLE=PHINEW(JRIS)
              SPH=SIN(ANGLE)
              CSPH=COS(ANGLE)
              TPP(2,1)=STHPP*CSPH
              TPP(2,2)=-CSTHPP*CSPH
              TPP(2,3)=SPH
```

```
                TPP(3,1)=STHPP*SPH
                TPP(3,2)=-CSTHPP*SPH
                TPP(3,3)=-CSPH
                CALL MATMAT(TPROD,TPP,TTEMP,3,3,3,3,3,3)
                IF(ICH) 330,340,340
  330           CALL MATVEC(TTEMP,VH1L,VECT,3,3,3,3)
                GO TO 350
  340           CALL MATVEC(TTEMP,VH1D,VECT,3,3,3,3)
  350           XNEW(1,JRIS)=XREF+VECT(1)
                YNEW(1,JRIS)=YREF+VECT(2)
                ZNEW(1,JRIS)=ZREF+VECT(3)
                IF(ICH) 360,370,370
  360           CALL MATVEC(TTEMP,VRL,VECT,3,3,3,3)
                GO TO 380
  370           CALL MATVEC(TTEMP,VRD,VECT,3,3,3,3)
  380           XNEW(2,JRIS)=XREF+VECT(1)
                YNEW(2,JRIS)=YREF+VECT(2)
                ZNEW(2,JRIS)=ZREF+VECT(3)
                CALL MATVEC(TTEMP,VC,VECT,3,3,3,3)
                XNEW(3,JRIS)=XREF+VECT(1)
                YNEW(3,JRIS)=YREF+VECT(2)
                ZNEW(3,JRIS)=ZREF+VECT(3)
  320       CONTINUE
            GO TO 400
C
  310       DO 390 JRIS=1,N
                ANGLE=PHINEW(JRIS)
                SPH=SIN(ANGLE)
                CSPH=COS(ANGLE)
                TP(2,1)=STHP*CSPH
                TP(2,2)=-CSTHP*CSPH
                TP(2,3)=SPH
                TP(3,1)=STHP*SPH
                TP(3,2)=-CSTHP*SPH
                TP(3,3)=-CSPH
                CALL MATMAT(TPROD,TP,TTEMP,3,3,3,3,3,3)
                CALL MATVEC(TTEMP,VH2,VECT,3,3,3,3)
                XNEW(1,JRIS)=XREF+VECT(1)
                YNEW(1,JRIS)=YREF+VECT(2)
                ZNEW(1,JRIS)=ZREF+VECT(3)
                CALL MATVEC(TTEMP,VH3,VECT,3,3,3,3)
                XNEW(2,JRIS)=XREF+VECT(1)
                YNEW(2,JRIS)=YREF+VECT(2)
                ZNEW(2,JRIS)=ZREF+VECT(3)
                CALL MATVEC(TTEMP,VC,VECT,3,3,3,3)
                XNEW(3,JRIS)=XREF+VECT(1)
                YNEW(3,JRIS)=YREF+VECT(2)
                ZNEW(3,JRIS)=ZREF+VECT(3)
  390       CONTINUE
C
C  Fold if necessary, imposing periodic continuation.
  400       DO 560 JRIS=1,N
                DO 560 IATOM=1,3
                    VECT(1)=XNEW(IATOM,JRIS)-ORIGIN(1)
                    VECT(2)=YNEW(IATOM,JRIS)-ORIGIN(2)
                    VECT(3)=ZNEW(IATOM,JRIS)-ORIGIN(3)
                    CALL VECVEC(VECT,AYCZ,XCRIT,3,3)
                    IF(XCRIT.LE.VOLUME) GO TO 510
                    LNEW(IATOM,JRIS)=LNEW(IATOM,JRIS)-1
                    XNEW(IATOM,JRIS)=XNEW(IATOM,JRIS)-AX(1)
```

```
                YNEW(IATOM,JRIS)=YNEW(IATOM,JRIS)-AX(2)
                ZNEW(IATOM,JRIS)=ZNEW(IATOM,JRIS)-AX(3)
                GO TO 520
  510           IF(XCRIT.GE.0.0) GO TO 520
                LNEW(IATOM,JRIS)=LNEW(IATOM,JRIS)+1
                XNEW(IATOM,JRIS)=XNEW(IATOM,JRIS)+AX(1)
                YNEW(IATOM,JRIS)=YNEW(IATOM,JRIS)+AX(2)
                ZNEW(IATOM,JRIS)=ZNEW(IATOM,JRIS)+AX(3)
C
  520           VECT(1)=XNEW(IATOM,JRIS)-ORIGIN(1)
                VECT(2)=YNEW(IATOM,JRIS)-ORIGIN(2)
                VECT(3)=ZNEW(IATOM,JRIS)-ORIGIN(3)
                CALL VECVEC(VECT,AZCX,YCRIT,3,3)
                IF(YCRIT.LE.VOLUME) GO TO 530
                MNEW(IATOM,JRIS)=MNEW(IATOM,JRIS)-1
                XNEW(IATOM,JRIS)=XNEW(IATOM,JRIS)-AY(1)
                YNEW(IATOM,JRIS)=YNEW(IATOM,JRIS)-AY(2)
                ZNEW(IATOM,JRIS)=ZNEW(IATOM,JRIS)-AY(3)
                GO TO 540
  530           IF(YCRIT.GE.0.0) GO TO 540
                MNEW(IATOM,JRIS)=MNEW(IATOM,JRIS)+1
                XNEW(IATOM,JRIS)=XNEW(IATOM,JRIS)+AY(1)
                YNEW(IATOM,JRIS)=YNEW(IATOM,JRIS)+AY(2)
                ZNEW(IATOM,JRIS)=ZNEW(IATOM,JRIS)+AY(3)
C
  540           VECT(1)=XNEW(IATOM,JRIS)-ORIGIN(1)
                VECT(2)=YNEW(IATOM,JRIS)-ORIGIN(2)
                VECT(3)=ZNEW(IATOM,JRIS)-ORIGIN(3)
                CALL VECVEC(VECT,AXCY,ZCRIT,3,3)
                IF(ZCRIT.LE.VOLUME) GO TO 550
                NNEW(IATOM,JRIS)=NNEW(IATOM,JRIS)-1
                XNEW(IATOM,JRIS)=XNEW(IATOM,JRIS)-AZ(1)
                YNEW(IATOM,JRIS)=YNEW(IATOM,JRIS)-AZ(2)
                ZNEW(IATOM,JRIS)=ZNEW(IATOM,JRIS)-AZ(3)
                GO TO 560
  550           IF(ZCRIT.GE.0.0) GO TO 560
                NNEW(IATOM,JRIS)=NNEW(IATOM,JRIS)+1
                XNEW(IATOM,JRIS)=XNEW(IATOM,JRIS)+AZ(1)
                YNEW(IATOM,JRIS)=YNEW(IATOM,JRIS)+AZ(2)
                ZNEW(IATOM,JRIS)=ZNEW(IATOM,JRIS)+AZ(3)
C
  560     CONTINUE
C
C  For each of the N possible rotational isomeric states of bond I compute
C  the increment in long range interaction energy caused by the addition of
C  atoms 3I, 3I+1 and 3I+2. Store these increments in array DENRGY.
          DO 500 JRIS=1,N
              DENLR(JRIS)=0.0
              DENSR(JRIS)=0.0
              DENRGY(JRIS)=0.0
C
              DO 505 IATOM=1,3
                  J1=IREF+IATOM
                  LAMJ1=LNEW(IATOM,JRIS)
                  MUJ1=MNEW(IATOM,JRIS)
                  NUJ1=NNEW(IATOM,JRIS)
                  X1=XNEW(IATOM,JRIS)
                  Y1=YNEW(IATOM,JRIS)
                  Z1=ZNEW(IATOM,JRIS)
                  CALL ENRGY(IDETAIL,ELR,ESR)
```

```
                IF (I.GE.4)  DENLR(JRIS)=DENLR(JRIS)+ELR
                DENSR(JRIS)=DENSR(JRIS)+ESR
                DENRGY(JRIS)=DENRGY(JRIS)+ELR
  505       CONTINUE
C
  500   CONTINUE
C
C  Skip Metropolis weight calculation for I<4.
        IF(I.GE.4) GO TO 570
        DO 580 JRIS=1,N
  580       WEIGHT(JRIS)=1.0
        GO TO 590
C
C  Form differences from the lowest energy increment
  570   DENMIN=DENRGY(1)
        DO 410 JRIS=2,N
            IF(DENRGY(JRIS).LT.DENMIN)  DENMIN=DENRGY(JRIS)
  410   CONTINUE
        DO 415 JRIS=1,N
  415       DENRGY(JRIS)=DENRGY(JRIS)-DENMIN
C
C  Form Boltzmann factors corresponding to the increments DENRGY(JRIS) and
C  store in array WEIGHT. These are the quasi-Metropolis probabilities
C  for bond I being in the various rotational isomeric states. Note that
C  the quasi-Metropolis scheme is purely Markovian, i.e. it does not take into
C  account what happens along the chain past the examined bond. This scheme,
C  however, is sensitive to long-range interactions.
        SUM=0.0
        DO 420 JRIS=1,N
  420       WEIGHT(JRIS)=0.0
        DO 425 JRIS=1,N
            ARGM=-DENRGY(JRIS)/RKCAL/TEMP
            IF(ARGM.LE.-50.) GO TO 425
            WEIGHT(JRIS)=EXP(ARGM)
  425   CONTINUE
C
C  Form probabilities of bond I being in the various rotational isomeric states
C  according to Flory's theory.
  590   CALL FLORY(I,NUNITS,NRISOLD)
C
C  Form the combined long- and short range probabilities for each of the
C  N rotational isomeric states of bond I, by multiplying Flory and Metropolis
C  probabilities, and normalizing.
        S=0.
        DO 575 JRIS=1,N
            PROB(JRIS)=Q(JRIS)*WEIGHT(JRIS)
  575       S=S+PROB(JRIS)
        IF(S.LT.1.0E-20) GO TO 586
        DO 585 JRIS=1,N
  585       PROB(JRIS)=PROB(JRIS)/S
        GO TO 587
C
C  If all probability products are equal to zero, proceed by pure Metropolis
C  scheme.
  586   S=0.
        DO 588 JRIS=1,N
  588       S=S+WEIGHT(JRIS)
        DO 589 JRIS=1,N
  589       PROB(JRIS)=WEIGHT(JRIS)/S
C
```

```
C  Choose rotational isomeric state of bond I by random number generation,
C  based on the combined probabilities.
  587     R1=RANDS1(SEED2)
          S=0.
          DO 430 NRIS=1,N
              S=S+PROB(NRIS)
              IF(S.GT.R1) GO TO 450
  430     CONTINUE
          NRIS=N
C
  450     IF(IWRPR.EQ.1) WRITE(6,455) I,RISNM(NRIS),(RISNM(JRIS),Q(JRIS),
     1                   WEIGHT(JRIS),PROB(JRIS),JRIS=1,N)
  455     FORMAT(//2X,'BOND :',I5,3X,'SELECTED STATE : ',A2/2X,33('-')//
     1          1X,'STATES',5X,'FLORY PROBABILITIES',3X,'METROPOLIS WEIGHTS',
     2          3X,'COMBINED PROBABILITIES'//(3X,A2,9X,E16.9,5X,E16.9,5X,
     3          E16.9))
          NRISOLD=NRIS
          CONFORM(I)=NRIS
          ANGLE=PHINEW(NRIS)
          PHI(I-1)=ANGLE/DEGRAD
          DO 470 IATOM=1,3
              J1=IREF+IATOM
              X(J1)=XNEW(IATOM,NRIS)
              Y(J1)=YNEW(IATOM,NRIS)
              Z(J1)=ZNEW(IATOM,NRIS)
              LAMDA(J1)=LNEW(IATOM,NRIS)
              MU(J1)=MNEW(IATOM,NRIS)
              NU(J1)=NNEW(IATOM,NRIS)
  470     CONTINUE
C
C  Update transfer matrix product
          IF(MOD(I,2)) 480,490,480
  480     SPH=SIN(ANGLE)
          CSPH=COS(ANGLE)
          TPP(2,1)=STHPP*CSPH
          TPP(2,2)=-CSTHPP*CSPH
          TPP(2,3)=SPH
          TPP(3,1)=STHPP*SPH
          TPP(3,2)=-CSTHPP*SPH
          TPP(3,3)=-CSPH
          CALL MATMAT(TPROD,TPP,TPROD,3,3,3,3,3,3)
          GO TO 600
C
  490     SPH=SIN(ANGLE)
          CSPH=COS(ANGLE)
          TP(2,1)=STHP*CSPH
          TP(2,2)=-CSTHP*CSPH
          TP(2,3)=SPH
          TP(3,1)=STHP*SPH
          TP(3,2)=-CSTHP*SPH
          TP(3,3)=-CSPH
          CALL MATMAT(TPROD,TP,TPROD,3,3,3,3,3,3)
C
  600     ETOTLR=ETOTLR+DENLR(NRIS)
          ETOTSR=ETOTSR+DENSR(NRIS)
          ETOTROT=ETOTROT+DENROT(NRIS)
C
  240 CONTINUE
C
      ETOTLJ=ETOTLR+ETOTSR
```

```
      ETOT=ETOTLJ+ETOTROT
C
      RETURN
C
      END



      SUBROUTINE FLORY(IBOND,X,NRISOLD)
C
C  In the course of chain generation, this subroutine forms the probabilities,
C  according to Flory's theory of the configurational statistical mechanics
C  of unperturbed chains, of bond I being in each of the N possible rotational
C  isomeric states, given that the previous bond was in a state NRISOLD.
C    Note that Flory's theory correctly incorporates the non-Markovian
C  character of configurational statistics, but takes into account only
C  long-range, and not short-range interactions.
C
      INTEGER*1 CONFORM(1000), TACTIC(500)
      INTEGER X
      CHARACTER RISNM(5)*2
      DIMENSION UM2(5,5), UR2(5,5), UO(5), UX(5), U(5,5), UP(5,5), UMPP(5,5),
     1          URPP(5,5), DIAG(5,5), Q(5), VEC(5), UPRODL(5,500),
     2          UPRODR(5,500), PHIO(5), PHI(1000), ROW(5), COL(5)
C
      COMMON UP,UMPP,URPP,DIAG,UO,UX,UM2,UR2,Q
      COMMON /BLOCK7/ N, N1, TEMP, PHIO, RISNM, CONFORM, TACTIC, PHI, IWRPR
      COMMON /BLOCK8/ UPRODL, UPRODR
C
      IF(IBOND.EQ.2) GO TO 10
      GO TO 20
C
C  Computation for bond 2
C  ----------------------
C  Compute vector of a' priori conformational probabilities for bond 2.
C  A' priori probability for bond 2 being in rotational isomeric state
C  j is stored in element Q(j)
C
C  Nominator calculation
   10 DO 31 I=1,N
   31     COL(I)=UPRODR(I,2)
      DO 26 J=1,N
          DO 27 I1=1,N
              DO 27 J1=1,N
   27             U(I1,J1)=0.0
          DO 28 I=1,N
   28         U(I,J)=UP(I,J)
          CALL VECMAT(UO, U, VEC, 5, 5, N, N)
          CALL VECMAT(VEC, DIAG, VEC, 5, 5, N, N)
          IF(TACTIC(1).NE.0) GO TO 29
          CALL VECMAT(VEC, UMPP, VEC, 5, 5, N, N)
          GO TO 30
   29     CALL VECMAT(VEC, URPP, VEC, 5, 5, N, N)
   30     CALL VECVEC(VEC, COL, PNOMINATOR, 5, N)
   26 Q(J)=PNOMINATOR
C
C  Calculate partition function Z, subject to the same normalizations as
C  those used in nominator calculations.
      CALL VECMAT(UO, UP, VEC, 5, 5, N, N)
```

```
      CALL VECMAT(VEC, DIAG, VEC, 5, 5, N, N)
      IF(TACTIC(1).NE.0) GO TO 32
      CALL VECMAT(VEC, UMPP, VEC, 5, 5, N, N)
      GO TO 33
   32 CALL VECMAT(VEC, URPP, VEC, 5, 5, N, N)
   33 CALL VECVEC(VEC, COL, Z, 5, N)
      DO 34 I=1,N
   34    Q(I)=Q(I)/Z
      GO TO 100
C
C  Subsequent bonds
C  ----------------
C  Even- and Odd- numbered bonds examined separately
C  Find number of dyad k of which considered bond is a part
C
   20 KDYAD=IBOND/2
      IF(KDYAD.EQ.1) GO TO 47
      DO 41 II=1,N
   41    ROW(II)=UPRODL(II,KDYAD-1)
   47 IF(KDYAD.EQ.X-1) GO TO 110
      DO 54 II=1,N
   54    COL(II)=UPRODR(II,KDYAD+1)
  110 IF(IBOND-2*KDYAD) 40, 80, 40
C
C
C  Case of odd- numbered bonds
C  ...........................
C  Bonds 3 and 2X-1 to be treated separately
C
   40 IF(IBOND.EQ.3)  GO TO 37
      IF(IBOND.EQ.2*X-1) GO TO 38
C
C  Computation of appropriate row of a' priori conformational
C  probability matrix P for the bond pair (IBOND-1, IBOND).
C  In element Q(J) is stored the probability that bond (IBOND-1)
C  will be found in state NRISOLD and bond IBOND in state J.
C  (NRISOLD,J = 1,2,3,...,N).
C
C  Compute partition function Z.
      IF(TACTIC(KDYAD).NE.0) GO TO 45
      CALL VECMAT(ROW, UM2, VEC, 5, 5, N, N)
      GO TO 46
   45 CALL VECMAT(ROW, UR2, VEC, 5, 5, N, N)
   46 CALL VECVEC(VEC, COL, Z, 5, N)
C  Compute nominators of P-matrix elements
      DO 42 J=1,N
         DO 39 I1=1,N
            DO 39 J1=1,N
   39          U(I1,J1)=0.0
         IF(TACTIC(KDYAD).NE.0) GO TO 43
         U(NRISOLD,J) = UMPP(NRISOLD,J)
         GO TO 44
   43    U(NRISOLD,J) = URPP(NRISOLD,J)
   44    CALL VECMAT(ROW, UP, VEC, 5, 5, N, N)
         CALL VECMAT(VEC, U, VEC, 5, 5, N, N)
         CALL VECVEC(VEC, COL, PNOMINATOR, 5, N)
C  Compute P-matrix elements
         Q(J)=PNOMINATOR/Z
   42 CONTINUE
      GO TO 90
```

```
C
C  P-Computation for bond 3
C                      ......
C  Computation of Z
   37 CALL VECMAT(UO, UP, VEC, 5, 5, N, N)
      CALL VECMAT(VEC, DIAG, VEC, 5, 5, N, N)
      IF(TACTIC(KDYAD).NE.0) GO TO 52
      CALL VECMAT(VEC, UMPP, VEC, 5, 5, N, N)
      GO TO 53
   52 CALL VECMAT(VEC, URPP, VEC, 5, 5, N, N)
   53 CALL VECVEC(VEC, COL, Z, 5, N)
C  Computation of nominators of P-matrix elements
      DO 48 J=1,N
          DO 49 I1=1,N
              DO 49 J1=1,N
   49             U(I1, J1)=0.0
          IF(TACTIC(KDYAD).NE.0) GO TO 50
          U(NRISOLD,J)=UMPP(NRISOLD,J)
          GO TO 51
   50     U(NRISOLD,J)=URPP(NRISOLD,J)
   51     CALL VECMAT(UO, UP, VEC, 5, 5, N, N)
          CALL VECMAT(VEC, DIAG, VEC, 5, 5, N, N)
          CALL VECMAT(VEC, U, VEC, 5, 5, N, N)
          CALL VECVEC(VEC, COL, PNOMINATOR, 5, N)
C  Computation of P- matrix elements
          Q(J)=PNOMINATOR/Z
   48 CONTINUE
      GO TO 90
C
C  P-Computation for bond 2X-1
C                          ....
C  Computation of Z
   38 IF(TACTIC(KDYAD).NE.0) GO TO 58
      CALL VECMAT(ROW, UM2, VEC, 5, 5, N, N)
      GO TO 59
   58 CALL VECMAT(ROW, UR2, VEC, 5, 5, N, N)
   59 CALL VECMAT(VEC, DIAG, VEC, 5, 5, N, N)
      CALL VECVEC(VEC, UX, Z, 5, N)
C  Computation of nominators of P- matrix elements
      DO 60 J=1,N
          CALL VECMAT(ROW, UP, VEC, 5, 5, N, N)
          DO 355 I1=1,N
              DO 355 J1=1,N
  355             U(I1,J1)=0.0
          IF(TACTIC(KDYAD).NE.0) GO TO 56
          U(NRISOLD,J)=UMPP(NRISOLD,J)
          GO TO 57
   56     U(NRISOLD,J)=URPP(NRISOLD,J)
   57     CALL VECMAT(VEC, U, VEC, 5, 5, N, N)
          CALL VECMAT(VEC, DIAG, VEC, 5, 5, N, N)
          CALL VECVEC(VEC, UX, PNOMINATOR, 5, N)
C  Computation of P- matrix elements
          Q(J)=PNOMINATOR/Z
   60 CONTINUE
C
C  Compute a' priori probability for bond (IBOND-1) being in state NRISOLD
C  by summing row NRISOLD of the P- matrix.
C
   90 PROB=0.0
      DO 61 J=1,N
```

```
   61      PROB=PROB+Q(J)
C
C  Form appropriate row of conditional probability matrix Q for bond I,
C  given bond (I-1), from a' priori probabilities for bond pair
C  (IBOND-1, IBOND) and bond (IBOND-1).
C
      DO 62 J=1,N
         Q(J)=Q(J)/PROB
   62 CONTINUE
C
      GO TO 100
C
C
C  Case of even- numbered bonds
C  ............................
C
C  Bond 2X-2 treated separately
C
   80 IF(IBOND.EQ.2*X-2) GO TO 72
C
C  Computation of appropriate row of a' priori conformational probability
C  matrix P for the  bond pair (IBOND-1, IBOND). In element Q(J) is stored
C  the probability that bond (IBOND-1) will be found in state I,
C  and bond IBOND in state J.    (NRISOLD,J=1,2,...,N)
C
C  Compute partition function Z
      CALL VECMAT(ROW, UP, VEC, 5, 5, N, N)
      IF(TACTIC(KDYAD).NE.0) GO TO 74
      CALL VECMAT(ROW, UM2, VEC, 5, 5, N, N)
      GO TO 75
   74 CALL VECMAT(ROW, UR2, VEC, 5, 5, N, N)
   75 CALL VECVEC(VEC, COL, Z, 5, N)
C  Computation of nominators of P- matrix elements
      DO 76 J=1,N
         DO 77 I1=1,N
            DO 77 J1=1,N
   77          U(I1,J1)=0.0
         U(NRISOLD,J)=UP(NRISOLD,J)
         CALL VECMAT(ROW, U, VEC, 5, 5, N, N)
         IF(TACTIC(KDYAD).NE.0) GO TO 78
         CALL VECMAT(VEC, UMPP, VEC, 5, 5, N, N)
         GO TO 79
   78    CALL VECMAT(VEC, URPP, VEC, 5, 5, N, N)
   79    CALL VECVEC(VEC, COL, PNOMINATOR, 5, N)
C  Computation of P- matrix elements
         Q(J)=PNOMINATOR/Z
   76 CONTINUE
      GO TO 95
C
C  P- computations for bond 2X-2
C                          ....
C  Computation of partition function, Z
   72 CALL VECMAT(ROW,UP,VEC,5,5,N,N)
      IF(TACTIC(KDYAD).NE.0) GO TO 574
      CALL VECMAT(ROW,UM2,VEC,5,5,N,N)
      GO TO 575
  574 CALL VECMAT(ROW,UR2,VEC,5,5,N,N)
  575 CALL VECMAT(VEC,DIAG,VEC,5,5,N,N)
      CALL VECVEC(VEC,UX,Z,5,N)
C  Computation of nominators of P- matrix elements
```

```
      DO 82 J=1,N
          DO 278 I1=1,N
              DO 278 J1=1,N
  278             U(I1,J1)=0.0
          U(NRISOLD,J)=UP(NRISOLD,J)
          CALL VECMAT(ROW, U, VEC, 5, 5, N, N)
          IF(TACTIC(KDYAD).NE.0) GO TO 279
          CALL VECMAT(VEC, UMPP, VEC, 5, 5, N, N)
          GO TO 81
  279     CALL VECMAT(VEC, URPP, VEC, 5, 5, N, N)
   81     CALL VECVEC(VEC, UX, PNOMINATOR, 5, N)
C  Computation of elements of P- matrix
          Q(J)=PNOMINATOR/Z
   82 CONTINUE
C
C  Compute a' priori probability for bond (IBOND-1) being in state NRISOLD by
C  summing row NRISOLD of the P- matrix.
C
   95 PROB=0.0
      DO 83 J=1,N
   83     PROB=PROB+Q(J)
C
C  Form appropriate row of conditional probability matrix for bond IBOND,i
C  given bond (IBOND-1), from a' priori probabilities for bond pair
C  (IBOND-1, IBOND) and bond (IBOND-1).
C
      DO 84 J=1,N
          Q(J)=Q(J)/PROB
   84 CONTINUE
C
  100 RETURN
      END



      SUBROUTINE ENRGY(IDETAIL, ELR, ESR)
C
C    Subroutine computes the increase in long range interaction energy of
C  a box of bulk amorphous polymer, brought about by the addition of a new
C  segment.
C    The gradients of the total energy with respect to the chain internal
C  degrees of freedom are also computed.
C    A chain model with rigid bond lengths and valence bond angles is used,
C  so that the only internal degrees of freedom of the chain are the
C  NDF=NBONDS-2 rotational angles of bonds 2,3,...,NBONDS-1.
C    Potential energy terms which do not change with conformation in the
C  rigid bond length and bond angle model employed here are not accounted for
C  in the energy computation. Thus, only interactions between atoms separated
C  by more than two bonds from each other are included in the energy and
C  derivative summations.
C    The parent chain has NBONDS=NDF+2 bonds, numbered from 1 to NDF+2, and
C  NATOMS=NDF+3 atoms, numbered from 0 to NDF+2.
C    The degree of polymerization is X=NDF/2+1.
C
      INTEGER*1 LAMDA(3000), MU(3000), NU(3000), KIND(3000), MODUL(3000),
     1          CONNECT(0:5,0:5), ICHIR(500)
      INTEGER*2 IC(0:1000), ISEG(3000)
      REAL L,LH,LR
      CHARACTER*4 NAME(3)
```

```
      DIMENSION X(3000), Y(3000), Z(3000), VC(3), VH1D(3), VH1L(3), VH2(3),
     1          VH3(3), VRD(3), VRL(3), R12(3), FORCE(3), TO(3,3), TP(3,3),
     2          TPP(3,3), TPROD(3,3), AX(3), AY(3), AZ(3), AXCY(3), AYCZ(3),
     3          AZCX(3),ORIGIN(3), ALFA(3), EFFNE(3), VDWR(3), EPS(3,3),
     4          SIGMA(3,3),RANGE(3,3), RANGEX(3,3), RANGEY(3,3), RANGEZ(3,3),
     5          VECT(3), EPSIG(3,3)
      COMMON /BLOCK1/ X, Y, Z
      COMMON /BLOCK2/ ICHIR, LAMDA, MU, NU, KIND, IC, ISEG, MODUL, CONNECT
      COMMON /BLOCK3/ NUNITS, NBONDS, NSEGMENTS, NATOMS, THETAP, THETAHP,
     1                THETAPP, THETAHPP, THETARPP, STHP, CSTHP, STHPP,
     2                CSTHPP, L, LH, LR, VC, VH1D, VH1L, VH2, VH3, VRD,
     3                VRL, TO, TP, TPP, TPROD
      COMMON /BLOCK4/ ALPHA, BETA, GAMMA, AX, AY, AZ, AXX, AYY, AZZ,
     1                AXCY, AYCZ, AZCX, ORIGIN, VOLUME
      COMMON /BLOCK5/ ALFA, EFFNE, VDWR, EPS, SIGMA, EPSIG, RANGE, RANGEX,
     1                RANGEY, RANGEZ, NAME, NNUC, RR1, RR2, DELRR, AU, BU,
     2                CU, AF, BF, CF, ROTBAR
      COMMON /BLOCK6/ J1, J2CM, LAMJ1, MUJ1, NUJ1, X1, Y1, Z1
C
      ELR=0.0
      ESR=0.0
      MODJ1=MODUL(J1)
      NUC1=KIND(J1)
C
C  Internal loop over all atoms up to now.
      DO 30 J2=1,J1-2
C
C  Skip interaction with carbon atom J2CM.
         IF(J2.EQ.J2CM) GO TO 30
C
C  Test if connectivity screening is necessary
         IF(J1-J2.GT.6) GO TO 40
C
C  Reject interaction if atoms J1 and J2 are less than three bonds apart,
C  using the connectivity table, CONNECT
         IF(CONNECT(MODJ1,MODUL(J2))) 40,30,40
C
C  Screening, to determine if the interaction between J1 and J2 should be
C  accounted for and, if yes, which image of J2 should be used
C
   40    NUC2=KIND(J2)
         RNG=RANGE(NUC1,NUC2)
         RNGX=RANGEX(NUC1,NUC2)
         RNGY=RANGEY(NUC1,NUC2)
         RNGZ=RANGEZ(NUC1,NUC2)
         DX=X1-X(J2)
         DY=Y1-Y(J2)
         DZ=Z1-Z(J2)
         ADX=ABS(DX)
         ADY=ABS(DY)
         ADZ=ABS(DZ)
C
         IF(ADX.GE.RNGX) GO TO 50
         LIMG=0
            IF(ADY.GE.RNGY) GO TO 60
            MIMG=0
               IF(ADZ.GE.RNGZ) GO TO 70
               NIMG=0
               GO TO 80
   70             IF(ADZ.LT.AZZ-RNGZ)          GO TO 30
```

```
                    NIMG=1
                        IF(DZ.LT.0.0) NIMG=-NIMG
                        GO TO 80
 60             IF(ADY.LT.AYY-RNGY)              GO TO 30
                    IF(ADZ.GE.RNGZ) GO TO 90
                    NIMG=0
                    MIMG=1
                        IF(DY.LT.0.0) MIMG=-MIMG
                        GO TO 80
 90                     IF(ADZ.LT.AZZ-RNGZ)              GO TO 30
                        MIMG=1
                            IF(DY.LT.0.0) MIMG=-MIMG
                            NIMG=1
                                IF(DZ.LT.0.0) NIMG=-NIMG
                                GO TO 80
 50         IF(ADX.LT.AXX-RNGX)              GO TO 30
                IF(ADY.GE.RNGY) GO TO 100
                MIMG=0
                    IF(ADZ.GE.RNGZ) GO TO 110
                    NIMG=0
                    LIMG=1
                        IF(DX.LT.0.0) LIMG=-LIMG
                        GO TO 80
 110                    IF(ADZ.LT.AZZ-RNGZ)              GO TO 30
                        LIMG=1
                            IF(DX.LT.0.0) LIMG=-LIMG
                            NIMG=1
                                IF(DZ.LT.0.0) NIMG=-NIMG
                                GO TO 80
 100                IF(ADY.LT.AYY-RNGY)              GO TO 30
                    IF(ADZ.GE.RNGZ) GO TO 120
                    NIMG=0
                    LIMG=1
                        IF(DX.LT.0.0) LIMG=-LIMG
                        MIMG=1
                            IF(DY.LT.0.0) MIMG=-MIMG
                            GO TO 80
 120                        IF(ADZ.LT.AZZ-RNGZ)              GO TO 30
                            LIMG=1
                                IF(DX.LT.0.0) LIMG=-LIMG
                                MIMG=1
                                    IF(DY.LT.0.0) MIMG=-MIMG
                                    NIMG=1
                                        IF(DZ.LT.0.0) NIMG=-NIMG
C
  80    R12(1)=DX-LIMG*AX(1)-MIMG*AY(1)-NIMG*AZ(1)
        R12(2)=DY-LIMG*AX(2)-MIMG*AY(2)-NIMG*AZ(2)
        R12(3)=DZ-LIMG*AX(3)-MIMG*AY(3)-NIMG*AZ(3)
        R=SQRT(R12(1)**2+R12(2)**2+R12(3)**2)
C
        IF(R.GE.RNG) GO TO 30
C
C  Calculate interaction energy and magnitude of interaction force
C  Find reduced radius RR=R/SIGMA
        RR=R/SIGMA(NUC1,NUC2)
C
C  Branch, according to relative magnitude of RR, RR1 (from screening, RR<RR2)
        IF(RR.GT.RR1) GO TO 130
C
C  Normal 6-12 potential expression used
```

```
          X6=(1./RR)**6
          X12=X6*X6
          EPSILON=EPS(NUC1,NUC2)
          ULJ=4.*EPSILON*(X12-X6)
          GO TO 140
C
C  Quintic spline used
  130     XI=(RR-RR1)/DELRR
          XI2=XI*XI
          XI1=1.-XI
          XI12=XI1*XI1
          ULJ=EPS(NUC1,NUC2)*XI12*XI1*(AU*XI2+BU*XI+CU)
C
C
C  Update energy
C  -------------
  140     IF(J2.EQ.J2CM.OR.J2.GT.J2CM+2) GO TO 150
          ELR=ELR+ULJ
          GO TO 160
  150     ESR=ESR+ULJ
  160     IF(IDETAIL.EQ.1) WRITE(6,121) J1,J2,NUC1,NUC2,R,ULJ
  121     FORMAT(2X,'J1=',I5,3X,'J2=',I5,3X,'NUC1=',I1,3X,'NUC2=',I1,3X,'R=',
     1            E16.9,3X,'ULJ=',E16.9)
C
   30 CONTINUE
C
      RETURN
C
      END



      SUBROUTINE VECMAT(V, A, VA, NFORM, LFORM, N, L)
C
C  Vector-matrix multiplication, VT.A=VAT
C
      DIMENSION V(NFORM), A(NFORM,LFORM), VA(LFORM), VAUX(25)
      DO 1 J=1,L
        X=0.0
        DO 2 K=1,N
    2   X=X+V(K)*A(K,J)
    1 VAUX(J)=X
      DO 3 J=1,L
    3 VA(J)=VAUX(J)
      RETURN
      END



      SUBROUTINE RENML(V, NFORM, N, ELMAX)
C
C  Normalization of a vector by division with its maximum element,
C  to avoid overflow during vector- matrix multiplications
C
      DIMENSION V(NFORM)
      ELMAX=0.
      DO 1 I=1,N
      IF(ABS(V(I)).GT.ELMAX) ELMAX=ABS(V(I))
```

```
    1 CONTINUE
      DO 2 I=1,N
    2 V(I)=V(I)/ELMAX
      RETURN
      END



      SUBROUTINE RISDATA(N, T, PHIO, RISNM)
      DIMENSION PHIO(5), UP(5,5), UMPP(5,5), URPP(5,5), DIAG(5,5),
     1          UO(5), UX(5), UM2(5,5), UR2(5,5), Q(5)
      CHARACTER RISNM(5)*2
      COMMON UP, UMPP, URPP, DIAG, UO, UX, UM2, UR2, Q
C
C  Subroutine contains all information relevant to the Rotational Isomeric
C  State Model used to describe vinyl polymer conformations.
C
C  Enter the number of Rotational Isomeric States and the values of
C  rotation angles.
C
C  Numbering convention for states in PP:
C
C  (1)=t, (2)=t*, (3)=g*, (4)=g, (5)=g-
C
      N=5
      RISNM(1)='t '
      RISNM(2)='t*'
      RISNM(3)='g*'
      RISNM(4)='g '
      RISNM(5)='g-'
      PHIO(1)=15.
      PHIO(2)=50.
      PHIO(3)=70.
      PHIO(4)=105.
      PHIO(5)=-115.
C
C  Calculate RIS weights and form weight matrices
C
      R=1.987
      ETA=1.0*EXP(-60./R/T)
      TAU=0.4*EXP(-500./R/T)
      OMEGASTAR=0.9*EXP(-1600./R/T)
      DO 7 I=1,N
      DO 7 J=1,N
        UP(I,J)=1.0
        UMPP(I,J)=0.0
    7 URPP(I,J)=0.0
      UP(3,3)=0.0
      UP(3,4)=0.0
      UP(4,3)=0.0
      UP(4,4)=0.0
      UP(5,5)=0.0
      UMPP(1,2)=ETA*OMEGASTAR
      UMPP(1,4)=ETA
      UMPP(2,1)=UMPP(1,2)
      UMPP(2,5)=TAU*OMEGASTAR
      UMPP(3,4)=OMEGASTAR
      UMPP(3,5)=TAU*OMEGASTAR
      UMPP(4,1)=UMPP(1,4)
```

```
      UMPP(4,3)=UMPP(3,4)
      UMPP(5,2)=UMPP(2,5)
      UMPP(5,3)=UMPP(3,5)
      URPP(1,1)=ETA*ETA
      URPP(1,3)=ETA*OMEGASTAR
      URPP(2,4)=OMEGASTAR
      URPP(2,5)=TAU*OMEGASTAR
      URPP(3,1)=URPP(1,3)
      URPP(3,5)=TAU*OMEGASTAR
      URPP(4,2)=OMEGASTAR
      URPP(4,4)=1.
      URPP(5,2)=URPP(2,5)
      URPP(5,3)=URPP(3,5)
C
C  Formation of diagonal matrix diag(1,1,1,eta,1)
C
      DO 13 I=1,N
      DO 13 J=1,N
   13 DIAG(I,J)=0.0
      DO 14 I=1,N
   14 DIAG(I,I)=1.
      DIAG(4,4)=ETA
      RETURN
      END



      REAL FUNCTION RANDS1 (SEED)
C
C  UNIFORM PSEUDO-RANDOM NUMBER GENERATOR; MIXED CONGRUENTIAL TYPE;
C  THE FUNCTION VALUE IS A REAL NUMBER FROM THE INTERVAL (0,1),
C  INCLUDING 0, EXCLUDING 1.
C
C  FOLLOWING D.E.KNUTH, "THE ART OF COMPUTER PROGRAMMING", VOL.2, 1969, P.155,
C                       ADDISON, READING(MASS.).
C  UWS 1982
C
C  SEED IS A 4-BYTE INTEGER
C
      INTEGER*4 SEED
      SEED=SEED*1592653589 + 453816691
      IF (SEED.LT.0) SEED=SEED + 1 + 2147483647
      RANDS1=SEED*4.65661287308E-10
      RETURN
      END



      SUBROUTINE POTINIT(ISHRINK,SHRINKRAD,SHRINKPOT,SHRINKROT,IPRINT)
C
C  Initialization of interatomic and rotational potential parameters
C
C  For  interatomic interaction, a modified Lennard-Jones potential is used:
C
C       - For R <= R1            use 6-12 LJ potential
C
C       - For R >= R2            no interaction (potential=0.0)
C
```

```
C        -  For R1 < R < R2          use quintic spline, designed so that the
C                                    potential function and its first and second
C                                    derivatives are continuous at R1=RR1*SIGMA
C                                    and zero at R2=R1+DELRR*SIGMA
C
C  Numbering convention for atomic species :
C      (1) : H    ,    (2) : C    ,    (3) : Methyl
C
C  For skeletal bond torsion, a symmetric threefold potential expression is
C  used, with rotational barrier equal to 2.8 kcal/mole.
C
      INTEGER*1 LAMDA(3000), MU(3000), NU(3000), ICHIR(500), KIND(3000),
     1          MODUL(3000), CONNECT(0:5,0:5)
      INTEGER*2 IC(0:1000), ISEG(3000)
      CHARACTER*4 NAME(3)
      DIMENSION AX(3), AY(3), AZ(3), AXCY(3), AYCZ(3), AZCX(3), ORIGIN(3),
     1          ALFA(3), EFFNE(3), VDWR(3), EPS(3,3), SIGMA(3,3), RANGE(3,3),
     2          RANGEX(3,3), RANGEY(3,3), RANGEZ(3,3), EPSIG(3,3)
      COMMON /BLOCK2/ ICHIR, LAMDA, MU, NU, KIND, IC, ISEG, MODUL, CONNECT
      COMMON /BLOCK4/ ALPHA, BETA, GAMMA, AX, AY, AZ, AXX, AYY, AZZ,
     1                AXCY, AYCZ, AZCX, ORIGIN, VOLUME
      COMMON /BLOCK5/ ALFA, EFFNE, VDWR, EPS, SIGMA, EPSIG, RANGE, RANGEX,
     1                RANGEY, RANGEZ, NAME, NNUC, RR1, RR2, DELRR, AU, BU,
     2                CU, AF, BF, CF, ROTBAR
C
C  Define number of chemical species used
      NNUC=3
C
C  Define names of species
      NAME(1)='H   '
      NAME(2)='C   '
      NAME(3)='CH3 '
C
C  Enter polarizabilities (A**3)
      ALFA(1)=0.42
      ALFA(2)=0.93
      ALFA(3)=1.77
C
C  Enter effective numbers of electrons
      EFFNE(1)=0.9
      EFFNE(2)=5.0
      EFFNE(3)=7.0
C
C  Enter Van der Waals radii
      VDWR(1)=1.3
      VDWR(2)=1.8
      VDWR(3)=2.0
C
C  Calculate Lennard-Jones Epsilons and Sigmas
      DO 30 I=1,NNUC
         DO 30 J=1,NNUC
C  Obtain coefficient Cij of r-6 attractive term from Slater-Kirkwood
C  formula
            CIJ=365.*ALFA(I)*ALFA(J)/(SQRT(ALFA(I)/EFFNE(I))+
     1           SQRT(ALFA(J)/EFFNE(J)))
C  Obtain coefficient AIJ from condition of potential minimum at
C      VDWR(I)+VDWR(J)
            AIJ=0.5*CIJ*(VDWR(I)+VDWR(J))**6
C  Obtain Lennard-Jones Epsilon(kcal/mol) and Sigma(A) for current pair
            EPS(I,J)=CIJ*CIJ/4./AIJ
```

```
            SIGMA(I,J)=(AIJ/CIJ)**(1./6)
   30 CONTINUE
C
C  If desired, scale Lennard-Jones sigmas by the factor SHRINKRAD
C  and Lennard-Jones epsilons by the factor SHRINKPOT.
      IF(ISHRINK.EQ.0) GO TO 35
      DO 25 J=1,3
          DO 25 I=1,3
              SIGMA(I,J)=SIGMA(I,J)*SHRINKRAD
   25         EPS(I,J)=EPS(I,J)*SHRINKPOT
C
   35 DO 40 J=1,3
          DO 40 I=1,3
   40         EPSIG(I,J)=EPS(I,J)/SIGMA(I,J)
C
C  Determine coefficients for quintic spline and derivative.
C  FR,DFR,DDFR symbolize the reduced LJ potential function and
C  its first and second derivatives, FR=ULJ/EPS, DFR=DULJ/(EPS/SIGMA),
C  DDFR=DDULJ/(EPS/SIGMA**2).
C  RR symbolizes the reduced distance RR=R/SIGMA
C
      RR2=RR1+DELRR
      X6=(1./RR1)**6
      X12=X6*X6
      FR=4.*(X12-X6)
      COEF=24./RR1
      DFR=-COEF*(2.*X12-X6)
      DDFR=COEF/RR1*(26.*X12-7.*X6)
      DELRR2=DELRR/2.
      AU=6.*FR+3.*DELRR*DFR+DELRR2*DELRR*DDFR
      BU=3.*FR+DELRR*DFR
      CU=FR
      AF=-5.*(6./DELRR*FR+3.*DFR+DELRR2*DDFR)
      BF=2.*(DFR+DELRR2*DDFR)
      CF=DFR
C
C  Form the matrices RANGE, RANGEX, RANGEY, RANGEZ of the  range of interatomic
C  interactions.
C  . RANGE(i,j) is simply the Lennard-Jones SIGMA corresponding to the atom
C    pair (i,j), multiplied by the reduced radial distance at which the
C    modified interatomic potential used in the energy calculations goes to 0
C  . RANGEX, RANGEY, RANGEZ are effective ranges, used in the screening
C    procedure to determine significant interactions between images of atoms
C    in the cube
       DO 60 I=1,NNUC
           DO 60 J=1,NNUC
   60          RANGE(I,J)=RR2*SIGMA(I,J)
      DO 65 I=1,NNUC
           DO 65 J=1,NNUC
               RANGEX(I,J)=RANGE(I,J)+ABS(AY(1))+ABS(AZ(1))
               RANGEY(I,J)=RANGE(I,J)+ABS(AZ(2))+ABS(AX(2))
               RANGEZ(I,J)=RANGE(I,J)+ABS(AX(3))+ABS(AY(3))
   65 CONTINUE
C
C  Form the projections AXX, AYY, AZZ of the continuation vectors AX, AY, AZ
C  on the x, y, z axes, respectively.
      AXX=AX(1)
      AYY=AY(2)
      AZZ=AZ(3)
C
```

```
C  Enter connectivity table (indices correspond to atom index in X,Y,Z, taken
C  modulo6)
      DO 160 I=0,5
         CONNECT(I,2)=0
  160    CONNECT(I,5)=0
      DO 170 I=3,5
         CONNECT(I,0)=1
  170    CONNECT(I,1)=1
      DO 180 I=0,2
         CONNECT(I,3)=1
  180    CONNECT(I,4)=1
      CONNECT(0,0)=1
      CONNECT(1,0)=0
      CONNECT(2,0)=0
      CONNECT(0,1)=1
      CONNECT(1,1)=1
      CONNECT(2,1)=0
      CONNECT(3,3)=1
      CONNECT(4,3)=0
      CONNECT(5,3)=0
      CONNECT(3,4)=1
      CONNECT(4,4)=1
      CONNECT(5,4)=0
C
C  Initialize the value of the rotational potential barrier ROTBAR
      ROTBAR=2.8
C
C  Shrink, if desired, the rotational barrier by a factor SHRINKROT
      IF(ISHRINK.NE.0) ROTBAR=ROTBAR*SHRINKROT
C
C  Optional printout
      IF(IPRINT.EQ.0) RETURN
      WRITE(6,70)
   70 FORMAT(///2X,'6-12 POTENTIAL PARAMETERS'//2X,'NUC.TYPE  VDW-R  ',
     1       'ALFA  EFF.NO. OF EL.'/)
      WRITE(6,80) (I, VDWR(I), ALFA(I), EFFNE(I), NAME(I), I=1,NNUC)
   80 FORMAT(8(4X,I2,5X,F5.2,2X,F5.2,5X,F5.2,8X,A/))
      WRITE(6,90) (I,I=1,NNUC)
   90 FORMAT(/2X,'EPSILON VALUES (KCAL/MOL) '/18X,8(I1,17X))
      DO 100 I=1,NNUC
  100    WRITE(6,110) I, (EPS(I,J), J=1,NNUC)
  110 FORMAT(I3,3X,8(4X,E15.8))
      WRITE(6,120) (I,I=1,NNUC)
  120 FORMAT(/2X,'SIGMA VALUES (ANGSTROMS) '/18X,8(I1,17X))
      DO 130 i=1,NNUC
  130 WRITE(6,110) I,(SIGMA(I,J), J=1,NNUC)
      WRITE(6,140) RR1,FR,RR2
  140 FORMAT(//2X,'6-12 POTENTIAL USED UP TO R/SIGMA = ',F10.6,5X,' WHERE ',
     1       ' ULJ/EPS = ',F9.6//2X,'ZERO POTENTIAL FROM R/SIGMA = ',F10.6//
     2      2X,'AND QUINTIC SPLINE WITH CONTINUOUS FIRST AND SECOND ',
     3       'DERIVATIVES IN BETWEEN')
      WRITE(6,150) ROTBAR
  150 FORMAT(///2X,'THREEFOLD ROTATIONAL POTENTIAL USED TO DESCRIBE ',
     1'SKELETAL BOND TORSION'//2X,'ROTATIONAL BARRIER ',E15.8,' KCAL/MOLE')
      IF(ISHRINK.NE.0) WRITE(6,135) SHRINKRAD,SHRINKPOT,SHRINKROT
  135 FORMAT(//2X,'IN THIS CALCULATION SIGMAS HAVE BEEN SHRUNK TO ',E15.8/
     1        4X,'EPSILONS TO ',E15.8,'  AND ROTBAR TO ',E15.8,
     2        /19X,' OF THEIR TRUE VALUE ')
      RETURN
      END
```

```
      SUBROUTINE MATVEC(A, V, AV, MFORM, NFORM, M, N)
C
C  Matrix- vector multiplication, A.V=AV
C
      DIMENSION A(MFORM,NFORM), V(NFORM), AV(MFORM), VAUX(25)
      DO 1 I=1,M
        X=0.0
        DO 2 K=1,N
    2   X=X+A(I,K)*V(K)
    1 VAUX(I)=X
      DO 3 I=1,M
    3 AV(I)=VAUX(I)
      RETURN
      END



      SUBROUTINE MATMAT(A,B,AB,MFORM,NFORM,LFORM,M,N,L)
C
C  Matrix multiplication A.B=AB
C
      DIMENSION A(MFORM,NFORM), B(NFORM,LFORM), AB(MFORM,LFORM), AUX(25,25)
      DO 1 I=1,M
      DO 1 J=1,L
        X=0.0
        DO 2 K=1,N
    2   X=X+A(I,K)*B(K,J)
    1 AUX(I,J)=X
      DO 3 I=1,M
      DO 3 J=1,L
    3 AB(I,J)=AUX(I,J)
      RETURN
      END



      SUBROUTINE VCROSSV(V1,V2,V3)
C
C  Formation of the external(cross) product of two vectors, V3=V1xV2
C  Subroutine is designed so that the product can be written in one of
C  the factors (V1 or V2 can be used in place of V3)
C
      DIMENSION V1(3), V2(3), V3(3)
C
      VAUX1=V1(2)*V2(3)-V2(2)*V1(3)
      VAUX2=V1(3)*V2(1)-V2(3)*V1(1)
      VAUX3=V1(1)*V2(2)-V2(1)*V1(2)
C
      V3(1)=VAUX1
      V3(2)=VAUX2
      V3(3)=VAUX3
C
      RETURN
      END
```

```
      SUBROUTINE VECVEC(V1, V2, PRODUCT, NFORM, N)
C
C  Vector multiplication, V1T.V2=PRODUCT
C
      DIMENSION V1(NFORM), V2(NFORM)
      PRODUCT=0.0
      DO 1 I=1,N
    1 PRODUCT=PRODUCT+V1(I)*V2(I)
      RETURN
      END



      SUBROUTINE CRDINIT(NDF)
C
C    Subroutine forms initializes coordinate calculations for a vinyl chain
C
C                  CH3-(CHR-CH2)nunits-H
C
C  of given tacticity, in a periodic box, given the position of the
C  first carbon of the chain, and the orientation of the first two skeletal
C  bonds
C
C    The chain has NBONDS=NDF+2 bonds, numbered from 1 to NDF+2
C    The chain has NSEGMENTS=NDF+3 skeletal segments, numbered from 0 to NDF+2
C    (Flory's convention).
C    Overall the chain has NATOMS=3NDF+5 atoms (or atomic groups), of which :
C               2  are terminal methyls
C         NDF/2+1  are chiral carbons
C           NDF/2  are achiral carbons
C        3NDF/2+1  are hydrogens
C         NDF/2+1  are R-substituents
C
C  NOTE ON BOOKKEEPING
C    The x-,y-,and z- coordinates of all atoms, regardless of type, are stored
C  in three unidimensional arrays X,Y,Z. The exact nature and position of an
C  atom in the parent chain can be inferred from its index in these arrays.
C    Specifically, the correspondence between indices and atoms is the
C  following:
C    Index = 1                                : terminal methyl at chain start
C            6i-4, i=1,2,...,NUNITS           : chiral skeletal carbon of unit (i)
C            6i-3, i=1,2,...,NUNITS           : hydrogen attached to chiral skeletal
C                                               carbon of unit (i) (either D- or L-)
C            6i-2, i=1,2,...,NUNITS           : substituent R attached to chiral
C                                               carbom of unit (i) (either D- or L-)
C            6i-1, i=1,2,...,NUNITS-1         : achiral skeletal atom of unit (i)
C            6i  , i=1,2,...,NUNITS-1         : D- hydrogen attached to achiral
C                                               skeletal carbon of unit (i)
C            6i+1, i=1,2,...,NUNITS-1         : L- hydrogen attached to achiral
C                                               skeletal carbon of unit (i)
C            6NUNITS-1                        : terminal methyl at chain end
C
C   . The chemical nature of an atom of index i is kept in array element
C     KIND(i)  (Code: 1=H, 2=C, 3=Methyl)
C   . In array element MODUL(i) is kept the remainder of the division of
```

```
C     the index i by 6, which is of use in connectivity screening.
C  .  In array element IC(iseg) is kept the index of the carbon atom
C     belonging to skeletal segment number iseg+1 (Flory's convention used
C     in numbering segments)
C  .  In array element ISEG(i) is kept the number of the segment (according
C     to Flory's convention, segments numbered from 0 to NDF+2), to which
C     atom i belongs.
C  .  Index ICHIR(i) designates the absolute configuration of the chiral
C     skeletal carbon atom (6i-4). A value of ICHIR=+1 indicates that the
C     chiral center is D- in a Fischer projection constructed so that the
C     beginning of the chain (atom 1) lies upwards. A value of ICHIR=-1
C     indicates an L- configuration, based on the same convention.
C  .  LAMDA(i), MU(i), NU(i) are integer multipliers, such that the vectors
C     LAMDA(i)*AX, MU(i)*AY, NU(i)*AZ, when added to the position vector
C     of atom i of the parent chain, give the position vector of an image
C     of i lying in the cube.
C
      INTEGER*1 LAMDA(3000), MU(3000), NU(3000), ICHIR(500), KIND(3000),
     1          MODUL(3000), CONNECT(0:5,0:5)
      INTEGER*2 IC(0:1000), ISEG(3000)
      REAL L, LH, LR
      DIMENSION X(3000), Y(3000), Z(3000), AX(3), AY(3), AZ(3),
     1          AXCY(3), AYCZ(3), AZCX(3), ORIGIN(3), VC(3), VH1D(3), VH1L(3),
     2          VH2(3), VH3(3), VRD(3), VRL(3), TO(3,3), TP(3,3), TPP(3,3),
     3          TPROD(3,3), VECT(3)
      COMMON /BLOCK1/ X, Y, Z
      COMMON /BLOCK2/ ICHIR, LAMDA, MU, NU, KIND, IC, ISEG, MODUL, CONNECT
      COMMON /BLOCK3/ NUNITS, NBONDS, NSEGMENTS, NATOMS, THETAP, THETAHP,
     1                THETAPP, THETAHPP, THETARPP, STHP, CSTHP, STHPP, CSTHPP,
     2                L, LH, LR, VC, VH1D, VH1L, VH2, VH3, VRD, VRL, TO, TP,
     3                TPP, TPROD
      COMMON /BLOCK4/ ALPHA, BETA, GAMMA, AX, AY, AZ, AXX, AYY, AZZ, AXCY,
     1                AYCZ, AZCX, ORIGIN, VOLUME
C
C  Initialize all coordinates to zero, except those of chain start
      DO 30 J=2,NATOMS
          X(J)=0.0
          Y(J)=0.0
          Z(J)=0.0
   30 CONTINUE
C
C  Setup parallel arrays KIND, IC and MODUL, keeping track of the chemical
C  nature and connectivity of the parent chain.
      ICARBON=-1
      DO 35 I=0,NDF
          ICARBON=ICARBON+3
          IC(I)=ICARBON
   35 CONTINUE
      IC(NDF+1)=NATOMS
C
      KIND(1)=3
C     (the follcwing are pseudo-definitions, used for convenience in updating)
      ISEG(1)=1
      MODUL(1)=1
      I=1
      ISEGM=0
C
   40 I=I+1
      ISEGM=ISEGM+1
      KIND(I)=2
```

```
      ISEG(I)=ISEGM
      MODUL(I)=2
C
      I=I+1
      KIND(I)=1
      ISEG(I)=ISEGM
      MODUL(I)=3
C
      I=I+1
      KIND(I)=3
      ISEG(I)=ISEGM
      MODUL(I)=4
C
      I=I+1
      IF(I.EQ.NATOMS) GO TO 50
      ISEGM=ISEGM+1
      KIND(I)=2
      ISEG(I)=ISEGM
      MODUL(I)=5
C
      I=I+1
      KIND(I)=1
      ISEG(I)=ISEGM
      MODUL(I)=0
C
      I=I+1
      KIND(I)=1
      ISEG(I)=ISEGM
      MODUL(I)=1
      GO TO 40
C
   50 KIND(NATOMS)=3
C     (the following is a pseudo-definition, used for convenience in updating)
      ISEG(NATOMS)=NDF+1
      MODUL(NATOMS)=5
C
C  Initialize coordinate transformation matrices
      STHP=SIN(THETAP)
      CSTHP=COS(THETAP)
      STHPP=SIN(THETAPP)
      CSTHPP=COS(THETAPP)
      TP(1,1)=CSTHP
      TP(1,2)=STHP
      TP(1,3)=0.0
C  Matrix TPP initially contains T- matrix corresponding to bond 1 (PHI1=0)
      TPP(1,1)=CSTHPP
      TPP(1,2)=STHPP
      TPP(1,3)=0.0
      TPP(2,1)=STHPP
      TPP(2,2)=-CSTHPP
      TPP(2,3)=0.0
      TPP(3,1)=0.0
      TPP(3,2)=0.0
      TPP(3,3)=-1.0
C
C  TO = Transformation matrix from local coordinate system of bond 1
C       to fixed coordinate system (x,y,z).
C
      TO(1,1)=COS(ALPHA)*SIN(BETA)
      TO(1,2)=-COS(ALPHA)*COS(BETA)*COS(GAMMA)-SIN(ALPHA)*SIN(GAMMA)
```

```
      TO(1,3)=-COS(ALPHA)*COS(BETA)*SIN(GAMMA)+SIN(ALPHA)*COS(GAMMA)
      TO(2,1)=SIN(ALPHA)*SIN(BETA)
      TO(2,2)=-SIN(ALPHA)*COS(BETA)*COS(GAMMA)+COS(ALPHA)*SIN(GAMMA)
      TO(2,3)=-SIN(ALPHA)*COS(BETA)*SIN(GAMMA)-COS(ALPHA)*COS(GAMMA)
      TO(3,1)=COS(BETA)
      TO(3,2)=SIN(BETA)*COS(GAMMA)
      TO(3,3)=SIN(BETA)*SIN(GAMMA)
C
C  Setup position vectors of skeletal carbons and substituents
C  with  respect to local coordinate systems of chain bonds.
C
C  VC = coordinate vector of skeletal carbon of segment i with
C       respect to coordinate system of bond i:
C
      VC(1)=L
      VC(2)=0.
      VC(3)=0.
C
C  VH1D = coordinate vector of hydrogen H1, connected to chiral
C         carbon atom of segment 2i-1 with respect to coordinate system of bond
C         (2i), for the case ICHIR(i)=+1 (D- configuration of carbon 2i-1)
C
      VH1D(1)=-LH*COS(THETAHPP)
      VH1D(2)=LH*COS(THETAHPP)/TAN(THETAPP/2.)
      VH1D(3)=LH*SQRT(1.-(COS(THETAHPP))**2/(SIN(THETAPP/2.))**2)
C
C  VRD = coordinate vector of substituent R, connected to the chiral
C        carbon atom of segment 2i-1 with respect to coordinate system of bond
C        (2i), for the case ICHIR(i)=+1
C        (D- configuration of carbon 2i-1)
C
      VRD(1)=-LR*COS(THETARPP)
      VRD(2)=LR*COS(THETARPP)/TAN(THETAPP/2.)
      VRD(3)=-LR*SQRT(1.-(COS(THETARPP))**2/(SIN(THETAPP/2.))**2)
C
C  Form respective coordinate vectors for L- configuration of segment
C  2i-1
C
      DO 60 I=1,3
        VH1L(I)=VH1D(I)
   60 VRL(I)=VRD(I)
      VH1L(3)=-VH1L(3)
      VRL(3)=-VRL(3)
C
C  VH2=coordinate vector of hydrogen H2, connected to achiral carbon
C      atom of segment 2i in the D- position, with respect to coordinate system
C      of bond (2i+1)
C
      VH2(1)=-LH*COS(THETAHP)
      VH2(2)=LH*COS(THETAHP)/TAN(THETAP/2.)
      VH2(3)=-LH*SQRT(1.-(COS(THETAHP))**2/(SIN(THETAP/2))**2)
C
C  VH3=coordinate vector of hydrogen H3, connected to achiral carbon
C      atom of segment 2i in the L- position, with respect to coordinate system
C      of bond (2i+1).
C
      VH3(1)=VH2(1)
      VH3(2)=VH2(2)
      VH3(3)=-VH2(3)
C
```

```
      LAMDA(1)=0
      MU(1)=0
      NU(1)=0
C
C  Form and store coordinates of chain atoms 2,3,4,5, which are independent
C  of the rotation angle vector PHI.
C
C  Atom 2 (Chiral carbon of segment1[Flory's conv.] of the chain)
      CALL MATVEC(TO,VC,VECT,3,3,3,3)
      X(2)=X(1)+VECT(1)
      Y(2)=Y(1)+VECT(2)
      Z(2)=Z(1)+VECT(3)
      LAMDA(2)=0
      MU(2)=0
      NU(2)=0
      CALL PERCONT(2)
C
C  Form and store transformation matrix product TPROD=TO*T1
      CALL MATMAT(TO,TPP,TPROD,3,3,3,3,3,3)
C
C  Atom 3 (Hydrogen connected to chiral carbon 2)
      IF(ICHIR(1)) 62,64,64
   62 CALL MATVEC(TPROD,VH1L,VECT,3,3,3,3)
      GO TO 70
   64 CALL MATVEC(TPROD,VH1D,VECT,3,3,3,3)
   70 X(3)=X(2)+VECT(1)
      Y(3)=Y(2)+VECT(2)
      Z(3)=Z(2)+VECT(3)
      LAMDA(3)=LAMDA(2)
      MU(3)=MU(2)
      NU(3)=NU(2)
      CALL PERCONT(3)
C
C  Atom 4 (Substituent R connected to chiral carbon 2)
      IF(ICHIR(1)) 72,74,74
   72 CALL MATVEC(TPROD,VRL,VECT,3,3,3,3)
      GO TO 80
   74 CALL MATVEC(TPROD,VRD,VECT,3,3,3,3)
   80 X(4)=X(2)+VECT(1)
      Y(4)=Y(2)+VECT(2)
      Z(4)=Z(2)+VECT(3)
      LAMDA(4)=LAMDA(2)
      MU(4)=MU(2)
      NU(4)=NU(2)
      CALL PERCONT(4)
C
C  Atom 5 (Achiral carbon of third segment of the chain)
      CALL MATVEC(TPROD,VC,VECT,3,3,3,3)
      X(5)=X(2)+VECT(1)
      Y(5)=Y(2)+VECT(2)
      Z(5)=Z(2)+VECT(3)
      LAMDA(5)=LAMDA(2)
      MU(5)=MU(2)
      NU(5)=NU(2)
      CALL PERCONT(5)
C
      RETURN
C
      END
```

```
      SUBROUTINE PERCONT(I)
C
C  Subroutine is used in the calculation of coordinates of atoms lying in
C  the cube.
C  Every time the coordinates of a new atom are calculated, the subroutine
C  checks whether the chain has exited the cube, and if yes it imposes an
C  appropriate periodic displacement to locate the image of the atom lying
C  within the cube
C
      INTEGER*1 LAMDA(3000), MU(3000), NU(3000), ICHIR(500), KIND(3000),
     1          MODUL(3000), CONNECT(0:5,0:5)
      INTEGER*2 IC(0:1000), ISEG(3000)
      DIMENSION X(3000), Y(3000), Z(3000), AX(3), AY(3), AZ(3), AXCY(3),
     1          AYCZ(3), AZCX(3), ORIGIN(3), VECT(3)
      COMMON /BLOCK1/ X, Y, Z
      COMMON /BLOCK2/ ICHIR, LAMDA, MU, NU, KIND, IC, ISEG, MODUL, CONNECT
      COMMON /BLOCK4/ ALPHA, BETA, GAMMA, AX, AY, AZ, AXX, AYY, AZZ, AXCY,
     1                AYCZ, AZCX, ORIGIN, VOLUME
C
      VECT(1)=X(I)-ORIGIN(1)
      VECT(2)=Y(I)-ORIGIN(2)
      VECT(3)=Z(I)-ORIGIN(3)
      CALL VECVEC(VECT, AYCZ, XCRIT, 3, 3)
      IF(XCRIT.LE.VOLUME) GO TO 10
      LAMDA(I)=LAMDA(I)-1
      X(I)=X(I)-AX(1)
      Y(I)=Y(I)-AX(2)
      Z(I)=Z(I)-AX(3)
      GO TO 20
   10 IF(XCRIT.GE.0.0) GO TO 20
      LAMDA(I)=LAMDA(I)+1
      X(I)=X(I)+AX(1)
      Y(I)=Y(I)+AX(2)
      Z(I)=Z(I)+AX(3)
C
   20 VECT(1)=X(I)-ORIGIN(1)
      VECT(2)=Y(I)-ORIGIN(2)
      VECT(3)=Z(I)-ORIGIN(3)
      CALL VECVEC(VECT, AZCX, YCRIT, 3, 3)
      IF(YCRIT.LE.VOLUME) GO TO 30
      MU(I)=MU(I)-1
      X(I)=X(I)-AY(1)
      Y(I)=Y(I)-AY(2)
      Z(I)=Z(I)-AY(3)
      GO TO 40
   30 IF(YCRIT.GE.0.0) GO TO 40
      MU(I)=MU(I)+1
      X(I)=X(I)+AY(1)
      Y(I)=Y(I)+AY(2)
      Z(I)=Z(I)+AY(3)
C
   40 VECT(1)=X(I)+ORIGIN(1)
      VECT(2)=Y(I)+ORIGIN(2)
      VECT(3)=Z(I)+ORIGIN(3)
      CALL VECVEC(VECT, AXCY, ZCRIT, 3, 3)
      IF(ZCRIT.LE.VOLUME) GO TO 50
      NU(I)=NU(I)-1
```

```
      X(I)=X(I)-AZ(1)
      Y(I)=Y(I)-AZ(2)
      Z(I)=Z(I)-AZ(3)
      GO TO 60
   50 IF(ZCRIT.GE.0.0) GO TO 60
      NU(I)=NU(I)+1
      X(I)=X(I)+AZ(1)
      Y(I)=Y(I)+AZ(2)
      Z(I)=Z(I)+AZ(3)
C
   60 CONTINUE
      RETURN
      END



      SUBROUTINE PRCD
C
C  Subroutine to print atom coordinates to output file
C
      INTEGER*1 ICHIR(500), LAMDA(3000), MU(3000), NU(3000), KIND(3000),
     1          MODUL(3000), CONNECT(0:5,0:5)
      INTEGER*2 IC(0:1000), ISEG(3000)
      REAL L, LH, LR
      DIMENSION X(3000), Y(3000), Z(3000), VC(3), VH1D(3), VH1L(3), VH2(3),
     1          VH3(3), VRD(3), VRL(3), TO(3,3), TP(3,3), TPP(3,3), TPROD(3,3)
      COMMON /BLOCK1/ X, Y, Z
      COMMON /BLOCK2/ ICHIR, LAMDA, MU, NU, KIND, IC, ISEG, MODUL, CONNECT
      COMMON /BLOCK3/ NUNITS, NBONDS, NSEGMENTS, NATOMS, THETAP, THETAHP,
     1                THETAPP, THETAHPP, THETARPP, STHP, CSTHP, STHPP,
     2                CSTHPP, L, LH, LR, VC, VH1D, VH1L, VH2, VH3, VRD, VRL,
     3                TO, TP, TPP, TPROD
      WRITE(6,10)
   10 FORMAT(////10X,'ATOM COORDINATES'/10X,16('-')//9X,'BACKBONE ATOM',13X,
     1       'L-SUBSTITUENT',10X,'D-SUBSTITUENT'/)
      ISEGM=0
      WRITE(6,20) ISEGM, X(1), Y(1), Z(1)
   20 FORMAT(/2X,I4,2X,'C ',E16.7,'(METHYL) '/10X,E16.7/10X,E16.7)
      ICARBON=-1
      DO 30 IUNIT=1,NUNITS-1
           ISEGM=ISEGM+1
           ICARBON=ICARBON+3
           IF(ICHIR(IUNIT)) 60,70,70
   60      WRITE(6,80) ISEGM,X(ICARBON),X(ICARBON+2),X(ICARBON+1)
   80      FORMAT(/2X,I4,2X,'C ',E16.7,5X,'R ',E16.7,5X,'H ',E16.7)
           WRITE(6,90) Y(ICARBON),Y(ICARBON+2),Y(ICARBON+1)
   90      FORMAT(10X,E16.7,7X,E16.7,7X,E16.7)
           WRITE(6,90) Z(ICARBON),Z(ICARBON+2),Z(ICARBON+1)
           GO TO 100
   70      WRITE(6,110) ISEGM,(X(I),I=ICARBON,ICARBON+2)
  110      FORMAT(/2X,I4,2X,'C ',E16.7,5X,'H ',E16.7,5X,'R ',E16.7)
           WRITE(6,90)  (Y(I),I=ICARBON,ICARBON+2)
           WRITE(6,90)  (Z(I),I=ICARBON,ICARBON+2)
  100      ISEGM=ISEGM+1
           ICARBON=ICARBON+3
           WRITE(6,120) ISEGM,X(ICARBON),X(ICARBON+2),X(ICARBON+1)
  120      FORMAT(/2X,I4,2X,'C ',E16.7,5X,'H ',E16.7,5X,'H ',E16.7)
           WRITE(6,90) Y(ICARBON),Y(ICARBON+2),Y(ICARBON+1)
           WRITE(6,90) Z(ICARBON),Z(ICARBON+2),Z(ICARBON+1)
```

```
   30 CONTINUE
      ISEGM=ISEGM+1
      ICARBON=ICARBON+3
      IF(ICHIR(NUNITS)) 130,140,140
  130 WRITE(6,80) ISEGM,X(ICARBON),X(ICARBON+2),X(ICARBON+1)
      WRITE(6,90) Y(ICARBON),Y(ICARBON+2),Y(ICARBON+1)
      WRITE(6,90) Z(ICARBON),Z(ICARBON+2),Z(ICARBON+1)
      GO TO 150
  140 WRITE(6,110) ISEGM,(X(I),I=ICARBON,ICARBON+2)
      WRITE(6,90) (Y(I),I=ICARBON,ICARBON+2)
      WRITE(6,90) (Z(I),I=ICARBON,ICARBON+2)
  150 ISEGM=ISEGM+1
      WRITE(6,20) ISEGM,X(NATOMS),Y(NATOMS),Z(NATOMS)
C
      RETURN
      END
```

APPENDIX J : Listing of the FORTRAN Program Used for the Relaxation to Mechanical Equilibrium, Described in Section 3.3.2

```
      PROGRAM CUBE
C
C
C  ***************************************************************************
C  *                                                                         *
C  *                        DOROS N. THEODOROU                               *
C  *                                                                         *
C  *                Department of Chemical Engineering                       *
C  *                                                                         *
C  *             Massachusetts Institute of Technology                       *
C  *                                                                         *
C  *                             June 1985                                   *
C  *                                                                         *
C  ***************************************************************************
C
C  Energy minimization in a cube of bulk amorphous polymer
C  Cube is filled with parts of a single polymer chain, displaced
C  according to the requirements of periodic boundary conditions,
C  with continuation vectors Ax, Ay, Az. Chain bond angles and
C  bond lengths are assumed constant.
C  The location of the chain start, and the orientation of the
C  first two skeletal bonds are fixed during the minimization.
C  thus, the degrees of freedom of the system are the
C  NDF-3=NBONDS-2 rotation angles of all the bonds of the chain,
C  and the three Eulerian angles alpha, beta, gamma.
C
      IMPLICIT REAL*8(A-H,O-Z)
      INTEGER ICHIR(100), KIND(600), MODUL(600), CONNECT(0:5,0:5)
      INTEGER IC(200), ISEG(600)
      REAL*8 L, LH, LR, MW, MWUNIT, MWR
      CHARACTER CHAINNM*20, NAME(3)*4
      DIMENSION X(600), Y(600), Z(600), PHI(200), SCALE(200), AX(3),
     1          AY(3), AZ(3), AXCY(3), AYCZ(3), AZCX(3), ORIGIN(3),
     2          VC(3), VH1D(3), VH1L(3), VH2(3), VH3(3), VRD(3),
     3          VRL(3), TO(3,3), TP(3,3), TPP(3,3), TPROD(3,3),
     4          VECT(3), R12(3), ALFA(3), EFFNE(3), VDWR(3), EPS(3,3),
     5          SIGMA(3,3), RANGE(3,3), RANGEX(3,3), RANGEY(3,3),
     6          RANGEZ(3,3), EPSIG(3,3), GRADX(200), GRADY(200),
     7          GRADZ(200), XP(600), YP(600), ZP(600)
      DIMENSION HESS(20100), SRHVEC(200), SOLVEC(200), GRDVEC(200),
     1          SCRVEC(200)
      COMMON /BLOCK1/ X, Y, Z
      COMMON /BLOCK2/ ICHIR, KIND, IC, ISEG, MODUL, CONNECT
      COMMON /BLOCK3/ NUNITS, NBONDS, NSEGMENTS, NATOMS, THETAP,
     1                THETAHP, THETAPP, THETAHPP, THETARPP, STHP,
     2                CSTHP, STHPP, CSTHPP, L, LH, LR, VC, VH1D,
     3                VH1L, VH2, VH3, VRD, VRL, TO, TP, TPP, TPROD
      COMMON /BLOCK4/SA,CSA,SB,CSB,SG,CSG, AX, AY, AZ, AXX, AYY, AZZ,
     1                AXCY, AYCZ, AZCX, ORIGIN, VOLUME
      COMMON /BLOCK5/ ALFA, EFFNE, VDWR, EPS, SIGMA, EPSIG, RANGE,
     1                RANGEX, RANGEY, RANGEZ, NAME, NNUC, RR1, RR2,
     2                DELRR, AU, BU, CU, AF, BF, CF, ROTBAR
      COMMON /BLOCK6/ ETOTLJ, ETOTROT, GRADY, GRADZ, SCALE
      COMMON /BLOCK7/ XP, YP, ZP
C
      OPEN(5,MODE='IN',ACCESS='SEQUENTIAL',FORM='FORMATTED',
     1       FILE='CUBE.DAT')
      OPEN(7,MODE='IN',ACCESS='SEQUENTIAL',FORM='FORMATTED',
     1       FILE='CHAIN.DF')
      OPEN(9,MODE='IN',ACCESS='SEQUENTIAL',FORM='FORMATTED',
```

```
     1        FILE='OPT.DAT')
      OPEN(6,MODE='OUT',ACCESS='SEQUENTIAL',FORM='FORMATTED',
     1        FILE='CUBE.OUT')
      OPEN(10,MODE='OUT',ACCESS='SEQUENTIAL',FORM='FORMATTED',
     1        FILE='OPT.OUT')
C
C  Enter chain type and size.
      READ(5,10) CHAINNM,MWR,NUNITS
   10 FORMAT(A20/F10.5/I5)
      NSEGMENTS=2*NUNITS+1
      NBONDS=2*NUNITS
      NDF=NBONDS+1
      NDF1=NDF-2
      NATOMS=3*NDF-4
      MWUNIT=MWR+27.04621
      MW=16.04303+NUNITS*MWUNIT
      WRITE(6,20) CHAINNM,NUNITS,NATOMS,NBONDS,NDF,MW
   20 FORMAT(/////2X,'MOLECULE : ',A20/13X,13('-')//2X,
     1 'DEGREE OF POLYMERIZATION : ',I5,5X,'(',I5,
     2 '  SKELETAL ATOMS,',3X,I5,'  BONDS )'//2X,
     3 'NUMBER OF SYSTEM DEGREES OF FREEDOM : ',I5//
     3 2X,'MOLECULAR WEIGHT : ',E16.8/)
C
C  Enter bond lengths (Angstroms) and bond angles (degrees)
      READ(5,30) L,LH,LR
      READ(5,30) THETAP,THETAHP
      READ(5,30) THETAPP,THETAHPP,THETARPP
   30 FORMAT(3F8.3)
      WRITE(6,40) L,LH,LR,THETAP,THETAPP,THETAHP,THETAHPP,THETARPP
   40 FORMAT(//2X,'BOND LENGTHS'/15X,'C - C  : ',F5.3,' ANGSTROMS'/
     115X,'C - H  : ',F5.3,' ANGSTROMS'/15X,'C - R  : ',F5.3,
     2' ANGSTROMS'/15X,'(R=SUBSTITUENT)'//2X,'BOND ANGLES'/15X,
     3'INTRADYAD C-C-C : ',F8.3,' DEG'/15X,'INTERDYAD C-C-C : ',
     4F8.3,' DEG'/15X,'INTRADYAD H-C-C : ',F8.3,' DEG'/15X,
     5'INTERDYAD H-C-C : ',F8.3,' DEG'/15X,'INTERDYAD R-C-C : ',
     6 F8.3,' DEG'/)
C
C  Enter continuation vectors of cube (coordinates in Angstroms)
      READ(5,50) (AX(I),I=1,3)
      READ(5,50) (AY(I),I=1,3)
      READ(5,50) (AZ(I),I=1,3)
   50 FORMAT(3E16.8)
      WRITE(6,60) (AX(I),I=1,3),(AY(I),I=1,3),(AZ(I),I=1,3)
   60 FORMAT(//2X,'CONTINUATION VECTORS FOR PERIODIC CUBE',
     1' (COMPONENTS IN ANGSTROMS) :'//5X,'AX :  ',3(E16.8,5X)//
     25X,'AY :  ',3(E16.8,5X)//5X,'AZ :  ',3(E16.8,5X))
C
C  Calculate cross products Ax x Ay, Ay x Az, Az x Ax
      CALL VCROSSV(AX, AY, AXCY)
      CALL VCROSSV(AY, AZ, AYCZ)
      CALL VCROSSV(AZ, AX, AZCX)
C  Calculate cube volume, V=Ax.(Ay x Az)
      VOLUME=AX(1)*AYCZ(1)+AX(2)*AYCZ(2)+AX(3)*AYCZ(3)
      WRITE(6,70) VOLUME
   70 FORMAT(/2X,'CUBE VOLUME = ',E16.8,2X,'CUBIC ANGSTROMS'/)
C
C  Calculate density
      DENSITY=MW/VOLUME*1.6603022
      WRITE(6,75) DENSITY
   75 FORMAT(2X,'CUBE MASS DENSITY = ',E16.8,2X,' G/CM3')
```

```
C
C  Enter coordinates of cube origin
      READ(5,50)  (ORIGIN(I),I=1,3)
      WRITE(6,80)  (ORIGIN(I),I=1,3)
   80 FORMAT(/2X,'CUBE ORIGIN AT (',E16.8,',',E16.8,',',E16.8,') ')
C
C  Read flag for specifying format of degree-of-freedom file
      READ(5,52)  ILONG
   52 FORMAT(I2,I2)
C
C  Read the necessary and sufficient parameters for completely
C  specifying the position, shape and orientation of the chain
C  (hence the coordinates of every atom or substituent belonging to it)
C
C  Position of first skeletal carbon (terminal methyl)
      IF(ILONG.NE.0) GO TO 95
      READ(7,90)  X(1), Y(1), Z(1)
C
C  Angles specifying the orientation of first two bonds (in DEGREES)
      READ(7,90)  PHI(1),PHI(2),PHI(3)
   90 FORMAT(3E16.9)
C
C  Chirality sequence for all chiral atoms of the molecule
C  Index ICHIR(I) designates the absolute configuration of the chiral
C  skeletal carbon atom (6I-4). A value of ICHIR=+1 indicates that the
C  chiral center is D- in a Fischer projection constructed so that
C  the beginning of the chain (atom 1) lies upwards.
C  A value of ICHIR=-1 indicates an L-configuration, based on the same
C  convention.
      READ(7,100)  (ICHIR(I),I=1,NUNITS)
  100 FORMAT(4012)
C
C  Read sequence of rotation angles of bonds 2,...,NBONDS-1.
C  Rotation angle of bond i is kept in element PHI(i+2). All values
C  measured in degrees.
      READ(7,110)  (PHI(I),I=4,NDF)
  110 FORMAT(5E16.9)
C
      GO TO 112
C
   95 READ(7,105)  X(1), Y(1), Z(1)
  105 FORMAT(2E40.33)
      READ(7,105)  (PHI(I),I=1,3)
      READ(7,100)  (ICHIR(I),I=1,NUNITS)
      READ(7,105)  (PHI(I),I=4,NDF)
C
  112 CLOSE(7)
      XP(1)=X(1)
      YP(1)=Y(1)
      ZP(1)=Z(1)
C
C  Printout characteristics of initial guess configuration
      WRITE(6,300)  (ICHIR(I),I=1,NUNITS)
  300 FORMAT(///2X,'SKELETAL CARBON CHIRALITY SEQUENCE OF CHAIN',
     1' FILLING THE CUBE :'/26X,'(+1=D, -1=L) '//3X,'* ',
     214(I2,' * ')/(5X,14(I2,' * ')))
      WM=0.0
      DO 115 I=2,NUNITS
         IF((ICHIR(I)-ICHIR(I-1)).NE.0) WM=WM+1.0
  115 CONTINUE
```

```
      WM=1.-WM/(NUNITS-1)
      WRITE(6,315) WM
  315 FORMAT(/2X,'FRACTION OF meso-DYADS, wm = ',F8.6)
      WRITE(6,310) X(1),Y(1),Z(1)
  310 FORMAT(///2X,'SPECIFICATION OF LOCATION OF METHYL AT CHAIN ',
     1'START'//2X,'. CARBON No 0 at ( ',F10.6,', ',2X,F10.6,', ',2X,
     2F10.6,') ')
C
C  Enter the left boundary and the width of the reduced radius interval
C  over which the Lennard-Jones potential will be approximated by a
C  quintic spline.
      READ(5,120) RR1,DELRR
  120 FORMAT(2F13.10)
C
C  Read option parameter for printing the potential parameters
C  initialized in POTINIT.
      READ(5,130) IPRPOT
C
C  ISHRINK is a flag determining how the Lennard-Jones epsilons
C  and sigmas are to be initialized within the subroutine.
C  . If ISHRINK=0, Lennard-Jones sigmas and epsilons, and the
C                  rotational potential, are given their true values
C  . If ISHRINK=1, Lennard-Jones sigmas are scaled, using the
C                  scaling parameter SHRINKRAD, Lennard-Jones
C                  epsilons are scaled, using the scaling parameter
C                  SHRINKPOT, and rotational potentials are scaled,
C                  using the scaling parameter SHRINKROT.
      READ(5,130) ISHRINK
  130 FORMAT(I2)
      IF(ISHRINK.EQ.0) GO TO 140
      READ(5,150) SHRINKRAD,SHRINKPOT,SHRINKROT
  150 FORMAT(3E15.8)
C
C  Read option parameter for scaling rotation angles
C       ISCALE=0 : Rotation angles not scaled
C       ISCALE=1 : Rotation angles scaled
      READ(5,130) ISCALE
C
C  Option input for printing coordinates in output file
C       IWRCD=1 : Coordinates printed
C       IWRCD=0 : Coordinates not printed
  140 READ(5,130) IWRCD
C
C  Read option parameter for printing detailed interactions
C
C  Convert valence bond angles and angles alpha, beta, gamma
C  to radians
      DEGRAD=ASIN(1.)/90.
      THETAP=THETAP*DEGRAD
      THETAHP=THETAHP*DEGRAD
      THETAPP=THETAPP*DEGRAD
      THETAHPP=THETAHPP*DEGRAD
      THETARPP=THETARPP*DEGRAD
C
C  Initialize scaling factors for rotation angles
      DO 135 I=1,NDF
  135    SCALE(I)=1.0
C
C
      ISTART=1
```

```
      CALL COORD(NDF, PHI, ISTART)
C
      ISTART=0
      IF(IWRCD.EQ.0.AND.ISCALE.NE.0) GO TO 182
      DO 185 I=1,NDF
  185    PHI(I)=PHI(I)*DEGRAD
      CALL COORD(NDF,PHI,0)
C
      DO 195 I=1,NDF
  195     PHI(I)=PHI(I)/DEGRAD
C
C  Invoke initializations in potential calculating routines
  182 CALL POTINIT(ISHRINK,SHRINKRAD,SHRINKPOT,SHRINKROT,IPRPOT)
C
      WRITE(6,196)
  196 FORMAT(////2X,'INITIAL GUESS CONFIGURATION'/2X,27('='))
      WRITE(6,320) PHI(1),PHI(2),PHI(3),NDF1,(PHI(I),I=4,NDF)
  320 FORMAT(///2X,'EXTERNAL ORIENTATION (EULERIAN) ANGLES'/
     12X,39('-')///
     2 2X,'. ANGLE BETW. x-AXIS AND PROJECTION OF BOND No',
     3' 1 ON PLANE xy  alpha = ',E16.9,'  DEG'//2X,'. ANGLE BETW.',
     4' z-AXIS AND BOND No 1  beta = ',E16.9,'  DEG'//2X,
     5'. DIHEDRAL ANGLE BETWEEN PLANES (bond1, z-axis) AND ',
     6'(bond1, bond2)  gamma = ',E16.9,'  DEG'///2X,
     72X,'SEQUENCE OF ROTATION ANGLES OF BONDS 2 THROUGH ',I5,
     8' (DEGREES) '/2X,62('-')/(/2X,5(F10.5,6X)))
C
      IF(ISCALE.EQ.0) GO TO 330
      CALL FUNCT(NDF,PHI,ENERGY,GRADX)
      IF(IWRCD.NE.0) CALL PRCD
      WRITE(6,270) ETOTLJ,ETOTROT,ENERGY
  270 FORMAT(///2X,'TOTAL ENERGY DUE TO INTERATOMIC INTERACTIONS :  ',
     1 1X,E16.9,' KCAL/MOLE'//2X,'TOTAL ENERGY DUE TO BOND ROTATIONAL',
     2 ' BARRIERS :   ',E16.9,' KCAL/MOLE'//2X,'TOTAL ENERGY (SUM OF',
     3 ' BOTH CONTRIBUTIONS) :  ',5X,E16.9,' KCAL/MOLE')
C
      WRITE(6,275) (GRADX(I),I=1,3)
  275 FORMAT(///2X,'DERIVATIVES OF TOTAL POTENTIAL ',
     1  'ENERGY wrt EULERIAN ANGLES (KCAL/MOLE/DEG) '//2X,
     2  75('-')///2X,'wrt. ALPHA : ',E16.9//2X,'wrt.  BETA : '
     3  ,E16.9//2X,'wrt. GAMMA : ',E16.9)
C
      WRITE(6,280) NDF1,(GRADX(I),I=4,NDF)
  280 FORMAT(///2X,'DERIVATIVES OF TOTAL POTENTIAL ENERGY wrt ',
     1'BOND ANGLES 2 THROUGH ',I5//2X,70('-')/28X,
     2 '(KCAL/MOLE/DEGREE) '//,(/2X,5(E14.7,2X)))
C
      GO TO 335
C
  330 IF(IWRCD.NE.0) CALL PRCD
C
C  Check whether conditions for screening algorithm are fulfilled.
  335 RANGEXM=0.0
      RANGEYM=0.0
      RANGEZM=0.0
      DO 180 J=1,3
          DO 180 I=1,3
              IF(RANGEX(I,J).GT.RANGEXM) RANGEXM=RANGEX(I,J)
              IF(RANGEY(I,J).GT.RANGEYM) RANGEYM=RANGEY(I,J)
              IF(RANGEZ(I,J).GT.RANGEZM) RANGEZM=RANGEZ(I,J)
```

```
  180 CONTINUE
      IF(2.*RANGEXM.GT.AXX) GO TO 190
      IF(2.*RANGEYM.GT.AYY) GO TO 190
      IF(2.*RANGEZM.GT.AZZ) GO TO 190
      GO TO 200
  190 WRITE(6,210)
  210 FORMAT(//2X,'INTERATOMIC INTERACTION RANGE TOO LONG'/2X,
     1'IN COMPARISON WITH SIZE OF CONTINUATION VECTORS'//2X,
     2'NECESSARY CRITERIA FOR VALIDITY OF SCREENING ALGORITHM',
     3' NOT FULFILLED'/)
      GO TO 220
C
C  Scale rotation angles
C  Within the minimization routines, angles are in scaled degrees.
  200 IF(ISCALE.NE.0) CALL SETSCALE(NDF,SCALE)
      DO 230 I=1,NDF
  230     PHI(I)=PHI(I)*SCALE(I)
C
C  Read optimization routine settings
      READ(9,400) MAXF, ISWTCH, IPRINT
  400 FORMAT(I10, I2, I2)
      READ(9,410) TOLX, TOLG
  410 FORMAT(3E10.4)
      READ(9,410) ENERGY, RFN
      READ(9,410) SPREC, EXTBND, HISTRY
      READ(9,415) IRHESS,IWRHESS
  415 FORMAT(2I2)
      IF(IRHESS.NE.0) OPEN(11,MODE='IN',ACCESS='SEQUENTIAL',FORM=
     1                 'FORMATTED',FILE='HESS.DF')
      IHESS=NDF*NDF1/2
C
      WRITE(10,420) ISWTCH
  420 FORMAT(/////5X, 'AMDLIB QUASI-NEWTON MINIMIZATION ROUTINE GCFLRV'
     1       ,' - ISWTCH = ',I1/5X,48('='),13('-'))
      IF(ISWTCH.EQ.1) WRITE(10,430)
      IF(ISWTCH.EQ.2) WRITE(10,440)
  430 FORMAT(23X,'(DFP HESSIAN UPDATING SCHEME USED)')
  440 FORMAT(23X,'(BFGS HESSIAN UPDATING SCHEME USED)')
      WRITE(10,450) NDF, MAXF, IPRINT
  450 FORMAT(///2X,'NVAR = ',I4, 6X, 'MAXF = ',I4, 6X, 'IPRINT = ',I4)
      WRITE(10,460) TOLX, TOLG
  460 FORMAT(//'TOLERANCES :    TOLX = ',E10.4, 4X,'TOLG = ',E10.4)
      WRITE(10,470) ENERGY, RFN
  470 FORMAT(//'APPROXIMATE LOCATION OF MIN. :    OBJF = ',E10.4, 4X,
     1'RFN = ',E10.4)
      WRITE(10,480) SPREC, EXTBND, HISTRY
  480 FORMAT(//'SPREC = ',E10.4, 6X, 'EXTBND = ',E10.4, 6X,
     1 'HISTRY = ',E10.4)
      WRITE(10,490) (I,PHI(I),I=1,NDF)
  490 FORMAT(//2X,'INITIAL VALUES OF PARAMETERS'//3(2X,'X(',I4,
     1') = ',E16.8))
C
      CALL GQBFGS(NDF,PHI,ISWTCH,MAXF,ITER,IPRINT,TOLX,TOLG,RFN,
     1            SPREC,EXTBND,ENERGY,IHESS,HESS,GRADX,IERR,NFCALL,
     2            SRHVEC,SOLVEC,GRDVEC,SCRVEC,HISTRY,IRHESS,IWRHESS)
      WRITE(10,500) IERR
  500 FORMAT(///2X,'RESULTS UPON EXIT FROM GQBFGS'/2X,29('-')//
     12X,'IERR = ',I2)
      WRITE(10,510) ENERGY
  510 FORMAT(//2X,'VALUE OF FUNCTION AT MINIMUM  OBJF = ',E15.8)
```

```
      WRITE(10,520)  (J,PHI(J),J=1,NDF)
  520 FORMAT(//2X,'VALUES OF PARAMETERS'//3(2X,'X(',I4,') = ',E16.8))
      WRITE(10,530)  (J,GRADX(J),J=1,NDF)
  530 FORMAT(//2X,'GRADIENT AT MINIMUM'//3(2X,'G(',I4,') = ', E16.8))
      WRITE(10,540)  ITER, NFCALL
  540 FORMAT(///2X,'TOTAL NUMBER OF ITERATIONS = ',I5/2X,
     1'TOTAL NUMBER OF FUNCTION EVALUATIONS = ',I5///)
C
      WRITE(6,340)
  340 FORMAT(////2X,'FINAL CONFIGURATION AFTER OPTIMIZATION'/
     12X,38('='))
C
C  Descale rotation angles to their true values (in degrees)
C  Form gradient with respect to true angle values (in degrees)
      DO 250 I=1,NDF
          ECHELLE=SCALE(I)
          PHI(I)=PHI(I)/ECHELLE
          GRADX(I)=GRADX(I)*ECHELLE
  250 CONTINUE
C
C  Print out rotation angles
      WRITE(6,320)  PHI(1),PHI(2),PHI(3),NDF1,(PHI(I),I=4,NDF)
C
      IF(IWRCD.EQ.0) GO TO 350
      CALL PRCD
C
C  Print out calculated energy
  350 WRITE(6,270)  ETOTLJ, ETOTROT, ENERGY
C
C  Print out gradient
      WRITE(6,275)  (GRADX(I),I=1,3)
      WRITE(6,280)  NDF1,(GRADX(I),I=4,NDF)
  220 CONTINUE
C
      OPEN(12,MODE='OUT',ACCESS='SEQUENTIAL',FORM='FORMATTED',
     1        FILE='LAST.DF')
      OPEN(14,MODE='OUT',ACCESS='SEQUENTIAL',FORM='FORMATTED',
     1        FILE='CHAIN.MIN')
      WRITE(12,90)  X(1),Y(1),Z(1)
      WRITE(14,560)  X(1), Y(1), Z(1)
  560 FORMAT(2E40.33)
      WRITE(12,90)   PHI(1), PHI(2), PHI(3)
      WRITE(14,560)  PHI(1), PHI(2), PHI(3)
      WRITE(12,100)  (ICHIR(I), I=1,NUNITS)
      WRITE(14,100)  (ICHIR(I), I=1,NUNITS)
      WRITE(12,110)  (PHI(I),I=4,NDF)
      WRITE(14,560)  (PHI(I),I=4,NDF)
      CLOSE(12)
      CLOSE(14)
C
      END



      SUBROUTINE POTINIT(ISHRINK,SHRINKRAD,SHRINKPOT,SHRINKROT,IPRINT)
C
C  Initialization of interatomic and rotational potential parameters
C
C  For  interatomic interaction, a modified Lennard-Jones potential is
```

```
C  used:
C
C        -  For R <= R1              use 6-12 LJ potential
C
C        -  For R >= R2              no interaction (potential=0.0)
C
C        -  For R1 < R < R2          use quintic spline, designed so that
C                                    the potential function and its first
C                                    and second derivatives are continuous
C                                    at R1=RR1*SIGMA and zero at
C                                    R2=R1+DELRR*SIGMA
C
C  Numbering convention for atomic species :
C      (1) : H    ,    (2) : C    ,    (3) : Methyl
C
C  For skeletal bond torsion, a symmetric threefold potential
C  expression used, with rotational barrier equal to 2.8 kcal/mole.
C
       IMPLICIT REAL*8(A-H,O-Z)
       INTEGER ICHIR(100), KIND(600), MODUL(600), CONNECT(0:5,0:5)
       INTEGER IC(200), ISEG(600)
       CHARACTER*4 NAME(3)
       DIMENSION AX(3), AY(3), AZ(3), AXCY(3), AYCZ(3), AZCX(3),
      1          ORIGIN(3), ALFA(3), EFFNE(3), VDWR(3), EPS(3,3),
      2          SIGMA(3,3), RANGE(3,3), RANGEX(3,3), RANGEY(3,3),
      3          RANGEZ(3,3), EPSIG(3,3)
       COMMON /BLOCK2/ ICHIR, KIND, IC, ISEG, MODUL, CONNECT
       COMMON /BLOCK4/SA,CSA,SB,CSB,SG,CSG, AX, AY, AZ, AXX, AYY, AZZ,
      1                AXCY, AYCZ, AZCX, ORIGIN, VOLUME
       COMMON /BLOCK5/ ALFA, EFFNE, VDWR, EPS, SIGMA, EPSIG, RANGE,
      1                RANGEX, RANGEY, RANGEZ, NAME, NNUC, RR1, RR2,
      2                DELRR, AU, BU, CU, AF, BF, CF, ROTBAR
C
C  Define number of chemical species used
       NNUC=3
C
C  Define names of species
       NAME(1)='H    '
       NAME(2)='C    '
       NAME(3)='CH3  '
C
C  Enter polarizabilities (A**3)
       ALFA(1)=0.42
       ALFA(2)=0.93
       ALFA(3)=1.77
C
C  Enter effective numbers of electrons
       EFFNE(1)=0.9
       EFFNE(2)=5.0
       EFFNE(3)=7.0
C
C  Enter Van der Waals radii
       VDWR(1)=1.2
       VDWR(2)=1.7
       VDWR(3)=2.0
C
C  Calculate Lennard-Jones Epsilons and Sigmas
       DO 30 I=1,NNUC
           DO 30 J=1,NNUC
C  Obtain coefficient Cij of r-6 attractive term from Slater-Kirkwood
```

```
C  formula
                CIJ=365.*ALFA(I)*ALFA(J)/(SQRT(ALFA(I)/EFFNE(I))+
     1              SQRT(ALFA(J)/EFFNE(J)))
C  Obtain coefficient AIJ from condition of potential minimum at
C       VDWR(I)+VDWR(J)
                AIJ=0.5*CIJ*(VDWR(I)+VDWR(J))**6
C  Obtain Lennard-Jones Epsilon(kcal/mol) and Sigma(A) for current pair
                EPS(I,J)=CIJ*CIJ/4./AIJ
                SIGMA(I,J)=(AIJ/CIJ)**(1./6)
   30 CONTINUE
C
C  If desired, scale Lennard-Jones sigmas by the factor SHRINKRAD
C  and Lennard-Jones epsilons by the factor SHRINKPOT.
      IF(ISHRINK.EQ.0) GO TO 35
      DO 25 J=1,3
          DO 25 I=1,3
              SIGMA(I,J)=SIGMA(I,J)*SHRINKRAD
   25         EPS(I,J)=EPS(I,J)*SHRINKPOT
C
   35 DO 40 J=1,3
          DO 40 I=1,3
   40         EPSIG(I,J)=EPS(I,J)/SIGMA(I,J)
C
C  Determine coefficients for quintic spline and derivative.
C  FR,DFR,DDFR symbolize the reduced LJ potential function and
C  its first and second derivatives, FR=ULJ/EPS, DFR=DULJ/(EPS/SIGMA),
C  DDFR=DDULJ/(EPS/SIGMA**2).
C  RR symbolizes the reduced distance RR=R/SIGMA
C
      RR2=RR1+DELRR
      X6=(1./RR1)**6
      X12=X6*X6
      FR=4.*(X12-X6)
      COEF=24./RR1
      DFR=-COEF*(2.*X12-X6)
      DDFR=COEF/RR1*(26.*X12-7.*X6)
      DELRR2=DELRR/2.
      AU=6.*FR+3.*DELRR*DFR+DELRR2*DELRR*DDFR
      BU=3.*FR+DELRR*DFR
      CU=FR
      AF=-5.*(6./DELRR*FR+3.*DFR+DELRR2*DDFR)
      BF=2.*(DFR+DELRR2*DDFR)
      CF=DFR
C
C  Form the matrices RANGE, RANGEX, RANGEY, RANGEZ of the  range of
C  interatomic interactions.
C  . RANGE(i,j) is simply the Lennard-Jones SIGMA corresponding to
C    the atom pair (i,j), multiplied by the reduced radial distance
C    at which the modified interatomic potential used in the energy
C    calculations goes to 0. RANGEX, RANGEY, RANGEZ are effective
C    ranges, used in the screening procedure to determine significant
C    interactions between images of atoms in the cube
      DO 60 I=1,NNUC
          DO 60 J=1,NNUC
   60         RANGE(I,J)=RR2*SIGMA(I,J)
      DO 65 I=1,NNUC
          DO 65 J=1,NNUC
              RANGEX(I,J)=RANGE(I,J)+ABS(AY(1))+ABS(AZ(1))
              RANGEY(I,J)=RANGE(I,J)+ABS(AZ(2))+ABS(AX(2))
              RANGEZ(I,J)=RANGE(I,J)+ABS(AX(3))+ABS(AY(3))
```

```
   65 CONTINUE
C
C  Store squared ranges in RANGE
      DO 67 I=1,NNUC
          DO 67 J=1,NNUC
   67         RANGE(I,J)=RANGE(I,J)**2
C
C  Form the projections AXX, AYY, AZZ of the continuation vectors
C  AX, AY, AZ on the x, y, z axes, respectively.
      AXX=AX(1)
      AYY=AY(2)
      AZZ=AZ(3)
C
C  Enter connectivity table (indices correspond to atom index in
C  X,Y,Z, taken modulo6)
      DO 160 I=0,5
          CONNECT(I,2)=0
  160     CONNECT(I,5)=0
      DO 170 I=3,5
          CONNECT(I,0)=1
  170     CONNECT(I,1)=1
      DO 180 I=0,2
          CONNECT(I,3)=1
  180     CONNECT(I,4)=1
      CONNECT(0,0)=1
      CONNECT(1,0)=0
      CONNECT(2,0)=0
      CONNECT(0,1)=1
      CONNECT(1,1)=1
      CONNECT(2,1)=0
      CONNECT(3,3)=1
      CONNECT(4,3)=0
      CONNECT(5,3)=0
      CONNECT(3,4)=1
      CONNECT(4,4)=1
      CONNECT(5,4)=0
C
C  Initialize the value of the rotational potential barrier ROTBAR
      ROTBAR=2.8
C
C  Shrink, if desired, the rotational barrier by a factor SHRINKROT
      IF(ISHRINK.NE.0) ROTBAR=ROTBAR*SHRINKROT
C
C  Optional printout
      IF(IPRINT.EQ.0) RETURN
      WRITE(6,70)
   70 FORMAT(///2X,'6-12 POTENTIAL PARAMETERS'//2X,'NUC.TYPE  VDW-R  ',
     1       'ALFA  EFF.NO. OF EL.'/)
      WRITE(6,80) (I, VDWR(I), ALFA(I), EFFNE(I), NAME(I), I=1,NNUC)
   80 FORMAT(8(4X,I2,5X,F5.2,2X,F5.2,5X,F5.2,8X,A/))
      WRITE(6,90) (I,I=1,NNUC)
   90 FORMAT(/2X,'EPSILON VALUES (KCAL/MOL) '/18X,8(I1,17X))
      DO 100 I=1,NNUC
  100     WRITE(6,110) I, (EPS(I,J), J=1,NNUC)
  110 FORMAT(I3,3X,8(4X,E15.8))
      WRITE(6,120) (I,I=1,NNUC)
  120 FORMAT(/2X,'SIGMA VALUES (ANGSTROMS) '/18X,8(I1,17X))
      DO 130 I=1,NNUC
  130 WRITE(6,110) I,(SIGMA(I,J), J=1,NNUC)
      WRITE(6,140) RR1,FR,RR2
```

```
  140 FORMAT(//2X,'6-12 POTENTIAL USED UP TO R/SIGMA = ',F10.6,5X,
     1      ' WHERE ULJ/EPS = ',F9.6//2X,'ZERO POTENTIAL FROM',
     2      ' R/SIGMA = ',F10.6//2X,'AND QUINTIC SPLINE WITH CONTINUOUS'
     3    ,' FIRST AND SECOND DERIVATIVES IN BETWEEN')
      WRITE(6,150) ROTBAR
  150 FORMAT(///2X,'THREEFOLD ROTATIONAL POTENTIAL USED TO DESCRIBE ',
     1'SKELETAL BOND TORSION'//2X,'ROTATIONAL BARRIER ',E15.8,
     2' KCAL/MOLE')
      IF(ISHRINK.NE.0) WRITE(6,135) SHRINKRAD,SHRINKPOT,SHRINKROT
  135 FORMAT(//2X,'IN THIS CALCULATION SIGMAS HAVE BEEN SHRUNK TO ',
     1E15.8/4X,'EPSILONS TO ',E15.8,'  AND ROTBAR TO ',E15.8,
     2        /19X,' OF THEIR TRUE VALUE ')
      RETURN
      END



      SUBROUTINE GQBFGS(NVAR,X,ISWTCH,MAXF,ITER,IPRINT,TOLX,TOLG,RFN,
     1                  SPREC,EXTBND,OBJF,IHESS,HESS,G,IERR,NFCALL,
     2                  SRHVEC,SOLVEC,GRDVEC,SCRVEC,HISTRY,IRHESS,
     3                  IWRHESS)
C
      IMPLICIT REAL*8(A-H,O-Z)
      DIMENSION  X(200),HESS(20100),G(200),SRHVEC(200),SOLVEC(200),
     1        GRDVEC(200),SCRVEC(200)
C
C       THIS SUBROUTINE MINIMIZES A FUNCTION OF SEVERAL VARIABLES
C     OBJF(X(1),X(2),...,X(NVAR))  USING A QUASI-NEWTON METHOD
C     OPTIONALLY EMPLOYING THE  DFP  AND  BFGS  UPDATING FORMULAS.
C     THE USER MUST PROVIDE A SUBROUTINE TO CALCULATE  OBJF(X)  AND
C     ITS GRADIENT(FIRST PARTIAL DERIVATIVE) VECTOR  G(X).
C
C     ****************************************************************
C       THIS ROUTINE INVOKES THE PACKAGE MODULES  SEARCH  AND  UPHESS
C     AND THE USER SUPPLIED SUBROUTINE  FUNCT.
C     ****************************************************************
C
C     ON INPUT
C
C        NVAR  IS THE NUMBER OF VARIABLES. IT IS ALSO THE DIMENSION OF
C           THE VECTORS  X, G, SRHVEC, SOLVEC, GRDVEC  AND  SCRVEC.
C
C        X  CONTAINS AN ESTIMATE OF THE SOLUTION VECTOR
C           (X(1),X(2),...,X(NVAR)).
C
C        ISWTCH  IS A PARAMETER SET EQUAL TO  K  WHICH SELECTS THE
C           FORMULA USED TO UPDATE THE APPROXIMATION TO THE HESSIAN
C           INVERSE. FOR
C
C           K = 1 - THE  DFP  UPDATE,
C           K = 2 - THE  BFGS  UPDATE.
C
C           THE  BFGS  UPDATE IS RECOMMENDED.
C
C        MAXF  IS THE LIMIT ON THE NUMBER OF CALLS TO THE FUNCTION
C           EVALUATION ROUTINE  FUNCT.
C
C        FUNCT  IS A USER SUPPLIED SUBROUTINE TO EVALUATE  OBJF(X)
C           AND THE COMPONENTS OF THE GRADIENT  G(X)  AT THE ESTIMATE
```

```
C          X(I), I = 1,2,...,NVAR.
C
C       TOLX,TOLG ARE THE ACCURACIES REQUIRED IN THE SOLUTION, I.E. A
C          NORMAL RETURN FROM THE ROUTINE OCCURS IF THE DIFFERENCE
C          BETWEEN THE COMPONENTS OF TWO SUCCESSIVE ESTIMATES OF THE
C          SOLUTION ARE NOT GREATER THAN  MAX(TOLX*ABS(X(I)),TOLX)
C          FOR ALL  I, AND THE L2 NORM OF THE GRADIENT IS NOT GREATER
C          THAN  TOLG.
C
C       RFN  IS AN ESTIMATE OF THE EXPECTED REDUCTION IN  OBJF(X).
C          THIS ESTIMATE IS USED ONLY ON THE FIRST ITERATION SO AN
C          ORDER OF MAGNITUDE ESTIMATE WILL SUFFICE. THE INFORMATION
C          CAN BE PROVIDED IN THE FOLLOWING WAYS DEPENDING UPON THE
C          VALUE OF  RFN. FOR
C
C             RFN .GT. 0.0 - THE SETTING OF  RFN  ITSELF WILL BE TAKEN
C                            AS THE EXPECTED REDUCTION IN  OBJF(X),
C
C             RFN = 0.0    - IT IS ASSUMED THAT AN ESTIMATE OF THE
C                            MINIMUM VALUE OF  OBJF(X)  HAS BEEN SET
C                            IN THE ARGUMENT  OBJF, AND THE EXPECTED
C                            REDUCTION IN  OBJF(X)  WILL BE COMPUTED
C                            AS (INITIAL FUNCTION VALUE) MINUS OBJF,
C
C             RFN .LT. 0.0 - A MULTIPLE  ABS(RFN)  OF THE MODULUS OF
C                            THE INITIAL FUNCTION VALUE WILL BE TAKEN
C                            AS THE EXPECTED REDUCTION.
C
C       SPREC  IS THE ACCURACY REQUIRED IN THE LINEAR SEARCH TECHNIQUE
C          INVOKED BY  GQBFGS, I.E. A POINT  XM  IS ACCEPTED AS THE
C          MINIMUM ALONG THE SEARCH DIRECTION IF THE RATIO OF THE
C          DIRECTIONAL DERIVATIVE AT  XM  OVER THE DIRECTIONAL
C          DERIVATIVE AT THE INITIAL POINT IS NOT GREATER THAN  SPREC.
C
C             THE SETTING  0.100  IS RECOMMENDED.
C
C       EXTBND  IS THE UPPER BOUND ON THE MULTIPLICATIVE INCREASE IN
C          THE SEARCH SCALAR DURING THE EXTRAPOLATION PHASE OF THE
C          LINEAR SEARCH TECHNIQUE.
C
C             THE SETTING  2.000  IS RECOMMENDED.
C
C       OBJF  CONTAINS AN ESTIMATE OF THE MINIMUM VALUE OF  OBJF(X)
C          IF  RFN = 0.0. OTHERWISE IT IS ONLY AN OUTPUT PARAMETER.
C
C       IHESS  IS A PARAMETER SET EQUAL TO THE DIMENSION OF  HESS
C          WHICH IS AT LEAST  NVAR*(NVAR+1)/2.
C
C       HISTRY  IS A DUMMY PARAMETER.
C
C     ON OUTPUT
C
C       X  CONTAINS THE BEST AVAILABLE ESTIMATE OF THE SOLUTION VECTOR.
C
C       OBJF  CONTAINS THE FUNCTION VALUE AT  X.
C
C
C       HESS  IS AN ARRAY OF DIMENSION  IHESS  WHICH CONTAINS THE
C          UPPER TRIANGLE OF THE MOST RECENT APPROXIMATION TO THE
C          HESSIAN INVERSE STORED ROW-WISE.
```

```
C
C        G  CONTAINS THE COMPONENTS OF THE GRADIENT AT  X.
C
C        IERR  IS A PARAMETER SET EQUAL TO  K  WHICH GIVES THE FOLLOWING
C           TERMINATION INDICATIONS
C
C           NORMAL TERMINATION,
C             K = 0,
C           INTERMEDIATE TERMINATION,
C             K = -N(N ANY INTEGER) - USER TERMINATION,
C             K = 1 - FAILURE TO CONVERGE IN  MAXF  CALLS OF  FUNCT,
C             K = 2 - LINEAR SEARCH TECHNIQUE INDICATES THAT IT IS
C                     LIKELY THAT NO MINIMUM EXISTS,
C
C        NFCALL  IS THE NUMBER OF CALLS TO  FUNCT.
C
C        SRHVEC  CONTAINS THE CURRENT SEARCH DIRECTION VECTOR.
C
C        SOLVEC  CONTAINS THE CURRENT SOLUTION VECTOR.
C
C        GRDVEC  CONTAINS THE CURRENT GRADIENT VECTOR.
C
C        SCRVEC  IS A SCRATCH VECTOR.
C
C     WRITTEN BY K. E. HILLSTROM, MARCH, 1976.
C
C
C     INITIALIZE THE FOLLOWING PARAMETERS
C
C       IERR   - THE TERMINATION INDICATOR
C       NFCALL - THE NUMBER OF CALLS TO  FUNCT
C       REDFCN - THE INITIAL PREDICTED REDUCTION IN  OBJF
C       ITER   - THE CURRENT ITERATION NUMBER
C
      IERR = 0
      ITER=0
      NFCALL = 1
      TEMP = OBJF
C
C     ************************************************************************
      CALL FUNCT(NVAR,X,OBJF,G)
C     ************************************************************************
C
      SQGRAD=0.0
      DO 220 III=1,NVAR
  220     SQGRAD=SQGRAD+G(III)**2
C
      IF (IERR .LT. 0) GO TO 410
      REDFCN = RFN
      IF (RFN .EQ. 0.0) REDFCN = OBJF - TEMP
      IF (RFN .LT. 0.0) REDFCN = ABS(REDFCN * OBJF)
      IF (REDFCN .LE. 0.0) REDFCN = 1.0
C
C    READ INITIAL ESTIMATE OF HESSIAN INVERSE, IF DESIRED
      IF(IRHESS.EQ.0) GO TO 200
      READ(11,202)  (HESS(II),II=1,IHESS)
202   FORMAT(5E16.9)
      GO TO 300
C
C     BEGIN THE QUASI-NEWTON PROCESS BY INITIALIZING THE APPROXIMATION
```

```
C       TO THE HESSIAN INVERSE TO UNITY
C
  200 IF(IPRINT.NE.0) WRITE(10,201)
  201 FORMAT(//2X,'>>>> QUASI-NEWTON PROCEDURE STARTED, WITH SEARCH',
     1       ' DIRECTION SET TO -G')
      K = 1 + NVAR * (NVAR+1) / 2
C
      DO 210 I = 1, NVAR
C
         DO 205 J = 1, I
            K = K - 1
            HESS(K) = 0.0
  205    CONTINUE
C
         HESS(K) = 1.0
  210 CONTINUE
C
  300 IF(IPRINT.EQ.0) GO TO 301
      EUCLID=SQRT(SQGRAD)
      IF(IPRINT.GE.20.AND.MOD(ITER,10).NE.0) GO TO 308
      WRITE(42,307) ITER,NFCALL,OBJF,EUCLID
  307 FORMAT(1X,'ITERATION: ',I5,26X,'FUNCTION EVALUATION: ',I6,
     1       /1X,'OBJECTIVE FUNCTION: ',E20.13,2X,'GRADIENT NORME: ',
     2        E20.13)
  308 IF(MOD(ITER,IPRINT).NE.  GO TO 301
      WRITE(10,302) ITER,NFCALL
  302 FORMAT(////2X,'ITERATION No ',I5//2X,'NUMBER OF FUNCTION AND ',
     1        'GRADIENT EVALUATIONS = ',I5//2X,'PARAMETER VALUES')
      WRITE(10,303) (J,X(J),J=1,NVAR)
  303 FORMAT(/3(2X,'X(',I4,') = ',E16.8))
      WRITE(10,304) OBJF
  304 FORMAT(//2X,'FUNCTION VALUE OBJF = ',E16.8///2X,'GRADIENT')
      WRITE(10,306) (J,G(J),J=1,NVAR)
  306 FORMAT(/3(2X,'G(',I4,') = ',E16.8))
  301 ITER=ITER+1
C
C     BEGIN AN ITERATION BY SAVING THE CURRENT BEST ESTIMATE OF THE
C       FUNCTION AND THE SOLUTION AND GRADIENT VECTORS.
C
      DO 310 I = 1, NVAR
         SOLVEC(I) = X(I)
         GRDVEC(I) = G(I)
  310 CONTINUE
C
      TOBJF = OBJF
C
C     CALCULATE THE SEARCH DIRECTION VECTOR IN  SRHVEC  AND THE
C       DIRECTIONAL DERIVATIVE IN  DIRDEV
C
      DO 340 I = 1, NVAR
         IJ = I
         Z = 0.0
C
         DO 330 J = 1, NVAR
            Z = Z - G(J) * HESS(IJ)
            IF (J .GE. I) GO TO 325
            IJ = IJ + NVAR - J
            GO TO 330
  325       IJ = IJ + 1
  330    CONTINUE
```

```
C
         SRHVEC(I) = Z
  340 CONTINUE
C
      DIRDEV = 0.0
C
      DO 350 I = 1, NVAR
         DIRDEV = DIRDEV + SRHVEC(I) * G(I)
  350 CONTINUE
C
C     IF THE DIRECTIONAL DERIVATIVE  DIRDEV  IS .GT. 0, THERE IS NO
C       GUARANTEE THAT A SEARCH IN THE  W  DIRECTION  WILL RESULT IN A
C       SMALLER  OBJF. THEREFORE, THE  QUASI-NEWTON  PROCESS IS
C       RESTARTED AT THE CURRENT ESTIMATE OF THE SOLUTION WITH  SRHVEC
C       SET TO  -G.
C
      IF (DIRDEV .GT. 0.0) GO TO 200
      IF (DIRDEV .EQ. 0.0) GO TO 500
C
C     COMPUTE THE INITIAL SEARCH SCALAR  ALPHA  AND CONDUCT THE
C       LINEAR SEARCH BY MEANS OF A CALL TO  SEARCH
C
      ALPHA = -2.0 * REDFCN / DIRDEV
      IF (ALPHA .GT. 1.0) ALPHA = 1.0
      REDFCN = OBJF
C
C     ******************************************************************
      CALL SEARCH(NVAR,X,G,SRHVEC,OBJF,ALPHA,DIRDEV,SPREC,
     1            EXTBND,NFCALL,SCRVEC,IERR)
C     ******************************************************************
C
C     TEST FOR ABNORMAL TERMINATION
C
      IF (IERR .LT. 0) GO TO 500
      IF (NFCALL .GE. MAXF) GO TO 400
      IF ((ALPHA .LT. 1.0E-20) .OR.
     1    (ALPHA .GT. 1.0E20)) GO TO 410
C
C     TEST FOR CONVERGENCE
C
      SQGRAD = 0.0
      ICONV = 0
C
      DO 360 I = 1, NVAR
         TEMP = ALPHA * SRHVEC(I)
         SQGRAD = SQGRAD + G(I) * G(I)
         T = TOLX * ABS(X(I))
         IF (T .LE. TOLX) T = TOLX
         IF (ABS(TEMP) .GT. T) ICONV = 1
  360 CONTINUE
C
      IF (SQGRAD .GT. TOLG*TOLG) ICONV = 1
      IF (SQGRAD .EQ. 0.0) ICONV = 0
      IF (ICONV .EQ. 0) GO TO 500
C
C     THE LINEAR SEARCH TECHNIQUE HAS LOCATED A MINIMUM. CALL  UPHESS
C       TO UPDATE THE APPROXIMATION TO THE HESSIAN INVERSE USING THE
C       DFP  OR  BFGS  UPDATING FORMULAS
C
C     ******************************************************************
```

```
      CALL UPHESS(NVAR,X,G,IHESS,HESS,SOLVEC,GRDVEC,SCRVEC,ISWTCH,IEXIT)
C     ******************************************************************
C
C     IF THE UPDATE IS NOT SUCCESSFUL THE QUASI-NEWTON PROCESS IS
C       RESTARTED WITH A DESCENT STEP AT THE CURRENT ESTIMATE OF THE
C       SOLUTION
C
      REDFCN = REDFCN - OBJF
      IF (IEXIT .NE. 0) GO TO 200
C
C     NOW START A NEW ITERATION
C
C  WRITE THE CURRENT ESTIMATE OF THE HESSIAN INVERSE, IF DESIRED.
      IF(IWRHESS.EQ.0) GO TO 300
      OPEN(14,MODE='OUT',ACCESS='SEQUENTIAL',FORM='FORMATTED',
     1       FILE='LAST.HESS')
      WRITE(14,202)  (HESS(II),II=1,IHESS)
      CLOSE(14)
C
      GO TO 300
C
C     ERROR RETURN BECAUSE THERE HAVE BEEN AT LEAST  MAXF  CALLS OF
C       FUNCT
C
  400 IERR = 1
      GO TO 450
C
C     ERROR RETURN BECAUSE LINEAR SEARCH TECHNIQUE INDICATES THAT IT IS
C       LIKELY THAT NO MINIMUM EXISTS
C
  410 IERR = 2
C
  450 DO 455 I = 1, NVAR
         X(I) = SOLVEC(I)
         G(I) = GRDVEC(I)
  455 CONTINUE
C
      OBJF = TOBJF
  500 RETURN
C
      END



      SUBROUTINE SEARCH(N,X,G,S,F,ALPHA,DIRDEV,SPREC,EXTBND,NFCALL,
     1                  W,IERR)
C
      IMPLICIT REAL*8(A-H,O-Z)
      DIMENSION  X(200),G(200),S(200),W(200)
C
C       THIS SUBROUTINE OBTAINS AN ESTIMATE OF THE SOLUTION
C     XM = XO + ALPHA * S  WHICH MINIMIZES  F  BY MEANS OF A LINEAR
C     SEARCH IN THE  S  DIRECTION.
C
C     ON INPUT
C
C        N  IS THE NUMBER OF VARIABLES. IT IS ALSO THE DIMENSION OF THE
C           VECTORS  X, G  AND  S.
C
```

```
C        X  CONTAINS AN ESTIMATE OF THE SOLUTION VECTOR
C           (XO(1),XO(2),...,XO(N)).
C
C        S  CONTAINS THE SEARCH DIRECTION VECTOR.
C
C        F  CONTAINS THE OBJECTIVE FUNCTION  F(X).
C
C        FUNCT  IS A USER SUPPLIED ROUTINE TO EVALUATE  F(X)  AND THE
C           COMPONENTS OF THE GRADIENT  G(X)  AT THE ESTIMATE IN  X.
C
C        ALPHA  IS  THE INITIAL STEP SCALAR.
C
C        DIRDEV  IS THE DIRECTIONAL DERIVATIVE AT X.
C
C        SPREC  IS THE ACCURACY REQUIRED IN THE SEARCH, I.E. A POINT  XM
C           IS ACCEPTED AS THE MINIMUM ALONG DIRECTION  S  IF THE RATIO
C           OF THE DIRECTIONAL DERIVATIVE AT  XM  OVER THE DIRECTIONAL
C           DERIVATIVE AT  XO  IS NOT GREATER THAN  SPREC.
C
C        EXTBND  IS THE UPPER BOUND ON THE MULTIPLICATIVE INCREASE IN
C           ALPHA  DURING EXTRAPOLATION.
C
C        NFCALL  IS THE NUMBER OF CALLS TO THE FUNCTION EVALUATION
C           SUBROUTINE  FCN.
C
C        W  IS A SCRATCH VECTOR.
C
C     ON OUTPUT
C
C        X  CONTAINS THE ESTIMATE OF THE MINIMUM
C           (XM(1),XM(2),...,XM(N))
C
C     IERR  IS A PARAMETER SET TO A NEGATIVE INTEGER IF THE USER
C           WISHES TO FORCE AN EXIT FROM  SEARCH. OTHERWISE IT IS
C           UNALTERED.
C
C        G  CONTAINS THE COMPONENTS OF THE GRADIENT AT  X.
C
C        F  CONTAINS THE FUNCTION VALUE  F(X).
C
C        ALPHA  IS THE FINAL STEP SCALAR.
C
C        DIRDEV  IS THE DIRECTIONAL DERIVATIVE AT  X.
C
C        NFCALL  IS THE NUMBER OF CALLS TO THE FUNCTION EVALUATION
C           SUBROUTINE  FUNCT.
C
C
C     INITIALIZE THE FOLLOWING PARAMETERS AND INDICATORS
C
C       TOT       -  THE SUM OF THE EXTRAPOLATION STEPS
C       CDIREV    -  THE CURRENT DIRECTIONAL DERIVATIVE
C       PDIREV    -  THE PREVIOUS DIRECTIONAL DERIVATIVE
C       IERR      -  THE ERROR INDICATOR
C
      TOT = 0.0
      CDIREV = DIRDEV
      PDIREV = DIRDEV
C
C     TEST WHETHER  ALPHA  IS TOO SMALL
```

```
C
  105 IF (ALPHA .LE. 1.0E-20) GO TO 150
C
C     BEGIN THE LINEAR SEARCH BY INCREMENTING THE SOLUTION VECTOR  X
C       AND CALCULATING THE FUNCTION AND GRADIENT AT THE INCREMENTED  X.
C
      DO 108 I = 1, N
         W(I) = X(I)
         X(I) = X(I) + ALPHA * S(I)
  108 CONTINUE
C
C     ***8**********************************************************
      CALL FUNCT(N,X,FTEST,G)
C     **********************************************8***************
C
      NFCALL = NFCALL + 1
      IF (IERR .LT. 0) GO TO 150
C
C     COMPUTE THE DIRECTIONAL DERIVATIVE  DIRDEV  AT  X + ALPHA * S
C
      DIRDEV = 0.0
C
      DO 110 I = 1, N
         DIRDEV = DIRDEV + G(I) * S(I)
  110 CONTINUE
C
C     TEST WHETHER  F(X + ALPHA * S)  IS LESS THAN  F(X).
C
      IF (FTEST .GE. F) GO TO 120
C
C     IF (DIRDEV / PDIREV) IS LESS THAN THE SEARCH PRECISION  SPREC,
C       ALPHA  IS ACCEPTED. OTHERWISE  ALPHA  IS MODIFIED
C
      IF (ABS(DIRDEV / PDIREV) .LE. SPREC) GO TO 140
C
C     ALPHA  IS MODIFIED. TEST WHETHER  ALPHA  IS TO BE REVISED BY
C       EXTRAPOLATION OR INTERPOLATION
C
      IF (DIRDEV .GT. 0.0) GO TO 120
C
C     ALPHA  IS REVISED USING AN EXTRAPOLATION FORMULA AND A NEW STEP
C       IS TAKEN IF THE SUM OF THE STEPS ALREADY MADE IS NOT TOO LARGE.
C       THE INPUT PARAMETER  EXTBND  LIMITS THE MULTIPLICATIVE CHANGE
C       IN  ALPHA
C
      TOT = TOT + ALPHA
      IF (TOT .GT. 1.0E10) GO TO 145
      TEMP = EXTBND
      IF (CDIREV .LT. DIRDEV) TEMP = DIRDEV / (CDIREV - DIRDEV)
      IF (TEMP .GT. EXTBND) TEMP = EXTBND
      F = FTEST
      CDIREV = DIRDEV
      ALPHA = ALPHA * TEMP
      GO TO 105
C
C     X  IS RESET TO THE CURRENT ESTIMATE, ALPHA  IS REVISED USING THE
C       CUBIC INTERPOLATION FORMULA AND A NEW STEP IS TAKEN IF THE
C       CONVERGENCE CRITERIA HAVE NOT BEEN SATISFIED.
C
  120 DO 130 I = 1, N
```

```
         X(I) = W(I)
  130 CONTINUE
C
      TEMP = 3.0 * (F - FTEST) / ALPHA + DIRDEV + CDIREV
      WT = ABS(TEMP)
      IF(WT.LT.ABS(DIRDEV)) WT=ABS(DIRDEV)
      IF(WT.LT.ABS(CDIREV)) WT=ABS(CDIREV)
      WW = TEMP / WT
      WW = WW * WW - CDIREV / WT * DIRDEV / WT
      IF (WW .LT. 0.0) WW = 0.0
      WW = SQRT(WW) * WT
      TEMP = 1.0 - (DIRDEV + WW - TEMP) / (2.0 * WW + DIRDEV -
     1       CDIREV)
      ALPHA = ALPHA * TEMP
      GO TO 105
C
C     ALPHA IS ACCEPTED
C
  140 F = FTEST
  145 ALPHA = TOT + ALPHA
  150 RETURN
C
      END



      SUBROUTINE UPHESS(N,X,G,IH,H,SOLVEC,GRDVEC,SCRVEC,ISWTCH,IEXIT)
C
      IMPLICIT REAL*8(A-H,O-Z)
      DIMENSION  X(200),G(200),H(20100),SOLVEC(200),GRDVEC(200),
     1           SCRVEC(200)
C
C     THIS SUBROUTINE UPDATES AN APPROXIMATION TO THE HESSIAN INVERSE
C       USING THE  DFP  OR  BFGS  FORMULA
C
C     ON INPUT
C
C        N  IS THE DIMENSION OF THE VECTORS  X, G, SOLVEC, GRDVEC  AND
C           SCRVEC.
C
C        X  CONTAINS AN ESTIMATE OF THE SOLUTION VECTOR.
C
C        G  CONTAINS THE COMPONENTS OF THE GRADIENT CORRESPONDING TO
C           THE  X  VECTOR.
C
C        IH  IS A PARAMETER SET EQUAL TO THE DIMENSION OF  H  WHICH IS
C           AT LEAST  N*(N+1)/2.
C
C        H  IS AN ARRAY OF DIMENSION  IH  WHICH CONTAINS THE UPPER
C           TRIANGLE OF AN APPROXIMATION TO THE HESSIAN INVERSE STORED
C           BY ROWS.
C
C        SOLVEC  CONTAINS THE CURRENT SOLUTION VECTOR.
C
C        GRDVEC  CONTAINS THE CURRENT GRADIENT VECTOR.
C
C        ISWTCH  IS A PARAMETER SET EQUAL TO  K  WHICH SELECTS THE
C           UPDATING FORMULA. FOR
C
```

```
C           K = 1 - THE  DFP  FORMULA IS USED,
C           K = 2 - THE  BFGS  FORMULA IS USED.
C
C     ON OUTPUT
C
C        IEXIT  IS A PARAMETER SET EQUAL TO  K  WHICH INDICATES THE
C           FOLLOWING. FOR
C
C           K = 0 - THE UPDATE WAS SUCCESSFUL,
C           K = 1 - THE UPDATE FAILED DUE TO ZERO DIVISORS.
C
C        H  CONTAINS THE UPDATED APPROXIMATION TO THE HESSIAN INVERSE
C           IF  IEXIT = 0.
C
C        SCRVEC  IS A SCRATCH VECTOR.
C
C     WRITTEN BY K. E. HILLSTROM, MARCH, 1976.
C
C
C     INITIALIZE THE EXIT INDICATOR  IEXIT
C
      IEXIT = 0
C
C     CALCULATE THE SOLUTION AND GRADIENT DIFFERENCE VECTORS FROM TWO
C       CONSECUTIVE ITERATIONS. FROM THIS SECTION ON
C
C       SOLVEC - CONTAINS  DELTA, THE SOLUTION DIFFERENCE VECTOR
C       GRDVEC - CONTAINS  GAMMA, THE GRADIENT DIFFERENCE VECTOR
C
  100 DO 110 I = 1, N
         SOLVEC(I) = X(I) - SOLVEC(I)
         GRDVEC(I) = G(I) - GRDVEC(I)
  110 CONTINUE
C
C     CALCULATE  Z = (GAMMA TRANSPOSE) * DELTA AND ALPHA =
C       (GAMMA TRANSPOSE) * (HESSIAN INVERSE) * GAMMA  OCCURING AS
C       DENOMINATORS IN THE  DFP  FORMULA. FROM THIS SECTION ON
C
C       H      - CONTAINS THE APPROXIMATION TO THE HESSIAN INVERSE
C       SCRVEC - CONTAINS THE SUCCESSIVE ELEMENTS OF  (GAMMA TRANSPOSE)
C                * (HESSIAN INVERSE)
C
      Z = 0.0
      ALPHA = 0.0
C
      DO 130 I = 1, N
         WT = GRDVEC(I)
         Z = Z + WT * SOLVEC(I)
         K = I
         WT = 0.0
C
         DO 120 J = 1, N
            WT = WT + GRDVEC(J) * H(K)
            IF (J .GE. I) GO TO 115
            K = K + N - J
            GO TO 120
  115       K = K + 1
  120    CONTINUE
C
         ALPHA = ALPHA + WT * GRDVEC(I)
```

```
         SCRVEC(I) = WT
  130 CONTINUE
C
C     ERROR EXIT IF THE  DFP  OR  BFGS  FORMULA BREAKS DOWN DUE TO ZERO
C       DIVISORS  Z  AND/OR  ALPHA
C
      IF ((Z .EQ. 0.0) .OR.
     1    (ALPHA .EQ. 0.0 .AND. ISWTCH .EQ. 1)) GO TO 200
C
C     UPDATE THE APPROXIMATION TO THE HESSIAN INVERSE USING THE  DFP
C       OR  BFGS  UPDATING FORMULA
C
      K = 1
C
      DO 160 I = 1, N
C
         DO 150 J = I, N
            IF (ISWTCH .EQ. 1) GO TO 135
            H(K) = H(K) - (SOLVEC(I) * SCRVEC(J) + SCRVEC(I) *
     1              SOLVEC(J)) / Z + (1.0 + ALPHA / Z) * (SOLVEC(I) *
     2              SOLVEC(J) / Z)
            GO TO 140
  135       H(K) = H(K) + SOLVEC(I) * SOLVEC(J) / Z - SCRVEC(I) *
     1              SCRVEC(J) / ALPHA
  140       K = K + 1
  150    CONTINUE
C
  160 CONTINUE
C
      GO TO 300
C
C     ERROR RETURN DUE TO ZERO DIVISORS IN THE UPDATING FORMULA
C
  200 IEXIT = 1
  300 RETURN
C
      END




      SUBROUTINE PRCD
C
C  Subroutine to print atom coordinates to output file
C
      IMPLICIT REAL*8(A-H,O-Z)
      INTEGER ICHIR(100), KIND(600), MODUL(600), CONNECT(0:5,0:5)
      INTEGER IC(200), ISEG(600)
      REAL*8 L, LH, LR
      DIMENSION X(600), Y(600), Z(600), VC(3), VH1D(3), VH1L(3),
     1          VH2(3), VH3(3), VRD(3), VRL(3), TO(3,3), TP(3,3),
     2          TPP(3,3), TPROD(3,3)
      COMMON /BLOCK1/ X, Y, Z
      COMMON /BLOCK2/ ICHIR, KIND, IC, ISEG, MODUL, CONNECT
      COMMON /BLOCK3/ NUNITS, NBONDS, NSEGMENTS, NATOMS, THETAP,
     1                THETAHP, THETAPP, THETAHPP, THETARPP, STHP,
     2                CSTHP, STHPP, CSTHPP, L, LH, LR, VC, VH1D,
     3                VH1L, VH2, VH3, VRD, VRL, TO, TP, TPP, TPROD
      WRITE(6,10)
   10 FORMAT(////10X,'ATOM COORDINATES'/10X,16('-')//9X,
```

```
     1        'BACKBONE ATOM',13X,'L-SUBSTITUENT',10X,'D-SUBSTITUENT'/)
      ISEGM=0
      WRITE(6,20) ISEGM, X(1), Y(1), Z(1)
   20 FORMAT(/2X,I4,2X,'C  ',E16.7,'(METHYL) '/10X,E16.7/10X,E16.7)
      ICARBON=-1
      DO 30 IUNIT=1,NUNITS-1
           ISEGM=ISEGM+1
           ICARBON=ICARBON+3
           IF(ICHIR(IUNIT)) 60,70,70
   60      WRITE(6,80) ISEGM,X(ICARBON),X(ICARBON+2),X(ICARBON+1)
   80      FORMAT(/2X,I4,2X,'C  ',E16.7,5X,'R  ',E16.7,5X,'H  ',E16.7)
           WRITE(6,90) Y(ICARBON),Y(ICARBON+2),Y(ICARBON+1)
   90      FORMAT(10X,E16.7,7X,E16.7,7X,E16.7)
           WRITE(6,90) Z(ICARBON),Z(ICARBON+2),Z(ICARBON+1)
           GO TO 100
   70      WRITE(6,110) ISEGM,(X(I),I=ICARBON,ICARBON+2)
  110      FORMAT(/2X,I4,2X,'C  ',E16.7,5X,'H  ',E16.7,5X,'R  ',E16.7)
           WRITE(6,90) (Y(I),I=ICARBON,ICARBON+2)
           WRITE(6,90) (Z(I),I=ICARBON,ICARBON+2)
  100      ISEGM=ISEGM+1
           ICARBON=ICARBON+3
           WRITE(6,120) ISEGM,X(ICARBON),X(ICARBON+2),X(ICARBON+1)
  120      FORMAT(/2X,I4,2X,'C  ',E16.7,5X,'H  ',E16.7,5X,'H  ',E16.7)
           WRITE(6,90) Y(ICARBON),Y(ICARBON+2),Y(ICARBON+1)
           WRITE(6,90) Z(ICARBON),Z(ICARBON+2),Z(ICARBON+1)
   30 CONTINUE
      ISEGM=ISEGM+1
      ICARBON=ICARBON+3
      IF(ICHIR(NUNITS)) 130,140,140
  130 WRITE(6,80) ISEGM,X(ICARBON),X(ICARBON+2),X(ICARBON+1)
      WRITE(6,90) Y(ICARBON),Y(ICARBON+2),Y(ICARBON+1)
      WRITE(6,90) Z(ICARBON),Z(ICARBON+2),Z(ICARBON+1)
      GO TO 150
  140 WRITE(6,110) ISEGM,(X(I),I=ICARBON,ICARBON+2)
      WRITE(6,90) (Y(I),I=ICARBON,ICARBON+2)
      WRITE(6,90) (Z(I),I=ICARBON,ICARBON+2)
  150 ISEGM=ISEGM+1
      WRITE(6,20) ISEGM,X(NATOMS),Y(NATOMS),Z(NATOMS)
C
      RETURN
      END



      SUBROUTINE MATVEC(A, V, AV, MFORM, NFORM, M, N)
C
C  Matrix- vector multiplication, A.V=AV
C
      IMPLICIT REAL*8(A-H,O-Z)
      DIMENSION A(MFORM,NFORM), V(NFORM), AV(MFORM), VAUX(25)
      DO 1 I=1,M
        X=0.0
        DO 2 K=1,N
    2   X=X+A(I,K)*V(K)
    1 VAUX(I)=X
      DO 3 I=1,M
    3 AV(I)=VAUX(I)
      RETURN
      END
```

```
      SUBROUTINE MATMAT(A,B,AB,MFORM,NFORM,LFORM,M,N,L)
C
C  Matrix multiplication A.B=AB
C
      IMPLICIT REAL*8(A-H,O-Z)
      DIMENSION A(MFORM,NFORM), B(NFORM,LFORM), AB(MFORM,LFORM),
     1          AUX(25,25)
      DO 1 I=1,M
      DO 1 J=1,L
        X=0.0
        DO 2 K=1,N
    2   X=X+A(I,K)*B(K,J)
    1 AUX(I,J)=X
      DO 3 I=1,M
      DO 3 J=1,L
    3 AB(I,J)=AUX(I,J)
      RETURN
      END



      SUBROUTINE VCROSSV(V1,V2,V3)
C
C  Formation of the external(cross) product of two vectors, V3=V1xV2
C  Subroutine is designed so that the product can be written in one of
C  the factors (V1 or V2 can be used in place of V3)
C
      IMPLICIT REAL*8(A-H,O-Z)
      DIMENSION V1(3), V2(3), V3(3)
C
      VAUX1=V1(2)*V2(3)-V2(2)*V1(3)
      VAUX2=V1(3)*V2(1)-V2(3)*V1(1)
      VAUX3=V1(1)*V2(2)-V2(1)*V1(2)
C
      V3(1)=VAUX1
      V3(2)=VAUX2
      V3(3)=VAUX3
C
      RETURN
      END



      SUBROUTINE VECVEC(V1, V2, PRODUCT, NFORM, N)
C
C  Vector multiplication, V1T.V2=PRODUCT
C
      IMPLICIT REAL*8(A-H,O-Z)
      DIMENSION V1(NFORM), V2(NFORM)
      PRODUCT=0.0
      DO 1 I=1,N
    1 PRODUCT=PRODUCT+V1(I)*V2(I)
      RETURN
      END
```

```
      SUBROUTINE SETSCALE(NDF,SCALE)
C
C  Subroutine to setup scaling factors for the rotation angles, to be used
C  in the minimization.
C
      IMPLICIT REAL*8(A-H,O-Z)
      DIMENSION SCALE(NDF)
      DO 5 I=1,3
    5     SCALE(I)=1.
C
      DO 10 I=4,NDF
   10     SCALE(I)=SQRT(1.-FLOAT(I-2)/(NDF-1))
C
      RETURN
      END



      SUBROUTINE FUNCT(NDF, PHI, ENERGY, GRADX)
C
C    Subroutine computes the total potential energy of a box of bulk
C  amorphous polymer, filled with segments of a single 'parent' chain,
C  displaced according to the requirements of periodic boundary
C  conditions.
C    The gradients of the total energy with respect to the chain
C   degrees of freedom are also computed.
C    A chain model with rigid bond lengths and valence bond angles
C  is used, so that the only internal degrees of freedom of the chain
C  are the NDF-3=NBONDS-2 rotational angles of bonds 2,3,...,NBONDS-1.
C    The three external orientation (Eulerian) angles alpha, beta,
C  gamma comprise three additional degrees of freedom.
C    Potential energy terms which do not change with conformation in
C  the rigid bond length and bond angle model employed here are not
C  accounted for in the energy computation. Thus, only interactions
C  between atoms separated  by more than two bonds from each other are
C  included in the energy and derivative summations.
C    The parent chain has NBONDS=NDF-1 bonds, numbered from 1 to NDF-1,
C  and NATOMS=3NDF-4 atoms, numbered from 0 to 3NDF-4.
C    The degree of polymerization is X=(NDF-1)/2.
C    The rotation angle of bond i is kept in array element PHI(i+2).
C    The respective component of the gradient of the energy is to be
C   found upon return in array element GRADX(i+2).
C    Eulerian angles alpha, beta, gamma are treated formally
C  as bond angles, stored in the elements 1,2,3 of the vector PHI.
C
      IMPLICIT REAL*8(A-H,O-Z)
      INTEGER KIND(600), MODUL(600), CONNECT(0:5,0:5), ICHIR(100)
      INTEGER IC(200), ISEG(600)
      REAL*8 L,LH,LR
      CHARACTER*4 NAME(3)
      DIMENSION X(600), Y(600), Z(600), VC(3), VH1D(3), VH1L(3),
     1          VH2(3), VH3(3), VRD(3), VRL(3), FORCE(3),
     2          TO(3,3), TP(3,3), TPP(3,3), TPROD(3,3), AX(3), AY(3),
     3          AZ(3), AXCY(3), AYCZ(3), AZCX(3),ORIGIN(3), ALFA(3),
     4          EFFNE(3), VDWR(3), EPS(3,3), SIGMA(3,3),RANGE(3,3),
```

```
     5          RANGEX(3,3), RANGEY(3,3), RANGEZ(3,3), PHI(200),
     6          SCALE(200), GRADX(200), GRADY(200), GRADZ(200),
     7          VECT(3), EPSIG(3,3), XP(600), YP(600), ZP(600)
      COMMON /BLOCK1/ X, Y, Z
      COMMON /BLOCK2/ ICHIR, KIND, IC, ISEG, MODUL, CONNECT
      COMMON /BLOCK3/ NUNITS, NBONDS, NSEGMENTS, NATOMS, THETAP,
     1                THETAHP, THETAPP, THETAHPP, THETARPP, STHP,
     2                CSTHP, STHPP, CSTHPP, L, LH, LR, VC, VH1D,
     3                VH1L, VH2, VH3, VRD, VRL, TO, TP, TPP, TPROD
      COMMON /BLOCK4/SA,CSA,SB,CSB,SG,CSG, AX, AY, AZ, AXX, AYY, AZZ,
     1                AXCY, AYCZ, AZCX, ORIGIN, VOLUME
      COMMON /BLOCK5/ ALFA, EFFNE, VDWR, EPS, SIGMA, EPSIG, RANGE,
     1                RANGEX, RANGEY, RANGEZ, NAME, NNUC, RR1, RR2,
     2                DELRR, AU, BU, CU, AF, BF, CF, ROTBAR
      COMMON /BLOCK6/ ETOTLJ, ETOTROT, GRADY, GRADZ, SCALE
      COMMON /BLOCK7/ XP, YP, ZP
C
C  Descale rotation angles to their true values
C  (artificial phi=scale*true phi)
C  After this conversion, rotation angles are in true degrees.
      DO 5 I=1,NDF
    5     PHI(I)=PHI(I)/SCALE(I)
C
C  Bring all rotation angles into the interval (-180,180)
      DO 6 I=1,NDF
         PHI(I)=PHI(I)-INT(PHI(I)/360.)*360
         IF(PHI(I).LT.-180.) PHI(I)=PHI(I)+360.
         IF(PHI(I).GT. 180.) PHI(I)=PHI(I)-360.
    6 CONTINUE
C
C  Write all degrees of freedom to file LAST.DF, which keeps
C  track of the latest system configuration.
      OPEN(12,MODE='OUT',ACCESS='SEQUENTIAL',FORM='FORMATTED',
     1        FILE='LAST.DF')
      WRITE(12,7) X(1),Y(1),Z(1)
    7 FORMAT(3E16.9)
      WRITE(12,7) PHI(1),PHI(2),PHI(3)
      WRITE(12,9) (ICHIR(I),I=1,NUNITS)
    9 FORMAT(40I2)
      WRITE(12,10) (PHI(I),I=4,NDF)
   10 FORMAT(5E16.9)
      CLOSE(12)
C
C  Convert angles from degrees to radians
C  After this conversion, angles are in true radians, lying between
C  -pi and pi.
      DEGRAD=ASIN(1.)/90.
      DO 15 I=1,NDF
   15    PHI(I)=PHI(I)*DEGRAD
C
C  Calculate coordinates of all atoms in the cube
      ISTART=0
      CALL COORD(NDF,PHI,ISTART)
C
C  Computation of that part of the energy and gradient, which is due to
C  LENNARD-JONES INTERATOMIC INTERACTIONS
C  ------------------------------------
C
C  Initialize energy and energy gradient
      ETOTLJ=0.0
```

```
      DO 20 I=1,NDF
           GRADX(I)=0.0
           GRADY(I)=0.0
           GRADZ(I)=0.0
   20 CONTINUE
C
C  Outer loop over all atoms
      DO 30 J1=6,NATOMS
           ISGJ13=ISEG(J1)+3
           ISGJ12=ISGJ13-1
           MODJ1=MODUL(J1)
           NUC1=KIND(J1)
           X1=X(J1)
           Y1=Y(J1)
           Z1=Z(J1)
           XP1=XP(J1)
           YP1=YP(J1)
           ZP1=ZP(J1)
C
C  Internal loop over all atoms
           DO 30 J2=1,J1-2
C
C  Test if connectivity screening is necessary
                IF(J1-J2.GT.6) GO TO 40
C
C  Reject interaction if atoms J1 and J2 are less than three bonds
C  apart using the connectivity table, CONNECT
                IF(CONNECT(MODJ1,MODUL(J2))) 40,30,40
C
C  Screening, to determine if the interaction between J1 and J2
C  should be accounted for and, if yes, which image of J2 should
C  be used
C
   40           NUC2=KIND(J2)
                RNG2=RANGE(NUC1,NUC2)
                RNGX=RANGEX(NUC1,NUC2)
                RNGY=RANGEY(NUC1,NUC2)
                RNGZ=RANGEZ(NUC1,NUC2)
C
                DX=X1-X(J2)
                DY=Y1-Y(J2)
                DZ=Z1-Z(J2)
                ADX=ABS(DX)
                ADY=ABS(DY)
                ADZ=ABS(DZ)
C
                IF(ADX.GE.RNGX) GO TO 50
                LIMG=0
                     IF(ADY.GE.RNGY) GO TO 60
                     MIMG=0
                          IF(ADZ.GE.RNGZ) GO TO 70
                          NIMG=0
                          GO TO 80
   70                          IF(ADZ.LT.AZZ-RNGZ)              GO TO 30
                               NIMG=1
                                    IF(DZ.LT.0.0) NIMG=-NIMG
                                    GO TO 80
   60                     IF(ADY.LT.AYY-RNGY)              GO TO 30
                               IF(ADZ.GE.RNGZ) GO TO 90
                               NIMG=0
```

```
                    MIMG=1
                        IF(DY.LT.0.0) MIMG=-MIMG
                        GO TO 80
 90                     IF(ADZ.LT.AZZ-RNGZ)              GO TO 30
                        MIMG=1
                            IF(DY.LT.0.0) MIMG=-MIMG
                            NIMG=1
                                IF(DZ.LT.0.0) NIMG=-NIMG
                                GO TO 80
 50             IF(ADX.LT.AXX-RNGX)              GO TO 30
                    IF(ADY.GE.RNGY) GO TO 100
                    MIMG=0
                        IF(ADZ.GE.RNGZ) GO TO 110
                        NIMG=0
                        LIMG=1
                            IF(DX.LT.0.0) LIMG=-LIMG
                            GO TO 80
110                         IF(ADZ.LT.AZZ-RNGZ)              GO TO 30
                            LIMG=1
                                IF(DX.LT.0.0) LIMG=-LIMG
                                NIMG=1
                                    IF(DZ.LT.0.0) NIMG=-NIMG
                                    GO TO 80
100                     IF(ADY.LT.AYY-RNGY)              GO TO 30
                            IF(ADZ.GE.RNGZ) GO TO 120
                            NIMG=0
                            LIMG=1
                                IF(DX.LT.0.0) LIMG=-LIMG
                                MIMG=1
                                    IF(DY.LT.0.0) MIMG=-MIMG
                                    GO TO 80
120                                 IF(ADZ.LT.AZZ-RNGZ)          GO TO 30
                                    LIMG=1
                                        IF(DX.LT.0.0) LIMG=-LIMG
                                        MIMG=1
                                            IF(DY.LT.0.0) MIMG=-MIMG
                                            NIMG=1
                                                IF(DZ.LT.0.0) NIMG=-NIMG
C
 80         IF(LIMG) 81,83,82
 81         DX=DX+AX(1)
            DY=DY+AX(2)
            DZ=DZ+AX(3)
            GO TO 83
 82         DX=DX-AX(1)
            DY=DY-AX(2)
            DZ=DZ-AX(3)
 83         IF(MIMG) 84,86,85
 84         DX=DX+AY(1)
            DY=DY+AY(2)
            DZ=DZ+AY(3)
            GO TO 86
 85         DX=DX-AY(1)
            DY=DY-AY(2)
            DZ=DZ-AY(3)
 86         IF(NIMG) 87,89,88
 87         DX=DX+AZ(1)
            DY=DY+AZ(2)
            DZ=DZ+AZ(3)
            GO TO 89
```

```
   88          DX=DX-AZ(1)
               DY=DY-AZ(2)
               DZ=DZ-AZ(3)
   89          R=DX*DX+DY*DY+DZ*DZ
C
               IF(R.GE.RNG2) GO TO 30
C
C  Calculate interaction energy and magnitude of interaction force
C  Find reduced radius RR=R/SIGMA
               R=SQRT(R)
               RR=R/SIGMA(NUC1,NUC2)
C
C  Branch, according to relative magnitude of RR, RR1 (from screening,
C  RR<RR2)
               IF(RR.GT.RR1) GO TO 130
C
C  Normal 6-12 potential expression used
               X6=(1./RR)**6
               X12=X6*X6
               EPSILON=EPS(NUC1,NUC2)
               ULJ=4.*EPSILON*(X12-X6)
               DULJ=-24.*EPSILON/R*(2.*X12-X6)
               GO TO 140
C
C  Quintic spline used
  130          XI=(RR-RR1)/DELRR
               XI2=XI*XI
               XI1=1.-XI
               XI12=XI1*XI1
               ULJ=EPS(NUC1,NUC2)*XI12*XI1*(AU*XI2+BU*XI+CU)
               DULJ=EPSIG(NUC1,NUC2)*XI12*(AF*XI2+BF*XI+CF)
C
C
C  Update energy
C  -------------
  140          ETOTLJ=ETOTLJ+ULJ
C     WRITE(42,121) J1,J2,NUC1,NUC2,R,ULJ,DULJ
C 121 FORMAT('J1=',I5,3X,'J2=',I5,3X,'NUC1=',I1,3X,'NUC2=',I1,3X,'R=',
C    1        E16.9,3X,'ULJ=',E16.9,3X,'DULJ=',E16.9)
C
C  Calculate components of force vector
               DULJR=DULJ/R
               FORCE(1)=DULJR*DX
               FORCE(2)=DULJR*DY
               FORCE(3)=DULJR*DZ
C
C  Update gradient
C  ---------------
C  Contribution to gradient components corresponding to rotation angles
C  of bonds lying between the segments to which parent atoms J1 and J2
C  are connected
               ISGJ23=ISEG(J2)+3
               ISGJ22=ISGJ23-1
               DO 150 I=ISGJ23,ISGJ12
                    ICARBON=IC(I)
                    VECT(1)=XP1-XP(ICARBON)
                    VECT(2)=YP1-YP(ICARBON)
                    VECT(3)=ZP1-ZP(ICARBON)
                    GRADX(I)=GRADX(I)+VECT(2)*FORCE(3)-VECT(3)*FORCE(2)
                    GRADY(I)=GRADY(I)+VECT(3)*FORCE(1)-VECT(1)*FORCE(3)
```

```
                GRADZ(I)=GRADZ(I)+VECT(1)*FORCE(2)-VECT(2)*FORCE(1)
  150         CONTINUE
C
C  Contribution to gradient components corresponding to rotation angles
C  of  bonds lying before the images of both J1 and J2 in the parent
C  chain
              VECT(1)=XP1-XP(J2)-DX
              VECT(2)=YP1-YP(J2)-DY
              VECT(3)=ZP1-ZP(J2)-DZ
              DO 155 I=1,ISGJ22
                  GRADX(I)=GRADX(I)+VECT(2)*FORCE(3)-VECT(3)*FORCE(2)
                  GRADY(I)=GRADY(I)+VECT(3)*FORCE(1)-VECT(1)*FORCE(3)
                  GRADZ(I)=GRADZ(I)+VECT(1)*FORCE(2)-VECT(2)*FORCE(1)
  155         CONTINUE
C
C
   30 CONTINUE
C
C
C  Calculate that part of the gradient which is due to interatomic
C  interactions from the vectorial elements accumulated in GRADX,
C  GRADY, GRADZ. Gradient is stored in GRADX.
C
      GRADX(1)=GRADZ(1)
      GRADX(2)=-SA*GRADX(2)+CSA*GRADY(2)
      GRADX(3)=(-CSA*GRADX(3)-SA*GRADY(3))*SB-CSB*GRADZ(3)
      DO 160 I=4,NDF
          ICARB=IC(I-1)
          ICARB1=IC(I)
          VECT(1)=(XP(ICARB1)-XP(ICARB))/L
          VECT(2)=(YP(ICARB1)-YP(ICARB))/L
          VECT(3)=(ZP(ICARB1)-ZP(ICARB))/L
          GRADX(I)=VECT(1)*GRADX(I)+VECT(2)*GRADY(I)+VECT(3)*GRADZ(I)
  160 CONTINUE
C
C
C  Computation of that part of the energy and energy gradient which is
C  due to the BOND ROTATIONAL POTENTIAL
C              ------------------------
      ETOTROT=0.0
      DO 170 I=4,NDF
          ANGLE=3.*PHI(I)
          ETOTROT=ETOTROT+ROTBAR/2.*(1.-COS(ANGLE))
          GRADX(I)=GRADX(I)+1.5*ROTBAR*SIN(ANGLE)
  170 CONTINUE
C
      ENERGY=ETOTLJ+ETOTROT
C
C  Scale rotational angles and convert angle measuring scale from
C  radians to degrees, to prepare for reentry to the optimization
C  routine.
C  Also form gradient with respect to the artificial(scaled) angles
C  from the true gradient (Elements of the artificial gradient should
C  be of roughly the same order of magnitude).
C  (Upon exit from FUNCT, angles are in scaled degrees)
      DO 180 I=1,NDF
          ECHELLE=SCALE(I)
          PHI(I)=PHI(I)*ECHELLE/DEGRAD
          GRADX(I)=GRADX(I)/ECHELLE*DEGRAD
  180 CONTINUE
```

```
C
      RETURN
      END



      SUBROUTINE COORD(NDF,PHI,ISTART)
C
C    Subroutine forms coordinates of all atoms of a vinyl chain
C
C                  CH3-(CHR-CH2)nunits-H
C
C  of given tacticity, in a periodic box, given the position of the
C  first carbon of the chain, the orientation of the first two skeletal
C  bonds, and the rotation angles of all subsequent bonds of the chain.
C
C    The chain has NBONDS=NDF-1 bonds, numbered from 1 to NDF-1
C    The chain has NSEGMENTS=NDF skeletal segments, numbered from 0 to
C    NDF-1 (Flory's convention).
C    Overall the chain has NATOMS=3NDF-4 atoms (or atomic groups),
C    of which :
C               2  are terminal methyls
C          (NDF-1)/2  are chiral carbons
C        (NDF-1)/2-1  are achiral carbons
C       (3NDF-1)/2-3  are hydrogens
C          (NDF-1)/2  are R-substituents
C
C  NOTE ON BOOKKEEPING
C    The rotation angle of bond i is kept in array element PHI(i+2)
C  (upon entrance to COORD, all angles must be in radians).
C    The x-,y-,and z- coordinates of all atoms, regardless of type,
C   are stored in three unidimensional arrays X,Y,Z. The exact nature
C   and position of an atom in the parent chain can be inferred from
C   its index in these arrays. Specifically, the correspondence between
C   indices and atoms is the
C  following:
C    Index = 1                                  : terminal methyl at chain
C                                                 start
C            6i-4, i=1,2,...,NUNITS             : chiral skeletal carbon of
C                                                 unit (i)
C            6i-3, i=1,2,...,NUNITS             : hydrogen attached to chiral
C                                                 skeletal carbon of unit
C                                                 (i) (either D- or L-)
C            6i-2, i=1,2,...,NUNITS             : substituent R attached
C                                                 to chiral carbon of unit
C                                                 (i) (either D- or L-)
C            6i-1, i=1,2,...,NUNITS-1           : achiral skeletal atom of
C                                                 unit (i)
C            6i  , i=1,2,...,NUNITS-1           : D- hydrogen attached to
C                                                 achiral skeletal carbon
C                                                 of unit (i)
C            6i+1, i=1,2,...,NUNITS-1           : L- hydrogen attached to
C                                                 achiral skeletal carbon
C                                                 of unit (i)
C            6NUNITS-1                          : terminal methyl at chain
C                                                 end
C
C   . The chemical nature of an atom of index i is kept in array
C     element KIND(i)   (Code: 1=H, 2=C, 3=Methyl)
```

```
C  .  In array element MODUL(i) is kept the remainder of the division
C     of the index i by 6, which is of use in connectivity screening.
C  .  In array element IC(iseg) is kept the index of the carbon atom
C     belonging to skeletal segment number iseg-2 (Flory's convention
C     used in numbering segments)
C  .  In array element ISEG(i) is kept the number of the segment
C     (according to Flory's convention, segments numbered from 0 to
C     NDF-1), to which atom i belongs.
C  .  Index ICHIR(i) designates the absolute configuration of the
C     chiral skeletal carbon atom (6i-4). A value of ICHIR=+1
C     indicates that the chiral center is D- in a Fischer projection
C     constructed so that the beginning of the chain (atom 1)
C     lies upwards. A value of ICHIR=-1 indicates an L- configuration,
C     based on the same convention.
C  .  XP(i), YP(i), ZP(i) are the coordinates of the parent
C     chain atom corresponding to cube atom i
C
      IMPLICIT REAL*8(A-H,O-Z)
      INTEGER ICHIR(100), KIND(600), MODUL(600), CONNECT(0:5,0:5)
      INTEGER IC(200), ISEG(600)
      REAL*8 L, LH, LR
      DIMENSION X(600), Y(600), Z(600), PHI(200), AX(3), AY(3), AZ(3),
     1          AXCY(3), AYCZ(3), AZCX(3), ORIGIN(3), VC(3), VH1D(3),
     2          VH1L(3), VH2(3), VH3(3), VRD(3), VRL(3), TO(3,3),
     3          TP(3,3), TPP(3,3), TPROD(3,3), VECT(3), XP(600),
     4          YP(600), ZP(600)
      COMMON /BLOCK1/ X, Y, Z
      COMMON /BLOCK2/ ICHIR, KIND, IC, ISEG, MODUL, CONNECT
      COMMON /BLOCK3/ NUNITS, NBONDS, NSEGMENTS, NATOMS, THETAP,
     1                THETAHP, THETAPP, THETAHPP, THETARPP, STHP,
     2                CSTHP, STHPP, CSTHPP, L, LH, LR, VC, VH1D, VH1L,
     3                VH2, VH3, VRD, VRL, TO, TP, TPP, TPROD
      COMMON /BLOCK4/SA,CSA,SB,CSB,SG,CSG, AX, AY, AZ, AXX, AYY, AZZ,
     1                AXCY, AYCZ, AZCX, ORIGIN, VOLUME
      COMMON /BLOCK7/ XP, YP, ZP
C
C  Initializations upon first call of subroutine (ISTART=1)
C
      IF(ISTART) 20,10,20
C
C  Initialize all coordinates to zero, except those of chain start
   20 DO 30 J=2,NATOMS
         X(J)=0.0
         Y(J)=0.0
         Z(J)=0.0
         XP(J)=0.0
         YP(J)=0.0
         ZP(J)=0.0
   30 CONTINUE
C
C  Setup parallel arrays KIND, IC and MODUL, keeping track of the
C  chemical nature and connectivity of the parent chain.
      ICARBON=-1
      DO 35 I=3,NDF
         ICARBON=ICARBON+3
         IC(I)=ICARBON
   35 CONTINUE
      IC(NDF+1)=NATOMS
C
      KIND(1)=3
```

```
C       (the following are pseudo-definitions, used for convenience
C        in updating)
        ISEG(1)=1
        MODUL(1)=1
        I=1
        ISEGM=0
C
   40   I=I+1
        ISEGM=ISEGM+1
        KIND(I)=2
        ISEG(I)=ISEGM
        MODUL(I)=2
C
        I=I+1
        KIND(I)=1
        ISEG(I)=ISEGM
        MODUL(I)=3
C
        I=I+1
        KIND(I)=3
        ISEG(I)=ISEGM
        MODUL(I)=4
C
        I=I+1
        IF(I.EQ.NATOMS) GO TO 50
        ISEGM=ISEGM+1
        KIND(I)=2
        ISEG(I)=ISEGM
        MODUL(I)=5
C
        I=I+1
        KIND(I)=1
        ISEG(I)=ISEGM
        MODUL(I)=0
C
        I=I+1
        KIND(I)=1
        ISEG(I)=ISEGM
        MODUL(I)=1
        GO TO 40
C
   50   KIND(NATOMS)=3
C       (the following is a pseudo-definition, used for convenience
C        in updating)
        ISEG(NATOMS)=NDF-2
        MODUL(NATOMS)=5
C
C  Initialize coordinate transformation matrices
        STHP=SIN(THETAP)
        CSTHP=COS(THETAP)
        STHPP=SIN(THETAPP)
        CSTHPP=COS(THETAPP)
        TP(1,1)=CSTHP
        TP(1,2)=STHP
        TP(1,3)=0.0
        TPP(1,1)=CSTHPP
        TPP(1,2)=STHPP
        TPP(1,3)=0.0
C
C  Setup position vectors of skeletal carbons and substituents
```

```
C  with  respect to local coordinate systems of chain bonds.
C
C  VC = coordinate vector of skeletal carbon of segment i with
C       respect to coordinate system of bond i:
C
      VC(1)=L
      VC(2)=0.
      VC(3)=0.
C
C  VH1D = coordinate vector of hydrogen H1, connected to chiral
C         carbon atom of segment 2i-1 with respect to coordinate
C         system of bond (2i), for the case ICHIR(i)=+1
C         (D- configuration of carbon 2i-1)
C
      VH1D(1)=-LH*COS(THETAHPP)
      VH1D(2)=LH*COS(THETAHPP)/TAN(THETAPP/2.)
      VH1D(3)=LH*SQRT(1.-(COS(THETAHPP))**2/(SIN(THETAPP/2.))**2)
C
C  VRD = coordinate vector of substituent R, connected to the chiral
C        carbon atom of segment 2i-1 with respect to coordinate system
C        of bond (2i), for the case ICHIR(i)=+1
C        (D- configuration of carbon 2i-1)
C
      VRD(1)=-LR*COS(THETARPP)
      VRD(2)=LR*COS(THETARPP)/TAN(THETAPP/2.)
      VRD(3)=-LR*SQRT(1.-(COS(THETARPP))**2/(SIN(THETAPP/2.))**2)
C
C  Form respective coordinate vectors for L- configuration of segment
C  2i-1
C
      DO 60 I=1,3
        VH1L(I)=VH1D(I)
   60 VRL(I)=VRD(I)
      VH1L(3)=-VH1L(3)
      VRL(3)=-VRL(3)
C
C  VH2=coordinate vector of hydrogen H2, connected to achiral carbon
C      atom of segment 2i in the D- position, with respect to
C      coordinate system of bond (2i+1)
C
      VH2(1)=-LH*COS(THETAHP)
      VH2(2)=LH*COS(THETAHP)/TAN(THETAP/2.)
      VH2(3)=-LH*SQRT(1.-(COS(THETAHP))**2/(SIN(THETAP/2))**2)
C
C  VH3=coordinate vector of hydrogen H3, connected to achiral carbon
C      atom of segment 2i in the L- position, with respect to
C      coordinate system of bond (2i+1).
C
      VH3(1)=VH2(1)
      VH3(2)=VH2(2)
      VH3(3)=-VH2(3)
C
C
      RETURN
C
C
C  Calculations upon normal call of subroutine
C  Matrix TPP initially contains T-matrix corresponding to
C  bond 1 (PHI=0).
   10 TPP(2,1)=STHPP
```

```
      TPP(2,2)=-CSTHPP
      TPP(2,3)=0.0
      TPP(3,1)=0.0
      TPP(3,2)=0.0
      TPP(3,3)=-1.0
C
C  TO = Transformation matrix from local coordinate system
C       of bond 1 to fixed coordinate system.
C
      CSA=COS(PHI(1))
      SA=SIN(PHI(1))
      CSB=COS(PHI(2))
      SB=SIN(PHI(2))
      CSG=COS(PHI(3))
      SG=SIN(PHI(3))
      TO(1,1)=CSA*SB
      TO(1,2)=-CSA*CSB*CSG-SA*SG
      TO(1,3)=-CSA*CSB*SG+SA*CSG
      TO(2,1)=SA*SB
      TO(2,2)=-SA*CSB*CSG+CSA*SG
      TO(2,3)=-SA*CSB*SG-CSA*CSG
      TO(3,1)=CSB
      TO(3,2)=SB*CSG
      TO(3,3)=SB*SG
C
C  Form and store coordinates of chain atoms 2,3,4,5, which are
C  independent of the rotation angle vector PHI.
C
C  Atom 2 (Chiral carbon of segment1[Flory's conv.] of the chain)
      CALL MATVEC(TO,VC,VECT,3,3,3,3)
      X(2)=X(1)+VECT(1)
      Y(2)=Y(1)+VECT(2)
      Z(2)=Z(1)+VECT(3)
      XP(2)=XP(1)+VECT(1)
      YP(2)=YP(1)+VECT(2)
      ZP(2)=ZP(1)+VECT(3)
      CALL PERCONT(2)
C
C  Form and store transformation matrix product TPROD=TO*T1
      CALL MATMAT(TO,TPP,TPROD,3,3,3,3,3,3)
C
C  Atom 3 (Hydrogen connected to chiral carbon 2)
      IF(ICHIR(1)) 62,64,64
   62 CALL MATVEC(TPROD,VH1L,VECT,3,3,3,3)
      GO TO 70
   64 CALL MATVEC(TPROD,VH1D,VECT,3,3,3,3)
   70 X(3)=X(2)+VECT(1)
      Y(3)=Y(2)+VECT(2)
      Z(3)=Z(2)+VECT(3)
      XP(3)=XP(2)+VECT(1)
      YP(3)=YP(2)+VECT(2)
      ZP(3)=ZP(2)+VECT(3)
      CALL PERCONT(3)
C
C  Atom 4 (Substituent R connected to chiral carbon 2)
      IF(ICHIR(1)) 72,74,74
   72 CALL MATVEC(TPROD,VRL,VECT,3,3,3,3)
      GO TO 80
   74 CALL MATVEC(TPROD,VRD,VECT,3,3,3,3)
   80 X(4)=X(2)+VECT(1)
```

```
      Y(4)=Y(2)+VECT(2)
      Z(4)=Z(2)+VECT(3)
      XP(4)=XP(2)+VECT(1)
      YP(4)=YP(2)+VECT(2)
      ZP(4)=ZP(2)+VECT(3)
      CALL PERCONT(4)
C
C  Atom 5 (Achiral carbon of third segment of the chain)
      CALL MATVEC(TPROD,VC,VECT,3,3,3,3)
      X(5)=X(2)+VECT(1)
      Y(5)=Y(2)+VECT(2)
      Z(5)=Z(2)+VECT(3)
      XP(5)=XP(2)+VECT(1)
      YP(5)=YP(2)+VECT(2)
      ZP(5)=ZP(2)+VECT(3)
      CALL PERCONT(5)
C
      ANGLE=PHI(4)
      SPH=SIN(ANGLE)
      CSPH=COS(ANGLE)
      TP(2,1)=STHP*CSPH
      TP(2,2)=-CSTHP*CSPH
      TP(2,3)=SPH
      TP(3,1)=STHP*SPH
      TP(3,2)=-CSTHP*SPH
      TP(3,3)=-CSPH
      CALL MATMAT(TPROD,TP,TPROD,3,3,3,3,3,3)
C
C  Loop over all atoms whose coordinates depend on the PHI's, but the
C  last one.
      DO 100 I=6,NATOMS-1
C
C  Differentiate, according to atom type
        GO TO (110,120,130,140,150) MODUL(I)
C
C  MODUL=0 : D-hydrogen attached to achiral skeletal carbon
        CALL MATVEC(TPROD,VH2,VECT,3,3,3,3)
        GO TO 170
C
C  MODUL=1 : L-hydrogen attached to achiral skeletal carbon
  110   CALL MATVEC(TPROD,VH3,VECT,3,3,3,3)
        GO TO 170
C
C  MODUL=3 : hydrogen attached to chiral skeletal carbon
  130   IF(ICHIR((I+3)/6)) 132,134,134
  132   CALL MATVEC(TPROD,VH1L,VECT,3,3,3,3)
        GO TO 170
  134   CALL MATVEC(TPROD,VH1D,VECT,3,3,3,3)
        GO TO 170
C
C  MODUL=4 : R-substituent attached to chiral skeletal carbon
  140   IF(ICHIR((I+2)/6)) 142,144,144
  142   CALL MATVEC(TPROD,VRL,VECT,3,3,3,3)
        GO TO 170
  144   CALL MATVEC(TPROD,VRD,VECT,3,3,3,3)
C
  170   IREF=IC(ISEG(I)+2)
        X(I)=X(IREF)+VECT(1)
        Y(I)=Y(IREF)+VECT(2)
        Z(I)=Z(IREF)+VECT(3)
```

```
          XP(I)=XP(IREF)+VECT(1)
          YP(I)=YP(IREF)+VECT(2)
          ZP(I)=ZP(IREF)+VECT(3)
          GO TO 190
C
C  MODUL=2 : chiral skeletal carbon
  120     CALL MATVEC(TPROD,VC,VECT,3,3,3,3)
C  Update transformation matrix product, taking into account the
C  rotation angle of bond (I+1)/3
          ANGLE=PHI((I+7)/3)
          SPH=SIN(ANGLE)
          CSPH=COS(ANGLE)
          TPP(2,1)=STHPP*CSPH
          TPP(2,2)=-CSTHPP*CSPH
          TPP(2,3)=SPH
          TPP(3,1)=STHPP*SPH
          TPP(3,2)=-CSTHPP*SPH
          TPP(3,3)=-CSPH
          CALL MATMAT(TPROD,TPP,TPROD,3,3,3,3,3,3)
C
          GO TO 180
C
C  MODUL=5 : Achiral skeletal carbon
  150     CALL MATVEC(TPROD,VC,VECT,3,3,3,3)
C  Update transformation matrix product, taking into account the
C  rotation angle of bond (I+1)/3
          ANGLE=PHI((I+7)/3)
          SPH=SIN(ANGLE)
          CSPH=COS(ANGLE)
          TP(2,1)=STHP*CSPH
          TP(2,2)=-CSTHP*CSPH
          TP(2,3)=SPH
          TP(3,1)=STHP*SPH
          TP(3,2)=-CSTHP*SPH
          TP(3,3)=-CSPH
          CALL MATMAT(TPROD,TP,TPROD,3,3,3,3,3,3)
C
  180     IREF=I-3
          X(I)=X(IREF)+VECT(1)
          Y(I)=Y(IREF)+VECT(2)
          Z(I)=Z(IREF)+VECT(3)
          XP(I)=XP(IREF)+VECT(1)
          YP(I)=YP(IREF)+VECT(2)
          ZP(I)=ZP(IREF)+VECT(3)
C
  190     CALL PERCONT(I)
C
  100 CONTINUE
C
C  Coordinate calculation for methyl at chain end
      CALL MATVEC(TPROD,VC,VECT,3,3,3,3)
      IREF=NATOMS-3
      X(NATOMS)=X(IREF)+VECT(1)
      Y(NATOMS)=Y(IREF)+VECT(2)
      Z(NATOMS)=Z(IREF)+VECT(3)
      XP(NATOMS)=XP(IREF)+VECT(1)
      YP(NATOMS)=YP(IREF)+VECT(2)
      ZP(NATOMS)=ZP(IREF)+VECT(3)
      CALL PERCONT(NATOMS)
C
```

```
      RETURN
      END



      SUBROUTINE PERCONT(I)
C
C  Subroutine is used in the calculation of coordinates of atoms lying
C  in the cube.
C  Every time the coordinates of a new atom are calculated, the
C  subroutine checks whether the chain has exited the cube, and if yes
C  it imposes an appropriate periodic displacement to locate the image
C  of the atom !ying within the cube
C
      IMPLICIT REAL*8(A-H,O-Z)
      INTEGER ICHIR(100), KIND(600), MODUL(600), CONNECT(0:5,0:5)
      INTEGER IC(200), ISEG(600)
      DIMENSION X(600), Y(600), Z(600), AX(3), AY(3), AZ(3), AXCY(3),
     1          AYCZ(3), AZCX(3), ORIGIN(3), VECT(3)
      COMMON /BLOCK1/ X, Y, Z
      COMMON /BLOCK2/ ICHIR, KIND, IC, ISEG, MODUL, CONNECT
      COMMON /BLOCK4/SA,CSA,SB,CSB,SG,CSG, AX, AY, AZ, AXX, AYY,
     1                AZZ, AXCY, AYCZ, AZCX, ORIGIN, VOLUME
C
      VECT(1)=X(I)-ORIGIN(1)
      VECT(2)=Y(I)-ORIGIN(2)
      VECT(3)=Z(I)-ORIGIN(3)
      XCRIT=VECT(1)*AYCZ(1)+VECT(2)*AYCZ(2)+VECT(3)*AYCZ(3)
      IF(XCRIT.LE.VOLUME) GO TO 10
      X(I)=X(I)-AX(1)
      Y(I)=Y(I)-AX(2)
      Z(I)=Z(I)-AX(3)
      GO TO 20
   10 IF(XCRIT.GE.0.0) GO TO 20
      X(I)=X(I)+AX(1)
      Y(I)=Y(I)+AX(2)
      Z(I)=Z(I)+AX(3)
C
   20 VECT(1)=X(I)-ORIGIN(1)
      VECT(2)=Y(I)-ORIGIN(2)
      VECT(3)=Z(I)-ORIGIN(3)
      YCRIT=VECT(1)*AZCX(1)+VECT(2)*AZCX(2)+VECT(3)*AZCX(3)
      IF(YCRIT.LE.VOLUME) GO TO 30
      X(I)=X(I)-AY(1)
      Y(I)=Y(I)-AY(2)
      Z(I)=Z(I)-AY(3)
      GO TO 40
   30 IF(YCRIT.GE.0.0) GO TO 40
      X(I)=X(I)+AY(1)
      Y(I)=Y(I)+AY(2)
      Z(I)=Z(I)+AY(3)
C
   40 VECT(1)=X(I)+ORIGIN(1)
      VECT(2)=Y(I)+ORIGIN(2)
      VECT(3)=Z(I)+ORIGIN(3)
      ZCRIT=VECT(1)*AXCY(1)+VECT(2)*AXCY(2)+VECT(3)*AXCY(3)
      IF(ZCRIT.LE.VOLUME) GO TO 50
      X(I)=X(I)-AZ(1)
      Y(I)=Y(I)-AZ(2)
```

```
      Z(I)=Z(I)-AZ(3)
      GO TO 60
   50 IF(ZCRIT.GE.0.0) GO TO 60
      X(I)=X(I)+AZ(1)
      Y(I)=Y(I)+AZ(2)
      Z(I)=Z(I)+AZ(3)
C
   60 RETURN
C
      END
```

APPENDIX K : **Listing of the FORTRAN Program used to Impose an Approximately Affine Deformation, as Described in Section 5.1**

```
C
C
C  ***********************************************************************
C  *                                                                     *
C  *                       DOROS N. THEODOROU                            *
C  *                                                                     *
C  *                 Department of Chemical Engineering                  *
C  *                                                                     *
C  *              Massachusetts Institute of Technology                  *
C  *                                                                     *
C  *                            June 1985                                *
C  *                                                                     *
C  ***********************************************************************
C
C  Program imposes an affine incremental deformation of specific type
C  and degree on a periodic system of bulk amorphous polymer, in the
C  least squares sense. That is, given a structure characterized by an
C  initial degree of compression, or shear, or uniaxial tension E0,
C  and a desired final degree of deformation  E, the program displaces
C  system boundaries so that they correspond to the new deformation,
C  and modifies system degrees of freedom so that the sum of squares
C  of the distances between actual atom positions and positions
C  obtained by affine deformation of the initial guess is at a minimum.
C  Chain bond angles and bond lengths are assumed constant.
C  The location of the chain start is variable during the minimization.
C  Thus, the degrees of freedom of the system are the 3 Eulerian angles,
C  specifying the overall orientation of the chain, the NBONDS-2
C  rotation angles of all the bonds of the chain, except the first and
C  last, and the 3 coordinates of the chain start.
C
      IMPLICIT REAL*8(A-H,O-Z)
      INTEGER LAMDA(600), MU(600), NU(600), ICHIR(100), KIND(600),
     1        MODUL(600), CONNECT(0:5,0:5)
      INTEGER IC(200), ISEG(600)
      REAL*8 L, LH, LR, MW, MWUNIT, MWR
      CHARACTER CHAINNM*20, NAME(3)*4, CHIRNM(-1:1)*1
      DIMENSION X(600), Y(600), Z(600), PHI(200), SCALE(200), AXO(3),
     1          AYO(3), AZO(3), AX(3), AY(3), AZ(3), AXCY(3), AYCZ(3),
     2          AZCX(3), ORIGINO(3), ORIGIN(3), VC(3), VH1D(3), VH1L(3),
     3          VH2(3), VH3(3), VRD(3), VRL(3), TO(3,3), TP(3,3),
     4          TPP(3,3), TPROD(3,3), VECT(3), GRADX(200), GRADY(200),
     5          GRADZ(200), XP(600), YP(600), ZP(600), XD(600), YD(600),
     6          ZD(600)
      DIMENSION HESS(20100), SRHVEC(200), SOLVEC(200), GRDVEC(200),
     1          SCRVEC(200)
      COMMON /BLOCK11/ X, Y, Z
      COMMON /BLOCK21/ ICHIR, LAMDA, MU, NU, KIND, IC, ISEG, MODUL,
     1                 CONNECT
      COMMON /BLOCK31/ NUNITS, NBONDS, NSEGMENTS, NATOMS, THETAP,
     1                 THETAHP, THETAPP, THETAHPP, THETARPP, STHP,
     2                 CSTHP, STHPP, CSTHPP, L, LH, LR, VC, VH1D,
     3                 VH1L, VH2, VH3, VRD, VRL, TO, TP, TPP, TPROD
      COMMON /BLOCK41/ SA, CSA, SB, CSB, SG, CSG, AX, AY, AZ, AXX, AYY,
     1                 AZZ, AXCY, AYCZ, AZCX, ORIGIN, VOLUME
      COMMON /BLOCK61/ GRADY, GRADZ, SCALE
      COMMON /BLOCK71/ XP, YP, ZP
      COMMON /BLOCK81/ XD, YD, ZD
C
      OPEN(5,MODE='IN',ACCESS='SEQUENTIAL',FORM='FORMATTED',
```

```
     1      FILE='DEFORM.DAT')
       OPEN(7,MODE='IN',ACCESS='SEQUENTIAL',FORM='FORMATTED',
     1      FILE='CHAIN.DF')
       OPEN(9,MODE='IN',ACCESS='SEQUENTIAL',FORM='FORMATTED',
     1      FILE='SSQ.DAT')
       OPEN(6,MODE='OUT',ACCESS='SEQUENTIAL',FORM='FORMATTED',
     1      FILE='DEFORM.OUT')
       OPEN(10,MODE='OUT',ACCESS='SEQUENTIAL',FORM='FORMATTED',
     1      FILE='SSQ.OUT')
       OPEN(16,MODE='OUT',ACCESS='SEQUENTIAL',FORM='FORMATTED',
     1      FILE='CUBE.NEW')
C
C  Enter chain type and size.
       READ(5,10) CHAINNM,MWR,NUNITS
       WRITE(16,10) CHAINNM,MWR,NUNITS
   10  FORMAT(A20/F10.5/I5)
       NSEGMENTS=2*NUNITS+1
       NBONDS=2*NUNITS
       NDF1=NBONDS+1
       NDFM2=NBONDS-1
       NVAR=NDF1+3
       NATOMS=3*NDF1-4
       MWUNIT=MWR+27.04621
       MW=16.04303+NUNITS*MWUNIT
       WRITE(6,20) CHAINNM,NUNITS,NATOMS,NBONDS,NVAR,MW
   20  FORMAT(/////2X,'MOLECULE : ',A20/13X,13('-')//2X,'DEGREE OF ',
     1  'POLYMERIZATION : ',I5,5X,'(',I5,'  SKELETAL ATOMS, ',3X,I5,
     2  '  BONDS )'//2X,'NUMBER OF SYSTEM DEGREES OF FREEDOM : ',I5//
     3  2X,'MOLECULAR WEIGHT : ',E16.8/)
C
C  Enter connectivity table (indices correspond to atom index in X,Y,Z,
C  taken modulo6)
       DO 16 I=0,5
          CONNECT(I,2)=0
   16     CONNECT(I,5)=0
       DO 17 I=3,5
          CONNECT(I,0)=1
   17     CONNECT(I,1)=1
       DO 18 I=0,2
          CONNECT(I,3)=1
   18     CONNECT(I,4)=1
       CONNECT(0,0)=1
       CONNECT(1,0)=0
       CONNECT(2,0)=0
       CONNECT(0,1)=1
       CONNECT(1,1)=1
       CONNECT(2,1)=0
       CONNECT(3,3)=1
       CONNECT(4,3)=0
       CONNECT(5,3)=0
       CONNECT(3,4)=1
       CONNECT(4,4)=1
       CONNECT(5,4)=0
C
C  Enter bond lengths (Angstroms) and bond angles (degrees)
       READ(5,30) L,LH,LR
       WRITE(16,30) L,LH,LR
       READ(5,30) THETAP,THETAHP
       WRITE(16,30) THETAP,THETAHP
       READ(5,30) THETAPP,THETAHPP,THETARPP
```

```
      WRITE(16,30) THETAPP,THETAHPP,THETARPP
   30 FORMAT(3F8.3)
      WRITE(6,40) L,LH,LR,THETAP,THETAPP,THETAHP,THETAHPP,THETARPP
   40 FORMAT(//2X,'BOND LENGTHS'/15X,'C - C  : ',F5.3,' ANGSTROMS'/
     115X,'C - H  : ',F5.3,' ANGSTROMS'/15X,'C - R  : ',F5.3,
     2' ANGSTROMS'/15X,'(R=SUBSTITUENT)'//2X,'BOND ANGLES'/15X,
     3'INTRADYAD C-C-C : ',F8.3,' DEG'/15X,'INTERDYAD C-C-C : ',F8.3,
     4' DEG'/15X,'INTRADYAD H-C-C : ',F8.3,' DEG'/15X,
     5'INTERDYAD H-C-C : ',F8.3,' DEG'/15X,'INTERDYAD R-C-C : ',F8.3,
     6' DEG'/)
C
C  Enter continuation vectors of original, equilibrium undeformed cube
C  from which initial structure has been obtained
      READ(5,50) (AXO(I),I=1,3)
      READ(5,50) (AYO(I),I=1,3)
      READ(5,50) (AZO(I),I=1,3)
   50 FORMAT(3E16.8)
      WRITE(6,59)
   59 FORMAT(///2X,'CHARACTERISTICS OF ORIGINAL (UNDEFORMED) CUBE'/2X,
     145('-'))
      WRITE(6,60) (AXO(I),I=1,3),(AYO(I),I=1,3),(AZO(I),I=1,3)
   60 FORMAT(//2X,'CONTINUATION VECTORS (COMPONENTS IN ',
     1'ANGSTROMS) :'//5X,'AX :  ',3(E16.8,5X)//5X,'AY :  ',3(E16.8,5X)
     2//5X,'AZ :  ',3(E16.8,5X))
C
C  Calculate cross products AxO x AyO, AyO x AzO, AzO x AxO
      CALL VCROSSV(AXO, AYO, AXCY)
      CALL VCROSSV(AYO, AZO, AYCZ)
      CALL VCROSSV(AZO, AXO, AZCX)
C  Calculate cube volume, V=Ax.(Ay x Az)
      VOLUMEO=AXO(1)*AYCZ(1)+AXO(2)*AYCZ(2)+AXO(3)*AYCZ(3)
      WRITE(6,70) VOLUMEO
   70 FORMAT(/2X,'SYSTEM VOLUME = ',E16.8,2X,'CUBIC ANGSTROMS'/)
C
C  Calculate density
      DENSITY=MW/VOLUMEO*1.6603022
      WRITE(6,75) DENSITY
   75 FORMAT(2X,'SYSTEM MASS DENSITY = ',E16.8,2X,' G/CM3')
C
C  Enter coordinates of undeformed cube origin
      READ(5,50) (ORIGINO(I),I=1,3)
      WRITE(6,80) (ORIGINO(I),I=1,3)
   80 FORMAT(/2X,'CUBE ORIGIN AT (',E16.8,',',E16.8,',',E16.8,')')
C
C  Read type of deformation, IDEF (1=compression, 2=shear, 3=uniaxial
C       tension)
C  Read direction in which deformation is imposed, IDIR
C       (applicable only to shear and tension; for IDEF=1 IDIR is a
C        dummy parameter)
C  Read direction perpendicular to which deformation is imposed, IPERP
C       (applicable only to shear; for IDEF=1 or 3 IPERP is a dummy
C        parameter)
C  Read initial (EO) and final (E) degree of imposed deformation
C        For IDEF=1, EO and E are fractional compressions relative to
C        the undeformed system
C        For IDEF=2, EO and E are shear strains relative to the
C                    undeformed system
C        For IDEF=3, EO and E are fractional elongations relative to
C                    the undeformed system.
      READ(5,85) IDEF,IDIR,IPERP,EO,E
```

```
   85 FORMAT(I2,I2,I2,E16.9,E16.9)
C
C  Read flag which specifies format of degree-of-freedom file
      READ(5,130) ILONG
  130 FORMAT(I2)
C
C
C  Read the necessary and sufficient parameters for completely
C  specifying the starting system.
C
C  Position of first skeletal carbon (terminal methyl)
      IF(ILONG.NE.0) GO TO 95
      READ(7,90)  (PHI(I),I=NDF1+1,NVAR)
   90 FORMAT(3E16.9)
C
C  Angles specifying the orientation of first two bonds (in DEGREES)
C  These angles are stored in the first three elements of array PHI.
      READ(7,90) PHI(1), PHI(2), PHI(3)
C
C  Chirality sequence for all chiral atoms of the molecule
C  Index ICHIR(I) designates the absolute configuration of the chiral
C  skeletal carbon atom (6I-4). A value of ICHIR=+1 indicates that the
C  chiral center is D- in a Fischer projection constructed so that the
C  beginning of the chain (atom 1) lies upwards.
C  A value of ICHIR=-1 indicates an L-configuration, based on the same
C  convention.
      READ(7,100)  (ICHIR(I),I=1,NUNITS)
  100 FORMAT(4012)
C
C  Read sequence of rotation angles of bonds 2,...,NBONDS-1.
C  Rotation angle of bond i is kept in element PHI(i+2). All values
C  measured in degrees.
      READ(7,110)  (PHI(I),I=4,NDF1)
  110 FORMAT(5E16.9)
      GO TO 112
C
   95 READ(7,105)  (PHI(I),I=NDF1+1,NVAR)
  105 FORMAT(2E40.33)
      READ(7,105)  (PHI(I),I=1,3)
      READ(7,100)  (ICHIR(I),I=1,NUNITS)
      READ(7,105)  (PHI(I),I=4,NDF1)
C
C
  112 CLOSE(7)
C
C  Printout characteristics of initial guess configuration
      CHIRNM(-1)='L'
      CHIRNM( 1)='D'
      CHIRNM( 0)='*'
      WRITE(6,300)  (CHIRNM(ICHIR(I)),I=1,NUNITS)
  300 FORMAT(///2X,'SKELETAL CARBON CHIRALITY SEQUENCE OF CHAIN FILLING'
     1       ,' THE CUBE :'//3X,'* ',17(A1,' * ')/(5X,17(A1,' * ')))
      WM=0.0
      DO 115 I=2,NUNITS
          IF((ICHIR(I)-ICHIR(I-1)).NE.0) WM=WM+1.0
  115 CONTINUE
      WM=1.-WM/(NUNITS-1)
      WRITE(6,315) WM
  315 FORMAT(/2X,'FRACTION OF meso-DYADS, wm = ',F8.6)
C
```

```
C  Read option parameter for scaling rotation angles
C       ISCALE=0 : Rotation angles not scaled
C       ISCALE=1 : Rotation angles scaled
      READ(5,130) ISCALE
C
C  Option input for printing coordinates in output file
C       IWRCD=1 : Coordinates printed
C       IWRCD=0 : Coordinates not printed
  140 READ(5,130) IWRCD
C
      IF(IDEF-2) 51,52,53
   51 WRITE(6,54) EO
   54 FORMAT(///2X,'MODE OF DEFORMATION : HYDROSTATIC COMPRESSION'/24X,
     1       23('-')//2X,'DEGREE OF DEFORMATION = FRACTIONAL REDUCTION',
     2       ' IN VOLUME'/26X,'RELATIVE TO UNDEFORMED SYSTEM'////2X,
     3       'INITIAL SYSTEM CHARACTERISTICS'/2X,30('-')//2X,
     4       'DEGREE OF DEFORMATION : ',E16.9)
      GO TO 55
   52 WRITE(6,56) IDIR,IPERP,EO
   56 FORMAT(///2X,'MODE OF DEFORMATION : PURE SHEAR ALONG COORDINATE',
     1       ' AXIS ',I2/24X,10('-'),' PERPENDICULAR TO  AXIS ',I2/
     2       /2X,'DEGREE OF DEFORMATION = ',
     3       'SHEAR STRAIN (TANGENT OF SHEAR ANGLE) '////2X,'INITIAL',
     4       ' SYSTEM CHARACTERISTICS'/2X,30('-')//2X,
     5       'DEGREE OF DEFORMATION : ',E16.9)
      GO TO 55
   53 WRITE(6,57) IDIR,EO
   57 FORMAT(///2X,'MODE OF DEFORMATION : PURE UNIAXIAL TENSION ALONG',
     1       ' COORD.AXIS ',I2/24X,21('-')//2X,'DEGREE OF DEFORMATION ',
     2       '= FRACTIONAL ELONGATION'/26X,'RELATIVE TO ORIGINAL',
     3       ' DIMENSIONS'////2X,'INITIAL SYSTEM CHARACTERISTICS'/2X,
     4       30('-')//2X,'DEGREE OF DEFORMATION : ',E16.9)
C
   55 INIT=1
      CALL AFFINE(IDEF,IDIR,IPERP,EO,E,ORIGINO,AXO,AYO,AZO,VOLUMEO,INIT)
      AXX=AX(1)
      AYY=AY(2)
      AZZ=AZ(3)
      WRITE(6,60)  (AX(I),I=1,3),(AY(I),I=1,3),(AZ(I),I=1,3)
      WRITE(6,70) VOLUME
      DENSITY=MW/VOLUME*1.6603022
      WRITE(6,75) DENSITY
      WRITE(6,80)  (ORIGIN(I),I=1,3)
C
C  Compute location vectors and continuation coefficients for all atoms
C  in the initial system.
C
C  Convert valence bond angles and angles alpha, beta, gamma to radians
      DEGRAD=ASIN(1.)/90.
      THETAP=THETAP*DEGRAD
      THETAHP=THETAHP*DEGRAD
      THETAPP=THETAPP*DEGRAD
      THETAHPP=THETAHPP*DEGRAD
      THETARPP=THETARPP*DEGRAD
C
C  Initialize scaling factors for rotation angles
      DO 135 I=1,NVAR
  135     SCALE(I)=1.0
C
      ISTART=1
```

```
      ICONT=1
      CALL CRD(NDF1,PHI,ISTART,ICONT)
C
      ISTART=0
C
C  Convert Eulerian and rotation angles to radians and compute coordinates
      DO 185 I=1,NDF1
  185      PHI(I)=PHI(I)*DEGRAD
      CALL CRD(NDF1,PHI,ISTART,ICONT)
      ICONT=0
C
C  Convert Eulerian and rotation angles back to degrees
      DO 195 I=1,NDF1
  195      PHI(I)=PHI(I)/DEGRAD
C
C  Compute origin and continuation vectors corresponding to final
C  system, as well as affinely deformed atom locations
      WRITE(6,89) E
   89 FORMAT(///2X,'FINAL SYSTEM CHARACTERISTICS'/2X,28('-')//2X,
     1        'DEGREE OF DEFORMATION : ',E16.9)
C
      INIT=0
      CALL AFFINE(IDEF,IDIR,IPERP,EO,E,ORIGINO,AXO,AYO,AZO,VOLUMEO,INIT)
      WRITE(16,50)  (AX(I),I=1,3)
      WRITE(16,50)  (AY(I),I=1,3)
      WRITE(16,50)  (AZ(I),I=1,3)
      WRITE(16,50)  (ORIGIN(I),I=1,3)
      CLOSE(16)
      WRITE(6,60)  (AX(I),I=1,3), (AY(I),I=1,3), (AZ(I),I=1,3)
      WRITE(6,70) VOLUME
      DENSITY=MW/VOLUME*1.6603022
      WRITE(6,75) DENSITY
      WRITE(6,80)  (ORIGIN(I),I=1,3)
C
      WRITE(6,384)
  384 FORMAT(////2X,'INITIAL SYSTEM CONFIGURATION'/2X,28('='))
      WRITE(6,320) PHI(NDF1+1), PHI(NDF1+2), PHI(NDF1+3),
     1             PHI(1), PHI(2), PHI(3), NDFM2, (PHI(I),I=4,NDF1)
  320 FORMAT(///2X,'COORDINATES OF CHAIN START '/2X,27('-')
     1 ///2X,'X - COORDINATE : ',E16.9,' Angstroms'//2X,
     2 'Y - COORDINATE : ',E16.9,' Angstroms'//2X,'Z - COORDINATE : ',
     3 E16.9,' Angstroms'////2X,'EXTERNAL ORIENTATION (EULERIAN) ANGLES'
     4 /2X,39('-')///2X,'. ANGLE BETW. x-AXIS AND PROJECTION OF',
     5 ' BOND No 1 ON PLANE xy alpha = ',E16.9,' DEG'//2X,
     6 '. ANGLE BETW. z-AXIS AND BOND No 1  beta = ',E19.9,' DEG'
     7 //2X,'. DIHEDRAL ANGLE BETWEEN PLANES (bond1, z-axis) AND',
     8 ' (bond1, bond2)  gamma = ',E16.9,' DEG'///2X,
     9 'SEQUENCE OF ROTATION ANGLES OF BONDS 2',
     6 ' THROUGH ',I5,' (DEGREES) '/2X,62('-')/(/2X,5(F10.5,6X)))
C
C  Compute objective function and derivatives at initial guess
      CALL EVLOBJ(NVAR,PHI,SSQ,GRADX)
C
      IF(IWRCD.NE.0) CALL PRCD
      WRITE(6,270) SSQ,(GRADX(I),I=NDF1+1,NVAR),(GRADX(I),I=1,3),
     1             NDFM2,(GRADX(I),I=4,NDF1)
  270 FORMAT(///9X,'SUM OF SQUARES OF DISTANCES BETWEEN ACTUAL AND ',
     1       'DESIRED'/9X,54('-')/2X,'(AFFINELY DEFORMED) ATOM ',
     2       'LOCATIONS SSQ : ',E16.9,' Angstroms2'/2X,68('-')////
     3       2X,'DERIVATIVES OF SSQ wrt. COORDINATES OF CHAIN START',
```

```
     4       ' (KCAL/MOLE/ANGSTROM) '/2X,71('-')///2X,3(E14.7,2X)////
     5       2X,'DERIVATIVES OF SSQ wrt EULERIAN ANGLES (KCAL/MOLE/',
     6       'DEGREE) '/2X,57('-')//2X,'wrt. ALPHA : ',E14.7,//2X,
     7       'wrt.  BETA : ',E14.7,//2X,'wrt. GAMMA : ',E14.7
     8       ////2X,'DERIVATIVES OF SSQ wrt BOND ANGLES 2 THROUGH ',
     9       I5,' (KCAL/MOLE/DEGREE) '/2X,69('-')//(/2X,5(E14.7,2X)))
C
C
C  Scale rotation angles
C  Within the minimization routine, angles are in scaled degrees
      IF(ISCALE.EQ.0) GO TO 235
      CALL SETSCALE(NVAR,SCALE)
      DO 230 I=1,NDF1
  230     PHI(I)=PHI(I)*SCALE(I)
C
C  Read optimization routine settings
  235 READ(9,400) MAXF, ISWTCH, IPRINT
  400 FORMAT(I10, I2, I2)
      READ(9,410) TOLX, TOLG
  410 FORMAT(3E10.4)
      READ(9,410) SSQ, RFN
      READ(9,410) SPREC, EXTBND, HISTRY
      READ(9,415) IRHESS,IWRHESS
  415 FORMAT(2I2)
      IHESS=NVAR*(NVAR+1)/2
C
      WRITE(10,420) ISWTCH
C
  420 FORMAT(/////5X, 'AMDLIB QUASI-NEWTON MINIMIZATION ROUTINE GQBFGS'
     1       ,' - ISWTCH = ',I1/5X,48('='),13('-'))
      IF(ISWTCH.EQ.1) WRITE(10,430)
      IF(ISWTCH.EQ.2) WRITE(10,440)
  430 FORMAT(23X,'(DFP HESSIAN UPDATING SCHEME USED) ')
  440 FORMAT(23X,'(BFGS HESSIAN UPDATING SCHEME USED) ')
      WRITE(10,450) NVAR, MAXF, IPRINT
  450 FORMAT(///2X,'NVAR = ',I4, 6X, 'MAXF = ',I4, 6X, 'IPRINT = ',I4)
      WRITE(10,460) TOLX, TOLG
  460 FORMAT(//'TOLERANCES :    TOLX = ',E10.4, 4X,'TOLG = ',E10.4)
      WRITE(10,470) SSQ, RFN
  470 FORMAT(//'APPROXIMATE LOCATION OF MIN. :    OBJF = ',E10.4, 4X,
     1 'RFN = ',E10.4)
      WRITE(10,480) SPREC, EXTBND, HISTRY
  480 FORMAT(//'SPREC = ',E10.4, 6X, 'EXTBND = ',E10.4, 6X, 'HISTRY = ',
     1       E10.4)
      WRITE(10,490) (I,PHI(I),I=1,NVAR)
  490 FORMAT(//2X,'INITIAL VALUES OF PARAMETERS'//3(2X,'X(',I4,') = ',
     1       E16.8))
C
      CALL GQBFGS(NVAR,PHI,ISWTCH,MAXF,ITER,IPRINT,TOLX,TOLG,RFN,SPREC,
     1            EXTBND,SSQ,IHESS,HESS,GRADX,IERR,NFCALL,SRHVEC,
     2            SOLVEC,GRDVEC,SCRVEC,HISTRY,IRHESS,IWRHESS)
C
      WRITE(10,500) IERR
  500 FORMAT(///2X,'RESULTS UPON EXIT FROM GQBFGS'/2X,29('-')//2X,
     1       'IERR = ',I2)
      WRITE(10,510) SSQ
  510 FORMAT(//2X,'VALUE OF FUNCTION AT MINIMUM  OBJF = ',E15.8)
      WRITE(10,520) (J,PHI(J),J=1,NDF1)
  520 FORMAT(//2X,'VALUES OF PARAMETERS'//3(2X,'X(',I4,') = ',E16.8))
      WRITE(10,530) (J,GRADX(J),J=1,NDF1)
```

```
  530 FORMAT(//2X,'GRADIENT AT MINIMUM'//3(2X,'G(',I4,') = ', E16.8))
      WRITE(10,540) ITER, NFCALL
  540 FORMAT(///2X,'TOTAL NUMBER OF ITERATIONS = ',I5/2X, 'TOTAL',
     1       ' NUMBER OF FUNCTION EVALUATIONS = ',I5///)
C
C  Descale Eulerian and rotation angles, and convert to radians.
C  Form gradient with respect to true angle values (in degrees)
C  Recalculate coordinates and continuation coefficients
      ICONT=1
      DO 250 I=1,NDF1
          ECHELLE=SCALE(I)
          GRADX(I)=GRADX(I)*ECHELLE
  250     PHI(I)=PHI(I)*DEGRAD/ECHELLE
      CALL CRD(NDF1,PHI,ISTART,ICONT)
C
C  Convert angles to degrees
      DO 255 I=1,NDF1
  255     PHI(I)=PHI(I)/DEGRAD
C
      WRITE(6,340)
  340 FORMAT(////2X,'FINAL CONFIGURATION AFTER OPTIMIZATION'/2X,38('='))
C
C  Print out rotation angles
      WRITE(6,320) PHI(NDF1+1), PHI(NDF1+2), PHI(NDF1+3),
     1             PHI(1), PHI(2), PHI(3), NDFM2, (PHI(I),I=4,NDF1)
C
      IF(IWRCD.EQ.0) GO TO 350
      CALL PRCD
C
C  Print out calculated objective function and gradient
  350 WRITE(6,270) SSQ,(GRADX(I),I=NDF1+1,NVAR),(GRADX(I),I=1,3),
     1             NDFM2,(GRADX(I),I=4,NDF1)
C
      OPEN(12,MODE='OUT',ACCESS='SEQUENTIAL',FORM='FORMATTED',
     1    FILE='LAST.DF')
      OPEN(14,MODE='OUT',ACCESS='SEQUENTIAL',FORM='FORMATTED',
     1    FILE='CHAIN.MIN')
      WRITE(12,90) X(1),Y(1),Z(1)
      WRITE(14,105) X(1),Y(1),Z(1)
      WRITE(12,90) PHI(1), PHI(2), PHI(3)
      WRITE(14,105) PHI(1), PHI(2), PHI(3)
      WRITE(12,100) (ICHIR(I),I=1,NUNITS)
      WRITE(14,100) (ICHIR(I),I=1,NUNITS)
      WRITE(12,110) (PHI(I),I=4,NDF1)
      WRITE(14,105) (PHI(I),I=4,NDF1)
      CLOSE(12)
      CLOSE(14)
C
      CONTINUE
C
      END



      SUBROUTINE EVLOBJ(NVAR, VAR, SSQ, GRADX)
C
C    Subroutine computes the sum of squares of the deviations between
C  present locations of all atoms of the system (X,Y,Z) and
C  corresponding desired locations (XD,YD,ZD).
```

```
C     The vector of degrees of freedom VAR, of length NVAR=2*NUNITS+4,
C   contains the Eulerian angles in the first 3 places, the rotation
C   angles of bonds 2 to 2*NUNITS-1 in places 3 to 2*NUNITS+1, and the
C   coordinates of the chain start in positions 2*NUNITS+2 to 2*NUNITS+4.
C     The corresponding components of the gradient are kept in GRADX,
C   in the same order.
C
      IMPLICIT REAL*8(A-H,O-Z)
      INTEGER LAMDA(600), MU(600), NU(600), KIND(600), MODUL(600),
     1          CONNECT(0:5,0:5), ICHIR(100)
      INTEGER IC(200), ISEG(600)
      REAL*8 L,LH,LR
      CHARACTER*4 NAME(3)
      DIMENSION X(600), Y(600), Z(600), VC(3), VH1D(3), VH1L(3), VH2(3),
     1          VH3(3), VRD(3), VRL(3), TO(3,3), TP(3,3), TPP(3,3),
     2          TPROD(3,3), AX(3), AY(3), AZ(3), AXCY(3), AYCZ(3),
     3          AZCX(3), ORIGIN(3), VAR(200), SCALE(200), GRADX(200),
     4          GRADY(200), GRADZ(200), VECT(3), XP(600), YP(600),
     5          ZP(600), XD(600), YD(600), ZD(600)
      COMMON /BLOCK11/ X, Y, Z
      COMMON /BLOCK21/ ICHIR, LAMDA, MU, NU, KIND, IC, ISEG, MODUL,
     1                 CONNECT
      COMMON /BLOCK31/ NUNITS, NBONDS, NSEGMENTS, NATOMS, THETAP,
     1                 THETAHP, THETAPP, THETAHPP, THETARPP, STHP,
     2                 CSTHP, STHPP, CSTHPP, L, LH, LR, VC, VH1D,
     3                 VH1L, VH2, VH3, VRD, VRL, TO, TP, TPP, TPROD
      COMMON /BLOCK41/ SA, CSA, SB, CSB, SG, CSG, AX, AY, AZ, AXX,
     1                 AYY, AZZ, AXCY, AYCZ, AZCX, ORIGIN, VOLUME
      COMMON /BLOCK61/ GRADY, GRADZ, SCALE
      COMMON /BLOCK71/ XP,YP,ZP
      COMMON /BLOCK81/ XD,YD,ZD
C
      NDF1=NVAR-3
      NDF2=NDF1+1
C
C  Descale rotation angles to their true values (artificial phi=scale*
C  true phi). After this conversion, rotation angles are in true
C  degrees.
      DO 5 I=1,NDF1
    5     VAR(I)=VAR(I)/SCALE(I)
C
C  Bring all rotation angles into the interval (-180,180)
      DO 6 I=1,NDF1
          VAR(I)=VAR(I)-INT(VAR(I)/360.)*360.
          IF(VAR(I).LT.-180.) VAR(I)=VAR(I)+360.
          IF(VAR(I).GT. 180.) VAR(I)=VAR(I)-360.
    6 CONTINUE
C
C  Convert angles from degrees to radians.
C  After this conversion, angles are in true radians, lying between -pi
C  and pi.
   11 DEGRAD=ASIN(1.)/90.
      DO 15 I=1,NDF1
   15     VAR(I)=VAR(I)*DEGRAD
C
C  Calculate coordinates of all atoms in the cube
      ISTART=0
      ICONT=0
      CALL CRD(NDF1,VAR,ISTART,ICONT)
C
```

```
      SSQ=0.0
      DO 20 I=1,NVAR
          GRADX(I)=0.0
          GRADY(I)=0.0
   20     GRADZ(I)=0.0
C
      XPSTART=XP(1)
      YPSTART=YP(1)
      ZPSTART=ZP(1)
C
C  Compute objective function and derivatives
C
C  Outer loop over all atoms
      DO 30 J=1,NATOMS
          XP1=XP(J)
          YP1=YP(J)
          ZP1=ZP(J)
          DX=X(J)-XD(J)
          DY=Y(J)-YD(J)
          DZ=Z(J)-ZD(J)
          SSQ=SSQ+DX*DX+DY*DY+DZ*DZ
          GRADX(NDF2)=GRADX(NDF2)+DX
          GRADX(NDF2+1)=GRADX(NDF2+1)+DY
          GRADX(NDF2+2)=GRADX(NDF2+2)+DZ
C
C  Inner loop over all degrees of freedom
          DO 40 I=1,3
              VECT(1)=XP1-XPSTART
              VECT(2)=YP1-YPSTART
              VECT(3)=ZP1-ZPSTART
              GRADX(I)=GRADX(I)+VECT(2)*DZ-VECT(3)*DY
              GRADY(I)=GRADY(I)+VECT(3)*DX-VECT(1)*DZ
              GRADZ(I)=GRADZ(I)+VECT(1)*DY-VECT(2)*DX
   40     CONTINUE
          ISGP2=ISEG(J)+2
          IF(ISGP2.LT.4) GO TO 30
          DO 50 I=4,ISGP2
              ICARBON=IC(I)
              VECT(1)=XP1-XP(ICARBON)
              VECT(2)=YP1-YP(ICARBON)
              VECT(3)=ZP1-ZP(ICARBON)
              GRADX(I)=GRADX(I)+VECT(2)*DZ-VECT(3)*DY
              GRADY(I)=GRADY(I)+VECT(3)*DX-VECT(1)*DZ
              GRADZ(I)=GRADZ(I)+VECT(1)*DY-VECT(2)*DX
   50     CONTINUE
C
   30 CONTINUE
C
C  Form gradient in GRADX
      DO 60 I=NDF2,NVAR
   60     GRADX(I)=2.*GRADX(I)
C
      GRADX(1)=2.*GRADZ(1)
      GRADX(2)=2.*(-SA*GRADX(2)+CSA*GRADY(2))
      GRADX(3)=2.*((-CSA*GRADX(3)-SA*GRADY(3))*SB-CSB*GRADZ(3))
      DO 70 I=4,NDF1
          ICARB=IC(I-1)
          ICARB1=IC(I)
          VECT(1)=XP(ICARB1)-XP(ICARB)
          VECT(2)=YP(ICARB1)-YP(ICARB)
```

```
          VECT(3)=ZP(ICARB1)-ZP(ICARB)
          GRADX(I)=(VECT(1)*GRADX(I)+VECT(2)*GRADY(I)+VECT(3)*GRADZ(I))
     1              *2./L
   70 CONTINUE
C
C  Scale rotation angles and convert from radians to degrees, to prepare
C  for reentry to the optimization routine. Also form gradient with
C  respect to the artificial (scaled) angles from the true gradient.
C  (Upon exit from EVLOBJ, angles are in scaled degrees).
      DO 80 I=1,NDF1
          ECHELLE=SCALE(I)
          VAR(I)=VAR(I)*ECHELLE/DEGRAD
          GRADX(I)=GRADX(I)/ECHELLE*DEGRAD
   80 CONTINUE
C
      RETURN
      END



      SUBROUTINE SETSCALE(NVAR,SCALE)
C
C  Subroutine to setup scaling factors for the rotation angles, to be
C  used in the minimization.
C
      IMPLICIT REAL*8(A-H,O-Z)
      DIMENSION SCALE(NVAR)
      NDF=NVAR-3
      DO 10 I=1,3
   10     SCALE(I)=1.
      DO 20 I=4,NDF
   20     SCALE(I)=SQRT(1.-FLOAT(I-2)/(NDF-1))
      DO 30 I=NDF+1,NVAR
   30     SCALE(I)=1.
C
      RETURN
      END



      SUBROUTINE AFFINE(IDEF,IDIR,IPERP,EO,E,ORIGINO,AXO,AYO,AZO,
     1                  VOLUMEO,INIT)
C
C  Subroutine performs an affine transformation of all atom coordinates
C  in the interior of the cube. Atom coordinates of the initial system
C  should be available upon entry in arrays X,Y,Z. Affinely deformed
C  coordinates are stored in arrays XD,YD,ZD.
C     IDEF is a flag indicating the type of deformation
C     IDEF=1 : hydrostatic compression
C          2 : pure shear
C          3 : pure uniaxial tension
C
C  For IDEF=2 (3), IDIR indicates the axis along which the system is
C  sheared (extended) : IDIR=1,2,3 stands for axis X,Y,Z respectively.
C  For IDEF=2, IPERP indicates the axis perpendicular to the sheared
C  faces of the cube. IPERP=1,2,3 stands for axis x,y,z, respectively.
C  EO, E are the initial and final (desired) degree of deformation
C  (fractional reduction in volume, shear strain relative to undeformed
```

```
C  system, or fractional elongation relative to undeformed system).
C
C  ORIGINO,AXO,AYO,AZO,VOLUMEO contain the location of the origin and
C  the edge vectors of the undeformed cube from which the initial
C  structure was obtained.
C
C  For INIT=1, the subroutine only determines the borders of the initial
C              system. Results are returned in variables ORIGIN,AX,AY,
C              AZ,AXCY,AYCZ,AZCX,VOLUME
C  For INIT=0, an affine transformation of the system borders (ORIGIN,
C              AX,AY,AZ,AXCY,AYCZ,AZCX,VOLUME) as well as of all atoms
C              in the system interior (XD,YD,ZD) is performed, from
C              degree of deformation EO to degree of deformation E.
C
      IMPLICIT REAL*8(A-H,O-Z)
      REAL*8 L, LH, LR
      DIMENSION X(600), Y(600), Z(600), AXO(3), AYO(3), AZO(3), AX(3),
     1          AY(3), AZ(3), AXCY(3), AYCZ(3), AZCX(3), ORIGINO(3),
     2          ORIGIN(3), VC(3), VH1D(3), VH1L(3), VH2(3), VH3(3),
     3          VRD(3), VRL(3), TO(3,3), TP(3,3), TPP(3,3), TPROD(3,3),
     4          XD(600), YD(600), ZD(600), VAUX(3), VAUX1(3)
      COMMON /BLOCK11/ X, Y, Z
      COMMON /BLOCK31/ NUNITS, NBONDS, NSEGMENTS, NATOMS, THETAP,
     1                 THETAHP, THETAPP, THETAHPP, THETARPP, STHP, CSTHP,
     2                 STHPP, CSTHPP, L, LH, LR, VC, VH1D, VH1L, VH2,
     3                 VH3, VRD, VRL, TO, TP, TPP, TPROD
      COMMON /BLOCK41/ SA, CSA, SB, CSB, SG, CSG, AX, AY, AZ, AXX, AYY,
     1                 AZZ, AXCY, AYCZ, AZCX, ORIGIN, VOLUME
      COMMON /BLOCK81/ XD, YD, ZD
C
C  Initialization
      EPS=EO
      IF(INIT.NE.1) EPS=E
C
      IF(IDEF-2) 30,40,50
C
C  Compression
   30 FRAC=(ABS(1.-EPS))**(1./3)
      IF(1.-EPS.LT.0.) FRAC=-FRAC
      DO 35 I=1,3
          ORIGIN(I)=ORIGINO(I)+(1.-FRAC)/2.*(AXO(I)+AYO(I)+AZO(I))
          AX(I)=FRAC*AXO(I)
          AY(I)=FRAC*AYO(I)
          AZ(I)=FRAC*AZO(I)
   35 CONTINUE
      GO TO 60
C
C  Pure Shear
   40 IF(IDIR-2) 42,44,46
C
C  Shear along x-axis
   42 DO 43 I=1,3
   43     VAUX(I)=EPS*AXO(I)
      GO TO 48
C
C  Shear along y-axis
   44 DO 45 I=1,3
   45     VAUX(I)=EPS*AYO(I)
      GO TO 48
C
```

```
C  Shear along z-axis
   46 DO 47 I=1,3
   47      VAUX(I)=EPS*AZO(I)
C
   48 DO 49 I=1,3
         ORIGIN(I)=ORIGINO(I)-0.5*VAUX(I)
         AX(I)=AXO(I)
         AY(I)=AYO(I)
   49    AZ(I)=AZO(I)
C
      IF(IPERP-2) 142,144,146
C
C  Shear perpendicular to x-axis
  142 DO 143 I=1,3
  143    AX(I)=AX(I)+VAUX(I)
      GO TO 60
C
C  Shear perpendicular to y-axis
  144 DO 145 I=1,3
  145    AY(I)=AY(I)+VAUX(I)
      GO TO 60
C
C  Shear perpendicular to z-axis
  146 DO 147 I=1,3
  147    AZ(I)=AZ(I)+VAUX(I)
      GO TO 60
C
C  Pure Uniaxial Tension
   50 IF(IDIR-2) 52,54,56
C
C  Elongation in x-direction
   52 DO 53 I=1,3
         ORIGIN(I)=ORIGINO(I)-EPS/2.*AXO(I)
         AX(I)=(1.+EPS)*AXO(I)
         AY(I)=AYO(I)
   53    AZ(I)=AZO(I)
      GO TO 60
C
C  Elongation in y-direction
   54 DO 55 I=1,3
         ORIGIN(I)=ORIGINO(I)-EPS/2.*AYO(I)
         AX(I)=AXO(I)
         AY(I)=(1.+EPS)*AYO(I)
   55    AZ(I)=AZO(I)
      GO TO 60
C
C  Elongation in z-direction
   56 DO 57 I=1,3
         ORIGIN(I)=ORIGINO(I)-EPS/2.*AZO(I)
         AX(I)=AXO(I)
         AY(I)=AYO(I)
   57    AZ(I)=(1.+EPS)*AZO(I)
C
   60 CALL VCROSSV(AX,AY,AXCY)
      CALL VCROSSV(AY,AZ,AYCZ)
      CALL VCROSSV(AZ,AX,AZCX)
      VOLUME=AX(1)*AYCZ(1)+AX(2)*AYCZ(2)+AX(3)*AYCZ(3)
C
      IF(INIT.EQ.1) RETURN
C
```

```
C  Affine Deformation of Interior
      IF(IDEF-2) 70,80,150
C
C  Compression
   70 FRAC1=(1.-E)/(1.-EO)
      FRAC=(ABS(FRAC1))**(1./3)
      IF(FRAC1.LT.O.) FRAC=-FRAC
      FRAC1=1.-FRAC
      FRAC12=FRAC1/2.
      DO 72 I=1,3
   72      VAUX(I)=FRAC1*ORIGINO(I)+FRAC12*(AXO(I)+AYO(I)+AZO(I))
      DO 75 IATOM=1,NATOMS
           XD(IATOM)=VAUX(1)+X(IATOM)*FRAC
           YD(IATOM)=VAUX(2)+Y(IATOM)*FRAC
   75      ZD(IATOM)=VAUX(3)+Z(IATOM)*FRAC
      RETURN
C
C  Pure Shear
   80 IF(IDIR.NE.IPERP) GO TO 81
      WRITE(6,89)
   89 FORMAT(///'*** IMPOSSIBLE SHEAR TRANSFORMATION')
      STOP
   81 IF(IDIR-2) 82,84,86
C
C  Along x-axis
   82 DO 83 I=1,3
   83      VAUX1(I)=AXO(I)
      GO TO 90
C
C  Along y-axis
   84 DO 85 I=1,3
   85      VAUX1(I)=AYO(I)
      GO TO 90
C
C  Along z-axis
   86 DO 87 I=1,3
   87      VAUX1(I)=AZO(I)
C
   90 IF(IPERP-2) 92,94,96
C
C  Perpendicular to x-axis
   92 CALL VCROSSV(AYO,AZO,VAUX)
      GO TO 100
C  Perpendicular to y-axis
   94 CALL VCROSSV(AZO,AXO,VAUX)
      GO TO 100
C  Perpendicular to z-axis
   96 CALL VCROSSV(AXO,AYO,VAUX)
C
  100 DO 110 I=1,3
  110      VAUX1(I)=VAUX1(I)*(E-EO)
      DO 120 IATOM=1,NATOMS
           FRAC=0.5-((X(IATOM)-ORIGINO(1))*VAUX(1)+(Y(IATOM)-ORIGINO(2))
     1          *VAUX(2)+(Z(IATOM)-ORIGINO(3))*VAUX(3))/VOLUMEO
           XD(IATOM)=X(IATOM)-FRAC*VAUX1(1)
           YD(IATOM)=Y(IATOM)-FRAC*VAUX1(2)
           ZD(IATOM)=Z(IATOM)-FRAC*VAUX1(3)
  120 CONTINUE
      RETURN
C
```

```
C  Pure Uniaxial Tension
  150 FRAC=(E-E0)/(1.+E0)
      IF(IDIR-2) 152,154,156
C
C  Tension in x-direction
  152 DO 153 I=1,3
  153     VAUX(I)=FRAC*AX0(I)
      CALL VCROSSV(AY0,AZ0,VAUX1)
      GO TO 160
C
C  Tension in y-direction
  154 DO 155 I=1,3
  155     VAUX(I)=FRAC*AY0(I)
      CALL VCROSSV(AZ0,AX0,VAUX1)
      GO TO 160
C
  156 DO 157 I=1,3
  157     VAUX(I)=FRAC*AZ0(I)
      CALL VCROSSV(AX0,AY0,VAUX1)
C
  160 DO 200 IATOM=1,NATOMS
          FRAC=((X(IATOM)-ORIGIN0(1))*VAUX1(1)+(Y(IATOM)-ORIGIN0(2))*
     1         VAUX1(2)+(Z(IATOM)-ORIGIN0(3))*VAUX1(3))/VOLUME0-0.5
          XD(IATOM)=X(IATOM)+FRAC*VAUX(1)
          YD(IATOM)=Y(IATOM)+FRAC*VAUX(2)
          ZD(IATOM)=Z(IATOM)+FRAC*VAUX(3)
  200 CONTINUE
      RETURN
C
      END



      SUBROUTINE GQBFGS(NVAR,X,ISWTCH,MAXF,ITER,IPRINT,TOLX,TOLG,RFN,
     1                  SPREC,EXTBND,OBJF,IHESS,HESS,G,IERR,NFCALL,
     2                  SRHVEC,SOLVEC,GRDVEC,SCRVEC,HISTRY,IRHESS,
     3                  IWRHESS)
C
      IMPLICIT REAL*8(A-H,O-Z)
      DIMENSION  X(200),HESS(20100),G(200),SRHVEC(200),SOLVEC(200),
     1         GRDVEC(200),SCRVEC(200)
C
C       THIS SUBROUTINE MINIMIZES A FUNCTION OF SEVERAL VARIABLES
C     OBJF(X(1),X(2),....,X(NVAR))  USING A QUASI-NEWTON METHOD
C     OPTIONALLY EMPLOYING THE  DFP  AND  BFGS  UPDATING FORMULAS.
C     THE USER MUST PROVIDE A SUBROUTINE TO CALCULATE  OBJF(X)  AND
C     ITS GRADIENT(FIRST PARTIAL DERIVATIVE) VECTOR  G(X).
C
C     ******************************************************************
C       THIS ROUTINE INVOKES THE PACKAGE MODULES  SEARCH  AND  UPHESS
C     AND THE USER SUPPLIED SUBROUTINE  FUNCT.
C     ******************************************************************
C
C     ON INPUT
C
C        NVAR  IS THE NUMBER OF VARIABLES. IT IS ALSO THE DIMENSION OF
C           THE VECTORS  X, G, SRHVEC, SOLVEC, GRDVEC  AND  SCRVEC.
C
C        X  CONTAINS AN ESTIMATE OF THE SOLUTION VECTOR
```

```
C          (X(1),X(2),...,X(NVAR)).
C
C       ISWTCH  IS A PARAMETER SET EQUAL TO  K  WHICH SELECTS THE
C          FORMULA USED TO UPDATE THE APPROXIMATION TO THE HESSIAN
C          INVERSE. FOR
C
C          K = 1 - THE  DFP  UPDATE,
C          K = 2 - THE  BFGS  UPDATE.
C
C          THE  BFGS  UPDATE IS RECOMMENDED.
C
C       MAXF  IS THE LIMIT ON THE NUMBER OF CALLS TO THE FUNCTION
C          EVALUATION ROUTINE  EVLOBJ.
C
C       EVLOBJ  IS A USER SUPPLIED SUBROUTINE TO EVALUATE  OBJF(X)
C          AND THE COMPONENTS OF THE GRADIENT  G(X)  AT THE ESTIMATE
C          X(I), I = 1,2,...,NVAR.
C
C       TOLX,TOLG ARE THE ACCURACIES REQUIRED IN THE SOLUTION, I.E. A
C          NORMAL RETURN FROM THE ROUTINE OCCURS IF THE DIFFERENCE
C          BETWEEN THE COMPONENTS OF TWO SUCCESSIVE ESTIMATES OF THE
C          SOLUTION ARE NOT GREATER THAN  MAX(TOLX*ABS(X(I)),TOLX)
C          FOR ALL  I, AND THE L2 NORM OF THE GRADIENT IS NOT GREATER
C          THAN  TOLG.
C
C       RFN  IS AN ESTIMATE OF THE EXPECTED REDUCTION IN  OBJF(X).
C          THIS ESTIMATE IS USED ONLY ON THE FIRST ITERATION SO AN
C          ORDER OF MAGNITUDE ESTIMATE WILL SUFFICE. THE INFORMATION
C          CAN BE PROVIDED IN THE FOLLOWING WAYS DEPENDING UPON THE
C          VALUE OF  RFN. FOR
C
C             RFN .GT. 0.0 - THE SETTING OF  RFN  ITSELF WILL BE TAKEN
C                            AS THE EXPECTED REDUCTION IN  OBJF(X),
C
C             RFN = 0.0    - IT IS ASSUMED THAT AN ESTIMATE OF THE
C                            MINIMUM VALUE OF  OBJF(X)  HAS BEEN SET
C                            IN THE ARGUMENT  OBJF, AND THE EXPECTED
C                            REDUCTION IN  OBJF(X)  WILL BE COMPUTED
C                            AS (INITIAL FUNCTION VALUE) MINUS OBJF,
C
C             RFN .LT. 0.0 - A MULTIPLE  ABS(RFN)  OF THE MODULUS OF
C                            THE INITIAL FUNCTION VALUE WILL BE TAKEN
C                            AS THE EXPECTED REDUCTION.
C
C       SPREC  IS THE ACCURACY REQUIRED IN THE LINEAR SEARCH TECHNIQUE
C          INVOKED BY  GQBFGS, I.E. A POINT  XM  IS ACCEPTED AS THE
C          MINIMUM ALONG THE SEARCH DIRECTION IF THE RATIO OF THE
C          DIRECTIONAL DERIVATIVE AT  XM  OVER THE DIRECTIONAL
C          DERIVATIVE AT THE INITIAL POINT IS NOT GREATER THAN  SPREC.
C
C          THE SETTING  0.100  IS RECOMMENDED.
C
C       EXTBND  IS THE UPPER BOUND ON THE MULTIPLICATIVE INCREASE IN
C          THE SEARCH SCALAR DURING THE EXTRAPOLATION PHASE OF THE
C          LINEAR SEARCH TECHNIQUE.
C
C          THE SETTING  2.000  IS RECOMMENDED.
C
C       OBJF  CONTAINS AN ESTIMATE OF THE MINIMUM VALUE OF  OBJF(X)
C          IF  RFN = 0.0. OTHERWISE IT IS ONLY AN OUTPUT PARAMETER.
```

```
C
C        IHESS  IS A PARAMETER SET EQUAL TO THE DIMENSION OF  HESS
C          WHICH IS AT LEAST  NVAR*(NVAR+1)/2.
C
C        HISTRY  IS A DUMMY PARAMETER.
C
C     ON OUTPUT
C
C        X  CONTAINS THE BEST AVAILABLE ESTIMATE OF THE SOLUTION VECTOR.
C
C        OBJF  CONTAINS THE FUNCTION VALUE AT  X.
C
C
C        HESS  IS AN ARRAY OF DIMENSION  IHESS  WHICH CONTAINS THE
C          UPPER TRIANGLE OF THE MOST RECENT APPROXIMATION TO THE
C          HESSIAN INVERSE STORED ROW-WISE.
C
C        G  CONTAINS THE COMPONENTS OF THE GRADIENT AT  X.
C
C        IERR  IS A PARAMETER SET EQUAL TO  K  WHICH GIVES THE FOLLOWING
C          TERMINATION INDICATIONS
C
C           NORMAL TERMINATION,
C             K = 0,
C           INTERMEDIATE TERMINATION,
C             K = -N(N ANY INTEGER) - USER TERMINATION,
C             K = 1 - FAILURE TO CONVERGE IN  MAXF  CALLS OF  FUNCT,
C             K = 2 - LINEAR SEARCH TECHNIQUE INDICATES THAT IT IS
C                   . LIKELY THAT NO MINIMUM EXISTS,
C
C        NFCALL  IS THE NUMBER OF CALLS TO  EVLOBJ.
C
C        SRHVEC  CONTAINS THE CURRENT SEARCH DIRECTION VECTOR.
C
C        SOLVEC  CONTAINS THE CURRENT SOLUTION VECTOR.
C
C        GRDVEC  CONTAINS THE CURRENT GRADIENT VECTOR.
C
C        SCRVEC  IS A SCRATCH VECTOR.
C
C     WRITTEN BY K. E. HILLSTROM, MARCH, 1976.
C
C
C     INITIALIZE THE FOLLOWING PARAMETERS
C
C       IERR   - THE TERMINATION INDICATOR
C       NFCALL - THE NUMBER OF CALLS TO  EVLOBJ
C       REDFCN - THE INITIAL PREDICTED REDUCTION IN  OBJF
C       ITER   - THE CURRENT ITERATION NUMBER
C
      IERR = 0
      ITER=0
      NFCALL = 1
      TEMP = OBJF
C
C     ***************************************************************
      CALL EVLOBJ(NVAR,X,OBJF,G)
C     ***************************************************************
C
      SQGRAD=0.0
```

```
      DO 220 III=1,NVAR
  220     SQGRAD=SQGRAD+G(III)**2
C
      IF (IERR .LT. 0) GO TO 410
      REDFCN = RFN
      IF (RFN .EQ. 0.0) REDFCN = OBJF - TEMP
      IF (RFN .LT. 0.0) REDFCN = ABS(REDFCN * OBJF)
      IF (REDFCN .LE. 0.0) REDFCN = 1.0
C
C     READ INITIAL ESTIMATE OF HESSIAN INVERSE, IF DESIRED
      IF(IRHESS.EQ.0) GO TO 200
      READ(11,202) (HESS(II),II=1,IHESS)
202   FORMAT(5E16.9)
      GO TO 300
C
C     BEGIN THE QUASI-NEWTON PROCESS BY INITIALIZING THE APPROXIMATION
C       TO THE HESSIAN INVERSE TO UNITY
C
  200 IF(IPRINT.NE.0) WRITE(10,201)
  201 FORMAT(//2X,'>>>> QUASI-NEWTON PROCEDURE STARTED, WITH SEARCH',
     1       ' DIRECTION SET TO -G')
      K = 1 + NVAR * (NVAR+1) / 2
C
      DO 210 I = 1, NVAR
C
         DO 205 J = 1, I
            K = K - 1
            HESS(K) = 0.0
  205    CONTINUE
C
         HESS(K) = 1.0
  210 CONTINUE
C
  300 IF(IPRINT.EQ.0) GO TO 301
      EUCLID=SQRT(SQGRAD)
      IF(IPRINT.GE.20.AND.MOD(ITER,20).NE.0) GO TO 308
      WRITE(42,307) ITER,NFCALL,OBJF,EUCLID
  307 FORMAT(1X,'ITERATION:',I5,26X,'FUNCTION EVALUATION:',I6,
     1       /1X,'OBJECTIVE FUNCTION:',E20.13,2X,'GRADIENT NORME:',
     2        E20.13)
  308 IF(MOD(ITER,IPRINT).NE.0) GO TO 301
      WRITE(10,302) ITER,NFCALL
  302 FORMAT(////2X,'ITERATION No ',I5//2X,'NUMBER OF FUNCTION AND ',
     1        'GRADIENT EVALUATIONS = ',I5//2X,'PARAMETER VALUES')
      WRITE(10,303) (J,X(J),J=1,NVAR)
  303 FORMAT(/3(2X,'X(',I4,') = ',E16.8))
      WRITE(10,304) OBJF
  304 FORMAT(//2X,'FUNCTION VALUE OBJF = ',E16.8///2X,'GRADIENT')
      WRITE(10,306) (J,G(J),J=1,NVAR)
  306 FORMAT(/3(2X,'G(',I4,') = ',E16.8))
  301 ITER=ITER+1
C
C     BEGIN AN ITERATION BY SAVING THE CURRENT BEST ESTIMATE OF THE
C       FUNCTION AND THE SOLUTION AND GRADIENT VECTORS.
C
      DO 310 I = 1, NVAR
         SOLVEC(I) = X(I)
         GRDVEC(I) = G(I)
  310 CONTINUE
C
```

```
      TOBJF = OBJF
C
C     CALCULATE THE SEARCH DIRECTION VECTOR IN  SRHVEC  AND THE
C       DIRECTIONAL DERIVATIVE IN  DIRDEV
C
      DO 340 I = 1, NVAR
         IJ = I
         Z = 0.0
C
         DO 330 J = 1, NVAR
            Z = Z - G(J) * HESS(IJ)
            IF (J .GE. I) GO TO 325
            IJ = IJ + NVAR - J
            GO TO 330
  325       IJ = IJ + 1
  330    CONTINUE
C
         SRHVEC(I) = Z
  340 CONTINUE
C
      DIRDEV = 0.0
C
      DO 350 I = 1, NVAR
         DIRDEV = DIRDEV + SRHVEC(I) * G(I)
  350 CONTINUE
C
C     IF THE DIRECTIONAL DERIVATIVE  DIRDEV  IS .GT. 0, THERE IS NO
C       GUARANTEE THAT A SEARCH IN THE  W  DIRECTION  WILL RESULT IN A
C       SMALLER  OBJF. THEREFORE, THE  QUASI-NEWTON  PROCESS IS
C       RESTARTED AT THE CURRENT ESTIMATE OF THE SOLUTION WITH  SRHVEC
C       SET TO  -G.
C
      IF (DIRDEV .GT. 0.0) GO TO 200
      IF (DIRDEV .EQ. 0.0) GO TO 500
C
C     COMPUTE THE INITIAL SEARCH SCALAR  ALPHA  AND CONDUCT THE
C       LINEAR SEARCH BY MEANS OF A CALL TO  SEARCH
C
      ALPHA = -2.0 * REDFCN / DIRDEV
      IF (ALPHA .GT. 1.0) ALPHA = 1.0
      REDFCN = OBJF
C
C     ******************************************************************
      CALL SEARCH(NVAR,X,G,SRHVEC,OBJF,ALPHA,DIRDEV,SPREC,
     1            EXTBND,NFCALL,SCRVEC,IERR)
C     ******************************************************************
C
C     TEST FOR ABNORMAL TERMINATION
C
      IF (IERR .LT. 0) GO TO 500
      IF (NFCALL .GE. MAXF) GO TO 400
      IF ((ALPHA .LT. 1.0E-20) .OR.
     1    (ALPHA .GT. 1.0E20)) GO TO 410
C
C     TEST FOR CONVERGENCE
C
      SQGRAD = 0.0
      ICONV = 0
C
      DO 360 I = 1, NVAR
```

```
         TEMP = ALPHA * SRHVEC(I)
         SQGRAD = SQGRAD + G(I) * G(I)
         T = TOLX * ABS(X(I))
         IF (T .LE. TOLX) T = TOLX
         IF (ABS(TEMP) .GT. T) ICONV = 1
  360 CONTINUE
C
      IF (SQGRAD .GT. TOLG*TOLG) ICONV = 1
      IF (SQGRAD .EQ. 0.0) ICONV = 0
      IF (ICONV .EQ. 0) GO TO 500
C
C     THE LINEAR SEARCH TECHNIQUE HAS LOCATED A MINIMUM. CALL  UPHESS
C       TO UPDATE THE APPROXIMATION TO THE HESSIAN INVERSE USING THE
C       DFP  OR  BFGS  UPDATING FORMULAS
C
C     ****************************************************************
      CALL UPHESS(NVAR,X,G,IHESS,HESS,SOLVEC,GRDVEC,SCRVEC,ISWTCH,IEXIT)
C     ****************************************************************
C
C     IF THE UPDATE IS NOT SUCCESSFUL THE QUASI-NEWTON PROCESS IS
C       RESTARTED WITH A DESCENT STEP AT THE CURRENT ESTIMATE OF THE
C       SOLUTION
C
      REDFCN = REDFCN - OBJF
      IF (IEXIT .NE. 0) GO TO 200
C
C     NOW START A NEW ITERATION
C
C  WRITE THE CURRENT ESTIMATE OF THE HESSIAN INVERSE, IF DESIRED.
      IF(IWRHESS.EQ.0) GO TO 300
      OPEN(14,MODE='OUT',ACCESS='SEQUENTIAL',FORM='FORMATTED',
     1       FILE='LAST.HESS')
      WRITE(14,202)  (HESS(II),II=1,IHESS)
      CLOSE(14)
C
      GO TO 300
C
C     ERROR RETURN BECAUSE THERE HAVE BEEN AT LEAST  MAXF  CALLS OF
C       EVLOBJ
C
  400 IERR = 1
      GO TO 450
C
C     ERROR RETURN BECAUSE LINEAR SEARCH TECHNIQUE INDICATES THAT IT IS
C       LIKELY THAT NO MINIMUM EXISTS
C
  410 IERR = 2
C
  450 DO 455 I = 1, NVAR
         X(I) = SOLVEC(I)
         G(I) = GRDVEC(I)
  455 CONTINUE
C
      OBJF = TOBJF
  500 RETURN
C
      END
```

```
      SUBROUTINE SEARCH(N,X,G,S,F,ALPHA,DIRDEV,SPREC,EXTBND,NFCALL,
     1                  W,IERR)
C
      IMPLICIT REAL*8(A-H,O-Z)
      DIMENSION  X(200),G(200),S(200),W(200)
C
C       THIS SUBROUTINE OBTAINS AN ESTIMATE OF THE SOLUTION
C     XM = XO + ALPHA * S  WHICH MINIMIZES  F  BY MEANS OF A LINEAR
C     SEARCH IN THE  S  DIRECTION.
C
C     ON INPUT
C
C        N  IS THE NUMBER OF VARIABLES. IT IS ALSO THE DIMENSION OF THE
C           VECTORS  X, G  AND  S.
C
C        X  CONTAINS AN ESTIMATE OF THE SOLUTION VECTOR
C           (XO(1),XO(2),...,XO(N)).
C
C        S  CONTAINS THE SEARCH DIRECTION VECTOR.
C
C        F  CONTAINS THE OBJECTIVE FUNCTION  F(X).
C
C        EVLOBJ  IS A USER SUPPLIED ROUTINE TO EVALUATE  F(X)  AND THE
C           COMPONENTS OF THE GRADIENT  G(X)  AT THE ESTIMATE IN  X.
C
C        ALPHA  IS  THE INITIAL STEP SCALAR.
C
C        DIRDEV  IS THE DIRECTIONAL DERIVATIVE AT X.
C
C        SPREC  IS THE ACCURACY REQUIRED IN THE SEARCH, I.E. A POINT  XM
C           IS ACCEPTED AS THE MINIMUM ALONG DIRECTION  S  IF THE RATIO
C           OF THE DIRECTIONAL DERIVATIVE AT  XM  OVER THE DIRECTIONAL
C           DERIVATIVE AT  XO  IS NOT GREATER THAN  SPREC.
C
C        EXTBND  IS THE UPPER BOUND ON THE MULTIPLICATIVE INCREASE IN
C           ALPHA  DURING EXTRAPOLATION.
C
C        NFCALL  IS THE NUMBER OF CALLS TO THE FUNCTION EVALUATION
C           SUBROUTINE  FCN.
C
C        W  IS A SCRATCH VECTOR.
C
C     ON OUTPUT
C
C        X  CONTAINS THE ESTIMATE OF THE MINIMUM
C           (XM(1),XM(2),...,XM(N))
C
C     IERR  IS A PARAMETER SET TO A NEGATIVE INTEGER IF THE USER
C           WISHES TO FORCE AN EXIT FROM  SEARCH. OTHERWISE IT IS
C           UNALTERED.
C
C        G  CONTAINS THE COMPONENTS OF THE GRADIENT AT  X.
C
C        F  CONTAINS THE FUNCTION VALUE  F(X).
C
C        ALPHA  IS THE FINAL STEP SCALAR.
C
C        DIRDEV  IS THE DIRECTIONAL DERIVATIVE AT  X.
C
```

```
C        NFCALL  IS THE NUMBER OF CALLS TO THE FUNCTION EVALUATION
C           SUBROUTINE  EVLOBJ.
C
C
C     INITIALIZE THE FOLLOWING PARAMETERS AND INDICATORS
C
C       TOT        -  THE SUM OF THE EXTRAPOLATION STEPS
C       CDIREV     -  THE CURRENT DIRECTIONAL DERIVATIVE
C       PDIREV     -  THE PREVIOUS DIRECTIONAL DERIVATIVE
C       IERR       -  THE ERROR INDICATOR
C
      TOT = 0.0
      CDIREV = DIRDEV
      PDIREV = DIRDEV
C
C     TEST WHETHER  ALPHA  IS TOO SMALL
C
  105 IF (ALPHA .LE. 1.0E-20) GO TO 150
C
C     BEGIN THE LINEAR SEARCH BY INCREMENTING THE SOLUTION VECTOR  X
C       AND CALCULATING THE FUNCTION AND GRADIENT AT THE INCREMENTED  X.
C
      DO 108 I = 1, N
         W(I) = X(I)
         X(I) = X(I) + ALPHA * S(I)
  108 CONTINUE
C
C     ***8****************************************************************
      CALL EVLOBJ(N,X,FTEST,G)
C     ****************************************************8***************
C
      NFCALL = NFCALL + 1
      IF (IERR .LT. 0) GO TO 150
C
C     COMPUTE THE DIRECTIONAL DERIVATIVE  DIRDEV  AT  X + ALPHA * S
C
      DIRDEV = 0.0
C
      DO 110 I = 1, N
         DIRDEV = DIRDEV + G(I) * S(I)
  110 CONTINUE
C
C     TEST WHETHER  F(X + ALPHA * S)  IS LESS THAN  F(X).
C
      IF (FTEST .GE. F) GO TO 120
C
C     IF (DIRDEV / PDIREV) IS LESS THAN THE SEARCH PRECISION  SPREC,
C       ALPHA  IS ACCEPTED. OTHERWISE  ALPHA  IS MODIFIED
C
      IF (ABS(DIRDEV / PDIREV) .LE. SPREC) GO TO 140
C
C     ALPHA  IS MODIFIED. TEST WHETHER  ALPHA  IS TO BE REVISED BY
C       EXTRAPOLATION OR INTERPOLATION
C
      IF (DIRDEV .GT. 0.0) GO TO 120
C
C     ALPHA  IS REVISED USING AN EXTRAPOLATION FORMULA AND A NEW STEP
C       IS TAKEN IF THE SUM OF THE STEPS ALREADY MADE IS NOT TOO LARGE.
C       THE INPUT PARAMETER  EXTBND  LIMITS THE MULTIPLICATIVE CHANGE
C       IN  ALPHA
```

```
C
      TOT = TOT + ALPHA
      IF (TOT .GT. 1.0E10) GO TO 145
      TEMP = EXTBND
      IF (CDIREV .LT. DIRDEV) TEMP = DIRDEV / (CDIREV - DIRDEV)
      IF (TEMP .GT. EXTBND) TEMP = EXTBND
      F = FTEST
      CDIREV = DIRDEV
      ALPHA = ALPHA * TEMP
      GO TO 105
C
C     X  IS RESET TO THE CURRENT ESTIMATE, ALPHA  IS REVISED USING THE
C       CUBIC INTERPOLATION FORMULA AND A NEW STEP IS TAKEN IF THE
C       CONVERGENCE CRITERIA HAVE NOT BEEN SATISFIED.
C
  120 DO 130 I = 1, N
         X(I) = W(I)
  130 CONTINUE
C
      TEMP = 3.0 * (F - FTEST) / ALPHA + DIRDEV + CDIREV
      WT = ABS(TEMP)
      IF(WT.LT.ABS(DIRDEV)) WT=ABS(DIRDEV)
      IF(WT.LT.ABS(CDIREV)) WT=ABS(CDIREV)
      WW = TEMP / WT
      WW = WW * WW - CDIREV / WT * DIRDEV / WT
      IF (WW .LT. 0.0) WW = 0.0
      WW = SQRT(WW) * WT
      TEMP = 1.0 - (DIRDEV + WW - TEMP) / (2.0 * WW + DIRDEV -
     1       CDIREV)
      ALPHA = ALPHA * TEMP
      GO TO 105
C
C     ALPHA IS ACCEPTED
C
  140 F = FTEST
  145 ALPHA = TOT + ALPHA
  150 RETURN
C
      END



      SUBROUTINE UPHESS(N,X,G,IH,H,SOLVEC,GRDVEC,SCRVEC,ISWTCH,IEXIT)
C
      IMPLICIT REAL*8(A-H,O-Z)
      DIMENSION  X(200),G(200),H(20100),SOLVEC(200),GRDVEC(200),
     1           SCRVEC(200)
C
C     THIS SUBROUTINE UPDATES AN APPROXIMATION TO THE HESSIAN INVERSE
C       USING THE  DFP  OR  BFGS  FORMULA
C
C     ON INPUT
C
C        N  IS THE DIMENSION OF THE VECTORS  X, G, SOLVEC, GRDVEC  AND
C           SCRVEC.
C
C        X  CONTAINS AN ESTIMATE OF THE SOLUTION VECTOR.
C
C        G  CONTAINS THE COMPONENTS OF THE GRADIENT CORRESPONDING TO
```

```
C           THE  X  VECTOR.
C
C        IH  IS A PARAMETER SET EQUAL TO THE DIMENSION OF  H  WHICH IS
C           AT LEAST  N*(N+1)/2.
C
C        H  IS AN ARRAY OF DIMENSION  IH  WHICH CONTAINS THE UPPER
C           TRIANGLE OF AN APPROXIMATION TO THE HESSIAN INVERSE STORED
C           BY ROWS.
C
C        SOLVEC  CONTAINS THE CURRENT SOLUTION VECTOR.
C
C        GRDVEC  CONTAINS THE CURRENT GRADIENT VECTOR.
C
C        ISWTCH  IS A PARAMETER SET EQUAL TO  K  WHICH SELECTS THE
C           UPDATING FORMULA. FOR
C
C           K = 1 - THE  DFP  FORMULA IS USED,
C           K = 2 - THE  BFGS  FORMULA IS USED.
C
C     ON OUTPUT
C
C        IEXIT  IS A PARAMETER SET EQUAL TO  K  WHICH INDICATES THE
C           FOLLOWING. FOR
C
C           K = 0 - THE UPDATE WAS SUCCESSFUL,
C           K = 1 - THE UPDATE FAILED DUE TO ZERO DIVISORS.
C
C        H  CONTAINS THE UPDATED APPROXIMATION TO THE HESSIAN INVERSE
C           IF  IEXIT = 0.
C
C        SCRVEC  IS A SCRATCH VECTOR.
C
C     WRITTEN BY K. E. HILLSTROM, MARCH, 1976.
C
C
C     INITIALIZE THE EXIT INDICATOR  IEXIT
C
      IEXIT = 0
C
C     CALCULATE THE SOLUTION AND GRADIENT DIFFERENCE VECTORS FROM TWO
C       CONSECUTIVE ITERATIONS. FROM THIS SECTION ON
C
C       SOLVEC - CONTAINS  DELTA, THE SOLUTION DIFFERENCE VECTOR
C       GRDVEC - CONTAINS  GAMMA, THE GRADIENT DIFFERENCE VECTOR
C
  100 DO 110 I = 1, N
         SOLVEC(I) = X(I) - SOLVEC(I)
         GRDVEC(I) = G(I) - GRDVEC(I)
  110 CONTINUE
C
C     CALCULATE  Z = (GAMMA TRANSPOSE) * DELTA AND ALPHA =
C       (GAMMA TRANSPOSE) * (HESSIAN INVERSE) * GAMMA  OCCURING AS
C       DENOMINATORS IN THE  DFP  FORMULA. FROM THIS SECTION ON
C
C       H      - CONTAINS THE APPROXIMATION TO THE HESSIAN INVERSE
C       SCRVEC - CONTAINS THE SUCCESSIVE ELEMENTS OF  (GAMMA TRANSPOSE)
C                * (HESSIAN INVERSE)
C
      Z = 0.0
      ALPHA = 0.0
```

```
C
      DO 130 I = 1, N
         WT = GRDVEC(I)
         Z = Z + WT * SOLVEC(I)
         K = I
         WT = 0.0
C
         DO 120 J = 1, N
            WT = WT + GRDVEC(J) * H(K)
            IF (J .GE. I) GO TO 115
            K = K + N - J
            GO TO 120
  115       K = K + 1
  120    CONTINUE
C
         ALPHA = ALPHA + WT * GRDVEC(I)
         SCRVEC(I) = WT
  130 CONTINUE
C
C     ERROR EXIT IF THE  DFP  OR  BFGS  FORMULA BREAKS DOWN DUE TO ZERO
C       DIVISORS  Z  AND/OR  ALPHA
C
      IF ((Z .EQ. 0.0) .OR.
     1    (ALPHA .EQ. 0.0 .AND. ISWTCH .EQ. 1)) GO TO 200
C
C     UPDATE THE APPROXIMATION TO THE HESSIAN INVERSE USING THE  DFP
C       OR  BFGS  UPDATING FORMULA
C
      K = 1
C
      DO 160 I = 1, N
C
         DO 150 J = I, N
            IF (ISWTCH .EQ. 1) GO TO 135
            H(K) = H(K) - (SOLVEC(I) * SCRVEC(J) + SCRVEC(I) *
     1              SOLVEC(J)) / Z + (1.0 + ALPHA / Z) * (SOLVEC(I) *
     2              SOLVEC(J) / Z)
            GO TO 140
  135       H(K) = H(K) + SOLVEC(I) * SOLVEC(J) / Z - SCRVEC(I) *
     1              SCRVEC(J) / ALPHA
  140       K = K + 1
  150    CONTINUE
C
  160 CONTINUE
C
      GO TO 300
C
C     ERROR RETURN DUE TO ZERO DIVISORS IN THE UPDATING FORMULA
C
  200 IEXIT = 1
  300 RETURN
C
      END



      SUBROUTINE PRCD
C
C  Subroutine to print atom coordinates to output file
```

```
C
      IMPLICIT REAL*8(A-H,O-Z)
      INTEGER ICHIR(100), LAMDA(600), MU(600), NU(600), KIND(600),
     1        MODUL(600), CONNECT(0:5,0:5)
      INTEGER IC(200), ISEG(600)
      REAL*8 L, LH, LR
      DIMENSION X(600), Y(600), Z(600), VC(3), VH1D(3), VH1L(3), VH2(3),
     1          VH3(3), VRD(3), VRL(3), TO(3,3), TP(3,3), TPP(3,3),
     2          TPROD(3,3)
      COMMON /BLOCK11/ X, Y, Z
      COMMON /BLOCK21/ ICHIR, LAMDA, MU, NU, KIND, IC, ISEG, MODUL,
     1                 CONNECT
      COMMON /BLOCK31/ NUNITS, NBONDS, NSEGMENTS, NATOMS, THETAP,
     1                 THETAHP, THETAPP, THETAHPP, THETARPP, STHP,
     2                 CSTHP, STHPP, CSTHPP, L, LH, LR, VC, VH1D, VH1L,
     3                 VH2, VH3, VRD, VRL, TO, TP, TPP, TPROD
      WRITE(6,10)
   10 FORMAT(////10X,'ATOM COORDINATES'/10X,16('-')//9X,'BACKBONE ATOM'
     1       ,13X,'L-SUBSTITUENT',10X,'D-SUBSTITUENT'/)
      ISEGM=0
      WRITE(6,20) ISEGM, X(1), Y(1), Z(1)
   20 FORMAT(/2X,I4,2X,'C ',E16.7,'(METHYL) '/10X,E16.7/10X,E16.7)
      ICARBON=-1
      DO 30 IUNIT=1,NUNITS-1
         ISEGM=ISEGM+1
         ICARBON=ICARBON+3
         IF(ICHIR(IUNIT)) 60,70,70
   60    WRITE(6,80) ISEGM,X(ICARBON),X(ICARBON+2),X(ICARBON+1)
   80    FORMAT(/2X,I4,2X,'C ',E16.7,5X,'R ',E16.7,5X,'H ',E16.7)
         WRITE(6,90) Y(ICARBON),Y(ICARBON+2),Y(ICARBON+1)
   90    FORMAT(10X,E16.7,7X,E16.7,7X,E16.7)
         WRITE(6,90) Z(ICARBON),Z(ICARBON+2),Z(ICARBON+1)
         GO TO 100
   70    WRITE(6,110) ISEGM,(X(I),I=ICARBON,ICARBON+2)
  110    FORMAT(/2X,I4,2X,'C ',E16.7,5X,'H ',E16.7,5X,'R ',E16.7)
         WRITE(6,90) (Y(I),I=ICARBON,ICARBON+2)
         WRITE(6,90) (Z(I),I=ICARBON,ICARBON+2)
  100    ISEGM=ISEGM+1
         ICARBON=ICARBON+3
         WRITE(6,120) ISEGM,X(ICARBON),X(ICARBON+2),X(ICARBON+1)
  120    FORMAT(/2X,I4,2X,'C ',E16.7,5X,'H ',E16.7,5X,'H ',E16.7)
         WRITE(6,90) Y(ICARBON),Y(ICARBON+2),Y(ICARBON+1)
         WRITE(6,90) Z(ICARBON),Z(ICARBON+2),Z(ICARBON+1)
   30 CONTINUE
      ISEGM=ISEGM+1
      ICARBON=ICARBON+3
      IF(ICHIR(NUNITS)) 130,140,140
  130 WRITE(6,80) ISEGM,X(ICARBON),X(ICARBON+2),X(ICARBON+1)
      WRITE(6,90) Y(ICARBON),Y(ICARBON+2),Y(ICARBON+1)
      WRITE(6,90) Z(ICARBON),Z(ICARBON+2),Z(ICARBON+1)
      GO TO 150
  140 WRITE(6,110) ISEGM,(X(I),I=ICARBON,ICARBON+2)
      WRITE(6,90) (Y(I),I=ICARBON,ICARBON+2)
      WRITE(6,90) (Z(I),I=ICARBON,ICARBON+2)
  150 ISEGM=ISEGM+1
      WRITE(6,20) ISEGM,X(NATOMS),Y(NATOMS),Z(NATOMS)
C
      RETURN
      END
```

```
      SUBROUTINE CRD(NDF, PHI, ISTART, ICONT)
C
C    Subroutine forms coordinates of all atoms of a vinyl chain
C
C                  CH3-(CHR-CH2)nunits-H
C
C  of given tacticity, in a periodic box, given the position of the
C  first carbon of the chain, the orientation of the first two skeletal
C  bonds, and the rotation angles of all subsequent bonds of the chain.
C
C    The chain has NBONDS=NDF-1 bonds, numbered from 1 to NDF-1
C    The chain has NSEGMENTS=NDF skeletal segments, numbered from 0 to
C    NDF-1 (Flory's convention).
C    Overall the chain has NATOMS=3NDF-4 atoms (or atomic groups), of
C    which :
C                2  are terminal methyls
C          (NDF-1)/2  are chiral carbons
C        (NDF-1)/2-1  are achiral carbons
C       (3NDF-1)/2-3  are hydrogens
C          (NDF-1)/2  are R-substituents
C
C  NOTE ON BOOKKEEPING
C    The three orientation angles (Eulerian angles,external degrees of
C  freedom) alpha,beta,gamma are kept in array elements PHI(1), PHI(2),
C  PHI(3).
C    The rotation angle of bond i is kept in array element PHI(i+1)
C  (upon entrance to CRD, all angles must be in radians).
C    The x-,y-,and z- coordinates of all atoms, regardless of type, are
C  stored in three unidimensional arrays X,Y,Z. The exact nature and
C  position of an atom in the parent chain can be inferred from its
C  index in these arrays.
C    Specifically, the correspondence between indices and atoms is the
C  following:
C  Index = 1                          : terminal methyl at chain start
C       6i-4, i=1,2,...,NUNITS        : chiral skeletal carbon of unit (i)
C       6i-3, i=1,2,...,NUNITS        : hydrogen attached to chiral skeletal
C                                       carbon of unit (i) (either D- or L-)
C       6i-2, i=1,2,...,NUNITS        : substituent R attached to chiral
C                                       carbom of unit (i) (either D- or L-)
C       6i-1, i=1,2,...,NUNITS-1      : achiral skeletal atom of unit (i)
C       6i  , i=1,2,...,NUNITS-1      : D- hydrogen attached to achiral
C                                          skeletal carbon of unit (i)
C       6i+1, i=1,2,...,NUNITS-1      : L- hydrogen attached to achiral
C                                          skeletal carbon of unit (i)
C       6NUNITS-1                     : terminal methyl at chain end
C
C   . The chemical nature of an atom of index i is kept in array element
C     KIND(i)  (Code: 1=H, 2=C, 3=Methyl)
C   . In array element MODUL(i) is kept the remainder of the division of
C     the index i by 6, which is of use in connectivity screening.
C   . In array element IC(iseg) is kept the index of the carbon atom
C     belonging to skeletal segment number iseg-2 (Flory's convention
C     used in numbering segments)
C   . In array element ISEG(i) is kept the number of the segment 0
C     (according to Flory's convention, segments numbered from 0 to
C      NDF-1), to which atom i belongs.
C   . Index ICHIR(i) designates the absolute configuration of the chiral
```

```
C     skeletal carbon atom (6i-4). A value of ICHIR=+1 indicates that
C     the chiral center is D- in a Fischer projection constructed so
C     that the beginning of the chain (atom 1) lies upwards. A value
C     of ICHIR=-1 indicates an L- configuration, based on the same
C     convention.
C  .  LAMDA(i), MU(i), NU(i) are integer multipliers, such that the
C     vectors LAMDA(i)*AX, MU(i)*AY, NU(i)*AZ, when added to the
C     position vector of atom i of the parent chain, give the position
C     vector of an image of i lying in the cube.
C  .  If ICONT=1, the routine calculates the continuation coefficients
C     LAMDA,MU,NU based on intersections of the parent chain with the
C     borders of the box.
C     If ICONT=0, the routine uses prespecified values for continuation
C     coefficients.
C
      IMPLICIT REAL*8(A-H,O-Z)
      INTEGER LAMDA(600), MU(600), NU(600), ICHIR(100), KIND(600),
     1        MODUL(600), CONNECT(0:5,0:5)
      INTEGER IC(200), ISEG(600)
      REAL*8 L, LH, LR
      DIMENSION X(600), Y(600), Z(600), PHI(200), AX(3), AY(3), AZ(3),
     1          AXCY(3), AYCZ(3), AZCX(3), ORIGIN(3), VC(3), VH1D(3),
     2          VH1L(3), VH2(3), VH3(3), VRD(3), VRL(3), TO(3,3),
     3          TP(3,3), TPP(3,3), TPROD(3,3), VECT(3),
     4          XP(600), YP(600), ZP(600)
      COMMON /BLOCK11/ X, Y, Z
      COMMON /BLOCK21/ ICHIR, LAMDA, MU, NU, KIND, IC, ISEG, MODUL,
     1                 CONNECT
      COMMON /BLOCK31/ NUNITS, NBONDS, NSEGMENTS, NATOMS, THETAP,
     1                 THETAHP, THETAPP, THETAHPP, THETARPP, STHP, CSTHP,
     2                 STHPP, CSTHPP, L, LH, LR, VC, VH1D, VH1L, VH2,
     3                 VH3, VRD, VRL, TO, TP, TPP, TPROD
      COMMON /BLOCK41/ SA, CSA, SB, CSB, SG, CSG, AX, AY, AZ, AXX, AYY,
     1                 AZZ, AXCY, AYCZ, AZCX, ORIGIN, VOLUME
      COMMON /BLOCK71/ XP, YP, ZP
C
C  Initializations upon first call of subroutine (ISTART=1)
C
      IF(ISTART) 20,10,20
C
C  Initialize all coordinates to zero, except those of chain start
   20 DO 30 J=2,NATOMS
         X(J)=0.0
         Y(J)=0.0
         Z(J)=0.0
   30 CONTINUE
C
C  Setup parallel arrays KIND, IC and MODUL, keeping track of the
C  chemical nature and connectivity of the parent chain.
      ICARBON=-1
      DO 35 I=3,NDF
         ICARBON=ICARBON+3
         IC(I)=ICARBON
   35 CONTINUE
      IC(2)=1
      IC(NDF+1)=NATOMS
C
      KIND(1)=3
C     (the following are pseudo-definitions, used for convenience in
C      updating)
```

```
      ISEG(1)=1
      MODUL(1)=1
      I=1
      ISEGM=0
C
   40 I=I+1
      ISEGM=ISEGM+1
      KIND(I)=2
      ISEG(I)=ISEGM
      MODUL(I)=2
C
      I=I+1
      KIND(I)=1
      ISEG(I)=ISEGM
      MODUL(I)=3
C
      I=I+1
      KIND(I)=3
      ISEG(I)=ISEGM
      MODUL(I)=4
C
      I=I+1
      IF(I.EQ.NATOMS) GO TO 50
      ISEGM=ISEGM+1
      KIND(I)=2
      ISEG(I)=ISEGM
      MODUL(I)=5
C
      I=I+1
      KIND(I)=1
      ISEG(I)=ISEGM
      MODUL(I)=0
C
      I=I+1
      KIND(I)=1
      ISEG(I)=ISEGM
      MODUL(I)=1
      GO TO 40
C
   50 KIND(NATOMS)=3
C     (the following is a pseudo-definition, used for convenience
C      in updating)
      ISEG(NATOMS)=NDF-2
      MODUL(NATOMS)=5
C
C  Initialize coordinate transformation matrices
      STHP=SIN(THETAP)
      CSTHP=COS(THETAP)
      STHPP=SIN(THETAPP)
      CSTHPP=COS(THETAPP)
      TP(1,1)=CSTHP
      TP(1,2)=STHP
      TP(1,3)=0.0
      TPP(1,1)=CSTHPP
      TPP(1,2)=STHPP
      TPP(1,3)=0.0
C
C  Setup position vectors of skeletal carbons and substituents
C  with  respect to local coordinate systems of chain bonds.
C
```

```
C  VC = coordinate vector of skeletal carbon of segment i with
C       respect to coordinate system of bond i:
C
      VC(1)=L
      VC(2)=0.
      VC(3)=0.
C
C  VH1D = coordinate vector of hydrogen H1, connected to chiral
C         carbon atom of segment 2i-1 with respect to coordinate system
C         of bond (2i), for the case ICHIR(i)=+1 (D- configuration of
C         carbon 2i-1)
C
      VH1D(1)=-LH*COS(THETAHPP)
      VH1D(2)=LH*COS(THETAHPP)/TAN(THETAPP/2.)
      VH1D(3)=LH*SQRT(1.-(COS(THETAHPP))**2/(SIN(THETAPP/2.))**2)
C
C  VRD = coordinate vector of substituent R, connected to the chiral
C        carbon atom of segment 2i-1 with respect to coordinate system
C        of bond (2i), for the case ICHIR(i)=+1
C        (D- configuration of carbon 2i-1)
C
      VRD(1)=-LR*COS(THETARPP)
      VRD(2)=LR*COS(THETARPP)/TAN(THETAPP/2.)
      VRD(3)=-LR*SQRT(1.-(COS(THETARPP))**2/(SIN(THETAPP/2.))**2)
C
C  Form respective coordinate vectors for L- configuration of segment
C  2i-1
C
      DO 60 I=1,3
        VH1L(I)=VH1D(I)
   60 VRL(I)=VRD(I)
      VH1L(3)=-VH1L(3)
      VRL(3)=-VRL(3)
C
C  VH2=coordinate vector of hydrogen H2, connected to achiral carbon
C      atom of segment 2i in the D- position, with respect to coordinate
C      system of bond (2i+1)
C
      VH2(1)=-LH*COS(THETAHP)
      VH2(2)=LH*COS(THETAHP)/TAN(THETAP/2.)
      VH2(3)=-LH*SQRT(1.-(COS(THETAHP))**2/(SIN(THETAP/2))**2)
C
C  VH3=coordinate vector of hydrogen H3, connected to achiral carbon
C      atom of segment 2i in the L- position, with respect to coordinate
C      system of bond (2i+1).
C
      VH3(1)=VH2(1)
      VH3(2)=VH2(2)
      VH3(3)=-VH2(3)
C
      LAMDA(1)=0
      MU(1)=0
      NU(1)=0
C
      RETURN
C
C
C  Calculations upon normal call of subroutine
C
C  Matrix TPP initially contains T- matrix corresponding to bond 1
```

```
C   (PHI=0)
   10 TPP(2,1)=STHPP
      TPP(2,2)=-CSTHPP
      TPP(2,3)=0.0
      TPP(3,1)=0.0
      TPP(3,2)=0.0
      TPP(3,3)=-1.0
C
C  TO = Transformation matrix from local coordinate system of bond 1
C       to fixed coordinate system (x,y,z).
C
      ALPHA=PHI(1)
      BETA=PHI(2)
      GAMMA=PHI(3)
      CSA=COS(ALPHA)
      SA=SIN(ALPHA)
      CSB=COS(BETA)
      SB=SIN(BETA)
      CSG=COS(GAMMA)
      SG=SIN(GAMMA)
      TO(1,1)=CSA*SB
      TO(1,2)=-CSA*CSB*CSG-SA*SG
      TO(1,3)=-CSA*CSB*SG+SA*CSG
      TO(2,1)=SA*SB
      TO(2,2)=-SA*CSB*CSG+CSA*SG
      TO(2,3)=-SA*CSB*SG-CSA*CSG
      TO(3,1)=CSB
      TO(3,2)=SB*CSG
      TO(3,3)=SB*SG
C
C  Store coordinates of chain atom 1 (terminal methyl)
      XP(1)=PHI(NDF+1)
      YP(1)=PHI(NDF+2)
      ZP(1)=PHI(NDF+3)
      IF(ICONT.EQ.0) GO TO 61
      X(1)=XP(1)
      Y(1)=YP(1)
      Z(1)=ZP(1)
      CALL PERCONT(1)
C
C  Form and store coordinates of chain atoms 2,3,4,5.
C
C  Atom 2 (Chiral carbon of segment1[Flory's conv.] of the chain)
   61 CALL MATVEC(TO,VC,VECT,3,3,3,3)
      XP(2)=XP(1)+VECT(1)
      YP(2)=YP(1)+VECT(2)
      ZP(2)=ZP(1)+VECT(3)
      IF(ICONT.EQ.0) GO TO 63
      X(2)=X(1)+VECT(1)
      Y(2)=Y(1)+VECT(2)
      Z(2)=Z(1)+VECT(3)
      LAMDA(2)=0
      MU(2)=0
      NU(2)=0
      CALL PERCONT(2)
C
C  Form and store transformation matrix product TPROD=TO*T1
   63 CALL MATMAT(TO,TPP,TPROD,3,3,3,3,3,3)
C
C  Atom 3 (Hydrogen connected to chiral carbon 2)
```

```
      IF(ICHIR(1)) 62,64,64
   62 CALL MATVEC(TPROD,VH1L,VECT,3,3,3,3)
      GO TO 70
   64 CALL MATVEC(TPROD,VH1D,VECT,3,3,3,3)
   70 XP(3)=XP(2)+VECT(1)
      YP(3)=YP(2)+VECT(2)
      ZP(3)=ZP(2)+VECT(3)
      IF(ICONT.EQ.0) GO TO 65
      X(3)=X(2)+VECT(1)
      Y(3)=Y(2)+VECT(2)
      Z(3)=Z(2)+VECT(3)
      LAMDA(3)=LAMDA(2)
      MU(3)=MU(2)
      NU(3)=NU(2)
      CALL PERCONT(3)
C
C  Atom 4 (Substituent R connected to chiral carbon 2)
   65 IF(ICHIR(1)) 72,74,74
   72 CALL MATVEC(TPROD,VRL,VECT,3,3,3,3)
      GO TO 80
   74 CALL MATVEC(TPROD,VRD,VECT,3,3,3,3)
   80 XP(4)=XP(2)+VECT(1)
      YP(4)=YP(2)+VECT(2)
      ZP(4)=ZP(2)+VECT(3)
      IF(ICONT.EQ.0) GO TO 73
      X(4)=X(2)+VECT(1)
      Y(4)=Y(2)+VECT(2)
      Z(4)=Z(2)+VECT(3)
      LAMDA(4)=LAMDA(2)
      MU(4)=MU(2)
      NU(4)=NU(2)
      CALL PERCONT(4)
C
C  Atom 5 (Achiral carbon of third segment of the chain)
   73 CALL MATVEC(TPROD,VC,VECT,3,3,3,3)
      XP(5)=XP(2)+VECT(1)
      YP(5)=YP(2)+VECT(2)
      ZP(5)=ZP(2)+VECT(3)
      IF(ICONT.EQ.0) GO TO 75
      X(5)=X(2)+VECT(1)
      Y(5)=Y(2)+VECT(2)
      Z(5)=Z(2)+VECT(3)
      LAMDA(5)=LAMDA(2)
      MU(5)=MU(2)
      NU(5)=NU(2)
      CALL PERCONT(5)
C
   75 ANGLE=PHI(4)
      SPH=SIN(ANGLE)
      CSPH=COS(ANGLE)
      TP(2,1)=STHP*CSPH
      TP(2,2)=-CSTHP*CSPH
      TP(2,3)=SPH
      TP(3,1)=STHP*SPH
      TP(3,2)=-CSTHP*SPH
      TP(3,3)=-CSPH
      CALL MATMAT(TPROD,TP,TPROD,3,3,3,3,3,3)
C
C  Loop over all atoms whose coordinates depend on the rotation angles,
C  but the last one.
```

```
      DO 100 I=6,NATOMS-1
C
C  Differentiate, accrding to atom type
         GO TO (110,120,130,140,150) MODUL(I)
C
C  MODUL=0 : D-hydrogen attached to achiral skeletal carbon
         CALL MATVEC(TPROD,VH2,VECT,3,3,3,3)
         GO TO 170
C
C  MODUL=1 : L-hydrogen attached to achiral skeletal carbon
  110    CALL MATVEC(TPROD,VH3,VECT,3,3,3,3)
         GO TO 170
C
C  MODUL=3 : hydrogen attached to chiral skeletal carbon
  130    IF(ICHIR((I+3)/6)) 132,134,134
  132    CALL MATVEC(TPROD,VH1L,VECT,3,3,3,3)
         GO TO 170
  134    CALL MATVEC(TPROD,VH1D,VECT,3,3,3,3)
         GO TO 170
C
C  MODUL=4 : R-substituent attached to chiral skeletal carbon
  140    IF(ICHIR((I+2)/6)) 142,144,144
  142    CALL MATVEC(TPROD,VRL,VECT,3,3,3,3)
         GO TO 170
  144    CALL MATVEC(TPROD,VRD,VECT,3,3,3,3)
C
  170    IREF=IC(ISEG(I)+2)
         XP(I)=XP(IREF)+VECT(1)
         YP(I)=YP(IREF)+VECT(2)
         ZP(I)=ZP(IREF)+VECT(3)
         IF(ICONT.EQ.0) GO TO 100
         X(I)=X(IREF)+VECT(1)
         Y(I)=Y(IREF)+VECT(2)
         Z(I)=Z(IREF)+VECT(3)
         LAMDA(I)=LAMDA(IREF)
         MU(I)=MU(IREF)
         NU(I)=NU(IREF)
         GO TO 190
C
C  MODUL=2 : chiral skeletal carbon
  120    CALL MATVEC(TPROD,VC,VECT,3,3,3,3)
C  Update transformation matrix product, taking into account the
C  rotation angle of bond (I+1)/3
         ANGLE=PHI((I+7)/3)
         SPH=SIN(ANGLE)
         CSPH=COS(ANGLE)
         TPP(2,1)=STHPP*CSPH
         TPP(2,2)=-CSTHPP*CSPH
         TPP(2,3)=SPH
         TPP(3,1)=STHPP*SPH
         TPP(3,2)=-CSTHPP*SPH
         TPP(3,3)=-CSPH
         CALL MATMAT(TPROD,TPP,TPROD,3,3,3,3,3,3)
C
         GO TO 180
C
C  MODUL=5 : Achiral skeletal carbon
  150    CALL MATVEC(TPROD,VC,VECT,3,3,3,3)
C  Update transformation matrix product, taking into account the
C  rotation  angle of bond (I+1)/3
```

```
          ANGLE=PHI((I+7)/3)
          SPH=SIN(ANGLE)
          CSPH=COS(ANGLE)
          TP(2,1)=STHP*CSPH
          TP(2,2)=-CSTHP*CSPH
          TP(2,3)=SPH
          TP(3,1)=STHP*SPH
          TP(3,2)=-CSTHP*SPH
          TP(3,3)=-CSPH
          CALL MATMAT(TPROD,TP,TPROD,3,3,3,3,3,3)
C
  180     IREF=I-3
          XP(I)=XP(IREF)+VECT(1)
          YP(I)=YP(IREF)+VECT(2)
          ZP(I)=ZP(IREF)+VECT(3)
          IF(ICONT.EQ.0) GO TO 100
          X(I)=X(IREF)+VECT(1)
          Y(I)=Y(IREF)+VECT(2)
          Z(I)=Z(IREF)+VECT(3)
          LAMDA(I)=LAMDA(IREF)
          MU(I)=MU(IREF)
          NU(I)=NU(IREF)
C
  190     CALL PERCONT(I)
C
  100 CONTINUE
C
C  Coordinate calculation for methyl at chain end
      CALL MATVEC(TPROD,VC,VECT,3,3,3,3)
      IREF=NATOMS-3
      XP(NATOMS)=XP(IREF)+VECT(1)
      YP(NATOMS)=YP(IREF)+VECT(2)
      ZP(NATOMS)=ZP(IREF)+VECT(3)
      IF(ICONT.EQ.0) GO TO 220
      X(NATOMS)=X(IREF)+VECT(1)
      Y(NATOMS)=Y(IREF)+VECT(2)
      Z(NATOMS)=Z(IREF)+VECT(3)
      LAMDA(NATOMS)=LAMDA(IREF)
      MU(NATOMS)=MU(IREF)
      NU(NATOMS)=NU(IREF)
      CALL PERCONT(NATOMS)
      RETURN
C
  220 DO 200 I=1,NATOMS
          X(I)=XP(I)+LAMDA(I)*AX(1)+MU(I)*AY(1)+NU(I)*AZ(1)
          Y(I)=YP(I)+LAMDA(I)*AX(2)+MU(I)*AY(2)+NU(I)*AZ(2)
          Z(I)=ZP(I)+LAMDA(I)*AX(3)+MU(I)*AY(3)+NU(I)*AZ(3)
  200 CONTINUE
C
      RETURN
      END



      SUBROUTINE PERCONT(I)
C
C  Subroutine is used in the calculation of coordinates of atoms lying
C  in the cube.
C  Every time the coordinates of a new atom are calculated, the
```

```
C  subroutine checks whether the chain has exited the cube, and
C  if yes it imposes an appropriate periodic displacement to
C  locate the image of the atom lying within the cube
C
      IMPLICIT REAL*8(A-H,O-Z)
      INTEGER LAMDA(600), MU(600), NU(600), ICHIR(100), KIND(600),
     1          MODUL(600), CONNECT(0:5,0:5)
      INTEGER IC(200), ISEG(600)
      DIMENSION X(600), Y(600), Z(600), AX(3), AY(3), AZ(3), AXCY(3),
     1          AYCZ(3), AZCX(3), ORIGIN(3), VECT(3)
      COMMON /BLOCK11/ X, Y, Z
      COMMON /BLOCK21/ ICHIR, LAMDA, MU, NU, KIND, IC, ISEG, MODUL,
     1                 CONNECT
      COMMON /BLOCK41/ SA, CSA, SB, CSB, SG, CSG, AX, AY, AZ, AXX,
     1                 AYY, AZZ, AXCY, AYCZ, AZCX, ORIGIN, VOLUME
C
      VECT(1)=X(I)-ORIGIN(1)
      VECT(2)=Y(I)-ORIGIN(2)
      VECT(3)=Z(I)-ORIGIN(3)
      CALL VECVEC(VECT, AYCZ, XCRIT, 3, 3)
      IF(XCRIT.LE.VOLUME) GO TO 10
      LAMDA(I)=LAMDA(I)-1
      X(I)=X(I)-AX(1)
      Y(I)=Y(I)-AX(2)
      Z(I)=Z(I)-AX(3)
      GO TO 20
   10 IF(XCRIT.GE.0.0) GO TO 20
      LAMDA(I)=LAMDA(I)+1
      X(I)=X(I)+AX(1)
      Y(I)=Y(I)+AX(2)
      Z(I)=Z(I)+AX(3)
C
   20 VECT(1)=X(I)-ORIGIN(1)
      VECT(2)=Y(I)-ORIGIN(2)
      VECT(3)=Z(I)-ORIGIN(3)
      CALL VECVEC(VECT, AZCX, YCRIT, 3, 3)
      IF(YCRIT.LE.VOLUME) GO TO 30
      MU(I)=MU(I)-1
      X(I)=X(I)-AY(1)
      Y(I)=Y(I)-AY(2)
      Z(I)=Z(I)-AY(3)
      GO TO 40
   30 IF(YCRIT.GE.0.0) GO TO 40
      MU(I)=MU(I)+1
      X(I)=X(I)+AY(1)
      Y(I)=Y(I)+AY(2)
      Z(I)=Z(I)+AY(3)
C
   40 VECT(1)=X(I)+ORIGIN(1)
      VECT(2)=Y(I)+ORIGIN(2)
      VECT(3)=Z(I)+ORIGIN(3)
      CALL VECVEC(VECT, AXCY, ZCRIT, 3, 3)
      IF(ZCRIT.LE.VOLUME) GO TO 50
      NU(I)=NU(I)-1
      X(I)=X(I)-AZ(1)
      Y(I)=Y(I)-AZ(2)
      Z(I)=Z(I)-AZ(3)
      GO TO 60
   50 IF(ZCRIT.GE.0.0) GO TO 60
      NU(I)=NU(I)+1
```

```
      X(I)=X(I)+AZ(1)
      Y(I)=Y(I)+AZ(2)
      Z(I)=Z(I)+AZ(3)
C
   60 RETURN
C
      END



      SUBROUTINE MATVEC(A, V, AV, MFORM, NFORM, M, N)
C
C  Matrix- vector multiplication, A.V=AV
C
      IMPLICIT REAL*8(A-H,O-Z)
      DIMENSION A(MFORM,NFORM), V(NFORM), AV(MFORM), VAUX(25)
      DO 1 I=1,M
        X=0.0
        DO 2 K=1,N
    2   X=X+A(I,K)*V(K)
    1 VAUX(I)=X
      DO 3 I=1,M
    3 AV(I)=VAUX(I)
      RETURN
      END



      SUBROUTINE MATMAT(A,B,AB,MFORM,NFORM,LFORM,M,N,L)
C
C  Matrix multiplication A.B=AB
C
      IMPLICIT REAL*8(A-H,O-Z)
      DIMENSION A(MFORM,NFORM), B(NFORM,LFORM), AB(MFORM,LFORM),
     1          AUX(25,25)
      DO 1 I=1,M
      DO 1 J=1,L
        X=0.0
        DO 2 K=1,N
    2   X=X+A(I,K)*B(K,J)
    1 AUX(I,J)=X
      DO 3 I=1,M
      DO 3 J=1,L
    3 AB(I,J)=AUX(I,J)
      RETURN
      END



      SUBROUTINE VCROSSV(V1,V2,V3)
C
C  Formation of the external(cross) product of two vectors, V3=V1xV2
C  Subroutine is designed so that the product can be written in one of
C  the factors (V1 or V2 can be used in place of V3)
C
      IMPLICIT REAL*8(A-H,O-Z)
      DIMENSION V1(3), V2(3), V3(3)
```

```
C
      VAUX1=V1(2)*V2(3)-V2(2)*V1(3)
      VAUX2=V1(3)*V2(1)-V2(3)*V1(1)
      VAUX3=V1(1)*V2(2)-V2(1)*V1(2)
C
      V3(1)=VAUX1
      V3(2)=VAUX2
      V3(3)=VAUX3
C
      RETURN
      END



      SUBROUTINE VECVEC(V1, V2, PRODUCT, NFORM, N)
C
C  Vector multiplication, V1T.V2=PRODUCT
C
      IMPLICIT REAL*8(A-H,O-Z)
      DIMENSION V1(NFORM), V2(NFORM)
      PRODUCT=0.0
      DO 1 I=1,N
    1 PRODUCT=PRODUCT+V1(I)*V2(I)
      RETURN
      END
```